# Investigation into Glycosylation of the *Aeromonas caviae* Polar Flagellum

Rebecca Catherine Lowry

A thesis submitted for the degree of Doctor of Philosophy

Department of Infection and Immunity

The University of Sheffield

February 2015

# Acknowledgements

I have found the past three and a half years both incredibly enjoyable, and immensely challenging. There are so many people I would like to thank who have helped and encouraged me along the way.

First of all I would like to start by thanking my supervisors, Dr Jonathan Shaw and Dr Graham Stafford, for their constant help and support during my PhD; and Dr Narciso Couto for all his patience and wisdom during the mass spectrometry work, whom without, Chapter 4 of this thesis would not have been possible. I would also like to thank Dr Jennifer Parker for being an amazing teacher and friend from day one of this project (and her husband Dr Matthew Hicks). A big thank you also to Dr Sabela Balboa-Mendez for all her help and support, and for the amazing Spanish feasts that have kept me going through all of this. I would also like to thank the other members of Infection and Immunity and the School of Clinical Dentistry, in particular: Jamie Hall, Helena Spiewak, Ben Harvey, Sayali Haldipurkar, Yu Hang Zhao, Hannah McMellon, Sarah Oates and Sam Harding, for so many useful discussions and coffee breaks that have really spurred me on. Also, thank you to the Department of Biological Engineering for all the support, particularly Tom Minshull and Andrew Landells for being computer and mass spec geniuses.

A big thank you also to the 'world food club' (ie. Beth and Megan) and the Spooner girls for being wonderful people, and getting me through the demanding times. A huge thank you also to my lovely undergraduate friends, Daniel Cozens, Liz Court, Kate Naylor and Charlotte Green, who have plied me with Fizzy Fangs and dry shampoo during the thesis writing period; I hope to return the favour when you guys are going through the same thing in a few months.

I would also like to thank the lovely Palmer family who are always amazing and supportive, and have made regular trips to Sheffield to cheer my day.

I would especially like to thank my mum, dad and Jason, for their continuous support with everything I do, and for their constant kindness – always making sure the larders are stocked and we have wood for the fire!

And finally, I would like to thank JP for everyday being incredibly supportive and understanding, I can't put into words how grateful I am. And you still want to marry me after all of my PhD craziness!

# Abstract

The bacterial flagellum is an important appendage at the bacterial cell surface, not only for motility, but for adherence to host cells, and therefore has an extensive role in bacterial colonisation and virulence. A number of pathogenic bacteria modify their flagellins with nonulosonic acids, such as *Aeromonas, Campylobacter* and *Helicobacter* species, via an *O*-linked glycosylation process. This modification is essential for their ability to form flagella, thus having implications in pathogen virulence. However, the role of flagellin glycosylation is currently undetermined.

The mesophilic aeromonad, *Aeromonas caviae*, forms a constitutively expressed polar flagellum necessary for motility in liquid environments. It is thought to be a good model for glycosylation as it decorates its flagellins solely with pseudaminic acid, and contains a genetically simple system for this process to occur. The work in this thesis has explored the pathway, and role of flagellin glycosylation in this microorganism.

The function of a putative deglycosylation enzyme (AHA0618) and its possible role in the fine tuning of flagellin glycosylation was examined, where it was concluded that this protein is likely to be involved in peptidoglycan crosslinking at the cell wall, and not the flagellin glycosylation pathway. This demonstrates that subtle changes to bacterial cellular morphology are able to affect bacterial behaviour.

Additionally, investigations into the sites of flagellin glycosylation via mass spectrometric methods concluded that the sites of modification on *A. caviae* flagellins can vary. However, certain residues were found to be predominantly glycosylated, suggesting partial selectivity to the glycosylation process via the putative glycosyltransferase, Maf1.

Finally, protein interaction studies have provided evidence that glycosylation is likely to occur in the cytoplasm before binding of the flagellin-specific chaperone and flagellin export. Moreover, Maf specificity investigations, together with these interaction studies have suggested that the Maf proteins may be recognising and docking to the N-terminal region of the flagellins.

# Abbreviations

| | |
|---|---|
| **ACN** | Acetonitrile |
| **Ambic** | Ammonium bicarbonate |
| **Amp** | Ampicillin |
| **ATP** | Adenosine triphosphate |
| **BHIB** | Brain heart infusion broth |
| **Bp** | Base pairs |
| **cAMP** | Cyclic adenosine monophosphate |
| **CAP** | Catabolite gene activator protein |
| **CBD** | Chaperone binding domain |
| **CID** | Collision induced dissociation |
| **Cm** | Chloramphenicol |
| **C-terminal** | Carboxy terminal |
| **DMSO** | Dimethyl sulfoxide |
| **DNA** | Deoxyribonucleic acid |
| **dNTPs** | Deoxynucleotides |
| **DTT** | Dithiothreitol |
| **ETD** | Electron transfer dissociation |
| **GlcNAc** | N-acetylglucosamine |
| **Gm** | Gentamycin |
| **HPLC** | High performance liquid chromatography |
| **Hrs** | Hours |
| **Hz** | Hurtz |
| **IPTG** | Isopropyl-β-thiogalactoside |
| **Kb** | kilobase |
| **Km** | Kanamycin |
| **LPS** | Lipopolysaccharide |
| **mAU** | milliabsorabance units |
| **Min** | Minutes |
| **MS** | Mass spectrometry |
| **MS/MS** | Tandem mass spectrometry |
| **Nal** | Nalidixic acid |
| **N-terminal** | Amino terminal |
| **NTR** | N-terminal region |
| **$OD_{600}$** | Optical density (measured at 600 nm) |
| **PBS** | Phosphate buffered saline |
| **PCR** | Polymerase chain reaction |
| **Pse5Ac7Ac** | Pseudaminic acid |
| **Q-TOF** | Quadrupole Time of Flight (Mass spectrometer) |
| **RNA** | Ribonucleic acid |
| **SDS-PAGE** | Sodium dodecyl sulphate polyacrylamide gel electrophoresis |
| **Strep** | Streptomycin |
| **T3SS** | Type three section system |
| **T6SS** | Type six secretion system |
| **Tm** | Melting temperature (primers) |
| **UV** | Ultraviolet |

# Table of Contents

**Chapter 1: Introduction** ..... 1
**1.1 – The genus *Aeromonas*** ..... 1
1.1.1 – Host interactions ..... 1
1.1.2 – Colonisation factors ..... 3
1.1.2.1 – Secreted factors ..... 3
1.1.2.2 – Adherence factors ..... 4
**1.2 – *Aeromonas* motility** ..... 8
1.2.1 – Polar Flagellum ..... 8
1.2.2 – Lateral Flagella ..... 13
1.2.3 – Export and assembly ..... 14
1.2.4 – Gene expression and regulation ..... 16
**1.3 – Protein Glycosylation** ..... 19
1.3.1 – Eukaryotic protein glycosylation ..... 19
1.3.2 – Bacterial glycosylation of surface proteins ..... 22
1.3.2.1 – *Campylobacter* ..... 22
1.3.2.2 – *Helicobacter* ..... 25
1.3.2.3 – *Pseudomonas* ..... 26
1.3.2.4 – *Neisseria* ..... 27
1.3.2.5 – Gram-positive bacterial glycosylation ..... 28
**1.4 – Glycosylation in *Aeromonas* species** ..... 29
1.4.1 – The *O*-linked flagellin glycosylation pathway in *A. caviae* Sch3 ..... 31
1.4.1.1 – Pseudaminic acid biosynthesis ..... 31
1.4.1.2 – Flagellin glycosylation ..... 33
**1.5 – Project aims** ..... 35
**Chapter 2 – Materials and methods** ..... 36
**2.1 – Strains and Plasmids** ..... 36
**2.2 – Media and Antibiotics** ..... 42
**2.3 – Solutions and Buffers** ..... 43
**2.4 – Growth Conditions and Genetic Manipulations** ..... 44
2.4.1 – Standard growth conditions ..... 44
2.4.2 – Glycerol stocks ..... 44
2.4.3 – Growth Curves ..... 44
2.4.4 – Swimming motility assays ..... 44

2.4.5 – Swarming motility assays ..... 45
2.4.6 – Bacterial adenylate cyclase two-hybrid system (BACTH system) ..... 45
2.4.7 – Isolation of Genomic DNA (Phenol/Chloroform Extraction) ..... 45
2.4.8 – Plasmid purification ..... 46
2.4.9 – Agarose gel electrophoresis ..... 46
2.4.10 – Gel extraction ..... 46
2.4.11 - Restriction digests ..... 46
2.4.12 – Ligation ..... 46
2.4.13 – Conjugation ..... 46
2.4.14 – Oxidase test ..... 47
2.4.15 – Bacterial transformation into chemically competent *E. coli* ..... 48
2.4.15.1 - Production of chemically competent cells ..... 48
2.4.15.2 - Transformation ..... 48
**2.6 – Polymerase Chain reaction (PCR)** ..... 49
2.6.1 – Primers ..... 50
2.6.2 – PCR cycles ..... 56
2.6.2.1 - Expand high fidelity PCR (Roche) ..... 56
2.6.2.2 – Q5 DNA polymerase (NEB) ..... 56
2.6.2.3 – Overlap extension PCR (for site-directed mutagenesis) ..... 56
2.6.2.4 – Colony PCR ..... 57
2.6.3 – PCR product purification ..... 57
2.6.4 – DNA sequencing ..... 59
**2.7 – Protein and Purification Methods** ..... 60
2.7.1 – Protein precipitation ..... 60
2.7.2 – SDS-PAGE (Sodium dodecyl sulphate polyacrylamide gel electrophoresis) ..... 60
2.7.3 – Western blotting ..... 60
2.7.4 – Flagella Isolation ..... 61
2.7.5 – LPS Extraction and Analysis ..... 61
2.7.6 – Peptidoglycan (PG) Extraction and Analysis ..... 62
2.7.6.1 - PG Extraction ..... 62
2.7.6.2 – PG analysis ..... 62
2.7.7 – Mass spectrometry (MS) ..... 63
2.7.7.1 - In-gel trypsin digestion of flagellin ..... 63
2.7.7.2 - High Performance Liquid Chromatography (HPLC) Mass Spectrometry (MS) Analysis ..... 64

2.7.7.3 - MS/MS Data Analysis ..... 65
**2.8 – Microscopy** ..... 66
2.8.1 – Fluorescence Microscopy ..... 66
2.8.2 – Scanning Electron Microscopy (SEM) ..... 66
**Chapter 3: Investigation into the Function of AHA0618 – a Flagellin Deglycosylase or Cell Wall Remodelling Enzyme?** ..... 67
**3.1 - Introduction** ..... 67
**3.2 – Results** ..... 69
3.2.1 – Bioinformatic analysis of AHA0618 ..... 69
3.2.2 - Analysis of *A. caviae AHA0618* mutant motility ..... 70
3.2.3 – Analysis of *AHA0618* mutant and wild type *A. caviae* containing pSRK_*AHA0618* 75
3.2.3.1 – Generation of pSRK_*AHA0618* ..... 75
3.2.3.2 – Motility analysis of *A. caviae* strains containing pSRK_*AHA0618* ..... 79
3.2.3.3 – Analysis of flagellin glycosylation levels via western blot analysis in the *AHA0618* mutant and strains containing pSRK_*AHA0618* ..... 82
3.2.4 – Analysis of *AHA0618* mutant and wild type *A. caviae* containing pSRK_*HP0518* ... 84
3.2.4.1 – Generation of pSRK_*HPO518* ..... 84
3.2.4.2 - Motility and flagellin glycosylation analysis of *A. caviae* strains containing pSRK_*HP0518* ..... 84
3.2.5 – Analysis of *AHA0618* mutant *A. caviae* cellular envelope ..... 88
3.2.6 – Analysis of *A. caviae* cellular morphology ..... 91
3.2.7 – *A. caviae* muropeptide analysis ..... 95
**3.3 – Discussion** ..... 97
**Chapter 4: Investigating the sites of *Aeromonas caviae* Sch3 Polar Flagellin Glycosylation** ..... 101
**4.1 – Introduction** ..... 101
**4.2 – Results** ..... 104
4.2.1 – Method of flagellin purification ..... 104
4.2.2 – Mass spectrometry analysis of *Aeromonas caviae* polar flagellins ..... 107
4.2.2.1 – Mass Spectrometry Methods for Glycoprotein Analysis ..... 107
4.2.2.2 - Manual analysis of CID-MS/MS spectra ..... 109
4.2.2.3 – EasyProt analysis of CID-MS/MS spectra ..... 114
4.2.3 – Flagellin Mutational Studies ..... 129
4.2.3.1 – Generation of pBBR1MCS-5_*flaB* ..... 129
4.2.3.2 – Site-directed Mutagenesis of FlaB Glycosylation Sites Identified via Mass Spectrometry ..... 129

4.2.3.3 – Analysis of Site-Directed Mutant pBBR1MCS-5_*flaB* constructs in *Aeromonas caviae* ..... 133
4.2.3.4 – Mass spectrometry analysis of the site-directed mutant flagellin, FlaB(S159/161A) ..... 138
4.2.3.5 – Further Site-Directed mutagenesis of FlaB ..... 142
**4.3 – Discussion** ..... 151
**Chapter 5: Investigations into Maf1 dependent polar flagellin glycosylation** ..... 160
**5.1 – Introduction** ..... 160
**5.2 – Results** ..... 162
5.2.1 – Interaction studies of the proteins of the *Aeromonas caviae* polar flagellum ..... 162
5.2.1.1 – Generation of the Bacterial two-hybrid system vectors ..... 162
5.2.1.2 – Interaction studies ..... 165
5.2.2 – The polar flagellar cap protein, FlaH, is not required for flagellin glycosylation ..... 169
5.2.3 – Flagellin swapping studies ..... 171
5.2.3.1 – Generation of pBBR1MCS-5 constructs containing *Aeromonas* flagellins ..... 171
5.2.3.2 – Analysis of pBBR1MCS-5_*flaA* constructs in *Aeromonas caviae* ..... 174
5.2.3.3 – Generation of pSRK(Gm) constructs containing *Aeromonas* flagellins ..... 174
5.2.3.4 – Analysis of pSRK_*flaA* constructs in *Aeromonas caviae* ..... 178
5.2.4 – *Helicobacter pylori* Maf studies ..... 181
5.2.4.1 – Generation of pSRK_*maf (H. pylori)* constructs ..... 181
5.2.4.2 - Analysis of pSRK_*maf (H. pylori)* constructs in *Aeromonas caviae* ..... 181
**5.3 – Discussion** ..... 188
**Chapter 6: General Discussion** ..... 197
**6.1 – General discussion of results** ..... 197
**6.2 – Future perspectives** ..... 201
6.2.1 – Short-term perspectives ..... 201
6.2.2 – Long-term perspectives ..... 203
**Chapter 7 - References** ..... 206
**Appendix** ..... 218
pSRK(Gm) ..... 218
pBBR1MCS-5 ..... 219
pGEM-T EASY ..... 219
BACTH vectors ..... 220
BACTH vector multiple cloning sites ..... 222

# Index to Figures


| | | |
|---|---|---|
| **Chapter 1** | **Introduction** | |
| **Figure 1.1** | Electron micrograph of *Aeromonas caviae* Sch3 | 7 |
| **Figure 1.2** | Schematic diagram of the bacterial flagellum | 11 |
| **Figure 1.3** | *Aeromonas caviae* Sch3 polar flagellin | 12 |
| **Figure 1.4** | Flagellar subunit export and assembly pathway | 15 |
| **Figure 1.5** | The major linkages formed during protein glycosylation | 20 |
| **Figure 1.6** | The structure of common nonulosonic acids | 23 |
| **Figure 1.7** | Polar flagella loci and glycosylation islands in *Aeromonas* species | 30 |
| **Figure 1.8** | Pseudaminic acid biosynthetic pathway in *Aeromonas caviae* Sch3 | 32 |
| **Chapter 2** | **Materials and Methods** | |
| **Figure 2.1** | Overlap extension PCR | 58 |
| **Chapter 3** | **AHA0618, a deglycosylase?** | |
| **Figure 3.1** | Alignment of AHA0618 and HP0518 | 71 |
| **Figure 3.2** | Alignment of YkuD superfamily proteins | 72 |
| **Figure 3.3** | The genetic context of *AHA0618* in the *A. caviae* Sch3 genome | 73 |
| **Figure 3.4** | Analysis of *A. caviae AHA0618* mutant swimming and swarming motility | 74 |
| **Figure 3.5** | Analysis of the growth of the *A. caviae AHA0618* mutant | 76 |
| **Figure 3.6** | Amplification of *AHA0618* from *A. caviae* Sch3 and insertion into pGEM-T EASY | 77 |
| **Figure 3.7** | Diagrammatic representation of the method used to clone *AHA0618* into pSRK(Gm) | 78 |
| **Figure 3.8** | Phenotypic analysis of the *A. caviae AHA0618* mutant containing pSRK_*AHA0618* | 80 |
| **Figure 3.9** | Phenotypic analysis of *A. caviae* Sch3 containing pSRK_*AHA0618* | 81 |
| **Figure 3.10** | Whole-cell Western blot analysis of *A. caviae* Sch3 and *AHA0618* mutant strains | 83 |
| **Figure 3.11** | Phenotypic analysis of the *A. caviae AHA0618* mutant containing pSRK_*HP0518* | 85 |
| **Figure 3.12** | Whole-cell Western blot analysis of the *A. caviae AHA0618* mutant containing pSRK_*HP0518* | 86 |
| **Figure 3.13** | Phenotypic analysis of *A. caviae* Sch3 containing pSRK_*HP0518* | 87 |
| **Figure 3.14** | Whole-cell Western blot analysis of *A. caviae* Sch3 containing pSRK_*HP0518* | 89 |
| **Figure 3.15** | LPS profile analysis of *A. caviae* Sch3 and *AHA0618* mutant strains | 90 |

| | | |
|---|---|---|
| **Figure 3.16** | Scanning electron microscopy analysis of *A. caviae* cell lengths | 92 |
| **Figure 3.17** | Fluorescence microscopy analysis of *A. caviae* cell lengths | 93 |
| **Figure 3.18** | Frequency distribution of the *A. caviae* cell lengths | 94 |
| **Figure 3.19** | HPLC analysis of peptidoglycan extracted from *A. caviae* Sch3 and the *AHA0618* mutant | 96 |
| **Chapter 4** | **Investigating the sites of *A. caviae* flagellin glycosylation** | |
| **Figure 4.1** | Flagella isolation | 105 |
| **Figure 4.2** | Percentage coverage of *A. caviae* flagellins detected via mass spectrometry | 106 |
| **Figure 4.3** | Fragmentation of the peptide backbone via CID and ETD-MS/MS | 108 |
| **Figure 4.4** | Manual analysis of FlaB peptide [146-173] in the CID-MS/MS spectra – Parker *et al.* (2014) | 110 |
| **Figures 4.5-4.9** | Analysis of the sites of glycosylation on the FlaB peptide [146-173] by CID-MS/MS | 115-120 |
| **Figures 4.10-4.17** | Analysis of the methylated flagellin peptides within the CID-MS/MS spectra | 121-128 |
| **Figure 4.18** | Swimming motility analysis of an *A. caviae flaAB* mutant containing pBBR1MCS-5_*flaB* | 130 |
| **Figure 4.19** | Diagrammatic representation of the method used to clone *flaB* (and the *flaB* site-directed mutants) into pBBR1MCS-5 | 131 |
| **Figure 4.20** | Analysis of FlaB(T155A) in the *A. caviae flaAB* mutant | 134 |
| **Figure 4.21** | Analysis of FlaB(S159/161A) in the *A. caviae flaAB* mutant | 135 |
| **Figure 4.22** | Analysis of FlaB(S167/169A) in the *A. caviae flaAB* mutant | 136 |
| **Figure 4.23** | Analysis of FlaB(S159/161/167/169A) in the *A. caviae flaAB* mutant | 137 |
| **Figure 4.24** | Western blot analysis of the FlaB site-directed mutants in the *A. caviae flaAB* mutant | 139 |
| **Figure 4.25** | The level of FlaB site-directed mutants in *A. caviae* whole-cell samples (densitometry) | 140 |
| **Figure 4.26** | The hydrophobic amino acids in *A. caviae* Sch3 FlaB | 144 |
| **Figure 4.27** | Analysis of FlaB(L160A) in the *A. caviae flaAB* mutant | 146 |
| **Figure 4.28** | Analysis of FlaB(I168A) in the *A. caviae flaAB* mutant | 147 |
| **Figure 4.29** | Analysis of FlaB(S208/210A) in the *A. caviae flaAB* mutant | 148 |
| **Figure 4.30** | Western blot analysis of the FlaB (L160A; I168A and S208/210A) site-directed mutants in the *A. caviae flaAB* mutant | 149 |
| **Figure 4.31** | Predicted three-dimensional structure of FlaB from *A. caviae* Sch3 | 154 |
| **Chapter 5** | **Investigations into Maf1-dependent flagellin glycosylation** | |
| **Figure 5.1** | The principle of the bacterial two-hybrid system | 163 |

| | | |
|---|---|---|
| **Figure 5.2** | Analysis of the flagellin in an *A. caviae flaH* mutant | 170 |
| **Figure 5.3** | Alignment of the flagellins from *Aeromonas* species | 172 |
| **Figure 5.4** | Motility analysis of an *A. caviae flaAB* mutant expressing heterologous *Aeromonas* flagellins (in pBBR1MCS-5) | 175 |
| **Figure 5.5** | Western blot analysis of whole-cell *A. caviae* expressing heterologous *Aeromonas* flagellins (in pBBR1MCS-5) | 176 |
| **Figure 5.6** | Western blot analysis of supernatant *A. caviae* expressing heterologous *Aeromonas* flagellins (in pBBR1MCS-5) | 177 |
| **Figure 5.7** | Motility analysis of an *A. caviae flaAB* mutant expressing heterologous *Aeromonas* flagellins [in pSRK(Gm)] | 179 |
| **Figure 5.8** | Western blot analysis of *A. caviae* expressing heterologous *Aeromonas* flagellins [in pSRK(Gm)] | 180 |
| **Figure 5.9** | The polar flagellar and glycosylation loci of *H. pylori* | 182 |
| **Figure 5.10** | Motility analysis of *A. caviae* Sch3 expressing *H. pylori maf1* | 183 |
| **Figure 5.11** | Western blot analysis of *A. caviae* flagellins when strains are expressing *H. pylori maf1* | 185 |
| **Figure 5.12** | Motility analysis of *A. caviae* Sch3 expressing *H. pylori maf2* | 186 |
| **Figure 5.13** | Western blot analysis of *A. caviae* flagellins when strains are expressing *H. pylori maf1* | 187 |
| **Figure 5.14** | A model of the flagellin glycosylation pathway in *A. caviae* Sch3 | 191 |
| **Figure 5.15** | Alignment of FlaA from *A. caviae* Sch3 and *H. pylori* 26995 | 194 |

# Index to Tables


| | | |
|---|---|---|
| **Chapter 2** | **Materials and Methods** | |
| **Table 2.1** | Strains | 36 |
| **Table 2.2** | Plasmids | 37 |
| **Table 2.3** | Media | 42 |
| **Table 2.4** | Antibiotics | 42 |
| **Table 2.5** | Solutions and Buffers | 43 |
| **Table 2.6** | Primers | 50 |
| **Chapter 4** | **Investigating the sites of *A. caviae* flagellin glycosylation** | |
| **Table 4.1** | Glycopeptides observed in the CID-MS/MS spectra | 113 |
| **Table 4.2** | Summary of the primers used to create the FlaB site-directed mutants | 132 |
| **Chapter 5** | **Investigations into Maf1-dependent flagellin glycosylation** | |
| **Table 5.1** | A summary of the primers used to amplify the genes for insertions into the bacterial two-hybrid vectors | 164 |
| **Table 5.2** | A summary of all the bacterial two-hybrid interactions analysed | 166 |
| **Table 5.3** | Summary of the bacterial two-hybrid interaction results | 168 |
| **Table 5.4** | Flagellin swapping gene and primer information | 173 |

# Chapter 1: Introduction

## 1.1 – The genus *Aeromonas*

The genus *Aeromonas* belongs to the family *Aeromonadaceae* (similar to *Vibrionaceae*), along with fellow genera *Tolumonas* and *Oceanomonas*, within the class of Gammaproteobacteria (Janda and Abbott, 2010). The genus consists of 25 species of Gram-negative, facultative anaerobic, rod-shaped bacteria that are ubiquitous in nature, but are generally associated with fresh or brackish water. They can be placed into two main groups, one being the motile mesophilic aeromonads that have optimal growth at temperatures between 30 and 37°C, and the other being the non-motile psychrophilic aeromonads (ie. *Aeromonas salmonicida*) that grow optimally between 22 and 28°C (Janda and Abbott, 2010; Parker and Shaw, 2011).

### 1.1.1 – Host interactions

Aeromonads are associated with disease in a variety of hosts, with the psychrophilic *A. salmonicia* subsp. *salmonicida* being a particular problem in fish disease (Beaz-Hidalgo and Figueras, 2013). *A. salmonicida* is able to cause the ulcerative disease, furunculosis, in economically important fish, such as: Atlantic salmon, channel catfish, halibut, turbot, Atlantic cod and many more, making it a problem in aquaculture worldwide (Beaz-Hidalgo and Figueras, 2013).

Mesophilic aeromonads are also able to cause fish disease, the infection of which displays similar symptoms to furunculosis and is known as 'motile *Aeormonas* septicaemia'. *A. hydrophila* has always been considered the main mesophilic aeromonad responsible for these infections, however, it is now clear that due to inaccurate identification methods the presence of this aeromonad has been overestimated (Beaz-Hidalgo *et al.*, 2010). Other mesophilic aeromonads have now been isolated from a variety of fish infections with the most prevalent being: *A veronii, A. sobria, A. bestiarum, A. piscicola* (Beaz-Hidalgo *et al.*, 2010; Beaz-Hidalgo and Figueras, 2013). Ultimately many infections result in fish death which has caused major financial losses in fish farming and any infected fish that are ingested have the potential to infect the recipient and cause further spread of disease.

Furthermore, mesophilic aeromonads are associated with human infections, such as gastrointestinal disease, as well as less common extraintestinal disease (wound and burn infections), in both immunocompromised and immunocompetent individuals (Parker and Shaw, 2011). Previously, misidentification of *Aeromonas* isolates led to *Aeromonas hydrophila* again to be thought of as one of the more important species linked with human disease;

however, it is now accepted that a number of other mesophilic aeromonads are able to cause disease, with *Aeromonas caviae, A. veronii* and *A. hydrophila*, being the most frequently isolated from patients, and therefore the most clinically significant (Janda and Abbott, 2010; Lowry *et al.*, 2014a; Parker and Shaw, 2011). Animal studies have shown that these species persistently colonise immunocompromised mice compared to other mesophilic *Aeromonas* species (Lye *et al.*, 2007).

Gastrointestinal diseases, such as gastroenteritis and traveller's diarrhoea (Vila *et al.*, 2003), are the most common diseases associated with *Aeromonas* infections, especially in the very young and usually in warmer months of the year. Early studies by Namdari and Bottone (1990) found *A. caviae* to be the sole pathogen isolated from 82% of paediatric patients studied, who showed symptoms such as watery diarrhoea, and Wilcox *et al.* (1992) also found *A. caviae* to be a particular pathogen isolated from children showing signs of gastroenteritis. Other studies, such as Guerra *et al.* (2007) from South Brazil, have shown *A. hydrophila* to be the most frequently isolated aeromonad in diseases connected with acute diarrhoea, but agree that prevalence is especially high in children.

*Aeromonas* species have also been found to infect wounds in both healthy individuals and those with underlying health problems. These infections usually occur when an individual is injured in an aquatic environment, and can lead to mild cellulitis, or more serious diseases such as necrotising fasciitis, which can result in mortality (Parker and Shaw, 2011). Although mesophilic aeromonads are generally associated with enteric disease, their widespread involvement in wound infections is becoming clear; for example *Aeromonas* species were the most commonly isolated organisms from soft tissue and skin infections from survivors of the 2004 Thailand tsunami (Hiransuthikul *et al.*, 2005), and *A. hydrophila* has been isolated from the wound infections from a number of animal-bite survivors around the world (bear, crocodile, alligator, shark, tiger) (Abrahamian and Goldstein, 2011; Easow and Tuladhar, 2007). Furthermore, a nationwide study of *Aeromonas* infections in France over a six month period also found wound infections to be the most common diseases linked with mesophilic aeromonads (Lamy *et al.*, 2009). Additionally, *Aeromonas* infections of burns can occur, but are extremely rare, and these microorganisms are often overlooked as causative agents when treating patients. However they have been known to occur, especially after a burnt individual has been exposed to contaminated water or soil (Barillo *et al.*, 1996; Kienzle *et al.*, 2000; Ribeiro *et al.*, 2010).

As well as aeromonads having a detrimental effect in their host, their colonisation can also be beneficial, where the bacterium and host live together in a symbiosis. For example, *Aeromonas*

species, in particular *A. veronii*, have been identified as symbionts of the medicinal leech gut (Nelson and Graf, 2012). It has been suggested that aeromonads may be able to utilise nutrients released from other leech gut symbionts (a *Rikenella*-like bacterium) (Bomar *et al.*, 2011) and in return, aeromonads may protect the leech from colonisation by pathogenic microorganisms, aid in the digestion of a blood meal or provide optimal nutrition for the leech with the release of nutrients (Bomar *et al.*, 2011; Nelson and Graf, 2012; Silver *et al.*, 2007). Furthermore, studies by Osei-Poku *et al.* (2012), have demonstrated that *Aeormonas* spp. are the most prevalent bacteria in the gut microbiota of wild Kenyan mosquitoes (around one third of the bacteria present).

Therefore it is clear that aeromonads have the ability to colonise a wide variety of environments, under many different circumstances, and can adapt to interact with their hosts in multiple ways.

## 1.1.2 – Colonisation factors

There are a number of virulence and colonisation factors that allow aeromonads to persist in their specific niche, and for clinically relevant species to allow them to infect their hosts. These consist of secreted factors that are exported via specific secretion systems and cause toxicity; and adherence factors, such monomeric proteins and appendages on the cell surface that are involved in motility and host cell interactions (Lowry *et al.*, 2014a; Tomas, 2012).

### 1.1.2.1 – Secreted factors

Secreted virulence determinants are exported via one of the five secretion systems that have been identified in aeromonads, out of the six that are currently known about in Gram negative bacteria (Type 1, 2, 3, 4 and 6). Very little is known about the type 1 secretion system and its effector proteins in aeromonads, however the type 2 system, which has so far only been studied in *A. hydrophila*, is thought to export proteins such as: haemolysin, amylases, proteases and DNases (Li *et al.*, 2011; Seshadri *et al.*, 2006); homologues of this system have also been identified in the genomes of other *Aeromonas* species, such as the psychrophilic *A. salmonicida* subspecies *salmonicida* (Reith *et al.*, 2008). The type 4 system is able to conjugally transfer DNA to other aeromonads, as well as transport effector proteins into host cells, and it is therefore thought to be responsible for the spread of antibiotic resistance amongst strains (Rangrez *et al.*, 2006).

In particular, type 3 and type 6 secretions systems (T3SS and T6SS respectively), which are both able to transfer virulence determinants directly into target eukaryotic cells, are involved in pathogenicity.

In the T3SS (the injectosome), five effectors proteins have so far been identified. Two of which are the ADP-ribosylating toxins: AexT (present in *A. salmonicida*) (Dacanay *et al.*, 2006; Reith *et al.*, 2008) and AexU (identified in *A. hydrophila*) (Sha *et al.*, 2007; Sierra *et al.*, 2007), that are able to disrupt the host cytoskeleton, leading to apoptosis. These proteins are directly involved in colonisation and infection as mutational studies have demonstrated that *aexT* deficient *A. salmonicida* subsp. *salmonicida* were unable to induce toxicity in a fish cell-line (RTG-2) (Braun *et al.,* 2002). Additionally, an *A. hydrophila aexU* mutant was found to be less virulent than the wild type when infection studies were carried out in a mouse model (Sha *et al.*, 2007).

The final three effectors of the T3SS are: AopH (tyrosine phosphatase), AopO (serine/threonine kinase) and AopP (NFκB inhibitor), which are likely to disrupt host-cell signalling pathways, and have also been identified in *A. salmonicida* species (Dacanay *et al.*, 2006; Reith *et al.*, 2008).

The T6SS has been studied in clinical isolate of *A. hydrophila*, and has so far been found to export four effector proteins (Suarez *et al.*, 2008; Suarez *et al.*, 2010). One of these proteins is the haemolysin coregulator protein (Hcp) which is thought to be involved in preventing the bacterium being phagocytosed by host macrophages and is also able to induce apoptosis in host cells (Suarez *et al.*, 2008). The other virulence determinants identified of this secretion system are: Vgr1, 2 and 3; and so far only the role of Vgr1, an ADP-ribosylating toxin, has been determined (Suarez *et al.*, 2008; Suarez *et al.*, 2010).

#### 1.1.2.2 – Adherence factors

Aeromonads also possess many adherence factors on their cell surfaces (filamentous and non-filamentous) that contribute to colonisation and host infection. For example, the lipopolysaccharide (LPS) O-antigen (O-Ag) has been shown to be important for aeromonad adherence and virulence, with mutational studies in *A. piscicola* AH-3 (previously classified as *A. hydrophila*) serotype O:34 demonstrating that strains unable to produce the O-Ag have an impaired ability to adhere to Hep-2 cells and are less virulent in fish and mice compared the wild type (Canals *et al.*, 2006b). In addition, a number of outer-membrane proteins (OMPs) are also important in *Aeromonas* spp. for adherence to target cells. VapA is the most abundant OMP, making up the S-layer, which is a crystallised layer of proteins covering the entire bacterium (Lowry *et al.*, 2014a). In species that can produce an S-layer, VapA makes up a substantial amount of their outer-membrane protein content (up to 60%). Studies in *A. salmonicida* have shown that VapA is directly associated with black rockfish colonisation, and have provided evidence that the S-layer here may be involved in host immune evasion, as the strains studied were able to evade opsonisation (Han *et al.*, 2011). Furthermore, in the absence of filamentous adhesins, a 43 kDa OMP protein has also been found to be important

for the adherence of *A. caviae* strains to Hep-2 cells (Rocha-De-Souza *et al.*, 2001), demonstrating that there are many factors that can contribute to *Aeromonas* colonisation. It is unknown as to why some *Aeromonas* strains are more pathogenic than others; intruigingly, a new set OMP proteins, which show homology to the Lig invasins in highly pathogenic *Leptospira* species (Cerqueira *et al.*, 2009; Choy *et al.*, 2007), have been identified in the genomes of *A. caviae* (Sch3) (Shaw unpublished) and *A. hydrophila* (ATCC 7966) (Seshadri *et al.,* 2006). These Lig proteins are currently unstudied in *Aeromonas* but are characteristic of extremely virulent *Leptospira* species, and therefore may be the reason why some mesophilic aeromonads are more invasive than others (Cerqueira *et al.,* 2009; Choy *et al.,* 2007).

Filamentous adhesins, such as pili are also involved in aeromonad colonisation. The type 4 MSHA (mannose-sensitive haemagglutinin)-like pilus, in particular, has a major role in mesophilic aeromonad adherence, and is also involved in biofilm formation (Hadi *et al.*, 2012). Pili are also present in psychrophilic aeromonads, and although they have a role in adherence, they are not essential for colonisation (Boyd *et al.*, 2008).

Flagella are also filamentous appendages on the bacterial cell surface, primarily allowing bacterial motility through aqueous environments, or movement across solid surfaces. Around 60% of mesophilic aeromonads, such as clinically relevant *A. hydrophila* and *A. caviae* species, possess dual flagella systems; a constitutively expressed polar flagellum, for motility in liquid environments (Fig. 1.1), and inducible peritrichous flagella (lateral flagella) for movement across solid surfaces (Gavin *et al.*, 2002; Kirov *et al.*, 2002; Rabaan *et al.*, 2001). Flagella are not only required for motility but also have an important role in cellular adherence (Haiko and Westerlund-Wikstrom, 2013), with mutational studies with *A. caviae* establishing that both flagella systems participate in the adherence and invasion of Hep-2 cells (Gavin *et al.*, 2002; Rabaan *et al.*, 2001).

Some *Aeromonas* species, such as *A. caviae* and *A. hydrophila*, are also able to post-translationally modify some of their surface proteins with sugar groups. One example of which is the O-linked glycosylation of the polar flagellins, which are the main component of the polar flagellar filament. Studies carried out in *A. caviae* and *A. hydrophila* have demonstrated that this modification is essential for the production of a functional flagellar filament (Canals *et al.*, 2006c; Canals *et al.*, 2007; Parker *et al.*, 2012; Tabei *et al.*, 2009), and therefore has implications in aeromonad virulence; although the precise role of glycosylation remains unclear. The pathway of flagellin glycosylation in *A. caviae* Sch3 is particularly intriguing as it possesses the smallest set of genes required for flagellin glycosylation currently identified in bacteria (Tabei *et al.*, 2009).

This chapter will focus on polar flagellar-mediated motility of *Aeromonas* spp. and the glycosylation of bacterial surface proteins (in particular the flagellins).

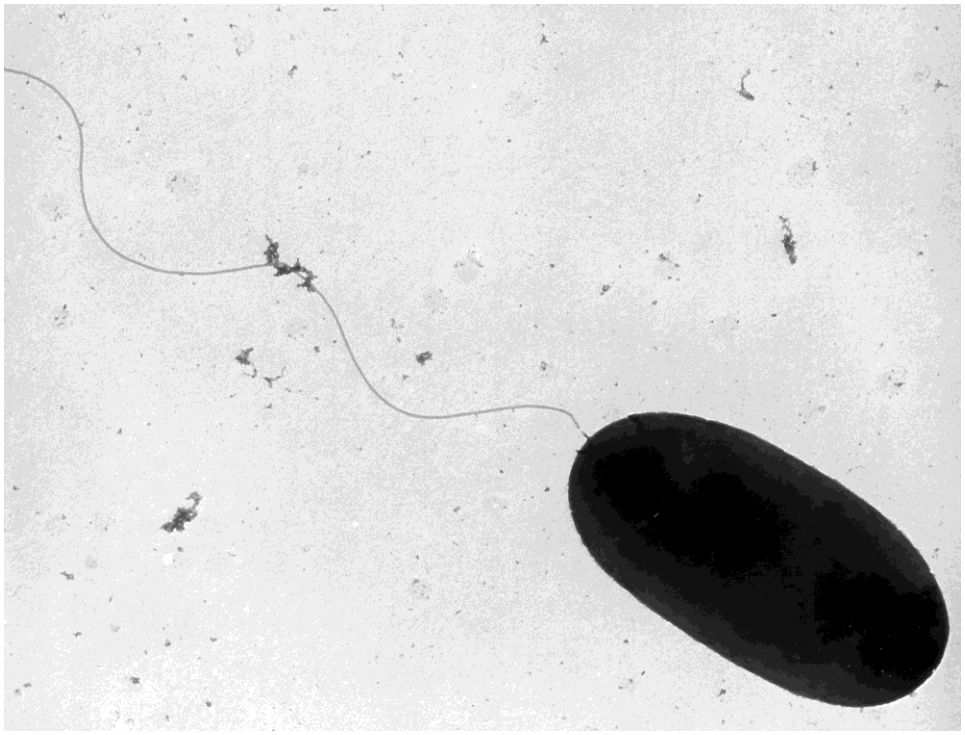

(Parker & Shaw, 2011)

**Figure 1.1** – A transmission electron micrograph from Parker & Shaw (2011) displaying *Aeromonas caviae* Sch3 and its constitutively expressed polar flagellum.

## 1.2 – *Aeromonas* motility

### 1.2.1 – Polar Flagellum

The polar flagellum in mesophilic aeromonads (Fig. 1.1) is constitutively expressed, unsheathed and encoded for by over 50 genes within five gene clusters in the genome (Lowry *et al.*, 2014a). This flagellum is required for motility in aqueous environments, and through the process of chemotaxis allows the movement towards nutrients and away from less desirable locations (Baker *et al.*, 2006; Terashima *et al.*, 2008). During chemotaxis, chemical gradients are sensed through transmembrane receptors called methyl-accepting proteins (MCPs), which transmit these signals to the Che proteins in the bacterial cytoplasm; the Che proteins then act to alter flagellar rotation in response to attractant levels through binding to the flagellar motor (Baker et al., 2006). This allows bacteria to move in a 'random biased walk' with a series of runs and tumbles. Chemotaxis has been extensively studied in *E. coli* which possesses peritrichous flagella. During runs, flagella rotate anticlockwise allowing the peritrichous arrangement to form a bundle at one pole of the cell which acts to push the bacterial cell forward. In order to change direction, the cells have to stop, or 'tumble', before setting off on another run; this is achieved by the chemotactic machinery signalling to the flagellar motor to change direction (clockwise rotation) which disrupts the bundle formation (Baker et al., 2006). Mesophilic aeromonads, however, possess only a single polar flagellum and therefore do not run and tumble by the same mechanisms due to their inability to form flagellar bundles. Although unstudied in *Aeromonas*, chemotaxis is likely to show similarity to the well-studied system in the polar flagellated bacterium *Rhodobacter sphaeroides* (Porter *et al.*, 2008). Here instead of altering the direction of flagellar rotation, the chemotactic system acts to stop the flagellar motor in order for the bacterium to tumble and reorient themselves before setting off on another run (Porter *et al.*, 2008).

The flagellum is made of three major components: the basal body, the hook and the flagellar filament (Fig. 1.2). The basal body spans the bacterial cell envelope and is composed of the rod and a series of rings (Fig. 1.2), within which resides a motor (made up of a stator and a rotor for flagellar rotation) and a narrow channel of around 2 nm (rod) which allows the export of unfolded flagellar subunits for the assembly of this nanomachine. The cytoplasmic ring (C-ring) is located within the bacterial cell and is composed of FliG, FliM and FliN, which together make up the rotor component of the flagellar motor. This part of the motor is also what controls flagellar rotation, and so responds to signals from the bacterial chemotactic system (Roberts *et al.*, 2010). The other component of the motor, the stator, is produced from four proteins in *Aeromonas* spp.: PomA and PomB (which are paralogs of MotA and MotB from *E. coli* and

*Salmonella*); and MotX and MotY, which are not present in *E. coli* and *Salmonella* systems, but are present in other bacteria such as *Vibrio* spp. MotX and MotY have been found to form a new ring, named the T-ring, in the polar flagellar basal body of *Vibrio spp.*, located below the periplasmic ring (P-ring, discussed below) (Molero *et al.*, 2011; Terashima *et al.*, 2006; Wilhelms *et al.*, 2009). The T-ring was found to be essential for incorporating the stator into the basal body (Terashima *et al.*, 2006). The rotor and stator components of the motor work together to harness the electrochemical energy of a proton or ion-motive force and generate torque; this then drives the rotation of the bacterial flagellum (Sowa and Berry, 2009). In the case of the *Aeromonas* polar flagellum, a sodium ion gradient is utilised. It is thought that the ions bind to the stator, and induce a conformational change which is then conferred to the rotor, allowing flagellar rotation (Sowa and Berry, 2009; Xing *et al.*, 2006). In addition, some aeromonads also appear to have two sets of Pom proteins (PomAB and $PomA_2B_2$), with studies in *A. piscicola* AH-3 demonstrating that only one set are required for motility in liquid culture (Wilhelms *et al.*, 2009). However, it was observed that $PomA_2B_2$ are more sensitive to lower sodium ion concentrations (Wilhelms *et al.*, 2009).

The C-ring is then linked to the membrane-supramembrane ring (MS-ring), which the rod is anchored to (Fig. 1.2). In Gram negative bacteria two further rings are present, the peptidoglycan ring (P-ring) and the lipopolysaccharide ring (L-ring), which allow the rod to penetrate the bacterial cell wall (Fig. 1.2) (Chevance *et al.*, 2007).

Attached to the rod is the hook, or the universal joint, which provides a flexible link from the engine of the flagellum to the helical flagellar filament, enabling work from the motor to be transmitted to the propeller (Fig. 1.3) (Samatey *et al.*, 2004). The hook allows different flagellar arrangements, such as peritrichous or lophotrichous flagella, to function correctly as a bundle (Terashima *et al.*, 2008).

The flagellar filament is joined to the hook via hook-filament junction proteins, and extends 15-20 µm from the cell surface (Samatey *et al.*, 2001; Yonekura *et al.*, 2003). It is created from thousands of monomer proteins (flagellins) which polymerise to form a helical, hollow tube that has a filament diameter of around 12-25 nm and a lumen diameter of around 2 nm (Fig. 1.2) (Samatey *et al.*, 2001; Yonekura *et al.*, 2003). A cap protein is also present at the tip of the filament (known as FlaH in aeromonads) and is required for the efficient polymerisation of the flagellins (Fig. 1.2) (Yonekura *et al.*, 2000). Cap proteins are also present in the early stages of flagellar assembly to control rod and hook formation. A dedicated T3SS, located within the basal body, is responsible for the export of all subunits of the bacterial flagellum.

The aeromonad polar flagellar filament is generated from the copolymerisation of two flagellins, FlaA and FlaB (Fig. 1.3); no dominant flagellin is present in this system as a mutation in one flagellin gene does not abolish motility, but instead mutants are able to form normal flagellar filaments from the remaining flagellin and display only slightly impaired motility (Rabaan *et al.*, 2001). This differs to other polar flagellated bacteria, such as *H.* pylori, that form flagella from two flagellin subunits which are present in the filament in different amounts (Kostrzynska *et al.*, 1991). The minor flagellin, FlaB, makes up the proximal end of the filament (close to the basal body), whereas the major subunit, FlaA, forms the majority of the filament and is necessary for the formation of a functional flagellum (Kostrzynska *et al.,* 1991). The stoichiometry of FlaA and FlaB in the flagellar filament of *Aeromonas*, however, is currently unknown.

Flagellin monomers are composed of three domains: the N-terminal domain which may contain a signal for protein export, a central D2/D3 region which is variable and is also glycosylated in a number of aeromonads, and the chaperone binding domain (CBD) which is essential for flagellin recognition by the flagellin-specific chaperone, FlaJ (Parker *et al.*, 2014). It has also been found that the D0 regions of the flagellins are directly involved in Toll-like receptor 5 (TLR-5) recognition of the flagellins by the host innate immune system (Fig. 1.3) (Hayashi *et al.*, 2001).

As previously mentioned, some mesophilic aeromonads (such as *A. caviae* and *A. hydrophila*) post-translationally modify their flagellins on their D2/D3 domains, through the *O*-linked glycosylation of serine or threonine residues with nonulosonate sugars. This modification is essential for aeromonad flagellar assembly and motility (Canals *et al.*, 2006c; Canals *et al.*, 2007; Parker *et al.*, 2012; Tabei *et al.*, 2009) and is also important for the flagellation of a number of other pathogenic bacteria, such as *Helicobacter* and *Campylobacter* spp. (Josenhans *et al.*, 2002; Schirm *et al.*, 2003; Thibault *et al.*, 2001). Bacterial protein glycosylation will be discussed in sections 1.3 and 1.4 in more detail, with a focus on *O*-linked glycosylation.

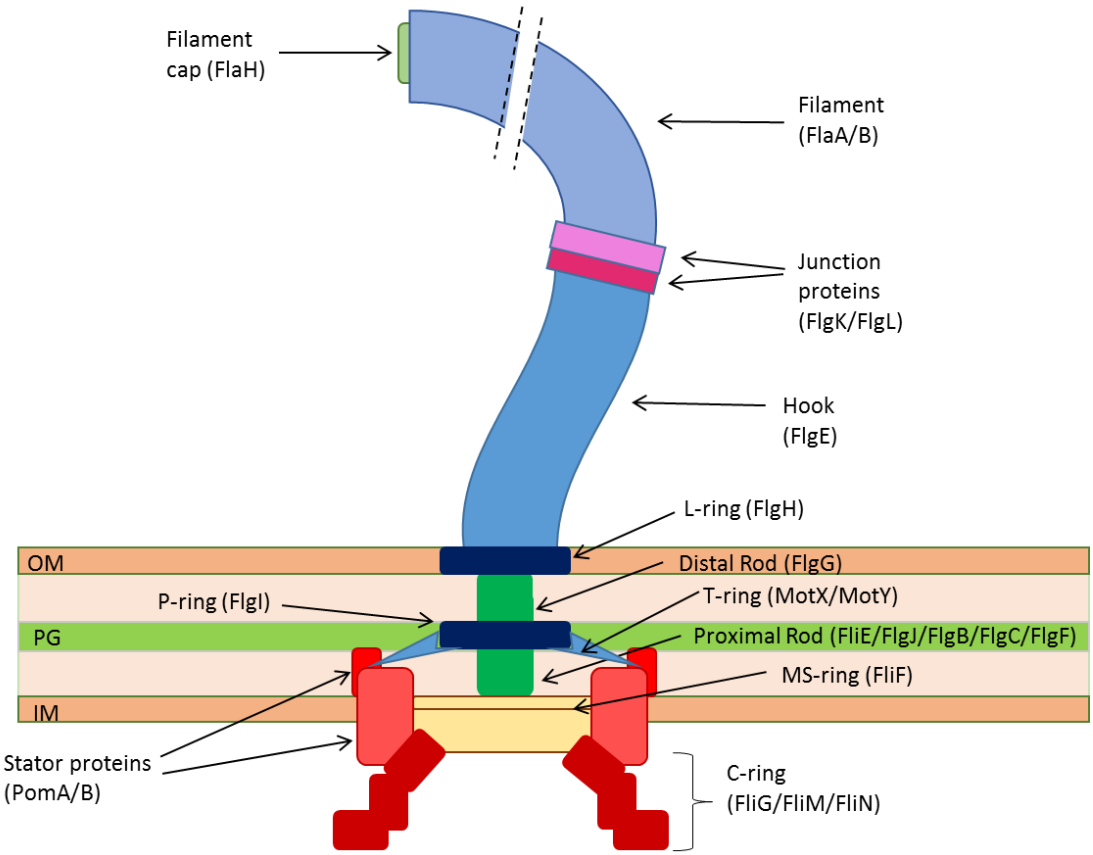


**Figure 1.2** – A schematic diagram of the bacterial flagellum, displaying the proteins present in the *Aeromonas* polar flagellum. OM = outer membrane; PG = peptidoglycan; IM = inner membrane.

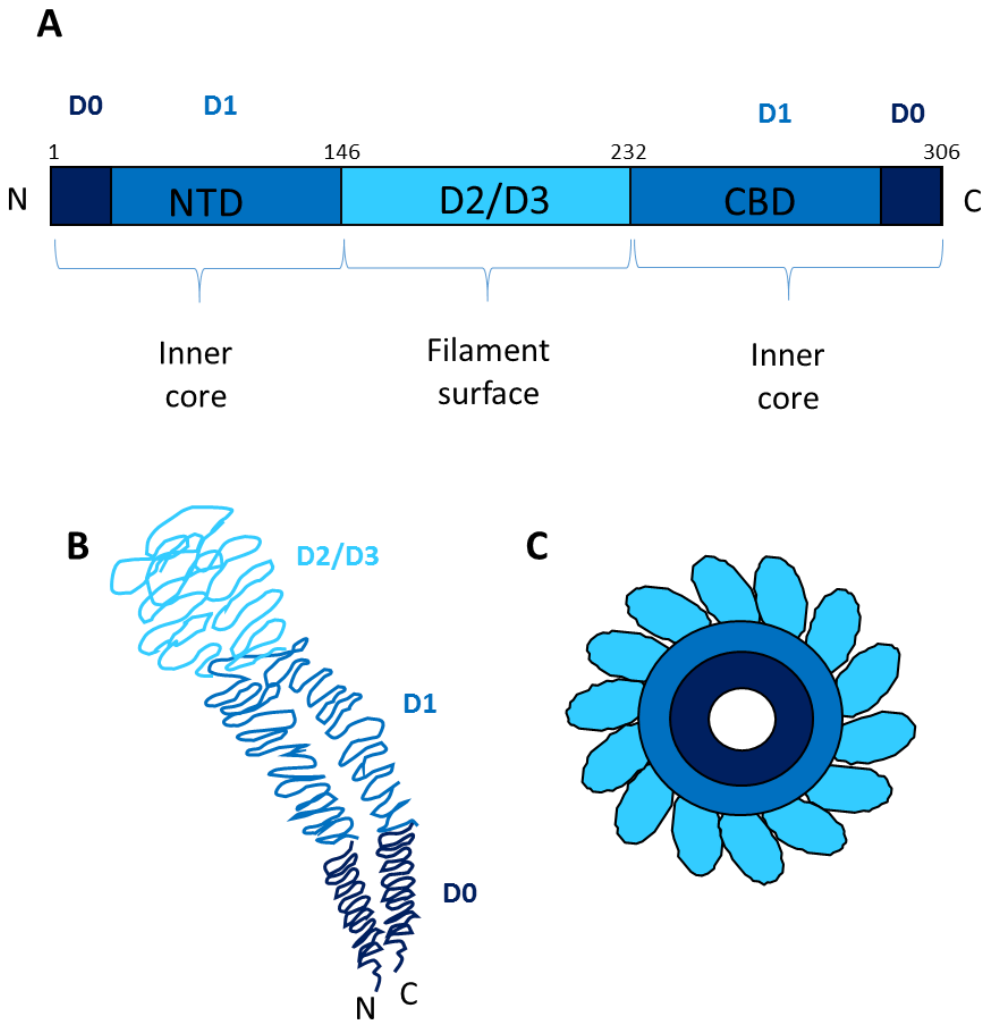


**Figure 1.3** – (**A**) This diagram depicts unfolded FlaA and its major domains from *Aeromonas* caviae Sch3: the N-terminal domain (NTD) (from amino acids around 1-146), the central D2/D3 domain (from amino acids around 146-232) and the chaperone binding domain (CBD) (from amino acids around 232-306). FlaA is 31.8 kDa (when post-translational modifications are not taken into account) composed of 306 amino acids. FlaB shows similar domains, however, contains 305 amino acids resulting in a 31.7 kDa protein when post-translational modifications are taken into account. (**B**) Diagrammatic representation of a flagellin monomer once it has folded. (**C**) A cross-section of the bacterial flagellum and where the D0, D1, D2 and D3 regions of the flagellins reside once they are incorporated into the flagellar filament. The D0 and D1 regions form the filament core, whereas the D2 and D3 regions form the filament surface.

## 1.2.2 – Lateral Flagella

The inducible, lateral flagellar system, which is found in a peritrichous arrangement around the bacterial cell, allows aeromonad movement in environments where the polar flagellum cannot function effectively; such as for movement across solid surfaces or through viscous solutions (Kirov *et al.*, 2002). Dual flagellar systems are also found in a number of other bacteria, but those found in *Aeromonas* species show most similarity to the systems described for *V. parahaemolyticus*, whose polar and lateral flagella are entirely distinct (Stewart and McCarter, 2003). Lateral flagella synthesis is regulated in response to environmental conditions, with the induction of gene expression being mainly associated with growth in viscous solutions or on solid surfaces (Kearns, 2010; Kirov *et al.*, 2002); however, the precise mechanisms of how bacteria sense surfaces and transduce these signals through their cell envelopes to affect gene expression is poorly understood (Kearns, 2010). One theory from early work in *V. parahaemolyticus* is that the polar flagellum is a mechanosensor, and when its movements are restricted from coming into contact with a surface this may alter the ion flux through the flagellar motor which the bacterial cell could then sense, and, in turn, alter lateral flagellar gene expression (Kawagishi *et al.*, 1996). Expression of the genes associated with polar and lateral flagellar systems have previously been linked in *V. parahaemolyticus*, as constitutive expression of lateral flagella occurs when there are defects in the polar flagellum (McCarter *et al.*, 1988). This is not the case in *Aeromonas* however, and so how they sense their environment, and coordinate polar and lateral gene expression, may differ (Altarriba *et al.*, 2003; Canals *et al.*, 2006a). The lateral flagellar system has been well studied in *A. piscicola* AH-3, which possesses 38 genes, known as the *laf* genes, in a single region of the chromosome required for lateral flagellar assembly (Canals *et al.*, 2006a).

Lateral flagella are formed from a T3SS system, similarly to the polar flagellum, and the filaments are unsheathed and produced from repeating units of the flagellin, LafA. However, in some aeromonads, such as *A. caviae* Sch3, two flagellins have been identified (similarly to in the polar system), known as LafA1 and LafA2 (Gavin *et al.*, 2002). In contrast to the polar system, the lateral system makes use of a proton motive force (pmf) for flagellar rotation, and therefore possesses a different stator complex, LafT and LafU (Gavin *et al.*, 2002; Wilhelms *et al.*, 2009).

There is also some evidence to suggest that the lateral flagellins may also be glycosylated (Wilhelms *et al.*, 2012), which will be further discussed in section 1.4.

## 1.2.3 – Export and assembly

The bacterial flagellum is assembled by the ordered export of its subunits through a dedicated T3SS (apart from the P and L-rings which are exported by the sec system) (Evans *et al.*, 2014). The export and assembly process has been most studied in *E. coli* and *Salmonella*, and involves subunits meeting at the export apparatus located at the base of the flagellum (Evans *et al.*, 2014). Subunits are exported in an unfolded state and these initial stages of export are energised by ATP hydrolysis and the pmf (Minamino and Namba, 2008). The transmembrane domains of six proteins: FlhA, FlhB, FliO, FliP, FliQ and FliR, all form the export gate, which resides below the MS-ring and extrudes into the cytoplasm (Fig. 1.4) (Chen *et al.*, 2011). This export gate can transition from an open and closed state, by aligning with the pore of the MS-ring when export is triggered. Below the export gate, the cytoplasmic domain of FlhA ($FlhA_c$) forms a homononomeric ring, which forms a platform connected to the export gate via the linker regions between the two FlhA domains (Fig. 1.4) (Abrusci *et al.*, 2013; Chen *et al.*, 2011). The export gate, together with the $FlhA_c$ platform, forms an 'export cage'. Furthermore, located below the export cage, is an ATPase complex which is anchored to the C-ring of the basal body (Evans *et al.*, 2014). This complex is formed from the homohexameric association of the ATPase, FliI, and two other proteins: FliJ (the central ATPase stalk) and FliH (the stator for anchoring the ATPase complex) (Abrusci *et al.*, 2013; Evans *et al.*, 2014; Ibuki *et al.*, 2011). It is thought that when active, the stalk of the ATPase spans the gap between itself and the export cage, interacting with the $FlhA_c$ homononomeric ring to allow the next stages of subunit export to occur (Abrusci *et al.*, 2013; Fraser *et al.*, 2003a).

Bacterial flagellar assembly is an ordered process, with early subunits, such as the rod and hook proteins, being required first, and the late subunits, such as the proteins for filament assembly, being required after. It is thought that both of these pathways, for the early and late subunits, are targeted to the ATPase (partially due to export sequences in the N –terminal regions of the subunits), before being presented to $FlhA_c$ of the export cage (Stafford *et al.*, 2007), due to interactions with FliJ of the ATPase complex with $FlhA_c$ (Abrusci *et al.*, 2013; Fraser *et al.*, 2003b). Ordered assembly at the $FlhA_c$ complex occurs, in part, due to chaperones and their subunits having different affinities for the hydrophobic pocket of $FlhA_c$ (Kinoshita *et al.*, 2013). This is therefore thought to allow the export of the junction and cap proteins before the flagellins, which in turn allows the efficient polymerisation of the flagellar filament which requires the cap protein to be present (Yonekura *et al.*, 2000).

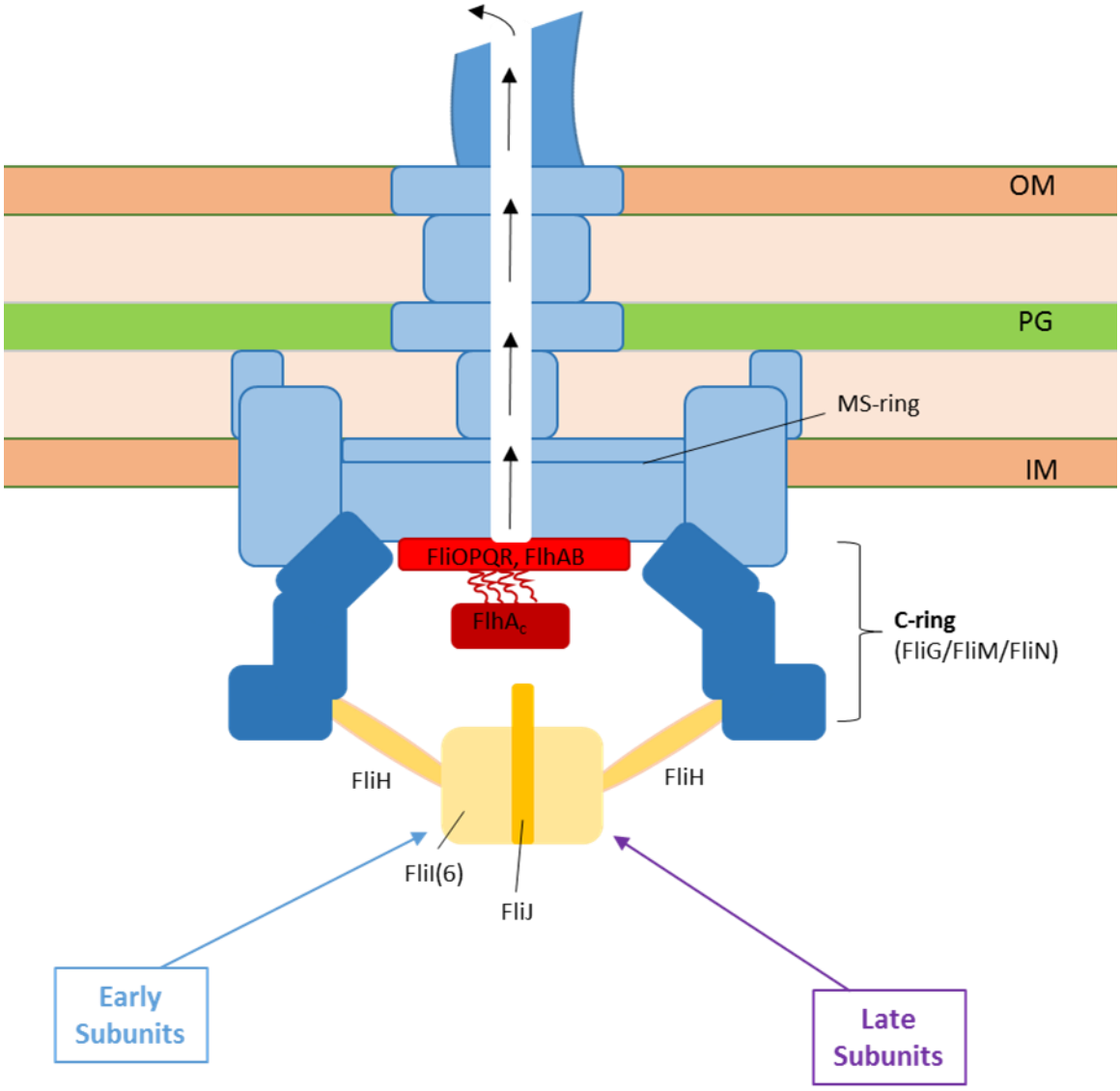


**Figure 1.4** – A schematic diagram of the export apparatus of the bacterial flagellum, displaying the export cage (FliOPQR, FlhAB) and the ATPase complex (FliHIJ), which are involved in subunit sorting, docking and export at the base of the flagellum. OM = outer membrane; PG = peptidoglycan; IM = inner membrane.

The details of the complete export process are not fully understood, however, it is known that the next stage of subunit export requires recruitment to FlhB of the export gate. This protein has a role in switching the specificity of the export gate, from the export of the early subunits, to export of the late subunits (Ferris and Minamino, 2006). FlhB is composed of a transmembrane and a cytoplasmic domain, connected via a flexible linker region. It is within this linker that FlhB undergoes cleavage essential for the export of the later subunits of the flagllum (Ferris *et al.*, 2005; Fraser *et al.*, 2003b). Mutational studies whereby FlhB can no longer undergo autocleavage locks the system for the permanent export of the early flagellar subunits (ie. rod and hook proteins) (Fraser *et al.*, 2003b). The precise mechanism of export specificity switching is not wholly understood, however, it also involves the 'molecular tape measure' FliK, which can bind to FlhB and is thought to detect hook length, initiating the switching of FlhB subunit specificity once the hook has reached the correct length (Erhardt *et al.*, 2010).

The bacterial flagellum has been shown to grow at a constant rate, independent of filament length (Turner *et al.*, 2012). Recent work by Evans *et al.* (2013) has proposed a chain mechanism of flagellar assembly that complements the observations by Turner *et al.* (2012), whereby the subunits move through the export gate, across the bacterial cell envelope and through the narrow tube of the filament, in an unfolded state, linked together in a chain. This is thought to occur through interactions of the opposing helices of each subunit with one another, allowing the subunits to travel through the tube of the flagellum, ending with the crystalisation of the subunits into the structure, beneath the cap proteins (Evans *et al.*, 2013). The folding and incorporation of a subunit into the flagellar structure is theorised to generate a pulling force and drive the entry of the next subunit into the flagellar lumen (Evans *et al.*, 2013).

### 1.2.4 – Gene expression and regulation

For the production of bacterial flagella, the genes are transcribed in a hierarchical manner due to the presence of a plethora of subunits which are required at different points of the assembly process, with each tier of the hierarchy being sensitive to the proteins at the previous level. Furthermore, at each tier of the hierarchy, the genes possess different promoter classes, either class I, II or III promoters, which allows the ordered expression of these genes at each stage (ie. early, middle or late gene expression). In addition, *Aeromonas* possesses two flagellar systems, making flagellar gene expression far more complex than in bacteria with only one system. However, it is thought that the different flagellar systems in this organism are entirely distinct as mutations that cause defects in the polar flagellum biogenesis do not affect lateral flagellar gene expression, and vice versa (Canals *et al.*, 2006a; Canals *et al.*,

2006c). This contrasts to *V. parahaemolyticus,* where expression of the dual flagellar systems is directly linked; mutational studies have demonstrated that when expression of polar flagellar system is impaired, the lateral flagellar system becomes constitutively expressed (McCarter *et al.,* 1988). The coordination of gene expression has been studied for both flagellar systems in *A. piscicola* AH-3 (Canals *et al.*, 2006a; Canals *et al.*, 2006c; Lowry *et al.*, 2014a; Wilhelms *et al.*, 2013; Wilhelms *et al.*, 2011).

With regards to polar flagellar gene expression, there are four tiers to the transcriptional hierarchy (I-IV), whose expression are under the regulation of either sigma factor 28 ($\sigma^{28}$) or sigma factor 54 ($\sigma^{54}$) (Wilhelms *et al.*, 2011). Level I encodes the $\sigma^{54}$ dependent enhancer binding protein, FlrA, which is the master regulator of the polar flagellar genes and whose gene-expression is independent of both $\sigma^{54}$ and $\sigma^{28}$. Level II encodes genes whose expression is dependent on FlrA and $\sigma^{54}$, such as: basal body components, the L and P rings, hook proteins, export apparatus, and FlrC, which is required for the expression of genes at the next level of the hierarchy (level III), along with its cognate kinase, FlrB. FlrC and $\sigma^{54}$ then go on to activate the genes at level III, which include the polar flagellar-specific sigma factor ($\sigma^{28}$ or FliA) and some of the motor proteins. Then, FliA initiates the expression of the genes at level IV, which include genes for the filament (FlaA/B), the flagellar cap (FlaH) and the flagellin-specific chaperone (FlaJ); along with an anti-sigma factor, FlgM, and additional motor proteins. FlgM negatively regulates the genes at level IV as its gene possesses a class II promoter. Therefore, FlgM brinds to FliA, preventing the early transcription of the later genes in this tier (ie. genes possessing class III promoters). Eventually, FlgM is exported, allowing the expression of the late genes by FliA in this tier (Wilhelms *et al.*, 2011).

As discussed in section 1.2.2, the lateral flagellar system is environmentally regulated, being induced when aeromonads come into contact with environments where the polar flagellum cannot function, such as on solid surfaces or within viscous solutions (Merino *et al.*, 2006). The expression of the lateral system is also tiered, having three levels in total (Canals *et al.*, 2006c; Wilhelms *et al.*, 2013). Level I genes are dependent on sigma factor 70 ($\sigma^{70}$) and encode the lateral flagellar system master regulator, LafK, and some structural components. The transcription of level I genes has been found to be constitutive in *A. piscicola*, however, translation only occurs when the bacteria encounter solid surfaces or viscous environments (Wilhelms *et al.*, 2013). Level II gene expression is dependent on $\sigma^{54}$ and LafK, which control the expression of the $\sigma^{28}$ of this system (LafS), and some other structural genes. Lastly, expression of genes the final level (III) is controlled by LafS, and its anti-sigma factor, FlgM, which is transcribed in the final tier. Here, genes for polar flagellar filament production are transcribed (Canals *et al.*, 2006c; Wilhelms *et al.*, 2013).

Furthermore, cyclic-di-GMP signalling is also thought to be involved in regulating flagellar gene expression in aeromonads, which is well known for being involved in bacterial lifestyle decisions (such as sessile or motile lifestyles) (Lowry *et al.*, 2014a). It is thought to modulate the activity of the master regulators and potentially interact with a PilZ domain-containing protein which has been identified in the *A. caviae* Sch3 genome (Shaw unpublished) likely to possess c-di-GMP binding capabilities. The homologue in *E. coli* (the PilZ domain-containing protein, YcgR) acts as a brake on the flagellar motor upon binding of this second messenger, preventing flagellar rotation and therefore favouring a sessile bacterial lifestyle when high levels of c-di-GMP are present (Lowry *et al.*, 2014a).

## 1.3 – Protein Glycosylation

Protein glycosylation was first identified in the 1930s when carbohydrate moieties were discovered on crystalline egg albumin (Neuberger, 1938). For a long time it was thought that only eukaryotes could post translationally modify their proteins and it was not until around four decades later when studies presented discoveries of prokaryotic protein glycosylation (Mescher and Strominger, 1976; Sleytr and Thorne, 1976). It is now accepted that glycosylation of proteins occurs in all the domains of life.

There are two major types of linkages for the attachment of sugars to proteins: N-linkages and *O*-linkages (Fig. 1.5). *N*-linked glycosylation is where the sugar forms a bond with the amide nitrogen of an asparagine residue in a protein; while *O*-linked glycosylation is where the carbohydrate is linked to the hydroxyl group of a threonine or serine residue, and less commonly a tyrosine (Fig. 1.5) (Zarschler *et al.*, 2010). Glycosylation is the most abundant and diverse post-translational modification present on eukaryotic proteins, and so the *N*- and *O*-linked pathways have been extensively studied (Spiro, 2002; Schwarz and Aebi, 2011).

### 1.3.1 – Eukaryotic protein glycosylation

Over two-thirds of eukaryotic proteins that carry out a diverse range of functions within the cell are predicted to be glycosylated, which highlights the importance of this post-translational modification in Eukaryotic systems.

N-linked glycosylation in Eukaryotes occurs on a vast array of proteins, at the specific consensus sequence: Asn-X-Ser/Thr (where X stands for any amino acid apart from proline) (Spiro, 2002). Generally, glycans are assembled on a lipid carrier on the cytosolic side of the endoplasmic reticulum (ER), via a team of glycosyltransferase enzymes. This glycan is then flipped across the membrane, into the ER lumen, via a flippase enzyme, where it is block transferred onto a target protein (at the correct consensus sequence) by an oligosaccharyltransferase. The glycan is transferred onto an unfolded protein, and can be modified further by further glycosyltransferases. This sequential processing step on the target protein is coupled to the protein's secretion, allowing for cell-specific *N*-linked glycosylation (Schwarz and Aebi, 2011). One of the most widely distributed sugar decorating eukaryotic proteins is *N*-acetylglucosamine (GlcNAc) which is found on proteins both within the cytosol and at the cell surface, such as on: enzymes, immunoglobulins and lectins (Spiro, 2002; Schwarz and Aebi, 2011). This pathway of *N*-linked glycosylation has some similarities to the heavily studied prokaryotic process of *N*-linked glycosylation in *C. jejuni*; however, the sugars generated in each case are vastly different. Eukaryotes initially produce a highly conserved sugar for *N*-linked glycosylation which can then

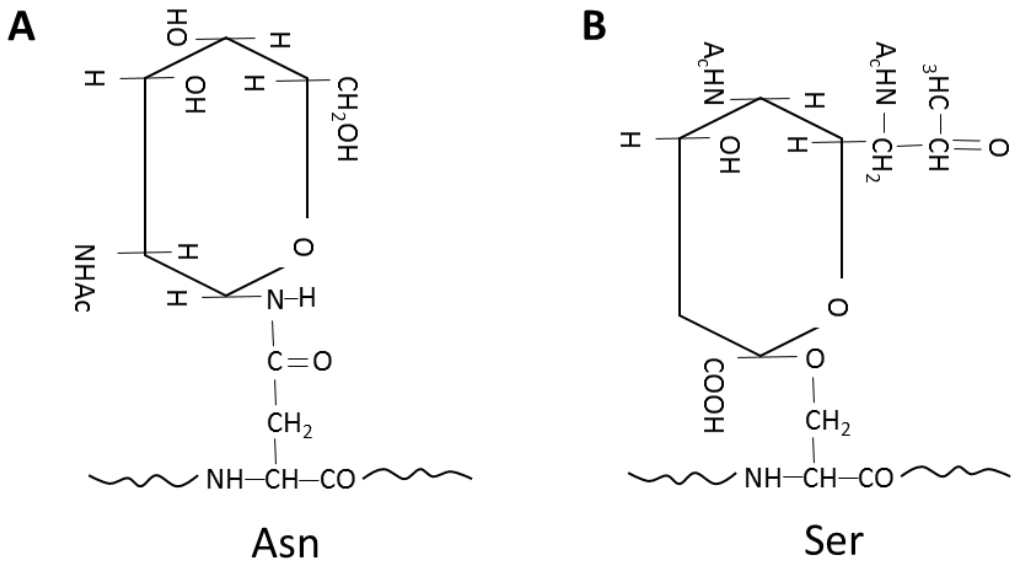


**Figure 1.5** – The major linkages formed during protein glycosylation. (**A**) *N*-linked glycosylation to an asparagine (Asn) residue (using *N*-acetlyglucosamine as an example sugar). (**B**) *O*-linked glycosylation to a serine residue (Ser) (using pseudaminic acid – Pse5Ac7Ac – as an example).

be diversified, in contrast to prokaryotes which produce an assortment of lipid-linked glycans (Schwarz and Aebi, 2011).

In addition, GlcNAc can also be *O*-linked onto target proteins, a modification which is important for the correct functioning of some cytoskeletal and nuclear proteins (Spiro, 2002). Eukaryotic proteins can also be *O*-mannosylated, which has been found to be extremely important in fungi for maintaining the cell wall. Mutational studies have demonstrated that knockout mutations of genes involved in *O*-mannosylation are lethal to *Saccharomyces cerevisiae* (Lommel and Strahl, 2009). Furthermore, *O*-mannosylation of fungal surface proteins is also involved in virulence and has a potential role in the solubilisation of misfolded proteins, demonstrating the wide variety of roles of this modification (Lommel and Strahl, 2009). In addition, with regards to humans, *O*-mannosylation is particularly important for the correct functioning of the dystrophin-glycoprotein complex in skeletal muscle; impaired ability to *O*-mannosylate this protein can lead to inherited muscular dystrophy (Blake *et al.*, 2002).

Glycans required for the *O*-linked glycosylation of proteins are, again, generally built onto a lipid carrier on the cytosolic side of the ER via glycosyltransferase enzymes. The sugar is then flipped into the lumen of the ER where it is transferred onto target proteins via an oligosaccharyltransferase. A consensus sequence for *O*-linked glycosylation has not yet been identified, so how these sugars are targeted to their proteins is not yet fully understood. Glycan diversification then takes place once it is covalently linked to the target protein, and this process can be carried out in the golgi where a number of glycosyltransferase enzymes reside (Lommel and Strahl, 2009).

## 1.3.2 – Bacterial glycosylation of surface proteins

Over recent years, research has demonstrated that some bacteria modify their proteins and surface appendages via these glycosylation pathways. In some cases, these post-translational modifications appear to be essential for bacterial virulence and colonisation; however, the precise role of glycosylation has not yet been determined (Nothaft and Szymanski, 2010). Bacterial protein glycosylation can either occur in an oligosaccharyltransferase dependent or independent manner (Nothaft and Szymanski, 2010). *N*-linked glycosylation has been well characterised in the bacterium *C. jejuni* and involves a lipid carrier for the glycan to be built onto, which is then transferred onto the target protein in the periplasm in an oligosaccharyltransferase dependent manner. This pathway shows some similarities the N-linked glycosylation present eukaryotes; however an alternative consensus sequence is present on target proteins (Glu-X-Asn-X-Ser/Thr, where X is any amino acid, except for proline) (Nothaft and Szymanski, 2010; Nothaft and Szymanski, 2013). Some atypical bacterial *N*-linked glycosylation pathways have also been identified. For example, in *Haemophilus influenzae*, some cell surface adhesins are modified with hexose residues via glycosyltransferase enzymes within the cytoplasm, and the consensus sequence for modification here is identical to that observed on target proteins in eukaryotes (Asn-X-Ser/Thr), despite this atypical pathway not being present within eukaryotic cells (Choi *et al.*, 2010; Grass *et al.*, 2010).

*O*-linked glycosylation pathways have been studied in a variety of bacteria, with the modification of the bacterial flagellum being particularly associated with the virulence of number of pathogens, especially in Gram-negative species. Many Gram-negative bacteria have been found to glycosylate their flagellins with nonulosonic acids, which can be essential for flagellation and therefore virulence (such as *Campylobacter, Helicobacter* and *Aeromonas* species) (Fig 1.6) (Merino and Tomas, 2014). Flagellin glycosylation occurs in an oligosaccharyltransferase independent manner and the Maf (motility associated factor) proteins are a novel group of proteins that have been recognised as the putative flagellin-specific glycosyltransferases (Karlyshev *et al.*, 2002; Schirm *et al.*, 2003; Canals *et al.*, 2007; Parker *et al.*, 2012).

### 1.3.2.1 – *Campylobacter*

The first bacterial *N*-linked glycosylation system was characterised in the gastrointestinal pathogen, *C. jejuni* (Szymanski *et al.*, 1999) and has also been reconstituted in *E. coli* (Linton *et al.*, 2005). The *pgl* locus contains the genes which encode the *N*-glycosylation system responsible for glycosylating over 60 *C. jejuni* periplasmic and membrane-bound proteins (Scott *et al.,* 2011). The process of N-linked glycosylation here is oligosaccharyltransferase

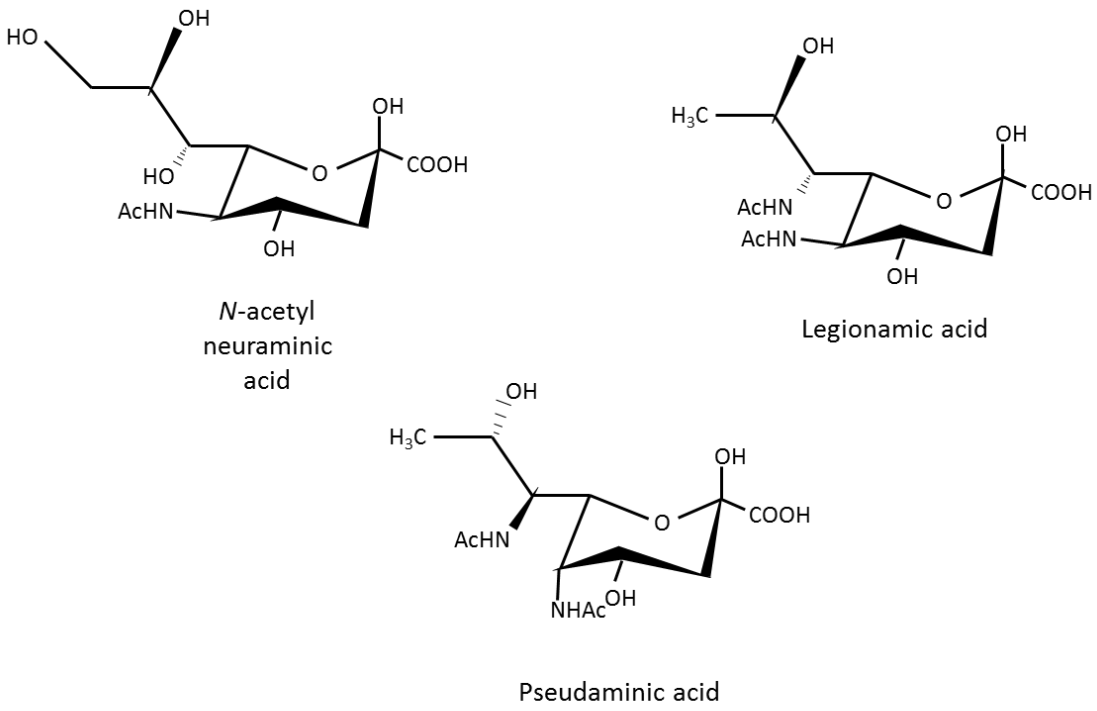


**Figure 1.6** – The structure of the common nonulosonic acids: *N*-acetyl neuraminic acid, pseudaminic acid and legionaminic acid.

dependent, with protein targets being modified with a heptasaccharide (Young *et al.*, 2002) which is manufactured on the cytoplasmic side of the inner membrane (via glycosyltransferase enzymes), on a lipid precursor molecule (Linton *et al.*, 2005). Once assembled, the glycan is 'flipped' across the membrane via an ATP-dependent flippase enzyme (Alaimo *et al.*, 2006) into the periplasm. Once in the periplasm, the sugar is block transferred onto the amide nitrogen of an asparagine residue located within a specific consensus sequence (Glu-X-Asn-X-Ser/Thr) (Kowarik *et al.*, 2006) on target folded proteins, via an oligosaccharyltransferase, which shows partial identity to the Eukaryotic version (Kowarik *et al.*, 2006). In *C. jejuni* N-linked glycosylation occurs on flexible loops of folded proteins, which is in contrast to the pathway of N-linked glycosylation in Eukaryotes where they modify unfolded proteins (Nothaft and Szymanski, 2010). N-glycosylation appears to be associated with pathogen virulence as mutational studies of the *pgl* locus revealed a decreased ability of *C. jejuni* to colonise chicks and bind to human epithelial cells (Karlyshev *et al.*, 2004). This modification may also allow modulation of the host immune response, as the heptasaccharide on the *C. jejuni* cell surface is recognised by a dendritic cell receptor, the human macrophage galactose-type lectin (MGL) (van Sorge *et al.*, 2009). A *C. jejuni pglA* mutant (where *pglA* encodes one of the glycosyltransferases required for building the heptasaccharide), which is unable to produce the glycan for N-linkage, has been shown to stimulate an increased cytokine response, with the release of interleukin 6 (IL-6), in dendritic cells, compared to the wild type strain (van Sorge *et al.*, 2009). This therefore suggests that *N*-linked glycosylation at the cell surface may dampen down the host immune response (van Sorge *et al.*, 2009).

Furthermore, *Campylobacter* species are also capable of modifying their flagellins via *O*-linked glycosylation with a variety of nonulosonate sugars, which are all derived from pseudaminic acid or legionaminic acid (Fig. 1.6) (Logan *et al.*, 2002; Logan *et al.*, 2009; McNally *et al.*, 2007; McNally *et al.*, 2006; Thibault *et al.*, 2001; Zampronio *et al.*, 2011). The Maf proteins are the putative glycosyltransferase enzymes that directly modify the central region of the flagellins (the D2/D3 domain) (Karlyshev *et al.*, 2002). This modification is essential for the formation of the *Campylobacter* polar flagellum, and is therefore implicated in the virulence of this pathogen and its ability to colonise the host gastrointestinal tract (Goon *et al.*, 2003; Guerry, 2007). Due to the presence of multiple sugars decorating the flagellum, the glycosylation islands required for sugar biosynthesis and flagellin modification are extremely vast and complex, and can encode up to seven *maf* homologues (Karlyshev *et al.*, 2002). However, mutational studies in *C. jejuni* and *C. coli* have demonstrated that pseudaminic acid is the essential, base sugar, required for flagellation and can make up for the absence of the other nonulosonic acids (Goon *et al.*, 2003; Logan *et al.*, 2002; Thibault *et al.*, 2001). The enzymes for

pseudaminic acid biosynthesis are encoded for by the *Pse* genes, which allow for the production of this sugar by a five step enzymatic pathway (Goon *et al.*, 2003) (discussed in section 1.4); orthologues of these genes are also present in other bacteria, such as *Helicobacter* and *Aeromonas* species that are also capable of synthesising nonulosonic acids (Canals *et al.*, 2007; Josenhans *et al.*, 2002; Schoenhofen *et al.*, 2006; Schirm *et al.*, 2003) (Tabei *et al.*, 2009). Although the precise role of flagellin glycosylation is unknown, there is some evidence to suggest that the expression of some Maf proteins may be phase variable, allowing *Campylobacter* to modify its flagellins with different nonulosonic acids during different stages of infection (van Alphen *et al.*, 2008). Mutational studies have also demonstrated that the surface charge of the *Campylobacter* flagellum changes when the glycosylation status of the flagellum is altered, affecting the ability of a population to autoagglutinate and form biofilms (Howard *et al.*, 2009). These changes were attributed to the loss of legionaminic acid on the *C. jejuni* flagellum, and were also shown to have a detrimental effect on the ability of this mutant strain to colonise chickens (Howard *et al.*, 2009). Therefore, flagellin glycosylation here may allow *Campylobacter* species to alter their behaviour, in order to produce favourable interactions with each other or their environments, even perhaps during different stages of infection (further discussed in Chapter 4).

#### 1.3.2.2 – *Helicobacter*

Some *Helicobacter* species, such as the gastric pathogen *H. pylori*, also *O*-glycosylate their flagellins, however the process is far simpler than in *Campylobacter* due to having less genetic diversity amongst species, and occurs solely with pseudaminic acid (Fig. 1.6) (Josenhans *et al.*, 2002; Schirm *et al.*, 2003). Mutational analysis of genes thought to be involved in flagellin glycosylation have demonstrated that glycosylation is crucial for polar flagellar assembly and motility (Schirm *et al.*, 2003); however why this is the case is not wholly understood. It is unlikely that *H. pylori* flagella are glycosylated to evade the host immune system, or for interactions with the external surroundings, as the flagella are sheathed (Geis *et al.*, 1993) and so are already sheltered from antibodies. It is possible, however, that flagellin glycosylation here has a structural role and is necessary for the co-polymerisation of the flagellin monomers (FlaA and FlaB), or for interactions with the secretion machinery; however, these theories have not yet been investigated. Although *H. pylori* flagellins are only modified with pseudaminic acid, it is intriguing that two *maf* homologues have been identified in the *H. pylori* genome (Schirm *et al.*, 2003; Tomb *et al.*, 1997); the roles of these proteins have not yet been determined however. It is possible that both of these proteins are required for flagellin modification, or perhaps other proteins are modified via the Maf proteins here. Nevertheless,

their presence demonstrates the importance of *O*-linked glycosylation in *H. pylori* flagellation and virulence.

In addition to the Maf proteins, a putative flagellin deglycosylation enzyme, named HP0518, has also been identified in *H. pylori*; a mutant of which is hypermotile and displays elevated levels of flagellin glycosylated (Asakura *et al.*, 2010). It is possible that a glycosylation homeostasis pathway is in place to modulate how *H. pylori* flagellins are glycosylated, perhaps depending on the environment, in order to alter bacterial behaviour. However, flagellin deglycosylation pathways have not yet been identified in other bacteria. *H. pylori* flagellin glycosylation is further discussed in results Chapters: 3, 4 and 5.

#### 1.3.2.3 – *Pseudomonas*

A number of pseudomonads are also capable of protein glycosylation. For example, the respiratory pathogen, *Pseudomonas aeruginosa* is able to modify cell surface appendages such as its type IV pilus and flagella (Nothaft and Szymanski, 2010).

Pilin glycosylation is *O*-linked, but the pathway shows similarities to *N*-linked glycosylation in *C. jejuni,* as it is oligosaccharyltransferase dependent, and requires a trisaccharide to be built on the cytoplasmic side of the inner membrane before it is flipped into the periplasm and block transferred onto subunits of the pilus (Nothaft and Szymanski, 2010). This modification is not essential for the formation of the type IV pilus, however, glycosylation has been found to alter the hydrophobicity of the pilus surface and increase *P. aeruginosa* colonisation capabilities when analysed in a pneumonia mouse model of infection (Smedley *et al.*, 2005).

*P. aeruginosa* can also *O*-glycosylate its flagellins, however, this modification is not essential for flagellation and does not involved nonulonsonate sugars, in contrast to flagellin glycosylation observed in *Campylobacter*, *Helicobacter* and *Aeormonas* species. Two types of flagellins are present in *P. aeruginosa* strains, a-type and b-type, which are classed due to their molecular weight and their anti-sera specificity (Nothaft and Szymanski, 2010). *P. aeruginosa* possessing a-type flagellins have been found to modify them with heterogeneous rhamnose-linked oligosaccharides, with some strains just modifying their flagellins with a single rhamnose moiety, and others modifying them with up to 11 additional monosaccharides (Schirm *et al.*, 2004). In contrast, strains containing b-type flagellins were found to modify them with less heterogeneous hexose residues linked to a 209 Da mass (to be determined) (Verma *et al.*, 2006).

Studies by Arora *et al.* (2005) have demonstrated that *P. aeruginosa* glycosylation defective mutants have attenuated virulence in a burned mouse model of infection, compared to the

wild type strain. Therefore, despite not being essential for flagellation, these sugars still have a clear role in the virulence of this pathogen. Furthermore, bacterial flagellins are recognised by a toll-like receptor on the surface of host immune cells (TLR-5) (Hayashi *et al.*, 2001) which induces the production of the proinflammatory cytokines. However, it has been suggested that the role of *P. aeruginosa* flagellin glycosylation is to aid this response, as studies have demonstrated that unglycosylated, mutant flagellins reduce IL-8 release considerably by the host immune cells (Verma *et al.*, 2005). Glycosylated flagellins may therefore be the reason why hyper-inflammation is usually present in *P. aeruginosa* respiratory infections, especially in cystic fibrosis patients.

Furthermore, the plant pathogen, *P. syringae*, is also able to *O*-glycosylate its flagellins with modified rhamnose residues (Takeuchi *et al.*, 2003). Similarly to *P. aeruginosa*, this modification is not essential for flagellation, however, it does have a role in the pathogen virulence, as glycosylation defective mutants are less able to adhere to surfaces and cause disease (Taguchi *et al.*, 2006). The glycosylated version of the *P. syringae* flagellum was also found to be more heat resistant than the unglycosylated form, which may prevent the flagellum from being broken down in the host (Taguchi *et al.*, 2009). (Further discussed in Chapter 4)

#### 1.3.2.4 – *Neisseria*

Pathogenic *Neisseria* species, such as *N. meningitidis* and *N. gonorrhoeae,* are able to *O*-glycosylate the monomeric constituents of their type IV pili (the pilins), which are major virulence determinants for these bacteria (Mattick, 2002). They contain a number of pilin glycosylation (*pgl*) genes required for pilin *O*-glycosylation of pili, and carry out this modification in a pathway related to that of the N-linked glycosylation pathway in *C. jejuni*, which involves a lipid-linked precursor (Aas *et al.*, 2007). *N. meningitidis* produces a trisaccharide with diacetamido trideoxyhexose at the base; this sugar is synthesised on the cytoplasmic side of the inner membrane, similarly to pilin glycosylation in *P. aeruginosa* and N-linked glycosylation in *C. jejuni*, before being flipped into the periplasm and transferred onto pilin via an oligosaccharyltransferase (Aas *et al.*, 2007; Power *et al.*, 2000).

*Neisseria spp.* also glycosylate another protein via the same *O*-linked glycosylated pathway, called AniA (Ku *et al.*, 2009; Vik *et al.*, 2009). AniA is an outer-membrane nitrate reductase exposed at the cell surface and there is some evidence to suggest that glycosylation of this protein shields it from the host immune system (Ku *et al.*, 2009; Vik *et al.*, 2009). Although the role of pilin glycosylation in *Neisseria* is unknown, it may also be involved in host immune evasion.

#### 1.3.2.5 – Gram-positive bacterial glycosylation

Much work on bacterial glycosylation has been carried out in Gram-negative bacteria, however, there have now reports of Gram-positive bacteria also possessing machinery to glycosylate their proteins, a number of which modify proteins at the cell surface. For example some *Clostridium* species are able to *O*-glycosylate their flagellins, such as the clinically relevant *C. botulinum* and *C. difficile* (Twine *et al.,* 2008; Twine *et al.,* 2009).

*C. botulinum* is able to modify its flagellins with nonulosonic acids (similarly to the glycosylation of many Gram-negative flagella), as well as hexnuronic acid (Twine *et al.*, 2008). Glycosylation was not found to be required for flagellar assembly, although more strains isolated from infant patients were found to modify their flagella with nonulosonate sugars, compared to strains not associated with disease; demonstrating that this modification has a clear role in pathogenicity (Twine *et al.*, 2008).

In contrast to *C. botulinum,* the glycosylation of *C. difficile* flagellins with *N*-acetylglucosamine is essential for pathogen flagellation (Twine *et al.*, 2009). Faulds-Pain *et al.* (2014) carried out recent studies altering the structure of this sugar at the *C. difficile* flagellar surface. Motility was not found to be required for colonisation, however, the structure of the glycan was, and when mutated, had a severe impact on the ability of this pathogen to colonise a mouse model of infection (Faulds-Pain *et al.*, 2014). Furthermore, some mutations on the glycan structure also affected bacterial motility and caused cellular aggregation, demonstrating that altering flagellar glycosylation can affect bacterial behaviour (Faulds-Pain *et al.*, 2014).

## 1.4 – Glycosylation in *Aeromonas* species

Mesophilic aeromonads are also able to *O*-glycosylate structures at their cell surfaces, such as their flagella, and in addition their LPS O-antigens (O-Ag). *A. caviae* Sch3 (which will be focused on here) modifies its polar flagellum solely with pseudaminic acid (316 Da) (similarly to flagellin glycosylation in *H. pylori*) and possesses the simplest set of genes currently known for *O*-linked flagellin glycosylation (Fig. 1.7A) (Tabei *et al.*, 2009). Within its polar flagellum locus is a single *maf* gene which encodes the putative flagellin-specific glycosyltransferase, Maf1 (Fig. 1.7A) (Parker *et al.*, 2012; Parker *et al.*, 2014). This modification is essential for the formation of the *A. caviae* polar flagellar filament. Other aeromonads also require glycosylation to form their flagella (Canals *et al.*, 2006c), however, appear to have more complex polar flagellin glycosylation than *A. caviae.* For example, *A. piscicola* AH-3 have a more complicated glycosylation island, encoding two *maf* homologues, and additional genes that are not found in *A. caviae* (Fig. 1.7B) (Canals *et al.*, 2007). In addition, flagellins have been found to be modified with a heptasaccharide which includes a 376 Da pseudaminic acid derivative (Wilhelms *et al.*, 2012); this therefore may explain the presence of these extra genes within the AH-3 genome (Canals *et al.*, 2007). Furthermore, recent work by Merino *et al.* (2014) has suggested that in *A. piscicola* AH-3, a lipid carrier protein (WecX) is involved in flagellin glycosylation, whereby pseudaminic acid is transferred onto the carrier, and the rest of the heptasaccharide is then built onto this sugar, before being block transferred onto the flagellin. This has not yet been reported for other *O*-linked flagellin glycosylation systems.

Similarly to *A. piscicola* AH-3, the glycosylation island of *A. hydrophila* ATCC 7966 (Fig. 1.7C) is also more complex than that of *A. caviae*, also possessing multiple *maf* homologues and additional genes which may be required for the more complex glycosylation of its flagellins.

Additionally, there is some evidence to suggest that the lateral flagellins are also glycosylated; however lateral flagellin glycosylation has not been studied as fervently as polar flagellin glycosylation. Both *A. caviae* and *A. piscicola* lateral flagellins were found to be larger than expected when analysed via SDS-PAGE, indicating that a post-translational modification may be present (Gavin *et al.*, 2002). Studies by Wilhelms *et al.* (2012) have demonstrated that this size discrepancy in *A. piscicola* AH-3 is due to the occurrence of a pseudaminic acid derivative (376 Da) decorating the lateral flagellins. This modification was found to be essential for the lateral flagellation and therefore the swarming motility of *A. piscicola* AH-3 when in contact with solid surfaces (Wilhelms *et al.*, 2012). Moreover, a *maf* homologue, *maf5*, has been identified in the lateral flagellar locus in *A. piscicola;* the mutation of which results in the abolition of lateral flagella (Canals *et al.*, 2006a).

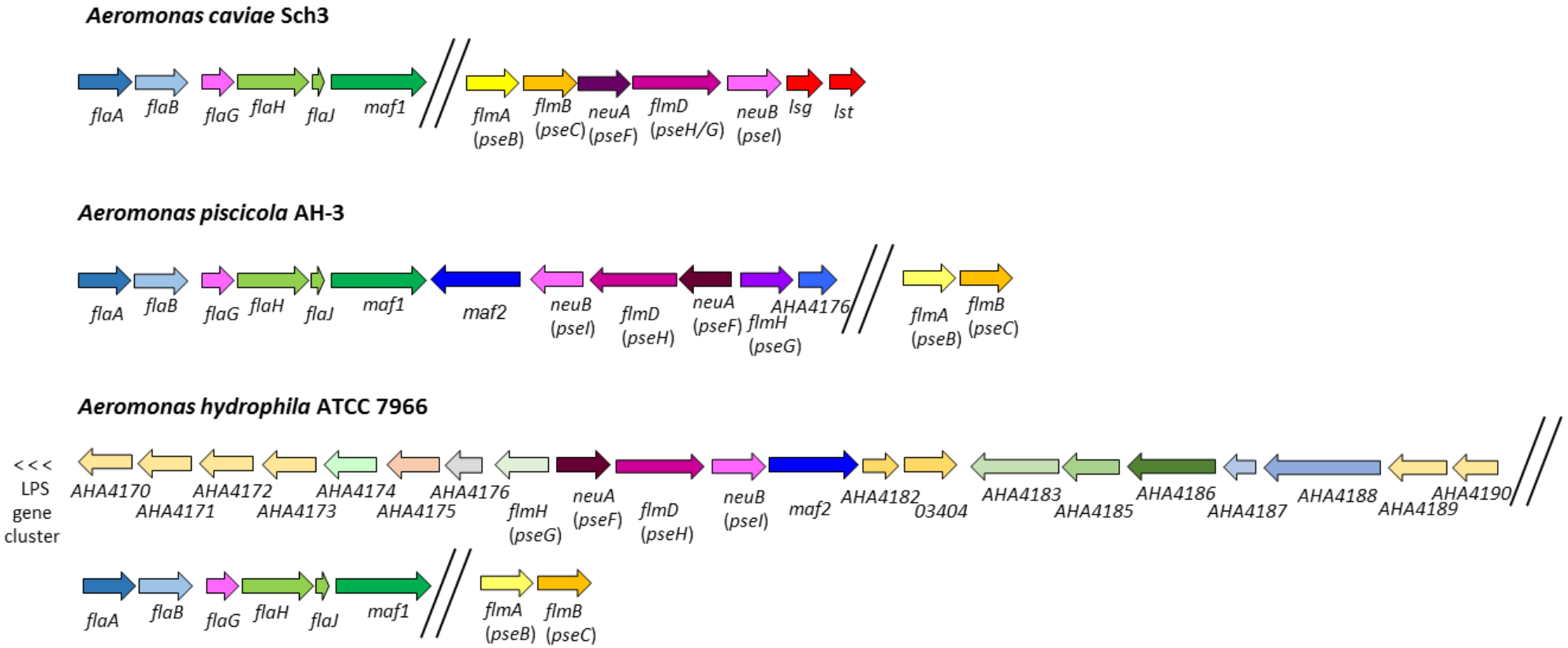


**Figure 1.7** – The polar flagellar loci and glycosylation islands in *Aeromonas* species. *Aeromonas caviae* Sch3 (Tabei *et al.,* 2009) contains the simplest glycosylation islands identified to date, whereas *A. piscicola* AH-3 (Canals *et al.,* 2006b and 2006c) and *A. hydrophila* ATCC 7966 (Seshradri *et al.,* 2006) display more complicated loci, with *A. hydrophila* in particular showing complexity, as the genes for pseudaminic acid biosynthesis, and the second *maf* homologue (*maf2*), here are surround by a series of currently uncharacterised genes. Within the genes for polar flagellar assembly, is also *flaG* which currently has an unknown function.

As *A. caviae* Sch3 glycosylates its polar flagellins exclusively with pseudaminic acid, and contains the simplest set of genes currently known to do this (Parker *et al.*, 2012; Tabei *et al.*, 2009), it is an ideal model organism for the study of the O-linked glycosylation pathway.

## 1.4.1 – The *O*-linked flagellin glycosylation pathway in *A. caviae* Sch3

### 1.4.1.1 – Pseudaminic acid biosynthesis

Pseudaminic acid (Pse5Ac7Ac), otherwise known as 5,7-diacetamido-3,5,7,9-tetradeoxy-L-glycero-L-manno-nonulosonic acid, is a nonulosonic acid (nine carbon sugar) related to the sialic acids. These sugars are all α-keto acids, which are a group of sugars well known for their important roles in a number of biological processes, such as the tricarboxylic acid cycle (TCA cycle) and glycolysis. The term 'sialic acid' relates to neuraminic acid and all *N*- or *O*-substituted derivatives. They are the most naturally abundant α-keto acids found in all domains of life, with the most common member of this group being *N*-acetylneuraminic acid (Neu5Ac) (Fig. 1.6) (Chen and Varki, 2010, Zunk and Kiefel, 2014). Some sialic acid derivatives , however (such as pseudaminic and legionaminic acid), appear to be exclusively found in bacteria, and have been linked with bacterial pathogenicity in a number of ways, making their biosynthetic pathways attractive therapeutic targets (Almagro-Moreno and Boyd, 2010). All sialic acid derivatives are synthesised in a similar way, whereby a nucleotide activated hexose residue is used as the precursor sugar. Then to this six carbon sugar a three carbon sugar is linked, which is generally a pyruvate derivative formed from the condensation of a six carbon compound to a three carbon compound. Therefore, these steps form the nine carbon skeleton of the nonulosonic acid. Furthermore, all nonulosonic acids are nucleotide activated before they are either transferred onto their target protein, or incorporated into a larger glycan structure (Almagro-Moreno and Boyd, 2010; Zunk and Kiefel, 2014).

With regards to Pse5Ac7Ac biosynthesis, a set of genes known as the *flm* locus are required for the conversion of uridine diphosphate *N*-acetlyglucosamine (UDP-GlcNAc) to Pse5Ac7Ac in mesophilic aeromonads (Fig 1.7A & 1.8) (Canals *et al.*, 2007; Gryllos *et al.*, 2001). This locus was initially identified in *A. caviae* Sch3, but homologues of these biosynthetic genes have now been identified in all mesophilic species analysed, and their orthologues are also found in *Campylobacter* and *Helicobacter* species (*Pse* genes) (Beatson *et al.*, 2011; Canals *et al.*, 2007; Goon *et al.*, 2003; Gryllos *et al.*, 2001; Schoenhofen *et al.*, 2006; Seshadri *et al.*, 2006; Tabei *et al.*, 2009). In *A.caviae* Sch3, Pse5Ac7Ac is produced from UDP-GlcNAc via a four step enzymatic pathway, carried out by the proteins: FlmA (a Pse5Ac7Ac nucleotide dehydratase and C-5 epimerase), FlmB (a pyridoxal dependent aminotransferase), FlmD (containing a glycosyltransferase domain and a RimL-like acetyltransferase domain) and NeuB (a Pse5Ac7Ac synthetase) (Fig. 1.8).

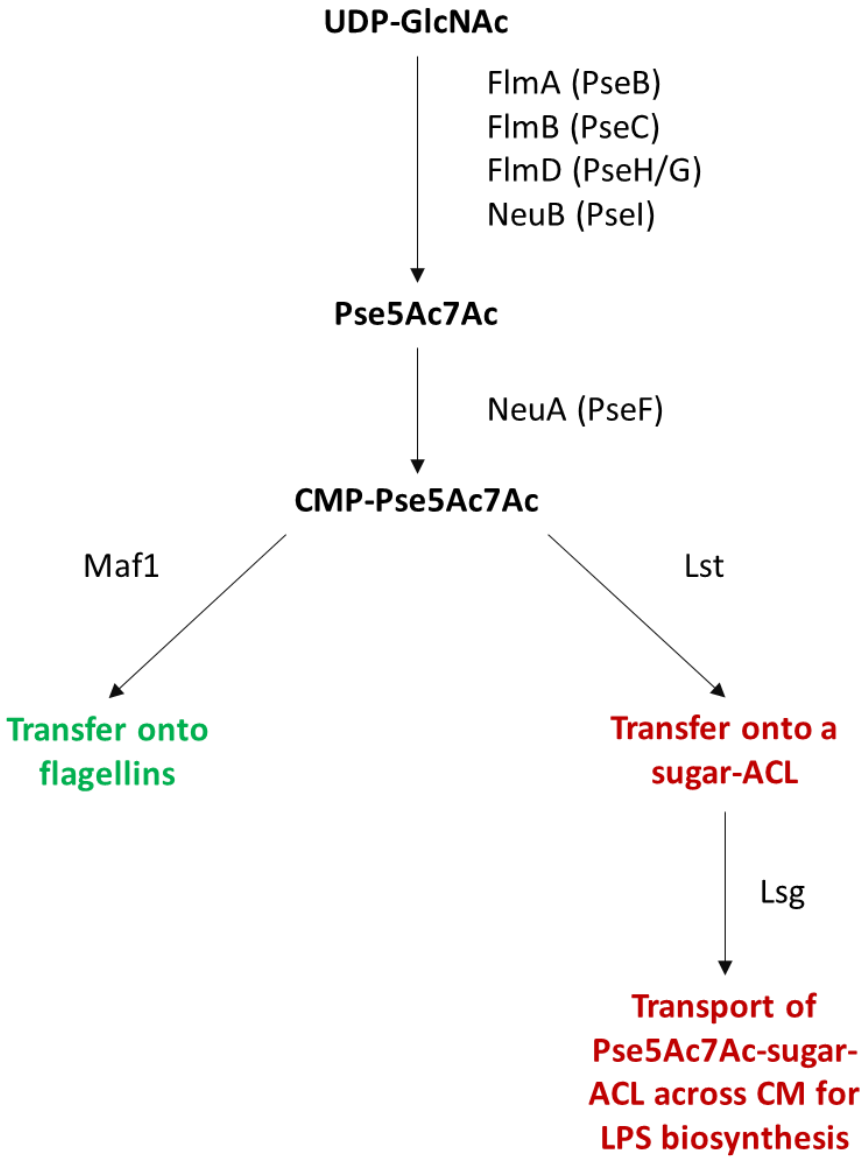


**Figure 1.8** – The four step pseudaminic acid biosynthetic pathway in *Aeromonas caviae* Sch3. Pse5Ac7Ac is produced from uridine diphosphate *N*-acetylglucosamine (UDP-GlcNAc) by: the nucleotide dehydratase and C-5 epimerase, FlmA; the pyridoxal-dependent aminotransferase, FlmB (rearranges the entire molecule), the chimeric protein (of FlmD and FlmH in other aeromonads), FlmD, which contains a glycosyltransferase domain and a RimL-like acetyltransferase domain; and the pseudaminic acid synthetase, NeuB. Pse5Ac7Ac is activated via the addition of cytidine monophosphate (CMP) by NeuA (CMP-Pse5Ac7Ac synthetase). Once active, the sugar can then be transferred onto the LPS O-antigen via the use of a sugar-antigen lipid carried (sugar-ALC); or onto the flagellins by the putative glycosyltransferase, Maf1. The figure also displays the orthologous proteins in *Campylobacter* (in the brackets).

Pse5Ac7Ac is then activated via the addition of cytidine monophosphate (CMP) by NeuA (a CMP-Pse5Ac7Ac synthetase) (Fig. 1.8).

The *flm* locus of *A. caviae* Sch3 has been found to have a dual role, as it is involved in both LPS O-Ag biosynthesis and flagellar assembly (Gryllos *et al.*, 2001; Tabei *et al.*, 2009). Mutations in the *flm* locus cause a loss of both the LPS O-Ag (LPS profile altered) and the loss of the polar flagellar system (Tabei *et al.*, 2009). There are also additional genes present in the locus, *lst* and *lsg,* which may be responsible for transferring the glycan group across the cytoplasmic membrane and onto the LPS (Fig. 1.7 and 1.8) (Tabei *et al.*, 2009). Therefore, once active, the sugar can go down one of two pathways: either the pathway of flagellin glycosylation, or LPS biosynthesis. Maf1 is the putative glycosyltransferase thought to be responsible for the transfer of activated Pse5Ac7Ac onto flagellins (Parker *et al.*, 2012; Parker *et al.*, 2014). In contrast, mutations in the *flm* locus of *A. piscicola* AH-3 only cause the loss of the flagella systems; there is no effect on the LPS profile (Canals *et al.*, 2007; Tabei *et al.*, 2009). This suggests that the *flm* locus is only involved in the assembly of the bacterial flagellum here, with a separate locus being present for LPS O-Ag biosynthesis. Despite their differences, the *flm* genes of both *A. caviae* Sch3 and *A. piscicola* AH-3 are still able to complement corresponding, non-polar, mutations in the other bacteria (Canals *et al.*, 2007).

Furthermore, *A. caviae* may have acquired the minimum gene cluster for Pse5Ac7Ac biosynthesis, as in addition to the pathways for both flagellar assembly and LPS biosynthesis being merged, the protein FlmD appears to be a chimera of the FlmD and FlmH proteins present in other aeromonads (and in other bacteriam such as *Campylobacter* , PseG and PseH) (Tabei *et al.*, 2009). It is possible that this gene cluster was acquired laterally as the G+C content of the *A. caviae* Sch3 *flm* locus is lower (around 42%) than that of the *A. piscicola* AH-3 locus, which is a characteristic 60% (similar to other aeromonads) (Tabei *et al.*, 2009).

#### 1.4.1.2 – Flagellin glycosylation

Once synthesised, Pse5Ac7Ac is transferred onto the polar flagellins by the putative glycosyltransferase, Maf1 (Parker *et al.*, 2012; Parker *et al.*, 2014). No consensus sequence has been identified for *O*-linked glycosylation, however *A. caviae* Sch3 flagellins have been found to be modified with six to eight sugars on serine/threonine residues within their D2/D3 domain (Tabei *et al.*, 2009); although the precise sites of modification are unknown. This modification is essential for *A. caviae* flagellation and virulence, as when *flm* mutants incapable of modifying their flagellins were examined in a mouse model they were found to be less virulent than the wild type strain and could no longer produce a polar flagellum (Tabei *et al.*, 2009). Furthermore, recent work by Parker *et al.* (2014), which includes some of the work carried out

here, has delved deeper into the flagellin glycosylation pathway of *A. caviae* Sch3 and demonstrated that Maf1 functions in the cytoplasm, glycosylating flagellins before the binding of the flagellin-specific chaperone, FlaJ. It was observed that unglycosylated flagellin can still be exported in *A. caviae* Sch3, therefore glycosylation is not required as a flagellin export signal, or for interactions with the export apparatus here (Parker *et al.*, 2014). However, it was demonstrated that FlaJ has less affinity for the unglycosylated flagellin, which is likely to promote the export of the glycosylated protein that can then be polymerised into a functional filament (Parker *et al.*, 2014).

The pathway of *O*-linked glycosylation is therefore very important for allowing this microorganism to thrive in its host and could potentially be a therapeutic target in the future; although the exact role of flagellin glycosylation is still to be determined.

## 1.5 – Project aims

The main aims of this project have been to explore the pathway and role of flagellin glycosylation with pseudaminic acid in *Aeromonas caviae* Sch3; a bacterium that contains the simplest set of genes currently known to synthesise this sugar and modify these proteins. These investigations were split into three distinct sections:

- A homologue of the putative deglycosylation enzyme, HP0518, known as AHA0618, was identified in *A. caviae* Sch3. Chapter 3 of this project investigates the potential existence of a flagellin deglycosylation pathway in *A. caviae*, whereby an *A. caviae AHA0618* mutant was phenotypically analysed and the glycosylation status of the wild type and mutant flagellins compared. Work here was published in Lowry *et al.,* (2014b).

- The exact sites of *A. caviae* Sch3 flagellin glycosylation are currently unknown, however work by Tabei *et al.* (2009) revealed that six to eight serine or threonine residues within the central region of the flagellins (D2/D3 domain) are occupied with pseudaminic acid. Chapter 4 of this work therefore explores the specific sites of flagellin glycosylation via mass spectrometric methods, and uses site-directed mutagenesis studies to determine the importance of the glycosylation sites identified on bacterial motility and flagellation.

- Chapter 5 of this work investigates the function of the *A. caviae* Sch3 putative flagellin glycosyltransferase, Maf1, with a series of mini-projects:
    - The location of Maf1-specific flagellin glycosylation in the flagellar assembly pathway was investigated via the bacterial adenylate cyclase two-hybrid system (BACTH).
    - Studies were carried out to determine whether the flagellar cap (FlaH) is required for flagellin glycosylation.
    - The specificity of Maf1 was investigated via flagellin domain swapping studies with the D2/D3 regions from *Aeromonas* species flagellins.
    - *A. caviae* Sch3 was also explored as a model of *O*-linked glycosylation for the heterologous expression of *H. pylori* glycosylation (Maf) proteins.

# Chapter 2 – Materials and methods

## 2.1 – Strains and Plasmids

Please refer to tables 2.1 and 2.2.

| Strain | Relevant Characteristics | Source/Reference |
|---|---|---|
| | ***Aeromonas* strains:** | |
| Sch3N | *Aeromonas caviae*, wild type, $Nal^R$ | Gryllos *et al.* (2001) |
| JPS04 | Sch3N *AHA0618*::Km | Lowry *et al.* (2014b) |
| JPS01 | Sch3N *maf1*::Km | Parker *et al.* (2012) |
| AAR59 | Sch3N *flaH*::Km | Rabaan *et al.* (2001) |
| AAR31 | Sch3N *flaA/B*::Km/Cm | Rabaan *et al.* (2001) |
| Ae398 | *Aeromonas caviae*, wild type | Beatson *et al.* (2011) |
| ATCC7966 | *Aeromonas hydrophila*, wild type | *Seshadri et al. (2006)* |
| AH-3 | *Aeormonas piscicola*, wild type | Merino *et al.* (1991) |
| | ***Escherichia coli* strains:** | |
| DH5α | Cloning/storage strain:<br>F-, endA, hdsR17 ($r_K$- $m_K$+) supE44, thi-1, *recA1* gyr-A96, ϕ80lacZ | Invitrogen Life TechnologiesTM, UK |
| BTH101 | Reporter strain for the bacterial two-hybrid system:<br>F-, *cya-99*, *araD139, galE15, galK16, rpsL1 (Str r)*, *hsdR2, mcrA1, mcrB1* | Euromedex |
| S17-1 λ *pir* | *thi rspL* ($Str^r$) *endA sbcB15 sbcC_hsdR* ($r_k^-$ $m_k^-$) Δ (*lac-proAB*) [F' *traD36_lacI*$^q$ Δ(*lacZ*)*M15 proA*$^+$*B*$^+$] | Herrero *et al.* (1990) |
| | **Other strains:** | |
| 26695 | *Helicobacter pylori, wild type* | Tomb *et al.* (1997) |

**Table 2.1** – Strains

$Nal^R$ (Nalidixic acid resistance); Km (kanamycin cassette); Cm (chloramphenicol cassette)

| Plasmid | Relevant Characteristics | Source/Reference |
|---|---|---|
| pGEM-T Easy | Cloning vector, $Amp^R$ | Promega |
| pSRK(Gm) | Broad-host-range expression vector, $Gm^R$ | Khan *et al.* (2008) |
| pSRK_*AHA0618* | pSRK(Gm) derivative containing *AHA0618* under the control of a *lac* promoter, $Gm^R$ | This work |
| pSRK_*HP0518* | pSRK(Gm) derivative containing *H. pylori* (26695) *HP0518* under the control of a *lac* promoter, $Gm^R$ | This work |
| pSRK_*flaA*(Sch3N) | pSRK(Gm) derivative containing *A. caviae* Sch3N *flaA* under the control of a *lac* promoter, $Gm^R$ | This work |
| pSRK_*flaA*(ATCC7966) | pSRK(Gm) derivative containing *A. hydrophila* ATCC7966 *flaA* under the control of a *lac* promoter, $Gm^R$ | This work |
| pSRK_*flaA*(AH-3) | pSRK(Gm) derivative containing *A. caviae* AH-3 *flaA* under the control of a *lac* promoter, $Gm^R$ | This work |
| pSRK_*maf1(H.p)* | pSRK(Gm) derivative containing *H. pylori* (26695) *maf1* under the control of a *lac* promoter, $Gm^R$ | This work |
| pSRK_*maf2(H.p)* | pSRK(Gm) derivative containing *H. pylori* (26695) *maf2* under the control of a *lac* promoter, $Gm^R$ | This work |
| pBBR1MCS-5 | Broad host range expression vector, $Gm^R$ | Kovach *et al.* (1995) |
| pBBR1MCS-5_*flaA* | pBBR1MCS-5 derivative containing Sch3N *flaA* under the control of its native promoter | This work |
| pBBR1MCS-5_*flaA*(Ae398) | pBBR1MCS-5 derivative containing the *A. caviae* Ae398 *flaA* under the control of its native promoter | This work |
| pBBR1MCS-5_*flaA*(AH-3) | pBBR1MCS-5 derivative containing the *Aeromonas piscicola* AH-3 *flaA* under the control of its native promoter | This work |
| pBBR1MCS-5_*flaA*(AH-3) | pBBR1MCS-5 derivative containing the *Aeromonas hydrophila* ATCC7966 *flaA* under the control of its native promoter | This work |

| | | |
|---|---|---|
| **Site-Directed Mutagenesis:** | | |
| pBBR1MCS-5_*flaB* | pBBR1MCS-5 derivative containing Sch3N *flaB* under the control of its native promoter | This work |
| pBBR1MCS-5_*flaB*(T155A) | pBBR1MCS-5 derivative containing Sch3N *flaB* with a Theronine155 to Alanine point mutation under the control of its native promoter | This work |
| pBBR1MCS-5_*flaB*(S159/161A) | pBBR1MCS-5 derivative containing Sch3N *flaB* with two point mutations (Serine159/161Alanine) under the control of its native promoter | This work |
| pBBR1MCS-5_*flaB*(S167/169A) | pBBR1MCS-5 derivative containing Sch3N *flaB* with two point mutations (Serine167/169Alanine) under the control of its native promoter | This work |
| pBBR1MCS-5_*flaB*(S159/161/167/169A) | pBBR1MCS-5 derivative containing Sch3N *flaB* with four point mutations (Serine159/161/167/169Alanine) under the control of its native promoter | This work |
| pBBR1MCS-5_*flaB*(S208/210A) | pBBR1MCS-5 derivative containing Sch3N *flaB* with two point mutations (Serine208/210Alanine) under the control of its native promoter | This work |
| pBBR1MCS-5_*flaB*(L160A) | pBBR1MCS-5 derivative containing Sch3N *flaB* with a Leucine160 to Alanine point mutation under the control of its native promoter | This work |
| pBBR1MCS-5_*flaB*(I168A) | pBBR1MCS-5 derivative containing Sch3N *flaB* with a Isoleucine168 to Alanine point mutation under the control of its native promoter | This work |
| **<u>Bacterial two-hybrid:</u>** | | |
| pUT18 | High copy number BACTH vector, allows in-frame fusion of desired protein to N-terminal of T18 | EUROMEDEX |

| | | |
|---|---|---|
| | adenylate cyclase (CyaA) domain, $Amp^R$ | |
| pUT18_*flaA* | pUT18 derivative containing Sch3N *flaA*, inserted into *Eco*R1/*Bam*HI site, $Amp^R$ | This work |
| pUT18_*flaA-CBD* | pUT18 containing Sch3N *flaA-CBD* (minus the chaperone binding domain), inserted into *Eco*R1/*Bam*HI site, $Amp^R$ | This work |
| pUT18_*flaA-D2/D3* | pUT18 containing Sch3N *flaA-D2/D3* (minus the central D2/D3 domain of FlaA), inserted into *Eco*R1/*Bam*HI site, $Amp^R$ | This work |
| pUT18_*flaB* | pUT18 derivative containing Sch3N *flaB*, inserted into *Eco*R1/*Bam*HI site, $Amp^R$ | This work |
| pUT18_*flaJ* | pUT18 derivative containing Sch3N *flaJ*, inserted into *Eco*R1/*Bam*HI site, $Amp^R$ | This work |
| pUT18_*maf1* | pUT18 derivative containing Sch3N *maf1*, inserted into *Eco*R1/*Bam*HI site, $Amp^R$ | This work |
| pUT18C | High copy number BACTH vector, allows in-frame fusion of desired protein to C-terminal of T18 adenylate cyclase domain, $Amp^R$ | EUROMEDEX |
| pUT18C_*flaA* | pUT18C derivative containing Sch3N *flaA*, inserted into *Eco*R1/*Bam*HI site, $Amp^R$ | This work |
| pUT18C_*flaA-CBD* | pUT18C containing Sch3N *flaA-CBD* (minus the chaperone binding domain), inserted into *Eco*R1/*Bam*HI site, $Amp^R$ | This work |
| pUT18C_*flaA-D2/D3* | pUT18C containing Sch3N *flaA-D2/D3* (minus the central D2/D3 domain of FlaA), inserted into *Eco*R1/*Bam*HI site, $Amp^R$ | This work |
| pUT18C_*flaB* | pUT18C derivative containing Sch3N *flaB*, inserted into *Eco*R1/*Bam*HI site, $Amp^R$ | This work |
| pUT18C_*flaJ* | pUT18C derivative containing Sch3N | This work |

| | | |
|---|---|---|
| | *flaJ*, inserted into *Eco*R1/*Bam*HI site, $Amp^R$ | |
| pUT18C_*maf1* | pUT18C derivative containing Sch3N *maf1*, inserted into *Eco*R1/*Bam*HI site, $Amp^R$ | This work |
| pKT25 | Low copy number BACTH vector, allows in-frame fusion of desired protein to C-terminal of T25 adenylate cyclase domain, $Km^R$ | EUROMEDEX |
| pKT25_*flaA* | pKT25 derivative containing Sch3N *flaA*, inserted into *Eco*R1/*Bam*HI site, $Km^R$ | This work |
| pKT25_*flaA-CBD* | pKT25 containing Sch3N *flaA-CBD* (minus the chaperone binding domain), inserted into *Eco*R1/*Bam*HI site, $Amp^R$ | This work |
| pKT25_*flaA-D2/D3* | pKT25 containing Sch3N *flaA-D2/D3* (minus the central D2/D3 domain of FlaA), inserted into *Eco*R1/*Bam*HI site, $Amp^R$ | This work |
| pKT25_*flaB* | pKT25 derivative containing Sch3N *flaB*, inserted into *Eco*R1/*Bam*HI site, $Km^R$ | This work |
| pKT25_*flaJ* | pKT25 derivative containing Sch3N *flaJ*, inserted into *Eco*R1/*Bam*HI site, $Km^R$ | This work |
| pKT25_*maf1* | pKT25 derivative containing Sch3N *maf1*, inserted into *Eco*R1/*Bam*HI site, $Km^R$ | This work |
| pKNT25 | Low copy number BACTH vector, allows in-frame fusion of desired protein to N-terminal of T25 adenylate cyclase domain, $Km^R$ | EUROMEDEX |
| pKNT25_*flaA* | pKNT25 derivative containing Sch3N *flaA*, inserted into *Eco*R1/*Bam*HI site, $Km^R$ | This work |
| pKNT25_*flaA-CBD* | pKNT25 containing Sch3N *flaA-CBD* (minus the chaperone binding domain), inserted into *Eco*R1/*Bam*HI site, $Amp^R$ | This work |
| pKNT25_*flaA-D2/D3* | pKNT25 containing Sch3N *flaA-* | This work |

| | | |
|---|---|---|
| | *D2/D3* (minus the central D2/D3 domain of FlaA), inserted into *Eco*R1/*Bam*HI site, $Amp^R$ | |
| pKNT25_*flaB* | pKNT25 derivative containing Sch3N *flaB*, inserted into *Eco*R1/*Bam*HI site, $Km^R$ | This work |
| pKNT25_*flaJ* | pKNT25 derivative containing Sch3N *flaJ*, inserted into *Eco*R1/*Bam*HI site, $Km^R$ | This work |
| pKNT25_*maf1* | pKNT25 derivative containing Sch3N *maf1*, inserted into *Eco*R1/*Bam*HI site, $Km^R$ | This work |
| pUT18C-zip | pUT18C derivative containing leucine zipper of GCN4 fused in-frame to C-terminal of T18 fragment CyaA, $Amp^R$ | EUROMEDEX (Karimova *et al.*, 1998) |
| pKT25-zip | pKT25 derivative containing leucine zipper of GCN4 fused in-frame to C-terminal of T25 fragment CyaA, $Km^R$ | EUROMEDEX (Karimova *et al.*, 1998) |

**Table 2.2** – Plasmids

$Km^R$ (kanamycin resistance), $Amp^R$ (ampicillin resistance), $Cm^R$ (chloramphenicol resistance) and $Gm^R$ (gentamicin resistance). Please refer to the appendix (page 221) for plasmid maps.

## 2.2 – Media and Antibiotics

Please refer to tables 2.3 and 2.4.

| Type of Media | Description |
|---|---|
| **Luria Broth (LB)** | 1% (w/v) tryptone (Oxoid), 0.5% (w/v) yeast extract (Oxoid), 1% (w/v) NaCl (Melford) In $dH_2O$ |
| **LB Agar** | LB (as above) 1.5% (w/v) agar (Oxoid) In $dH_2O$ |
| **Motility Agar** | 1% (w/v) tryptone (Oxoid), 0.5% (w/v) NaCl (Melford), 0.25% (w/v)agar (Oxoid) In $dH_2O$ |
| **Swarming Agar** | 0.6% (w/v) 'Eiken' agar, 0.8% (w/v) Nutrient broth (Difco), 0.5% (w/v) NaCl (Melford) In tap water |
| **Blood Agar** | Oxoid horse blood agar plates |
| **Brain-Heat Infusion Broth (BHIB)** | Difco BHI mix (40 g in 1 L $dH_2O$) |
| **BHI agar** | BHIB containing 1.5% (w/v) agar (Oxoid) |
| **MacConkey Agar** | For use in the bacterial two-hybrid system Difco MacConkey agar mix (40 g in 1 L $dH_2O$), supplemented with 1% (w/v) maltose (Melford) |

**Table 2.3** – Media

| Antibiotic | Final concentration |
|---|---|
| **Ampicillin (Melford)** | 100 µg/ml |
| **Chloramphenicol (Melford)** | 25 µg/ml |
| **Gentamicin (Melford)** | 25 µg/ml |
| **Kanamycin (Melford)** | 50 µg/ml |
| **Nalidixic Acid (Ducgefa Biochemie)** | 50 µg/ml |
| **Streptomycin (Melford)** | 50 µg/ml |

**Table 2.4** - Antibiotics

## 2.3 – Solutions and Buffers

| Solution/Buffer | Description |
|---|---|
| **Phosphate Buffered Saline (PBS)** | 10 X - 137 mM NaCl (Melford), 27 mM KCl (Melford), 14 mM $Na_2HPO_4$ (Fischer), 43 mM $KH_2PO_4$ (Sigma) - Adjust to pH 7.4<br><br>1 X - Dilute 10 X 1:9 in $dH_2O$ |
| **TAE buffer** | 50 X - 40 mM Tris (Fischer), 1.142% (w/v) Acetic acid (Melford), 1 mM EDTA (Melford)<br><br>1 X - Dilute 50 X 1:49 in $dH_2O$ |
| **SDS-PAGE running buffer (1X)** | 200 mM Glycine (Sigma), 0.1% (w/v) SDS (Sigma), 25 mM Tris base (Fisher) |
| **Western blot transfer buffer** | 10 X - 25 mM Tris base (Fischer), 200 mM Glycine (Sigma)<br><br>1 X - Dilute 10 X 1:9 in $dH_2O$ and methanol (20% methanol overall) |
| **RF1 (production of chem comp cells)** | 100 mM KCl (Melford), 50 mM $MnCl_2.4H_2O$ (Fischer), 30 mM KAc (Fischer), 10 mM $CaCl_2.2H_2O$ (Sigma), 15% (v/v) glycerol (Sigma) |
| **RF2 (production of chem comp cells)** | 10 mM MOPS (Fischer), 10 mM KCl (Melford), 75 mM $CaCl_2$ (Sigma), 15% (v/v) glycerol (Sigma) |
| **Ethidium bromide solution** | 15% (w/v) ethidium bromide (Invitrogen) in 1% TAE buffer |
| **Laemmeli Buffer (protein loading)** | 62.5 mM Tris HCl (Invitrogen) 10% (v/v) glycerol (Sigma), 2% (w/v) SDS (Sigma), 0.01 mg/ml Bromophenol blue (Invitrogen), 5% (v/v) β-Mercaptoethanol (Melford) |
| **Nitrocellulose membrane blocking buffer** | 5% (w/v) skimmed milk powder (Marvel) in 1 X PBS |
| **Lysozyme solution (for genomic DNA isolation)** | 25 mM Tris-HCl (pH8) (Invitrogen)<br>25 mM EDTA (pH8) (Invitrogen)<br>2 mg/ml Lysozyme (Sigma) |

**Table 2.5** – Solutions and buffers

## 2.4 – Growth Conditions and Genetic Manipulations

### 2.4.1 – Standard growth conditions

Overnight subcultures were set up with 10 ml of the required growth media in a 25 ml sterile universal tube and inoculated with the chosen bacterial strain. A list of bacterial strains and plasmids used in this work are shown in tables 2.1 and 2.2. Both *E. coli* and *A. caviae* were generally grown at 37°C, with agitation, or as directed.

### 2.4.2 – Glycerol stocks

Glycerol stocks were created by making an overnight subculture of the desired strain and pipetting 500 µl of the culture into a 1.5 ml microcentrifuge containing 500 µl of 50% glycerol (25% glycerol overall). Stocks were stored at -80°C.

### 2.4.3 – Growth Curves

Growth curves were carried out in triplicate, in BHIB, over the course of 7 hrs for the required strains. Overnight subcultures were set up of the desired strain and used to inoculate 50 ml flasks of BHIB the following day (1:100). The optical density was measured of each flask every hour by pipetting 1 ml samples into a 1 ml plastic cuvette (Sarstedt) and measuring the $OD_{600}$ on a Pharmacia LKB spectrophotometer. Average measurements were obtained for each time-point (n=3) and GraphPad Prism was used to analyse the data collected.

### 2.4.4 – Swimming motility assays

Swimming motility assays were carried out by setting up an overnight subculture of the desired bacterial strain. Motility agar was melted using a bench top autoclave and allowed to cool to around 50°C before pouring. If required, IPTG was added to the media at a final concentration of 1 mM. The assays were carried out on large square petri dishes (300 X 300 mm) (Fischer) holding 250 ml of motility agar. 1 ml of the overnight subculture was pelleted (13000 X *g*) in a 1.5 ml microcentrifuge tube (Eppendorf) and the supernatant removed. The motility agar was inoculated by dipping a sterile cocktail stick into the remaining bacterial pellet and piercing the agar; large motility plates could fit between 16 – 24 individual inoculants on them. Motility plates were incubated aerobically, overnight, at room temperature. Plates were analysed by manually measuring the radius of any motility halos present, usually after 16 hr incubations (unless otherwise stated) and data was analysed with GraphPad Prism.

## 2.4.5 – Swarming motility assays

Swarming motility assays were carried out as above (section 2.4.3) but with swarming motility agar.

## 2.4.6 – Bacterial adenylate cyclase two-hybrid system (BACTH system)

The bacterial two-hybrid system was carried out using the Euromedex BACTH system kit following the protocol provided. The required BACTH plasmids (containing genes of interest) (plasmid diagrams in the appendix, page 221) were co-transformed into chemically competent *E. coli* BTH101 (section 2.4.15) and plated onto MacConkey agar supplemented with 1% (w/v) maltose for analysis of interactions. Plates were incubated for 1-3 days at 30°C (incubation up to 5 days if necessary).

## 2.4.7 – Isolation of Genomic DNA (Phenol/Chloroform Extraction)

Bacteria were harvested from 10 ml BHIB overnight subcultures via centrifugation at 3,000 X *g* for 10 mins at 4°C. Cell pellets were resuspended in 500 µl of lysozyme solution (Table 2.5), transferred to 1.5 ml microcentrifuge tubes and incubated at 37°C for 1 hr. Following incubation, 50 µl of 10% (w/v) SDS was added and samples incubated for a further 15 mins at 37°C. Samples were then gently mixed (by inverting the tube) for 5 mins or until the solutions became less viscous. Subsequently, 300 µl of phenol/chloroform/isoamyl alcohol was added to the samples which were then gently mixed and centrifuged at 16,000 X *g* for 8 mins. The aqueous phase was removed following centrifugation and transferred to a fresh microcentrifuge tube. The aqueous phase of each sample was mixed with 200 µl of $dH_2O$ to decrease the viscosity and the Phenol/Chloroform step repeated. DNA precipitation was achieved by adding 1 volume of ice-cold isopropanol and 0.1 volumes of 3 M sodium acetate to the samples and incubating on ice for 10 mins. DNA was recovered via centrifugation at 16,000 X *g* for 5 mins. The DNA pellet was washed with 70% (v/v) ethanol before being dissolved in 500 µl of elution buffer (Qiagen) for 2 hours at room temperature. DNase free RNase at a final concentration of 40 µg/ml was added to the samples and incubated at 37°C for 30 mins. Finally, the DNA was precipitated as before, washed with 70% (v/v) ethanol and dissolved in 100 µl of elution buffer.

DNA precipitation was achieved by adding 0.1 volumes of 3 M sodium acetate and 1 volume of ice cold isopropanol and incubating on ice for 10 minutes. Genomic DNA was diluted to a concentration of 50 ng/µl for PCR reactions.

## 2.4.8 – Plasmid purification

Plasmid purification was carried out from an overnight subculture of the bacterial strain containing the desired plasmid in LB. An Omega E.Z.N.A plasmid miniprep kit II was used to extract and purify the plasmid according to the manufacturer's guidelines, from 1.5 ml of bacterial culture. Pure plasmids were eluted into a 1.5 ml microcentrifuge tube in 30 µl of elution buffer from the kit (unless otherwise stated) and stored at -20°C.

## 2.4.9 – Agarose gel electrophoresis

To determine the size of DNA samples, agarose gel electrophoresis was used. TAE-based 1% agarose gels (Fischer) were produced and samples loaded onto the gel with Qiagen Gelpilot loading dye. Samples were run alongside a DNA ladder, such as Q step 4 DNA ladder (YorkBio), at 90 V for 1 hr with a BIO-RAD power pack. The gels were post-stained with ethidium bromide solution (table 2.5) for 10 mins to allow visualisation of DNA under UV light.

## 2.4.10 – Gel extraction

Gel extractions were carried out to isolate DNA fragments from an agarose gel after agarose gel electrophoresis with the use of QIAGEN gel extraction buffers according to the manufacturer's guidelines.

## 2.4.11 - Restriction digests

Restriction digests were set up to check the size of plasmids or produce DNA fragments/plasmids with the required sticky ends for cloning. The digests were set up with the appropriate restriction enzyme and corresponding buffer according to the manufacturer's guidelines (NEB). Typically 5 units of enzyme was used per 1 µg of DNA to be digested. The size of digested DNA was checked via agarose gel electrophoresis (section 2.4.9).

## 2.4.12 – Ligation

Ligation reactions were set up with T4 DNA ligase (Promega) and the corresponding buffer according to the manufacturer's guidelines (Promega).

The 10 µl reactions were carried out with insert DNA and vector DNA at a 3:1 molar ratio, using 0.1-1 units of T4 DNA ligase. Reactions were incubated at room temperature for 16 hrs.

## 2.4.13 – Conjugation

The *E. coli* strain S17-1 λ *pir* (table 2.1) was used as the donor strain to conjugate the desired expression vector [such as pSRK(Gm) or pBBR1MCS-5 containing an insert] into an *A. caviae* (recipient) strain.

In preparation for conjugative transfer, the expression vector was transformed into chemically competent *E. coli* S17-1 λ *pir* (section 2.4.15). Overnight subcultures were set up of the resulting *E. coli* S17-1 λ *pir* strains and the required *A. caviae* (recipient) strains.

The 10 ml subcultures were centrifuged in sterile 15 ml falcon tubes for 8 mins (2,800 X *g*). The supernatant was removed and pellet resuspended in 5 ml of sterile PBS to remove any antibiotics present and centrifugation was carried out as before. The PBS wash step was repeated and the final *E. coli* S17-1 λ *pir* pellets were resuspended in 1 ml PBS (more/less depending on number of conjugations carried out).

The recipient pellet was then resuspended in 0.5 ml of the *E. coli* S17-1 λ *pir* suspension and 200 µl of the resulting suspension was plated onto a blood agar plate (Oxoid). Plates were incubated for 8 h at 37°C.

After incubation the bacterial lawn was scraped off the blood agar plate and resuspended in 1 ml of sterile PBS and pipetted into a 1.5 ml microcentrifuge tube. The cell suspension collected was serially diluted 3 times (1:10/1:100/1:1000) into separate 1.5 ml microcentrifuge tubes (100 µl cell suspension added to 900 µl PBS).

A volume of 200 µl from each cell suspension was spread onto BHI agar containing the appropriate antibiotics to select for *A. caviae* containing the vector. Plates were incubated overnight at 37°C.

An oxidase test (section 2.4.14) was carried out on resulting colonies to ensure the bacterial growth was *Aeromonas* and colony PCR (section 2.6.2.4) carried out where required to ensure the strain contained the desired gene. Suitable controls were carried out with empty expression vectors.

## 2.4.14 – Oxidase test

Oxidase tests were carried out on the resulting colonies from bacterial conjugation to test for the presence of *Aeromonas caviae*. Filter paper was soaked in 1% tetramethyl-p-phenylenediamine dihydrochloride (electron donor) and a single bacterial colony was rubbed onto the paper using a sterile loop. A colour change (dark purple) can be visualised if the bacteria are oxidase positive (*Aeromonas*) or no colour change if oxidase negative (*E. coli*).

## 2.4.15 – Bacterial transformation into chemically competent *E. coli*

### 2.4.15.1 - Production of chemically competent cells

An overnight subculture was set up of the *E. coli* strain to be made chemically competent for the uptake of plasmid DNA. Subsequently, the subculture was used to inoculate a flask of LB (100 ml) (1:100) which was then incubated for around 2 hrs at 37°C until an $OD_{600}$ of 0.6 (exponential phase of growth) was reached. Once at the desired $OD_{600}$ the culture was incubated on ice for 15 mins, after which it was transferred to a 50 ml falcon tube and centrifuged at 2,800 X *g* for 10 mins at 5°C. The supernatant was discarded and cell pellet gently resuspended in 20 ml of sterile ice-cold RF1 (table 2.5). The cell suspension was incubated on ice for 30 mins and then centrifuged at 2,800 X *g* for 10 mins at 5°C. The supernatant was discarded and cell pellet gently resuspended in 700 µl of sterile ice-cold RF2. The chemically competent cells were then pipetted into separate 1.5 ml microcentrifuge tubes in 100 µl aliquots and stored at -80°C.

### 2.4.15.2 - Transformation

Chemically competent cells to be transformed and plasmid DNA to be introduced into these cells were thawed on ice. The required amount of plasmid DNA (Generally 1 µl of a plasmid miniprep) was transferred into a sterile microcentrifuge tube and gently mixed with 100 µl of chemically competent cells. The DNA/cell mixture was incubated on ice for 30 mins before being heat shocked at 42°C for 1 min 30 secs. Cells were cooled on ice for a further 5 mins before 900 µl of LB was added to the samples. Cells were allowed to recover by incubation at 37°C for 1 hr.

Recovered cell samples were then centrifuged at 16,000 X *g* for 1 min and the supernatant discarded. Cell pellets were resuspended in 100 µl of fresh LB and plated onto agar plates containing suitable antibiotics to select for any transformants. The plates were incubated overnight at 37°C (unless otherwise stated). Where IPTG induction of plasmid genes was required, IPTG (Invitrogen) was added to the agar plates at a final concentration of 1 mM.

## 2.6 – Polymerase Chain reaction (PCR)

Polymerase chain reaction (PCR) was carried out in 50 µl reactions, in thin-walled PCR tubes (Eppendorf) using a BIO-RAD T100$^{TM}$ Thermal Cycler (PCR machine).

Different PCR conditions were utilised depending on the reaction being carried out. The general PCR reaction mixture used was as follows:

- 1 µl Forward primer (2 pmol/µl)
- 1 µl Reverse primer (2 pmol/µl)
- 1 µl Template DNA (50-200 ng)
- 1 µl 25 mM $MgCl_2$ (Where necessary)
- 5 µl 10 X buffer (or 10 µl 5 X buffer for Q5 DNA polymerase)
- 2.5 µl 100% Dimethyl sulfoxide (DMSO)
- 1 µl dNTPs (10 mM stock, Roche)
- 1 µl polymerase (2.5 U per reaction)
- Make up to 50 µl with molecular grade $dH_2O$

## 2.6.1 – Primers

Please refer to table 2.6 below.

| Primer | Relevant Characteristics | Reference |
|---|---|---|
| JLP_28 | 5'ATATATAT**CATATG**GTGGTGGTGAAGAAGTC 3' (Forward)<br><br>Insertion of *AHA0618* into the expression vector pSRK(Gm), contains an **NdeI** restriction site | This work |
| JLP_29 | 5'TATTAT**GGATCC**TCAGGGCTCGATGATGATGG 3'(Reverse)<br><br>Insertion of *AHA0618* into the expression vector pSRK(Gm), contains a **BamHI** restriction site | This work |
| JLP_108 | 5'**CATATG**AAAAAGGTATTACCGGCTTTATTAATG 3'(Forward)<br><br>Insertion of *H. pylori* 26695 *HP0518* into the expression vector pSRK(Gm), contains an **NdeI** restriction site | This work |
| JLP_109 | 5'**GGATCC**CTATTTTTCCATTATAATAGACACTTGATTGTT 3'<br><br>(Reverse)<br><br>Insertion of *H. pylori* 26695 *HP0518* into the expression vector pSRK(Gm), contains a **BamHI** restriction site | This work |
| RCL_53 | 5'GCGC**CATATG**AGTCTGTATATCAATACCAACGTTTC 3' (Forward)<br><br>Insertion of *A. caviae* Sch3N *flaA* into the expression vector pSRK(Gm), contains an **NdeI** restriction site | This work |
| RCL_54 | 5' GCGC**AAGCTT**TTATTTCTGCAGCAGGGAG 3' (Reverse)<br><br>Insertion of *A. caviae* Sch3N *flaA* into the expression vector pSRK(Gm), contains a **HindIII** restriction site | This work |
| RCL_49 | 5' GCGC**CATATG**GGTCTTTATATCAATACGAACGTTTC 3' (Forward)<br><br>Insertion of *A. piscicola* AH-3 *flaA* into the expression vector pSRK(Gm), contains an **NdeI** restriction site | This work |
| RCL_50 | 5' GCGC**AAGCTT**TTAGCCTTGCAGCAGCG 3' (Reverse)<br><br>Insertion of *A. piscicola* AH-3 *flaA* into the expression vector pSRK(Gm), contains an **HindIII** restriction site | This work |
| RCL_51 | 5' GCGC**CATATG**GCCATGTATATCAACACGAATACT 3' (Forward)<br><br>Insertion of *A. hydrophila* ATCC7966 *flaA* into the expression vector pSRK(Gm), contains an **NdeI** restriction site | This work |

| | | |
|---|---|---|
| RCL_52 | 5’ GCGC**AAGCTT**TTAACCCAGCAGGGACAG 3’ (Reverse)<br><br>Insertion of *A. hydrophila* ATCC7966 *flaA* into the expression vector pSRK(Gm), contains an **HindIII** restriction site | This work |
| RCL_60 | 5’ GCGC**CATATG**ATGGATATTTATCAAAAAAACTTGC 3’ (Forward)<br><br>Insertion of *H. pylori* 26695 *maf1* into the expression vector pSRK(Gm), contains an **NdeI** restriction site | This work |
| RCL_61 | 5’ GCGC**GGATCC**TTACCATTCTTTTAAAGCCATTT 3’ (Reverse)<br><br>Insertion of *H. pylori* 26695 *maf1* into the expression vector pSRK(Gm), contains an **BamHI** restriction site | This work |
| RCL_62 | 5’ GCGC**CATATG**CCCTTTTTAAAAGCCCTAGAAT 3’ (Forward)<br><br>Insertion of *H. pylori* 26695 *maf2* into the expression vector pSRK(Gm), contains an **NdeI** restriction site | This work |
| RCL_63 | 5’ GCGC**GGATCC**TCATGGTTGTTTGAGTTGC 3’ (Reverse)<br><br>Insertion of *H. pylori* 26695 *maf2* into the expression vector pSRK(Gm), contains an **BamHI** restriction site | This work |
| RCL_71 | 5’ GCGC**AAGCTT**GTCTTGTGAAAAGGCGCCG 3’ (Forward)<br><br>Insertion of *A. caviae* Sch3N *flaA* into pBBR1MCS-5, including the native promoter and contains a **HindIII** restriction site | This work |
| RCL_72 | 5’ GCGC**GGATCC**CTTCAGAACCTTATTTCTGCAGCAG 3’ (Reverse)<br><br>Insertion of *A. caviae* Sch3N *flaA* into pBBR1MCS-5 and contains a **BamHI** restriction site | This work |
| RCL_28 | 5’ GCGC**AAGCTT**GCCGTTAACTAAACATATCAGG 3’ (Forward)<br><br>Insertion of *A. caviae* Ae398 *flaA* into pBBR1MCS-5, including the native promoter and contains a **HindIII** restriction site | This work |
| RCL_29 | 5’ GCGC**GGATCC**CATGTTGACGGTTTAACCG 3’ (Reverse)<br><br>Insertion of *A. caviae* Ae398 *flaA* into pBBR1MCS-5 and contains a **BamHI** restriction site | This work |
| RCL_30 | 5’ GCGC**AAGCTT**CATCGAACATGAAAGACAATAAAG 3’ (Forward)<br><br>Insertion of *A. piscicola* AH-3 *flaA* into pBBR1MCS-5, including the native promoter and contains a **HindIII** restriction site | This work |

| | | |
|---|---|---|
| RCL_31 | 5’ GCGC**GGATCC**CAACCGCCCTGTTTTC 3’ (Reverse)<br><br>Insertion of *A. piscicola* AH-3 *flaA* into pBBR1MCS-5 and contains a **BamHI** restriction site | This work |
| RCL_32 | 5’ GCGC**AAGCTT**GGATCGTTCAACCTGTTC 3’ (Forward)<br><br>Insertion of *A. hydrophila* ATCC7966 *flaA* into pBBR1MCS-5, including the native promoter and contains a **HindIII** restriction site | This work |
| RCL_34 | 5’ GCGC**TCTAGA**CTATCTCATCACTGCGTTTC 3’ (Reverse)<br><br>Insertion of *A. hydrophila* ATCC7966 *flaA* into pBBR1MCS-5 and contains a **XbaI** restriction site | This work |
| | **Site-Directed Mutagenesis Primers** | |
| RCL_55 | 5’ GCGC**AAGCTT**AGGCAGACTCGTTCAAGCTGT 3’ (Forward)<br><br>Insertion of *A. cavie* Sch3N *flaB* into pBBR1MCS-5 and contains a **HindIII** restriction site | This work |
| RCL_56 | 5’ GCGC**GGATCC**CTGCTCCTCATATCAATGATGTTG 3’ (Reverse)<br><br>Insertion of *A. cavie* Sch3N *flaB* into pBBR1MCS-5 and contains a **BamHI** restriction site | This work |
| B T155A (R) | 5’ CTAAACCCAAT**GGC**CTGATTGGC 3’ (Reverse)<br><br>To be used in conjunction with RCL_55 to form the front section of *flaB* for overlap extension PCR. Incorporates a T155A site-directed mutation into FlaB. | This work |
| B T155A (F) | 5’ 3’ GCCAATCAG**GCC**ATTGGGTTTAG (Forward)<br><br>To be used in conjunction with RCL_56 to form the back section of *flaB* for overlap extension PCR. Incorporates a T155A site-directed mutation into FlaB. | This work |
| B S159/161A (R) | 5’ GGCTT**GAG**CCA**AGG**CAAACCCAA 3’ (Reverse)<br><br>To be used in conjunction with RCL_55 to form the front section of *flaB* for overlap extension PCR. Incorporates S159/161A site-directed mutations into FlaB. | This work |
| B S159/161A (F) | 5’ TTGGGTTTG**CCT**TGG**CTC**AAGCC 3’ (Forward)<br><br>To be used in conjunction with RCL_56 to form the back section of Sch3N *flaB* for overlap extension PCR. Incorporates S159/161A site-directed mutations into FlaB. | This work |
| B S167/169A (R) | 5’ CAATCCC**AGC**AAT**GGC**GAACCCTC 3’ (Reverse) | This work |

| | | |
|---|---|---|
| | To be used in conjunction with RCL_55 to form the front section of *flaB* for overlap extension PCR. Incorporates S167/169A site-directed mutations into FlaB. | |
| B S167/169A (F) | 5’ GAGGGTTC**GCC**ATT**GCT**GGGATTG 3’ (Forward)<br><br>To be used in conjunction with RCL_56 to form the back section of *flaB* for overlap extension PCR. Incorporates S167/169A site-directed mutations into FlaB. | This work |
| B L160A (R) | 5’ GGCTTGAGA**CGC**GCTAAACCCAA 3’ (Reverse)<br><br>To be used in conjunction with RCL_55 to form the front section of *flaB* for overlap extension PCR. Incorporates an L160A site-directed mutation into FlaB. | This work |
| B L160A (F) | 5’ TTGGGTTTAGC**GCG**TCTCAAGCC 3’ (Forward)<br><br>To be used in conjunction with RCL_56 to form the back section of *flaB* for overlap extension PCR. Incorporates an L160A site-directed mutation into FlaB. | This work |
| B I168A (R) | 5’ CAATCCCAGA**AGC**GCTGAACCCTC 3’ (Reverse)<br><br>To be used in conjunction with RCL_55 to form the front section of *flaB* for overlap extension PCR. Incorporate an I168A site-directed mutation into FlaB. | This work |
| B I168A (F) | 5’ GAGGGTTCAGC**GCT**TCTGGGATTG 3’ (Forward)<br><br>To be used in conjunction with RCL_56 to form the back section of *flaB* for overlap extension PCR. Incorporates an I168A site-directed mutation into FlaB. | This work |
| B S208/210A (R) | 5’ CTCTGAGT**AGC**AAT**AGC**GATGCCACC 3’ (Reverse)<br><br>To be used in conjunction with RCL_55 to form the front section of *flaB* for overlap extension PCR. Incorporates S208/210A site-directed mutations into FlaB. | This work |
| B S208/210A (F) | 5’ GGTGGCATC**GCT**ATT**GCT**ACTCAGAG 3’ (Forward)<br><br>To be used in conjunction with RCL_56 to form the back section of *flaB* for overlap extension PCR. Incorporates S208/210A site-directed mutations into FlaB. | This work |
| | **Bacterial Two-Hybrid Primers**<br><br>All forward primers contain *Bam*HI restriction sites and reverse primers contain *Eco*RI sites | |
| JLP_39 | 5’ **GGATCC**CATGAGTCTGTATATCAATACCAAC 3’ (Forward)<br><br>Insertion of *flaA*, *flaA*-CBD and *flaA*-D2/D3, in to all four | Lab collection |

| | | |
|---|---|---|
| | bacterial two-hybrid vectors (pUT18, pUT18C, pKT25 & pKNT25) | |
| JLP_40 | 5' **GAATTC**TTATTTCTGCAGCAGGGAGA 3' (Reverse)<br><br>Insertion of *flaA* and *flaA*-D2/D3 into pUT18C and pKT25 (tag at N-terminal) | Lab collection |
| JLP_53 | 5' **GAATTC**GAGTTCTGCAGCAGGGAGAG 3' (Reverse)<br><br>Insertion of *flaA* and *flaA*-D2/D3 into pUT18 and pKNT25 (tag at C-terminal) | Lab collection |
| RCL_01 | 5' **GAATT**CTTATGCATCGCGGATACGAGA 3' (Reverse)<br><br>Insertion of *flaA*-CBD into pUT18C and pKT25 (tag at N-terminal) | This work |
| RCL_02 | 5' **GAATT**CGATGCATCGCGGATACGAGA 3' (Reverse)<br><br>Insertion of *flaA*-CBD into pUT18 and pKNT25 (tag at C-terminal) | This work |
| RCL_17 | 5'GGTTCTGCACCGCACCCAGTTCTGCTCGAGTACCGCTAAATGAACCATCAAG 3' (Reverse)<br><br>To be used with JLP_39 to create the front section of *flaA*-D2/D3. The construct was then created via overlap extension PCR with the back sections of the gene | This work |
| RCL_18 | 5'CTGCTTGATGGTTCATTTAGCGGTACTCGAGCAGAACTGGGTGCG 3' (Forward)<br><br>To be used alongside either JLP_40 or JLP_53 to create the back sections of *flaA*-D2/D3. Overlap extension PCR was then used with the front gene fragment to create *flaA-D2/D3* | This work |
| JLP_47 | 5' **GGATCC**CATGGCCATGTATATCAATACCAATAC 3' (Forward)<br><br>Insertion of *flaB* into all four bacterial two-hybrid vectors | Lab collection |
| JLP_48 | 5' **GAATTC**TTAACCCAGCAGCTGCAG 3' (Reverse)<br><br>Insertion of *flaB* into pUT18C and pKT25 (tag at N-terminal) | Lab collection |
| JLP_52 | 5' **GAATTC**GAACCCAGCAGCTGCAG 3' (Reverse)<br><br>Insertion of *flaB* into pUT18 and pKNT25 (tag at C-terminal) | Lab collection |
| JLP_41 | 5' **GGATCC**CATGTACAAGCGCAATATCAAAGC 3' (Forward)<br><br>Insertion of *flaJ* into all four bacterial two-hybrid vectors | This work |
| RCL_20 | 5' **GAATTC**TCATAGCTCACCCAACTGC 3' (Reverse) | This work |

| | | |
|---|---|---|
| | Insertion of *flaJ* into pUT18 and pKNT25 (tag at C-terminal) | |
| RCL_21 | 5' **GAATTC**GATAGCTCACCCAACTGCTG 3' (Reverse)<br><br>Insertion of *flaJ* into pUT18C and pKT25 (tag at N-terminal) | This work |
| RCL_79 | 5' ATAT**GGATCC**CATGTCACTCAATATAGATGTAGCTTTG 3' (Forward)<br><br>Insertion of *maf1* into all four bacterial two-hybrid vectors | This work |
| JLP_44 | 5' **GAATTC**TTATTTTTTGAATAGTACAATAACTTCATTG 3' (Reverse)<br><br>Insertion of *maf1* into pUT18C and pKT25 (tag at N-terminal) | This work |
| JLP_50 | 5'**GAATTC**GATTTTTTGAATAGTACAATAACTTCATTGTCTATC 3' (Reverse)<br><br>Insertion of *maf1* into pUT18 and pKNT25 (tag at C-terminal) | This work |

**Table 2.6 – Primers**

Primers were obtained at an initial concentration of 100 pmol/µl. With regards to the bacterial two-hybrid primers: Reverse primers for the insertion of desired genes into pKNT25 and pUT18 have the stop codon removed due to being able to make use of the adenylate cyclase domain stop codon downstream (tagged at the C-terminal). All forward primers possess an EcoRI restriction site (GAATTC) and all reverse primers a BamHI restriction site (GGATCC) at the 5' end. Together these allow insertion of the amplified gene fragments into the bacterial two-hybrid plasmids cut with these enzymes.

JLP primers were created by Dr Jennifer L Parker.

## 2.6.2 – PCR cycles

### 2.6.2.1 - Expand high fidelity PCR (Roche)

The Roche Expand High Fidelity PCR kit was utilised due to being a mixture of 2 polymerases: one allowing high fidelity amplification of target genes due to its proofreading (3'-5' exonuclease) activity and another for the addition of non-templated adenines to the PCR product (useful in TA-cloning). This allowed the amplified gene to be ligated into the storage vector, pGEM-T-EASY (Promega). A general PCR cycle was used to amplify target genes (see below) and was tailored according to the size of the gene and the primers used. An annealing temperature of 5°C below the melting temperature (Tm) of the primers was used

- Initial denaturation step - 94°C – 2 mins
- Denaturation - 94°C - 15 secs
- Annealing – 45 - 65°C - 30 secs
- Extension - 72°C - 1 min/kb

X 10

- Denaturation - 94°C - 15 secs
- Annealing (generally 1°C increase) – 45- 68 - 30 secs
- Extension - 72°C - 1 min/kb

X 20

- Final elongation - 72°C - 2 mins

### 2.6.2.2 – Q5 DNA polymerase (NEB)

With Q5 DNA polymerase (NEB), again the PCR cycle was adjusted according to the size of the gene being amplified and to the Tm of the primers. NEB suggest an annealing temperature of 3°C above the Tm (of the primer with the lowest Tm). The following PCR cycle was used:

- Initial denaturation - 98°C – 30 secs
- Denaturation - 98°C – 10 secs
- Annealing – 50-72°C – 30 secs
- Extension - 72°C – 30 secs/kb

X 30

- Final extension - 72°C – 2 mins

### 2.6.2.3 – Overlap extension PCR (for site-directed mutagenesis)

Overlap extension PCR (OE-PCR) was carried out to introduce point mutations into proteins or to splice together different sections of a gene using Q5 DNA polymerase (section 2.6.2.2). Two rounds of PCR reactions were carried out:

**Round 1** – The first round of OE-PCR was carried out to amplify individually the desired sections of a gene to be spliced together. Generally two reactions were carried out, using the

cycle described for Q5 DNA polymerase in section 2.6.2.2. Reverse primer 1 and forward primer 2 (please refer to figure 2.1) were designed containing overlapping tails complementary to the opposite PCR product, enabling the PCR products from round 1 to bind and become a single PCR product during round 2.

**Round 2** – PCR products from round 1 were both used as the template DNA in this round of OE-PCR (in equal quantities) with both of the outside primers (forward primer 1 and reverse primer 2) being used to produce one large PCR product (Fig 2.1). The following PCR cycle was used, with the annealing temperature and extension time depending on the size of the desired gene product and the Tm of the primers:

- Initial denaturation - 98°C – 5 mins
- Denaturation - 98°C – 10 secs
- Annealing – 50-72°C – 30 secs
- Extension - 72°C – 1 min/kb

X 30

- Final extension - 72°C – 5 mins

### 2.6.2.4 – Colony PCR

Colony PCRs were carried out with Taq DNA polymerase (NEB). General PCR mixtures were set up on ice without any template DNA and a fresh bacterial colony of interest inoculated into the mixture using a sterile pipette tip. The following PCR cycle was used, with the extension time and annealing temperature adjusted where necessary depending on the gene being screened for and the Tm of the primers (annealing temperature of 5°C lower than the Tm was used):

- Initial denaturation - 95°C – 5 mins
- Denaturation - 95°C – 15 secs
- Annealing – 45-68°C – 30 secs
- Extension - 68°C – 1 min/kb

X 30

- Final extension - 68°C – 5 mins

## 2.6.3 – PCR product purification

PCR product size was checked by running 5 µl of the PCR reaction on an agarose gel (section 2.4.9) and if correct was purified with QIAGEN buffers: buffer PB (binding buffer), buffer PE (wash buffer) and buffer EB (elution buffer), following the manufacturer's guidelines.

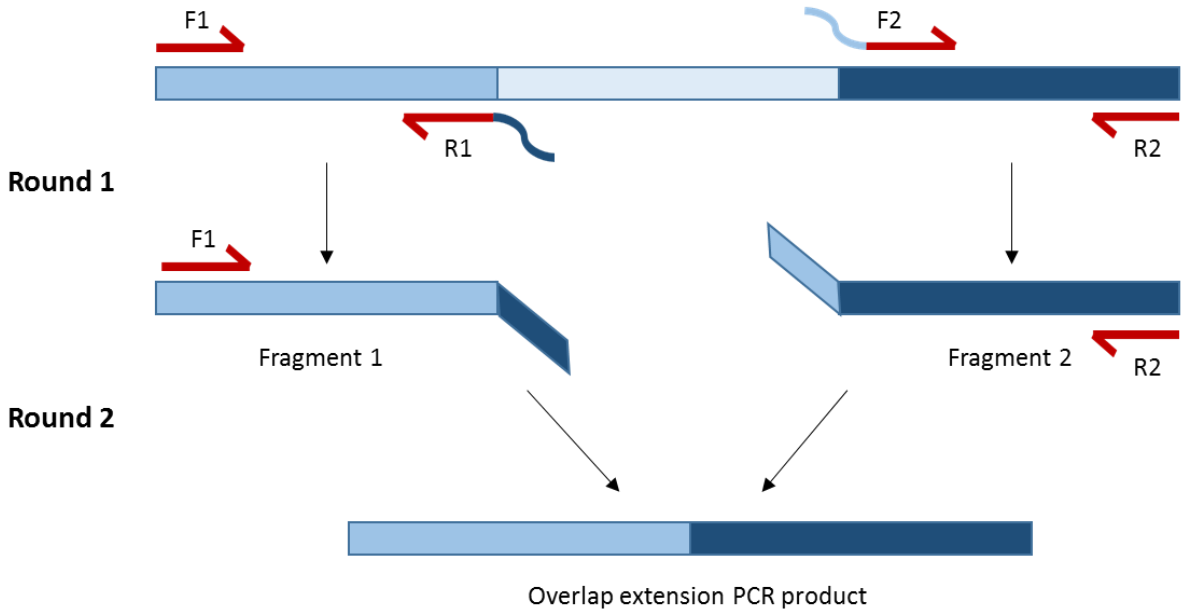


**Figure 2.1 – Overlap extension PCR (OE-PCR)**

Diagram summarising the two rounds of PCR carried out in OE-PCR. Round one amplifies the desired gene fragments to be spliced together. Fragment one is amplified from forward primer one (F1) and reverse primer one (R1) and fragment two amplified from forward primer two (F2) and reverse primer two (R2). During round two of OE-PCR, fragment one and two are merged together using primers F1 and R2.

### 2.6.4 – DNA sequencing

DNA was sequenced by the Genomic Medicine Service at the Medical School of Sheffield University.

Sequencing reaction results were checked using FinchTV software and the online application, EMBOSS NEEDLE Pairwise Sequence Alignment (Nucleotide):

http://www.ebi.ac.uk/Tools/psa/emboss_needle/nucleotide

## 2.7 – Protein and Purification Methods

### 2.7.1 – Protein precipitation

Protein precipitation (ie. precipitation of supernatant proteins) was carried out by adding two volumes of ice-cold ethanol to the desired proteins (in solution) and incubating on ice for 1-3 hrs. Precipitated proteins were pelleted at 3,900 x *g* for 30 mins at 4°C. After centrifugation, the supernatant was discarded and the protein pellet allowed to dry in the air for 10 mins. Precipitated protein samples were then boiled in Laemmli buffer and analysed by SDS-PAGE (Section 2.7.2). In general, for Western blot analysis of bacterial supernatant samples, 10 ml overnight subcultures were used (unless otherwise stated).

### 2.7.2 – SDS-PAGE (Sodium dodecyl sulphate polyacrylamide gel electrophoresis)

Whole cell protein samples and pure protein samples were analysed on a 12% polyacrylamide gel in a geneflow (OmniPAGE Mini) SDS-PAGE gel tank.

To produce two gels (approximately 7 mls each) the following recipe was used:

**Resolving gel:** 3.3 ml $dH_2O$, 4 ml 30% acrylamide (37.5:1 acrylamide:bisacrylamide) (Geneflow), 2.5 ml 1.5 M Tris-HCl (pH 8.8), 50 µl 20% SDS (Melford), 200 µl 10% (w/v) Ammonium persulphate (APS) (Melford), 7 µl Tetramethylethylenediamine (TEMED) (Fluka).

**Stacking gel:** 2.7 ml $dH_2O$, 0.67 ml 30% Acrylamide (Geneflow), 1 ml 0.5 M Tris-HCl (pH 6.8), 40 µl 20% (w/v) SDS (Melford), 40 µl 10% (w/v) APS, 5 µl TEMED (Fluka).

Two sets of gel plates compatible with the geneflow (OmniPAGE Mini) SDS-PAGE gel tank were inserted into the gel casting apparatus. The resolving gel was produced first and levelled off with the addition of 0.5 ml of isopropanol. Once set, the isopropanol was removed from the top of each gel before the stacking gel was prepared and pipetted on top of the resolving gels. A comb compatible with the gel plates was inserted into the stacking gel to form the wells and the gel was allowed to set. The gel units were then transferred into the gel tank containing 1 X SDS-PAGE running buffer. Samples, boiled in laemmli buffer, were pipetted into the stacking gel wells and were run alongside a protein marker (geneflow 17-190 kD prestained ladder) at 160 V via a QIAGEN power pack until the loading dye had passed through the length of the gel.

Once run, protein gels were stained with instant blue (Gentaur) to visualise proteins present.

### 2.7.3 – Western blotting

Protein gels were run according to section 2.7.2. Once run, the gel was removed from the gel plates and placed in a Western blotting cassette (BIO-RAD), along with a nitrocellulose

membrane (Invitrogen) for proteins to be transferred onto, sandwiched between sponges and blotting paper. The cassette was placed into a BIO-RAD Western blotting tank containing 1 X transfer buffer and the transfer was carried out overnight at 10 V.

Following transfer the nitrocellulose membrane was incubated in 20 mls of blocking buffer for 1 hr with shaking. The blocking buffer was removed and the membrane was incubated in 20 mls of PBS (containing 0.3% [w/v] skimmed milk powder - Marvel) and the required primary antibody for 1 h. The primary antibody was removed and the membrane was three times washed in 20 mls of PBS for 10 minutes. The membrane was then incubated in 20 mls of PBS (containing 0.3% [w/v] skimmed milk powder - Marvel) and the required secondary antibody conjugated to horseradish peroxidase (1:1000) for 1 h. The membrane was washed as before with PBS. Bands were visualised using ECL Western blotting detection reagents (Pierce) according to the manufacturer's instructions. For detection of the signal the membrane was exposed to X-ray film (Thermo), adjusting the exposure time to allow for optimisation of the signal.

Densitometry analysis of Western blots was carried out using ImageJ software.

### 2.7.4 – Flagella Isolation

*Aeromonas* flagella were isolated via a shearing and centrifugation method developed from Wilhelms *et al.* (2012). An overnight subculture of the desired strain (5 ml) was spread onto a large swarm plate (section 2.4.5) and incubated overnight at 37°C. Subsequent bacterial growth was scraped off the swarm plate using 20 ml PBS and transferred to a 50 ml oakridge polypropylene centrifuge tube (Thermo Scientific)centrifuge tube. Cell suspensions were vortexed and manually shaken for 10 mins to shear the flagella from the cell bodies and three centrifugation steps carried out to pellet the flagella. Cell suspensions were centrifuged first at 8,000 x *g* for 30 mins; the supernatant was collected in a fresh tube and centrifuged at 18,000 x *g* for 20 mins. Again the supernatant was collected in a fresh tube and centrifuged at 75,000 x *g* for 1.5 hrs. The supernatant was then discarded and the jelly pellet present in the centrifuge tube (containing the flagella) resuspended in PBS and stored at -20°C.

### 2.7.5 – LPS Extraction and Analysis

LPS extractions were carried out using the LPS extraction kit from ChemBio according to the manufacturer's guidelines. LPS was analysed on a 12% polyacrylamide gel (section 2.7.2) containing 4 M urea in both the resolving and stacking gels and visualised by silver staining (Guardpetter *et al.*, 1995). Silver staining was carried out using the BioRad silver staining kit.

## 2.7.6 – Peptidoglycan (PG) Extraction and Analysis

### 2.7.6.1 - PG Extraction

To extract the PG of Gram negative bacteria, a 10 ml overnight bacterial subcultures were used to inoculate a 1 L flasks of BHIB (1:100). Cultures were grown to an $OD_{600}$ of 0.7 and cells harvested at 5,000 x *g* for 10 mins at room temperature. Cell pellets were resuspended in 5 ml MiliQ water, transferred to a 50 ml falcon tubes (SLS) and frozen at -80°C. A beaker of water was boiled on a hot-plate (SLS) and holes were made in the 50 ml falcon tube lids before they were plunged into the boiling water. Magnetic stirring bars (7 mm x 2 mm) were added to the thawed cell suspensions, allowing continuous mixing. Slowly, 5 ml of boiling 8% SDS was added to the cell suspensions and permitted to boil for 30 mins. Samples were then removed from the boiling water and allowed to cool overnight at room temperature.

The boiled samples were centrifuged for 30 mins at 75,000 x *g*, the supernatant discarded and the jelly pellets washed with MilliQ water. This process was repeated five times, with the final pellets being resuspended in 2 ml of 10 mM Tris-HCl (pH 7.4) containing 2 mg/ml of pronase (Sigma). Samples were incubated at 60°C for 3 hrs with continuous, gentle agitation to allow pronase digestion of PG to occur. After incubation, pronase was washed from the samples with MilliQ water and ultracentrifugation at 175,000 x *g* for 1.5 hrs; this was repeated three times. Final peptidoglycan samples were resuspended in 100 µl MilliQ water and stored at -20°C before analysis.

### 2.7.6.2 – PG analysis

PG was analysed in the department of Molecular Biology and Biotechnology at the University of Sheffield, with the help of Dr Stephane Mesnage. In brief, PG (1mg) was digested with 50 units of mutanolysin (Sigma) in a final volume of 150µl containing: 20 mM phosphate buffer (pH 6.5), 0.1 mM $MgCl_2$ and 25µg of enzyme. The mixture was incubated for 16 hrs at 37 °C. After heat inactivation (5 min at 100 °C), the soluble fraction was recovered by centrifugation at 20,000 x *g* for 20 mins at 4°C. To reduce the amino sugars to their alditol derivatives, an equal volume of borate buffer (250 mM, pH 9.0 - Sigma) was added to the solution of disaccharide peptides. Two milligrams of sodium borohydride (Sigma) was added and the solution was incubated for 20 mins at room temperature. The solution was adjusted to pH 4.0 with 20% orthophosphoric acid (Fisher Scientific). Reduced muropeptides were separated by reversed phase high performance liquid chromatography (rp-HPLC) on a Hypersil aQ $C_{18}$ column (3 µm, 2.1 mm × 200 mm; Thermofisher) connected to an Ultimate 3000 system (Thermofisher) at a flow rate of 0.25 ml/min. Muropeptides were eluted for 10 mins with

10 mM ammonium phosphate buffer (pH 5.6; buffer A) (Fisher scientific), and then with a 65-min methanol linear gradient (0–20%) in buffer A.

## 2.7.7 – Mass spectrometry (MS)

### 2.7.7.1 - In-gel trypsin digestion of flagellin

After isolation, flagella samples were incubated at 75°C for 10 minutes in Laemmli buffer (1 x final concentration) to cause depolymerisation of the flagella, yielding monomeric flagellins. Flagellin samples were run on a 12% polyacrylamide gel and directly excised from the gel using a clean scalpel after staining with Instant Blue (Gentaur). To minimise the protein loss due to protein absorption to normal microcentrifuge tube surfaces, gel slices were transferred to LoBind 1.5 mL microcentrifuge tubes (Eppendorf). All solutions for in-gel trypsin digestion were prepared with high performance liquid chromatography (HPLC) grade solvents and chemicals (Fischer Scientific); incubations were carried out at room temperature unless otherwise stated. Initially, gel slices were washed with 200 µL of HPLC water, followed by 200 µL of 100 mM ammonium bicarbonate (Ambic). Gel slices were then destained with a 50:50 (v/v) solution of 100 mM Ambic and 100% acetonitrile (ACN) for 20 mins; the supernatant was removed and the destain process repeated until the gel slices were colourless. Once destained, 500 µL of 100% ACN was added to dehydrate the gel slices for 10 mins. The supernatant was once again removed before the reduction and alkylation steps were carried out. For the reduction step, gel slices were incubated in 200 µL of 10 mM dithiothritol (DTT) in 100 mM Ambic for 30 minutes at 56°C. After incubation, the liquid was removed and the LoBind tubes chilled on ice before adding 500 µL 100% ACN to dehydrate the gel slices (10 mins). The supernatant was removed and alkylation was performed by addition of 200 µL of 55 mM iodoacetamide in 100 mM Ambic to the gel slices. Reaction was performed in dark at room temperature for 30 mins. The excess liquid was discarded from the tubes and 500 µL of 100% ACN added to dehydrate the gel slices once again (10 mins). The supernatant was removed and gel slices left to air dry (10 mins) before trypsin (Promega) (in 100 mM Ambic) was added to the gel slices at a ratio of 20:1 (protein:enzyme w/w) (0.5 µg). In-gel trypsin digestions were carried out at 37°C for 18 hours.

After digestion, tryptic peptides were extracted from the gel slices. Tubes were vortexed and the peptide solution pipetted into clean LoBind microcentrifuge tubes before 60 µL of 100 mM Ambic was added to the gel slices (incubated at 37°C for 15 mins). Again, tubes were vortexed before the supernatant was collected and combined into the tubes. Peptides were extracted a further three times, with each step incubating the gel slices at 37°C for 15 mins before collecting the excess liquid. Gel slices were first incubated with 50µL of 100% ACN, then with

50 µL of a 5% (v/v) formic acid solution (in HPLC water) and finally in 50% (v/v) ACN containing 5% (v/v) formic acid. Extracted peptides were dried in a vacuum concentrator (Eppendorf) at room temperature and stored at -20°C before mass spectrometric analysis.

#### 2.7.7.2 - High Performance Liquid Chromatography (HPLC) Mass Spectrometry (MS) Analysis

Tryptic peptides were separated via reverse phase liquid chromatography (LC) on a U3000 HPLC system (ThermoFisher) and MS analysed on both a maXis™ (Bruker) Quadrupole Time of Flight (Q-TOF) system (for collision induced dissociation [CID] tandem mass spectrometry [MS/MS] analysis) and an amaZon™ (Bruker) ion trap system (for electron transfer dissociation [ETD] MS/MS analysis). Both mass spectrometers were interfaced with an electrospray ion source.

For analysis on both mass spectrometers, the HPLC system was equipped with a 75 µm x 15 cm C18 analytical column (LC Packings) and a 300 µm x 5 cm micro precolumn packed with C18 material (LC Packings). Peptides were separated at a flow rate of 300 nL/min and 30 µL/min respectively at 30°C.

Reverse phase separation of peptides was achieved, in both cases, using the following buffers: buffer A (3% (v/v) HPLC ACN and 97% (v/v) HPLC water, incorporating 0.1% (v/v) formic acid) and buffer B (97% (v/v) HPLC ACN and 3% (v/v) HPLC water, incorporating 0.1% (v/v) formic acid). A gradient from 5% (v/v) buffer B to 40% (v/v) buffer B was set up over the course of 90 mins to elute the peptides.

Both mass spectrometers were set up for positive ion detection at an m/z range of 50 – 2200 (Q-TOF) and 200 – 2000 (ion trap). To generate the spray, the Q-TOF parameters were set at: endplate offset of -500 V, capillary voltage of 1,700 V, nebuliser gas at 0.4 bar, dry gas at 6 L/min and a dry temperature of 180°C. The ion trap parameters were set at: endplate offset of -500 V, capillary voltage of 2,700 V, dry gas of 6 L/min and a dry temperature of 180°C. Ion transmission was optimised for detection of glycopeptide diagnostic ions in the MS/MS analysis.

Peptide information was generated by CID (on the Q-TOF) and ETD (on the ion trap) MS/MS using an auto Ms(n) setting where the top three most intense peaks were selected for dissociation with the total ion count above the threshold of 5,000 (Q-TOF) and 25,000 (ion trap). The Q-TOF included a lock mass for internal calibration using hexakis ion at an m/z of 1221 to obtain exact mass measurements. The following software was used in both MS: for operating the LC system, Chromeleon was used (LC Packings) and MS operating parameters were integrated via Hystar software.

#### 2.7.7.3 - MS/MS Data Analysis

Using DataAnalysis™ software (Version 4.1) (Bruker) raw mass spectrometric data was converted into mascot generic files (.mgf) for examination via the graphical platform, EasyProt (Gluck *et al.*, 2013). On EasyProt, the proteins of interest (FlaA and FlaB from *Aeormonas caviae* Sch3, Shaw Unpublished) were uploaded as a database and pseudaminic acid (able to modify serine and threonine residues) was added to the modifications list. For EasyProt analysis of data, trypsin was selected as the protease, with up to two miscleavages considered. A fixed modification of carbamidomethyl on cysteine was set and the following variable modifications were considered: methionine oxidation, glycosylation of serine/threonine residues with pseudaminic acid and methylation of lysine residues (methyl/dimethyl/trimethyl). Protein Prospector (http://prospector.ucsf.edu/) was used to aid manual analysis of spectra.

## 2.8 – Microscopy

### 2.8.1 – Fluorescence Microscopy

Fluorescence microscopy samples were prepared from overnight bacterial cultures in LB broth. Samples were allowed to dry on L-lysine-coated coverslips (Neuvitro) and were then fixed with 4% paraformaldehyde for 30 mins. After fixing, paraformaldehyde was washed off the coverslips with phosphate buffered saline (PBS). The samples were then post-stained with Alexafluor 594 (Life Technologies) by submerging the coverslips in 200 µl PBS and adding 20 µl of a 5mg/ml Alexa Fluor solution in DMSO to the PBS. Residual fluorescent dye was removed by washing cells with PBS. Samples were mounted onto glass microscope slides (Fisher Scientific) with ProLong Antifade Gold with DAPI (Life Technologies) and incubated in the dark for 24 hrs. Samples were analysed on Zeiss Axiovert fluorescence microscope at 1000 x magnification.

### 2.8.2 – Scanning Electron Microscopy (SEM)

Bacterial subcultures (10 mls) were grown overnight in LB and samples, normalised to an $OD_{600}$ of one, were pelleted at 16,000 X *g* and submitted to Mr Chris Hill at the Sheffield University Electron Microscopy Unit (Dept. Biomedical Sciences) for SEM sample preparation in a gold sputter coater (Edwards S150b). Samples were analysed on a Philips XL-20 SEM and cell lengths measured manually.

# Chapter 3: Investigation into the Function of AHA0618 – a Flagellin Deglycosylase or Cell Wall Remodelling Enzyme?

## 3.1 - Introduction

The Maf proteins have been described in a number of bacteria as the putative glycosyltransferases thought to be responsible for the O-glycosylation of the bacterial flagellum. Some *Campylobacter* species possess seven *maf* genes and it has been suggested that the expression of the genes can be phase variable, which may allow different Maf proteins to decorate the *Campylobacter* flagellum with different nonulosonate sugars (ie. Pseudaminic or legionaminic acid) at different stages of infection and has been shown to alter autoagglutination ability of cells (van Alphen *et al.*, 2008; Karlyshev *et al.*, 2002). This suggests that tailoring the amount of flagellin glycosylation may modulate bacterial behaviour. In addition, mutational studies carried out by Howard *et al.* (2009) demonstrated that the behaviour of *Campylobacter* could be altered (such as ability to form biofilm and autoagglutinate) by modifying glycosylation and changing the overall surface charge of the flagellum.

*Helicobacter pylori* glycosylates its flagellins solely with pseudaminic acid, similarly to *Aeromonas caviae* Sch3 (Josenhans *et al.*, 2002; Schirm *et al.*, 2003). In recent years, a possible flagellin deglycosylation pathway has been highlighted by Asakura *et al.* (2010) in *H. pylori* which may be allowing modulation of flagellin glycosylation and therefore bacterial behaviour. The putative deglycosylation enzyme, HP0518, was identified and a mutant of which was hypermotile on semisolid agar. *H.* pylori flagellins (FlaA) displayed increased glycosylation levels which could be detected clearly by western blot analysis and was confirmed by mass spectrometry. In addition, the mutant exhibited 'superior colonisation capabilities', whereby it was able to interact more efficiently with host cells (work carried out on a human gastric carcinoma cell line), leading to enhanced CagA (cytotoxin-associated gene A) phosphorylation and the subsequent host cell responses caused by this toxin (Asakura *et al.*, 2010).

Sycuro *et al.,* 2012 called into question the true function of HP0518, renamed Cds6 in this study, as they demonstrated the protein to have LD-carboxypeptidase activity, a hydrolytic enzyme which was found to be responsible for cleaving uncross-linked tetrapeptides in the peptidoglycan structure to yield tripeptides (Sycuro *et al.*, 2013). This study identified a number of genes important for *H. pylori* cell morphology and demonstrated that by mutating

*cds6* (ie. *HP0518*), *H. pylori* exhibited a straight-rod cell morphology compared to its usual characteristic helical shape (Sycuro *et al.*, 2013).

In light of these studies this chapter focuses on the characterisation of a HP0518 homologue, AHA0618, and looks into the potential existence of a flagellin deglycosylation pathway in *A. caviae* Sch3. This work resulted in Lowry *et al.* (2014b).

## 3.2 – Results

### 3.2.1 – Bioinformatic analysis of AHA0618

*AHA0618*, was identified from analysis of the *A. caviae* Sch3 genome sequence (Shaw unpublished) by probing the genome with the gene sequence of a putative deglycosylation enzyme, *HP0518*, from *H. pylori* (ncbi BLAST) (Askura *et al.,* 2010). The predicted amino acid sequence was found to have 37% homology to the central region of the putative deglycosylation enzyme, HP0518 (Asakura *et al.*, 2010), at the primary level (Fig. 3.1 A/B). Furthermore, the identified *AHA0618* gene sequence was also used to re-probe the *H. pylori* genome for homologues (ncbi BLAST); *HP0518* was the top match suggesting that *AHA0618* and *HP0518* are true orthologues.

Cellular localisation of AHA0618 could not be accurately determined from further analysis of the amino acid sequence using the Cello server (http://cello.life.nctu.edu.tw/) which suggested this protein to be either cytoplasmic or periplasmic, and no signal peptide could be detected when the protein sequence was run through the SignalP server (http://www.cbs.dtu.dk/services/SignalP/) for export to the periplasm. Conserved domain searches through the Pfam (http://pfam.xfam.org/) and ncbi conserved domain servers revealed this protein to be in the YkuD-superfamily of proteins. YkuD was originally characterised in *Bacillus subtilis* and contains a his/cys motif invariant amongst members of this superfamily (Bielnicki *et al.*, 2006). *E. coli* possess five YkuD protein homologues: ErfK, YbiS, YcfS, YnhG and YcbB, and studies have indicated that these are a family of L,D-transpeptidases that allow the formation 3-3 type peptidoglycan cross linkages at the cell wall (Magnet *et al.*, 2007; Magnet *et al.*, 2008). In addition these proteins are also thought to be associated with anchoring of the Lpp lipoproteins (or Braun's lipoprotein) to peptidoglycan, with three out of the five *E. coli* homologues (ErfK/YbiS/YcfS) being shown to have this function (Magnet *et al.*, 2007). Mutational studies by Sanders and Pavelka (2013) demonstrated that *E. coli* lacking the three L,D-transpeptidases responsible for Lpp anchoring to peptidoglycan resulted in loss of outer-membrane stability and cells showed altered stress resistance. In addition, deletion of all YkuD homologues was detrimental to *E. coli* growth under stressful conditions (Sanders and Pavelka, 2013).

When aligned with characterised and predicted YkuD-superfamily proteins, both AHA0618 and HP0518 were found to contain the histidine and cysteine residues thought to be characteristic of the YkuD family catalytic domain (Fig. 3.2). However, HP0518 is significantly larger than AHA0618, similarly to YkuD domain containing proteins (such as the *E. coli* homologues YbiS/ErfK/YcfS) which may indicate the presence of multiple domains in HP0518, perhaps

giving this protein an additional role in the cell, compared to AHA0618. Analysis of the primary amino acid sequence of HP0518 suggests this to be the case as when submitted to both ncbi conserved domain and Pfam prediction servers, results suggested that as well as belonging to the YkuD superfamily of proteins, an additional, uncharacterised 'SnoaL' domain of unknown function is also present.

The position of *AHA0618* in the *A. caviae* genome is interesting as it is not associated with either of the two known loci associated with flagellin glycosylation, where the putative glycosyltransferase, Maf1, and pseudaminic biosynthetic genes are located (Fig. 3.3) (Rabaan *et al.*, 2001; Parker *et al.*, 2012; Tabei *et al.*, 2009). Instead, *AHA0618* is close to homologues of the cellulose synthase operon from *Yersinia enterocolitica (Fuchs et al., 2011)* and genes encoding nutrient uptake apparatus (eg. ABC transport systems)(Fig. 3.3). It is flanked by an M3 family oligoendopeptidase and an AzlC family protein which is predicted to be involved in amino acid transport/metabolism; these being drastically different from genes involved in bacterial motility and flagellin post-translational modification (Fig. 3.3).

Bioinformatic analysis therefore suggests that AHA0618 is unlikely to be involved in flagellin modification and motility, but that it instead may have a role in cell wall maintenance.

In order to explore further the function of AHA0618, phenotypic analysis of an insertional mutant previously created in the Shaw group, was carried out. This mutant was created by inserting a kanamycin resistance cassette into the *AHA0618* gene in the same transcriptional orientation, with an outward reading promoter to decrease the chance of polar effects downstream of the mutation. PCR was used to confirm the location and orientation of the resistance cassette.

### 3.2.2 - Analysis of *A. caviae AHA0618* mutant motility

In order to assess whether the *AHA0618* mutation had an effect on the motility of *A. caviae*, swimming motility assays were carried out on semi-solid agar alongside the wild type strain (Chapter 2, section 2.4.4). Motility assays were carried out on large plates, allowing eight technical repeats for each strain to be carried out per plate; in addition, three biological replicates were carried out. Figure 3.4 A displays a close up of motility halos from each strain, taken from one of the motility plates analysed, however is representative of each of the biological repeats. The radius of each halo was measured and an average measurement calculated. The *AHA0618* mutant was found to swim significantly more than the wild type strain ($p < 0.0001$), having a mean radius, in this case, of 20.8 mm compared to the wild type mean measurement of 13.6 mm, therefore showing a 1.5 fold increase in motility (Fig. 3.4 A/B).

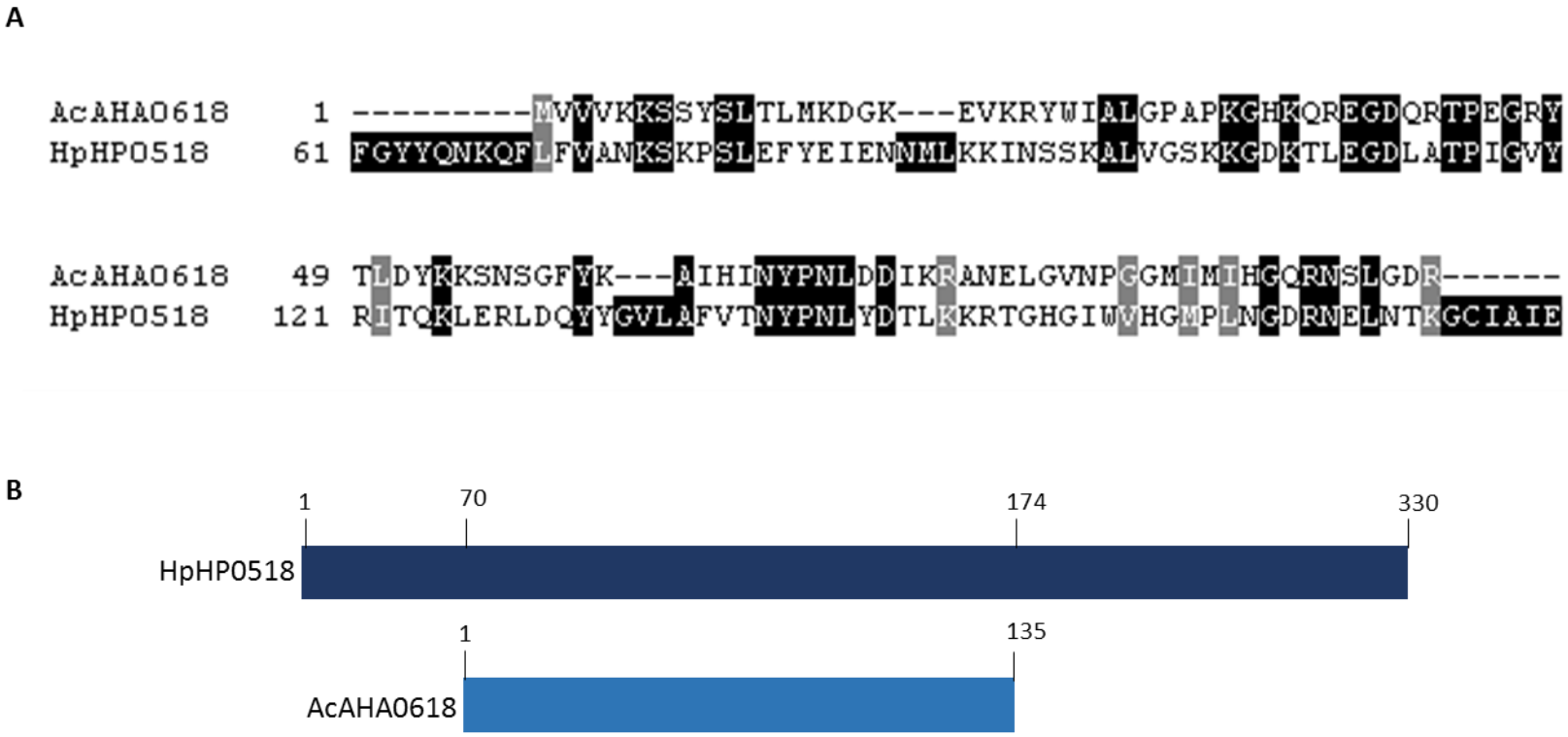


**Figure 3.1**: (**A**) Alignment of *Aeromonas caviae* Sch3 AHA0618 (Accession HG934767) (AcAHA0618) primary amino acid sequence with the central region of the homologue HP0518 form *Helicobacter pylori* 26695 (HpHP0518) (amino acids 51 – 200) (Asakura *et al.*, 2010). The alignment was executed using CLUSTALW (Thompson *et al.*, 1994) and displayed with box-shade. (**B**) Diagrammatic representation of *A. caviae* Sch3 AHA0618 (AcAHA0618) compared to *H. pylori* 26695 HP0518 (HpHP0518) in their unfolded state.

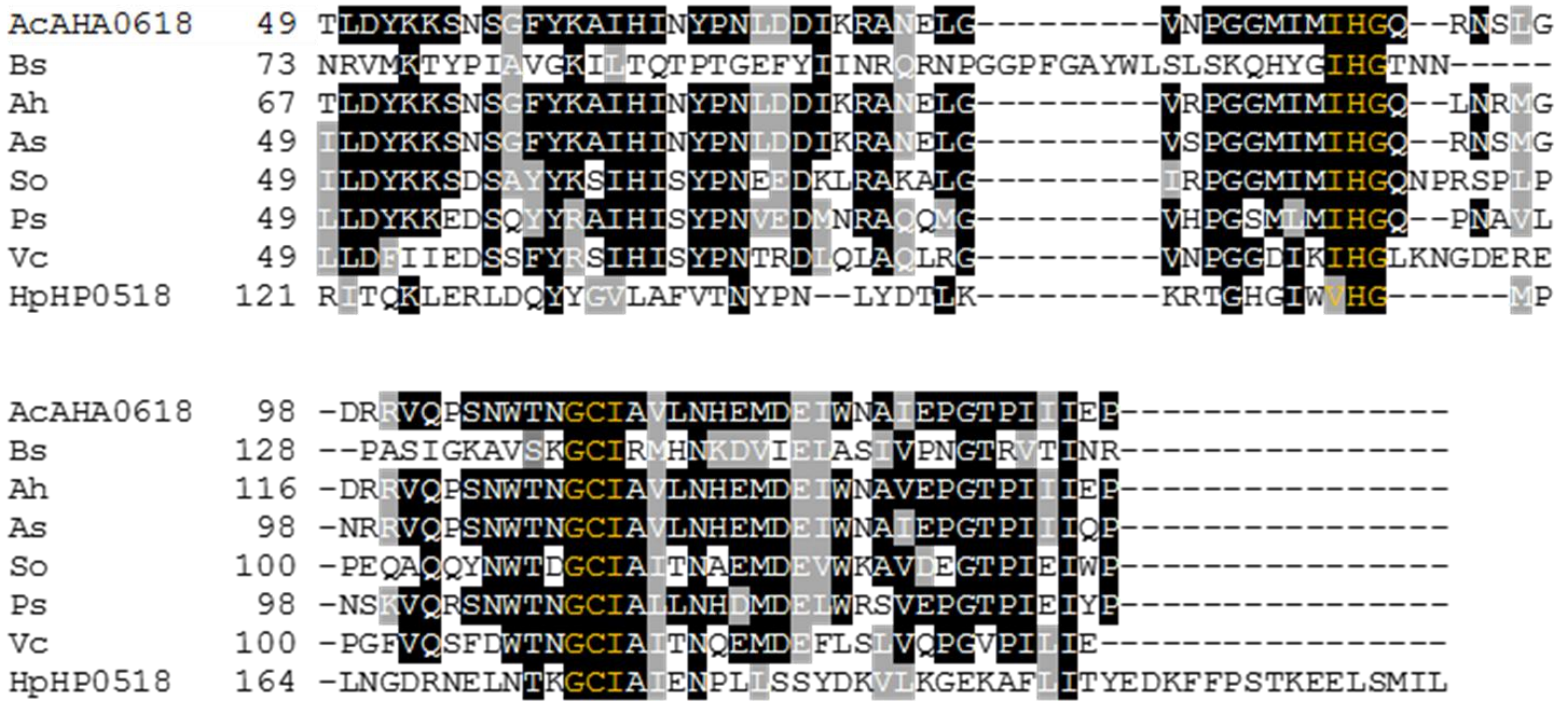


**Figure 3.2**: Alignment of *Aeromonas caviae* Sch3 AHA0618 (AcAHA0618) and *Helicobacter pylori* 26695 HP0518 (HpHP0518) with other YkuD superfamily proteins: *Bacillus subtilis* (Bs) (accession NP_389287), *Aeromonas hydrophila* (Ah) (accession AHE48181), *Aeromonas salmonicida* (As) (accession WP_021138855), *Shewanella oneidensis* (So) (accession NP_717783), *Pleisiomonas shigelloides* (Ps) (accession WP_010864114), *Vibrio cholerae* (Vc) (accession NP_232564). The conserved histidine and cysteine residues from the his/cys motif in the YkuD predicted catalytic domain are highlighted in orange.

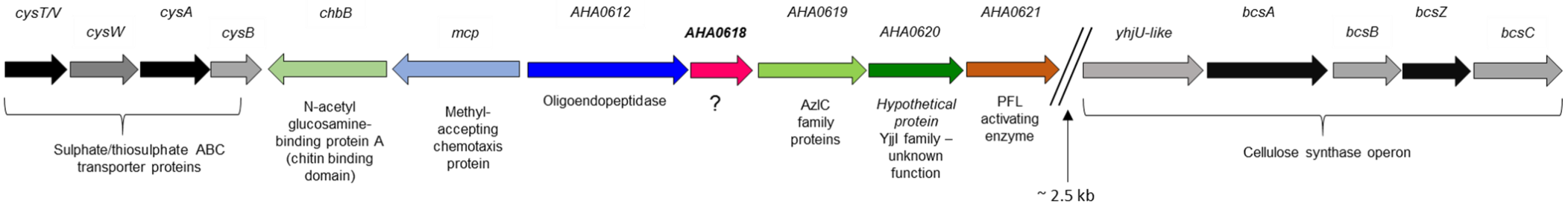


**Figure 3.3** - The genetic context of *AHA0618* in the *A. caviae* Sch3 genome and surrounding genes, showing their predicted functions (Shaw, unpublished). The arrows depict the open reading frames present.

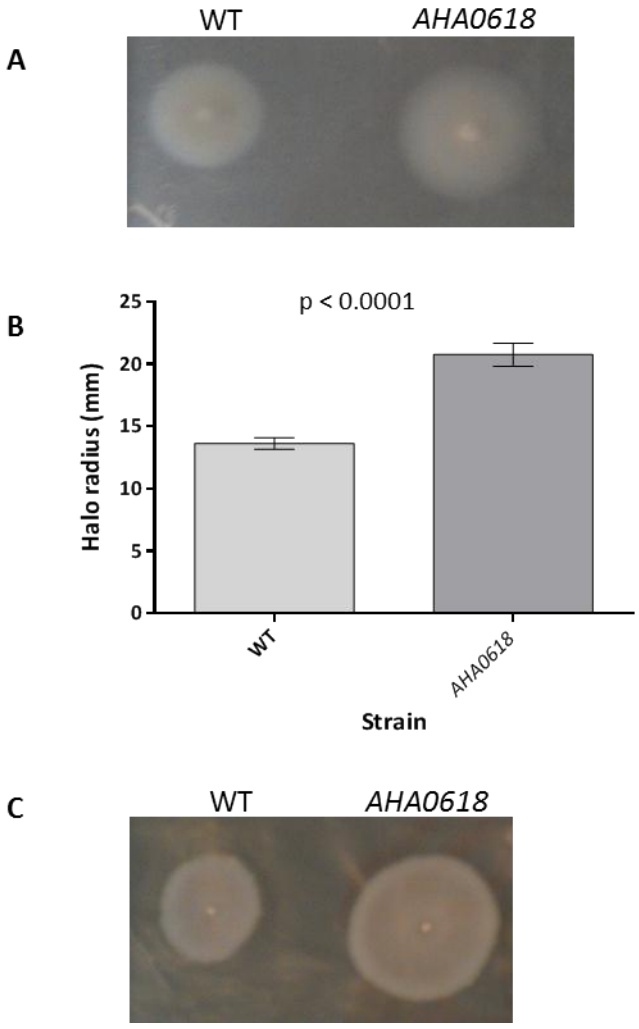


**Figure 3.4**: (**A**) Swimming motility analysis of *Aeromonas caviae* Sch3 (WT) compared to the *A. caviae AHA0618* mutant (*AHA0618*). Assays were carried out on 0.25% (w/v) agar. (**B**) The radius of each motility halo was measured and average measurements for *A. caviae* Sch3 (WT) and *AHA0618* mutant (*AHA0618*) motility are presented here (n=8) ± the standard error of the mean. A p-value of < 0.0001 was generated when a paired T-test was carried out on the data sets. (**C**) Swarming motility analysis of *A. caviae* Sch3 (WT) compared to the *A. caviae AHA0618* mutant (*AHA0618*). Assays were carried out on 0.6% (w/v) swarming agar.

Swarming motility assays were also carried out (0.5% 'Eiken' Agar) (Chapter 2, section 2.4.5) and the *AHA0618* displayed increased motility when compared to the wild type (Fig. 3.4 C). However, swarming motility could not be quantified like swimming motility due to irregular colony formation and was therefore only visually analysed. The lateral flagellar system of *A. caviae* is induced when grown on solid media (Shimada *et al.*, 1985) and there is some evidence to suggest that this system also glycosylates its flagellins (Gavin *et al.*, 2002; Wilhelms *et al.*, 2012; Wilhelms *et al.*, 2013); however, nothing is known about the *A. caviae* lateral flagellar glycan or mechanism. The hypermotility observed on swarming agar suggests that *AHA0618* may have a wider role than solely effecting polar flagella mediated motility.

A growth curve was carried out of wild type and *AHA0618* mutant *A. caviae* to assess whether the strains were growing at different rates and that being the reason why the mutant was displaying increased swimming and swarming motility (Chapter 2, section 2.4.3). Growth curves were carried out in triplicate for each strain, results of which are displayed in figure 3.5 and demonstrate that both strains grow similarly.

## 3.2.3 – Analysis of *AHA0618* mutant and wild type *A. caviae* containing pSRK_*AHA0618*

In order to explore whether the observed hypermotility phenotype of the *A. caviae AHA0618* mutant was due to the *AHA0618* mutation itself, or due to any downstream effects of this mutation, complementation analysis was carried out whereby *AHA0618* was cloned into the IPTG inducible vector pSRK(Gm), expressed in the mutant strain and the effect on both motility and flagellin glycosylation status investigated. Furthermore, this construct was also analysed in the wild type strain to examine the effects of AHA0618 overexpression; overexpression analysis can give an indication of protein roles due to producing mutant or exaggerated phenotypes.

### 3.2.3.1 – Generation of pSRK_*AHA0618*

Initially *AHA0618* was amplified using the primers JLP_28 and JLP_29 (Chapter2, Table 2.6) using the Expand high fidelity PCR system (Roche) (Chapter 2, section 2.6.2.1) with *A. caviae* Sch3 genomic DNA as the template. The expected size of the PCR product was around 410 bp (gene size of 408 bp) which was checked via agarose gel electrophoresis (Fig. 3.6). The Expand High Fidelity DNA polymerase system allows TA-cloning due to the addition of non-templated adenines to the PCR product; the correct size PCR product was therefore ligated into the TA-cloning vector pGEM-T EASY (Promega) (Fig. 3.7 A) and subsequently transformed into chemically competent *E. coli* DH5α. An *Eco*RI digest was carried out on the plasmid DNA

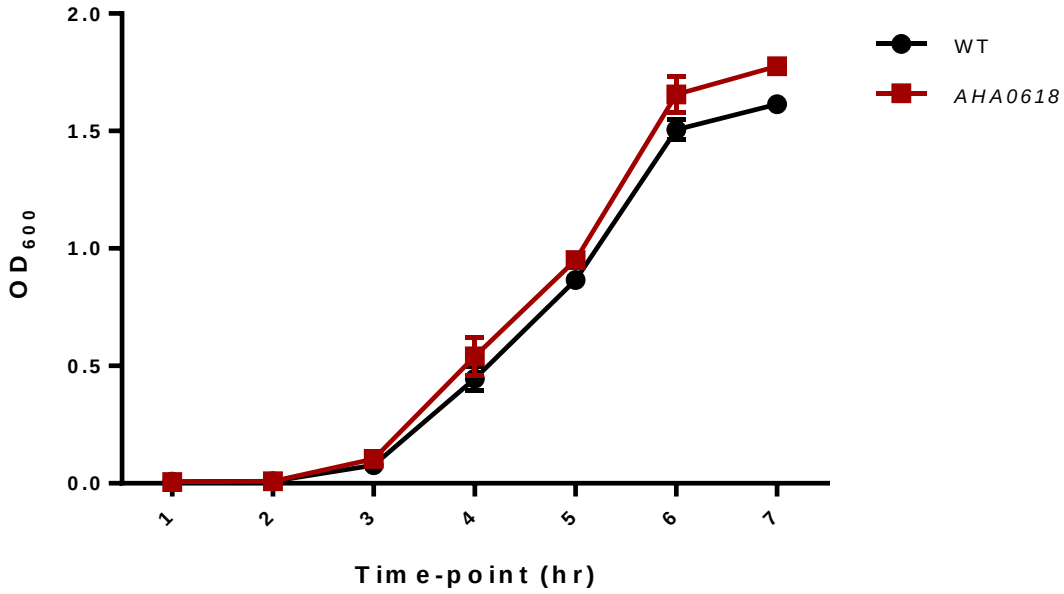


**Fig. 3.5** – Growth Curves comparing the growth of *Aeromonas caviae* Sch3 (WT) and the *AHA0618* mutant (*AHA0618*) over 7 hours. Growth curves were carried out in triplicate, at 37°C, in BHIB (Table 2.3) and average measurements plotted here ± the standard error of the mean.

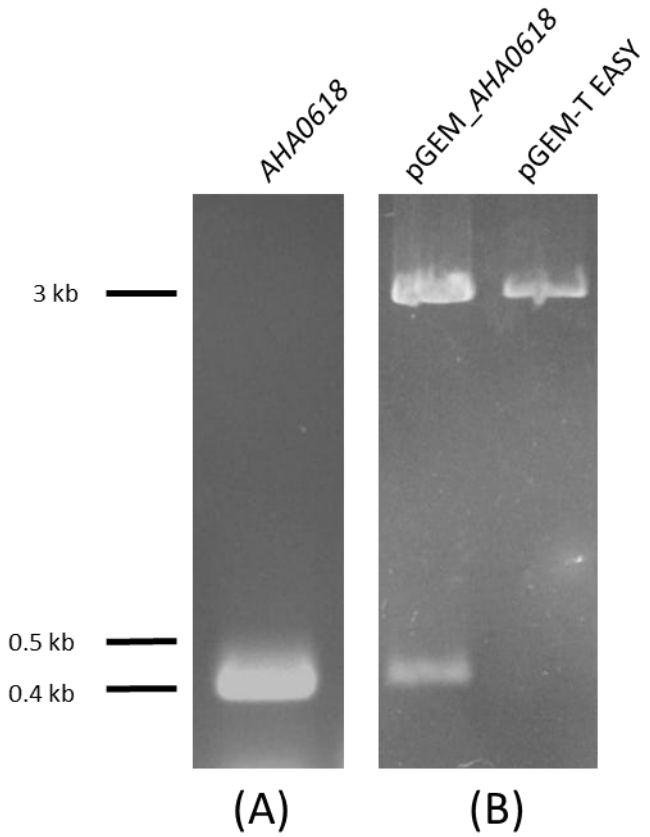


**Figure 3.6** – 1% agarose gels displaying (**A**) the *AHA0618* PCR product and (**B**) EcoRI digested pGEM_*AHA0618* (with empty pGEM-T EASY as a negative control.

A

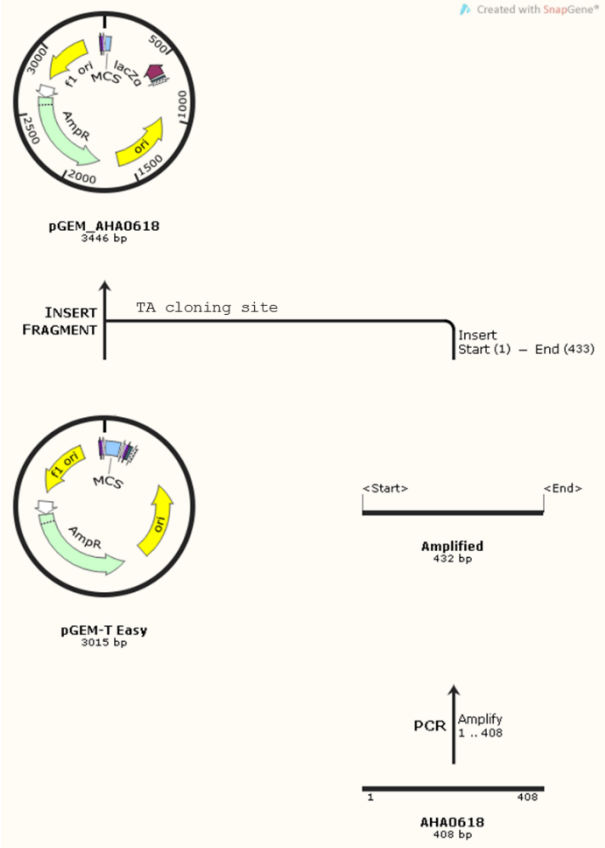


B

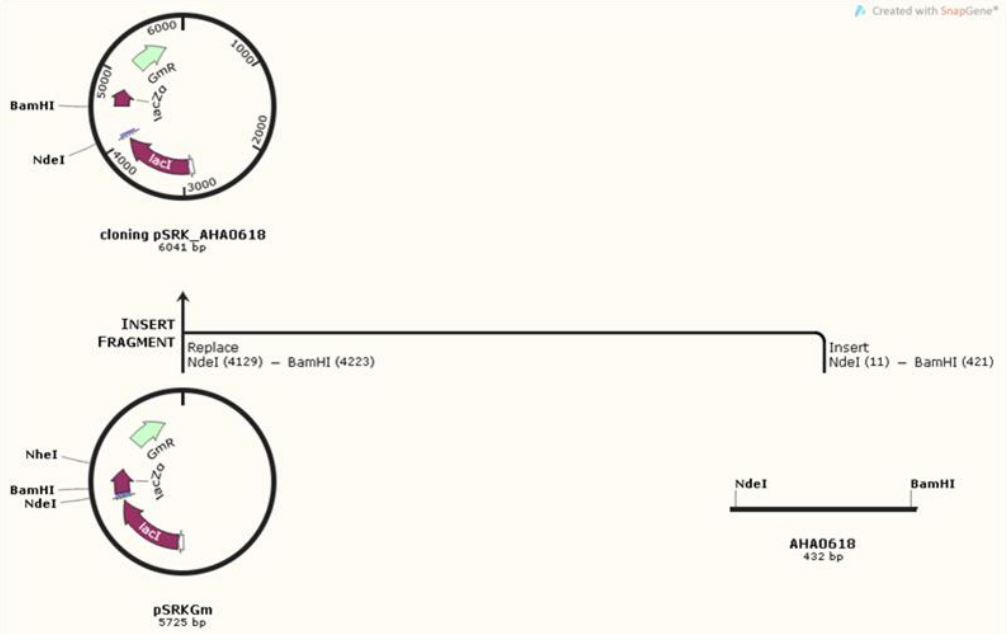


**Figure 3.7** – Diagrammatic representation of the cloning method of: (A) *AHA0618* from *Aeromonas caviae* Sch3 into pGEM-T EASY, and (B) *AHA0618* from *Aeromonas caviae* Sch3 into pSRK(Gm) (Khan *et al.*, 2008) (pSRK_AHA0618) using SnapGene software.

isolated from the resulting transformants (present at each side of the pGEM-T EASY multiple cloning site) to check for the presence of the *AHA0618* gene which was excised from the vector (agarose gel electrophoresis) (Fig. 3.6 & 3.7 A). The presence of *AHA0618* was confirmed by sequencing using sequencing primers T7 forward and SP6 reverse. This construct was then digested with a combination of NdeI and BamHI restriction enzymes to excise *AHA0618* from the vector and ligated into NdeI/BamHI cut pSRK(Gm) (Khan *et al,.* 2008) (Fig. 3.7 B). Ligations were transformed into *E. coli* DH5α (selected for on Gm plates) and overnight subcultures made from resulting transformants. Plasmids were isolated from the subcultures and digested with BamHI to linearise. Digested vector was finally run on an agarose gel alongside empty, BamHI cut pSRK(Gm); a size shift of the correct size between the empty vector and the one potentially carrying the desired gene indicated the presence of *AHA0618*.

#### 3.2.3.2 – Motility analysis of *A. caviae* strains containing pSRK_*AHA0618*

The pSRK_*AHA0618* and empty pSRK(Gm) vectors were transformed into *E. coli* S17-1 λ *pir*, a strain containing conjugal transfer genes, allowing conjugation of plasmid DNA into *A. caviae* strains. The gene, *AHA0618*, was reintroduced into the *A. caviae AHA0618* mutant to test whether the hypermotility phenotype observed could be complemented (Chapter 2, section 2.4.13). Three transconjugants from each conjugation were selected to phenotypically analyse. Swimming motility assays were carried out with each conjugant on large motility plates (0.25 % w/v) containing 1 mM IPTG to induce the expression of *AHA0618* from pSRK(Gm), alongside wild type *A. caviae*, the *AHA0618* mutant and the *AHA0618* mutant containing empty pSRK(Gm). Conjugants were analysed on separate plates, therefore allowing five technical repeats to be carried out per strain on each plate (in addition three biological repeats were carried out) (Fig. 3.8). The measurements from one motility plate (from one transconjugant) are displayed in figure 3.8 but are representative of all transconjugants and plates measured. Reintroduction of *AHA0618* was able to partially complement the mutant strain, significantly reducing its motility, therefore discounting polar effects on genes downstream of the mutation. The pSRK_*AHA0618* construct was also introduced into the wild type *A. caviae* strain by bacterial conjugation (method as above) and the effect of *AHA0618* overexpression was investigated. Again, three transconjugants were selected for phenotypic analysis via swimming motility assays (as above). Motility of the overexpression strain (wild type *A. caviae* containing pSRK_*AHA618*) was compared solely to wild type containing the empty vector as the empty vector was found to have a great negative effect on motility (Fig 3.9 A). The measurements from one motility plate (from one conjugant) are displayed in figure 3.9 (B/C) and demonstrates there are no discernible differences in motility between the overexpression strain and wild type containing the empty vector on swimming motility agar containing 1 mM

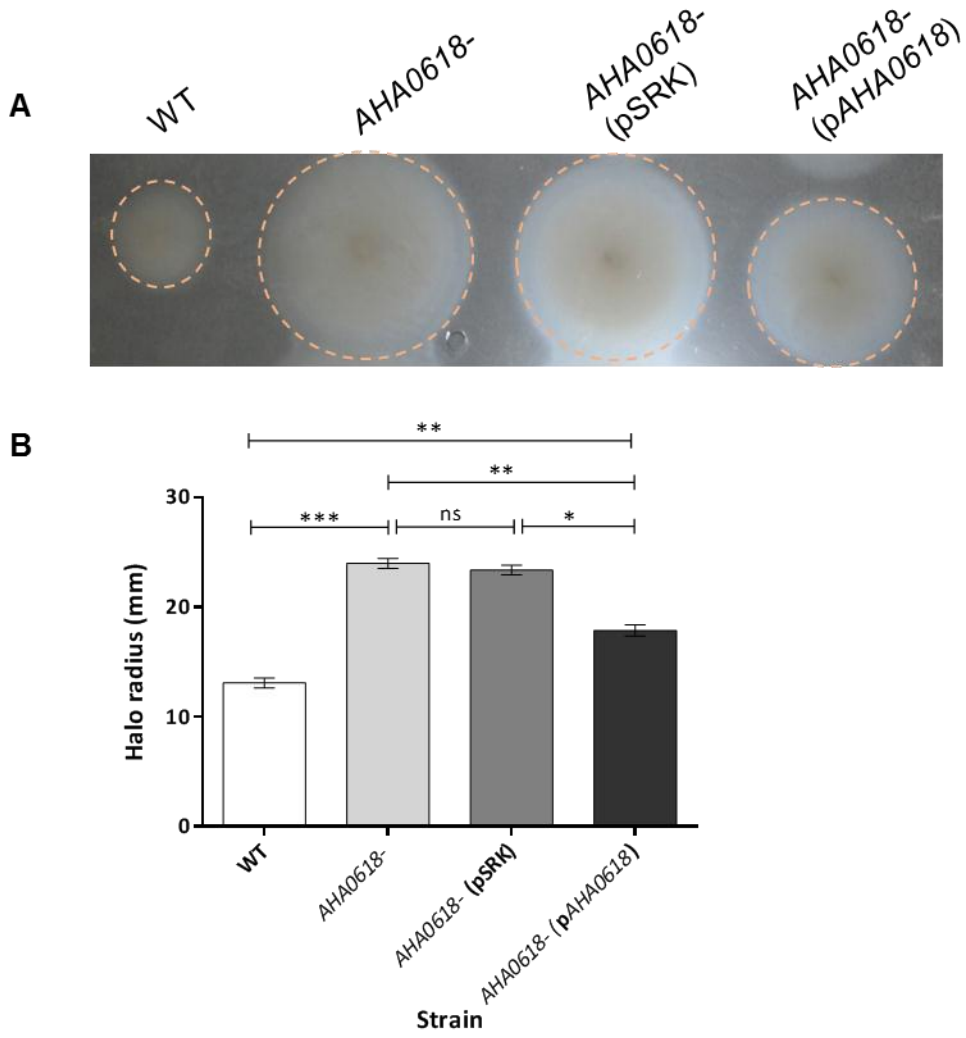


**Figure 3.8** – Analysis of pSRK_*AHA0618* expression in an *Aeromonas caviae AHA0618* mutant (**A**) Swimming motility assays were carried out on 0.25% (w/v) agar containing 1 mM IPTG for: *A. caviae* Sch3 (WT) , the *AHA0618* mutant (*AHA0618*-), the mutant containing empty pSRK(Gm) [*AHA0618*- (pSRK)] and the mutant containing pSRK_AHA0618 [*AHA0618*-(pAHA0618)]. (**B**) The radius of each motility halo was measured and average measurements are presented here (n=5) ± the standard error of the mean. A one-way ANOVA, with a Tukey's multiple comparisons test, was carried out on the data sets. *p = 0.01-0.05, **p = 0.001-0.009, ***p = 0.0001-0.0009, ns = not significant.

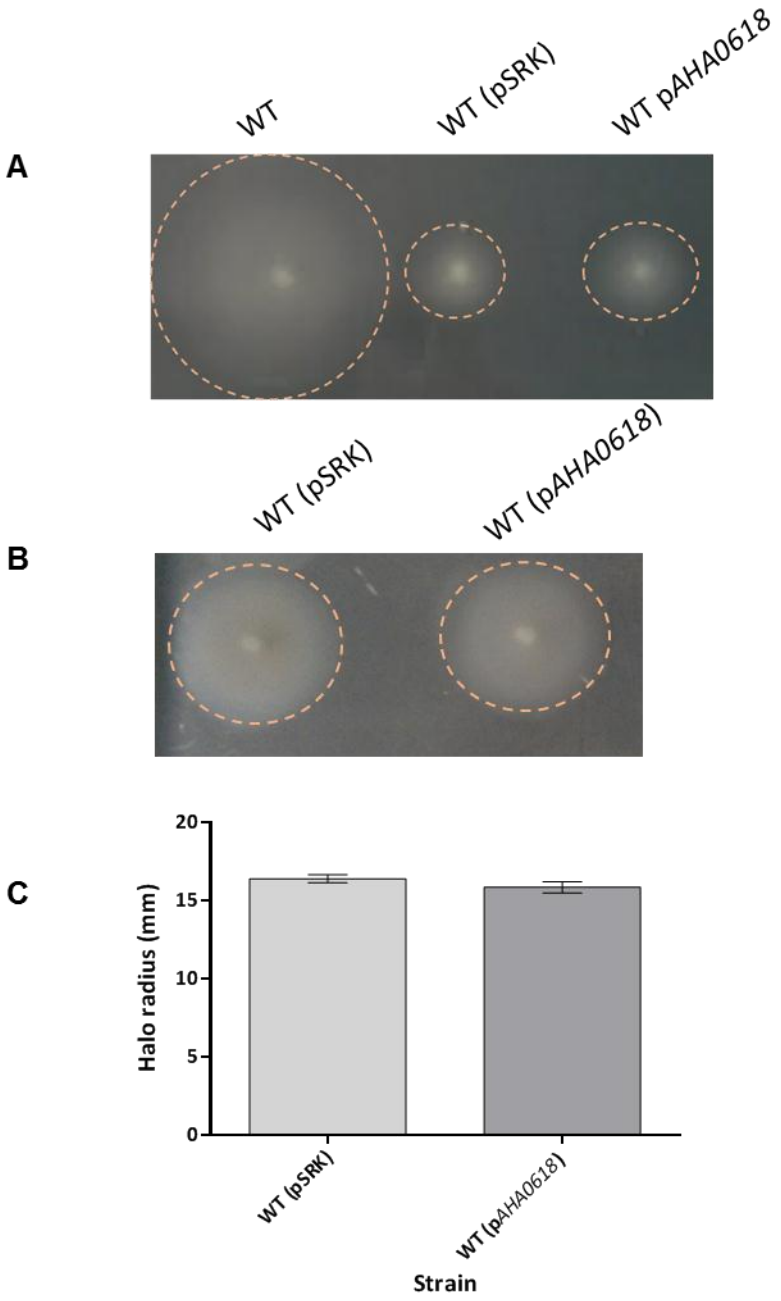


**Figure 3.9** – Analysis of pSRK_*AHA0618* overexpression in *Aeromonas caviae* Sch3. Swimming motility assays (**A/B**) were carried out on 0.25% (w/v) agar containing 1 mM IPTG. (**A**) Motility assay to demonstrate the difference in *A. caviae* Sch3 motility (WT) compared to that of *A. caviae* containing empty pSRK(Gm) [WT(pSRK)] or pSRK_*AHA0618* [WT(p*AHA0618*)]. (**B**) Swimming motility analysis of *A. caviae* Sch3 containing empty pSRK(Gm) compared to *A. caviae* Sch3 containing pSRK_*AHA0618.* (**C**) The radius of each motility halo (from **B**) was measured and average measurements for *A. caviae* Sch3 motility when containing either empty pSRK(Gm) or pSRK_*AHA0618* are presented here (n=10) ± the standard error of the mean. No statistical significance between the motility of each strain was seen when a paired T-test was carried out on the data sets.

IPTG. The results of one large motility plate are displayed in figure 3.9 and are representative of the motility of all transconjugants analysed.

### 3.2.3.3 – Analysis of flagellin glycosylation levels via western blot analysis in the *AHA0618* mutant and strains containing pSRK_*AHA0618*

As AHA0618 shows 37% homology to HP0518 of *H. pylori* and mutating the gene gives a hypermotility phenotype in each case (Asakura *et al.,* 2010), it was hypothesised that AHA0618 from *A. caviae* may therefore be having a similar role to HP0518 and elevated glycosylation levels on the *AHA0618* mutant polar flagellins (FlaA/B) may be the reason for the increased motility compared to the wild type. In order to assess whether AHA0618 has an effect on flagellin glycosylation, whole cell Western blots (Chapter 2, section 2.7.3) were carried out with wild type and the *A. caviae AHA0618* mutant (Fig. 3.10 A). Samples were probed with an anti-FlaA/B(+Pse) antibody that recognises only glycosylated flagellin and an anti-FlaA/B antibody that recognises both unglycosylated and glycosylated flagellins (Fig. 3.10 A). An *A. caviae maf1* mutant (overexpressing *flaA*) was used as a negative control when samples were probed with the antibody that recognises only glycosylated flagellin, anti-FlaA/B(+Pse). Maf1 is the putative polar flagellin glycosyltransferase, a mutant of which is non-motile and lacks the ability to glycosylate its flagellins (Parker *et al.*, 2012). Unglycosylated flagellin in a *maf1* mutant strain cannot be detected via whole cell western blot analysis due to very low levels, however when *flaA* is overexpressed in the multicopy vector pSRK(Gm) in this strain, unglycosylated flagellin can then be detected by the anti-FlaA/B antibody. A size shift can be clearly seen when unglycosylated flagellin is compared to the glycosylated version; however, there is no size shift between the wild type and *AHA0618* mutant flagellins (Fig. 3.10 A). This therefore suggests that both wild type and *AHA0618* mutant polar flagellins are glycosylated similarly and it is unlikely that AHA0618 is affecting flagellin glycosylation levels.

Whole cell western blots were also carried out to investigate the glycosylation status of wild type and *AHA0618* mutant strains containing pSRK_*AHA0618* (Fig. 3.10 B/C). Again, samples were probed with both antibodies and flagellins appeared to be identical in size. Western blots in figure 3.10 B and C display the results of a whole cell sample taken from one of the transconjugants previously phenotypically analysed in section 3.2.3.2, but is representative of all the transconjugants analysed.

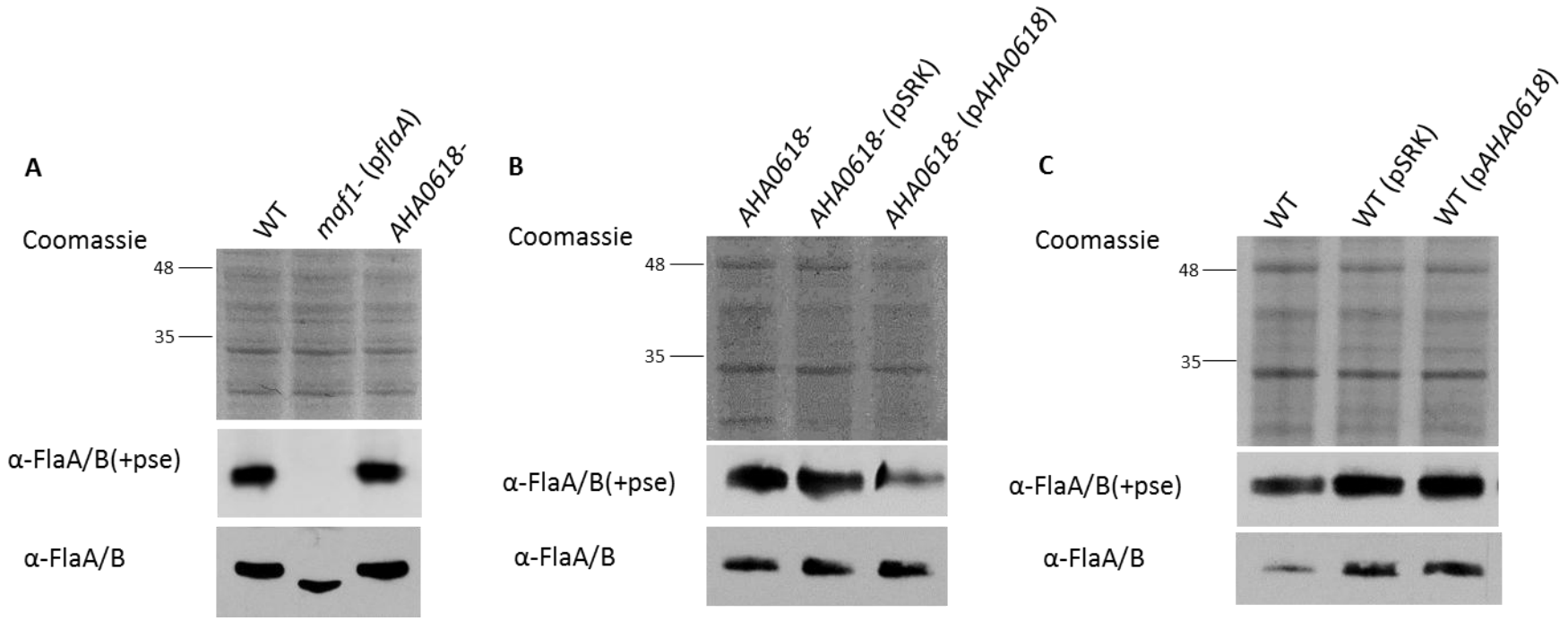


**Figure 3.10** – Western blot analysis of *Aeromonas caviae* whole-cell samples probed with a rabbit, anti-polar flagellin antibody that recognises only glycosylated polar flagellin [α-FlaA/B(+Pse)] (1:10,000) and a rat, anti-polar flagellin antibody that recognises both glycosylated and unglycosylated polar flagellin [α-FlaA/B] (1:1,000) . (**A**) Lane 1, *A. caviae* Sch3 (WT); lane 2, *maf1* mutant containing pSRK_*flaA* [*maf1*- (p*flaA*)]; lane 3, *AHA0618* mutant (*AHA0618*-). (**B**) Lane 1, *AHA0618* mutant (*AHA0618*-); lane 2, *AHA0618* mutant containing pSRK(Gm) [*AHA0618*- (pSRK)]; lane 3, *AHA0618* mutant containing pSRK_*AHA0618* [*AHA0618*- (p*AHA0618*)]. (**C**) Lane 1, *A. caviae* Sch3 (WT); lane 2, Sch3 containing pSRK(Gm) [WT (pSRK)]; lane 3, Sch3 containing pSRK_*AHA0618* [WT (p*AHA0618*)].

## 3.2.4 – Analysis of *AHA0618* mutant and wild type *A. caviae* containing pSRK_*HP0518*

HP0518 of *H. pylori* was shown by Asakura *et al.* (2010) to be a putative flagellin deglycosylation enzyme and mutant flagellin had elevated levels of flagellin glycosylation. The effect of *HP0518* expression was therefore assessed in wild type and *AHA0618* mutant *A. caviae* to see if the resultant protein had an effect on *A. caviae* motility or flagellin glycosylation. *HP0518* was cloned into the IPTG inducible vector, pSRK(Gm), similarly to *AHA0618.*

### 3.2.4.1 – Generation of pSRK_*HPO518*

The same cloning method previously described for creating pSRK_*AHA0618* (section3.2.3.1) was adopted for creating pSRK_*HP0518*. However, HP0518 was amplified via PCR by the primers JLP_108 and JLP_109 (Chapter 2, Table 2.6) using *H. pylori* 26695 genomic DNA as the template. The expected PCR product size of *HP0518* was around 1 kb (gene size of 993 bp) and was again cloned with NdeI and BamHI restriction sites either side of the gene for insertion into pSRK(Gm). Once the sequence of *HP0518* was confirmed by sequencing, pSRK_*HP0518* was transformed into *E. coli* S17-1 λ *pir* for conjugation into the *A. caviae AHA0618* mutant and the wild type strain. Please refer to section 3.2.3.1 for the specific method of cloning used.

### 3.2.4.2 - Motility and flagellin glycosylation analysis of *A. caviae* strains containing pSRK_*HP0518*

Following conjugal transfer of pSRK_*HP0518* into wild type *A. caviae* and the *AHA0618* mutant, three transconjugants were selected for analysis of motility on motility agar plates and flagellin glycosylation status via western blotting.

Motility assays were carried out as previously stated in section 3.2.3.2 and revealed that *HP0518* is able to complement the increased motility phenotype of the *AHA0618* mutant strain, significantly reducing motility to slightly below wild type levels (Fig. 3.11 A/B). However, whole cell western blot analysis of polar flagellins revealed no size difference between flagellins from the *AHA0618* mutant and the mutant expressing *HP0518*, when samples were probed with both anti-FlaA/B(+Pse) and anti-FlaA/B, suggesting that glycosylation levels are not affected by the expression of this gene (Fig. 3.12).

In contrast to *AHA0618* overexpression in wild type *A. caviae,* overexpression of *HP0518* in the wild type strain significantly reduced motility when compared to the motility of the wild type containing empty pSRK(Gm) (Fig. 3.13 A/B). In this case motility was reduced by 26.5% ($p = 0.0001$) in comparison to motility of wild type containing the empty vector.

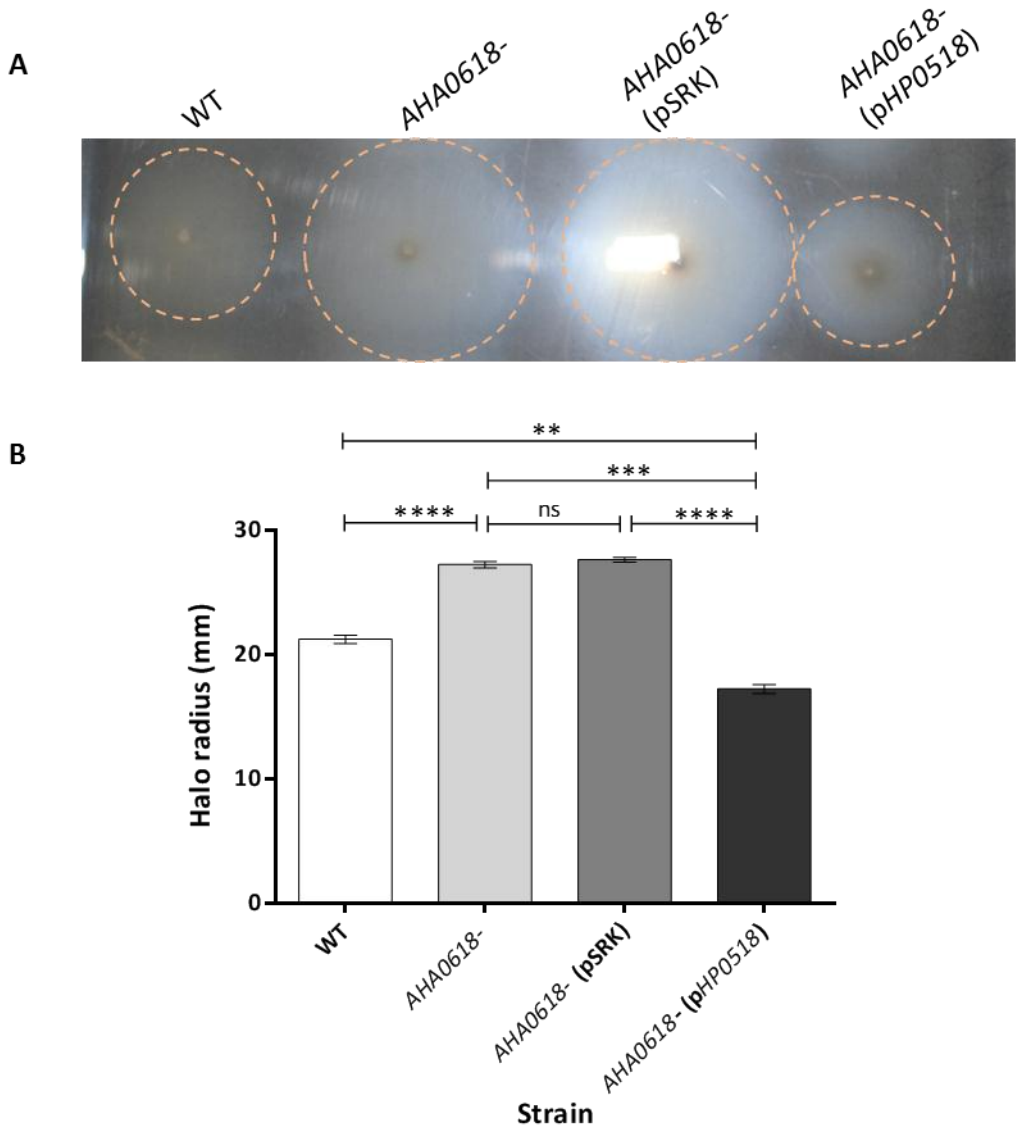


**Figure 3.11** - Analysis of pSRK_*HP0518* overexpression in *AHA0618* mutant *Aeromonas caviae*. (A) Swimming motility assays were carried out on 0.25% (w/v) agar containing 1 mM IPTG for *A. caviae* Sch3 (WT), the *AHA06108* mutant (*AHA0618*-), the mutant containing pSRK(Gm) [*AHA0618*- (pSRK)] and the mutant containing pSRK_*HP058* [*AHA0618*- (pHP0518)]. (**C**) The radius of each motility halo was measured and average measurements are presented here (n=5) ± the standard error of the mean. A one-way ANOVA, with a Tukey's multiple comparisons test, was carried out on the data sets. **p = 0.001-0.009, ***p = 0.0001-0.0009, ****p < 0.0001, ns = not significant.

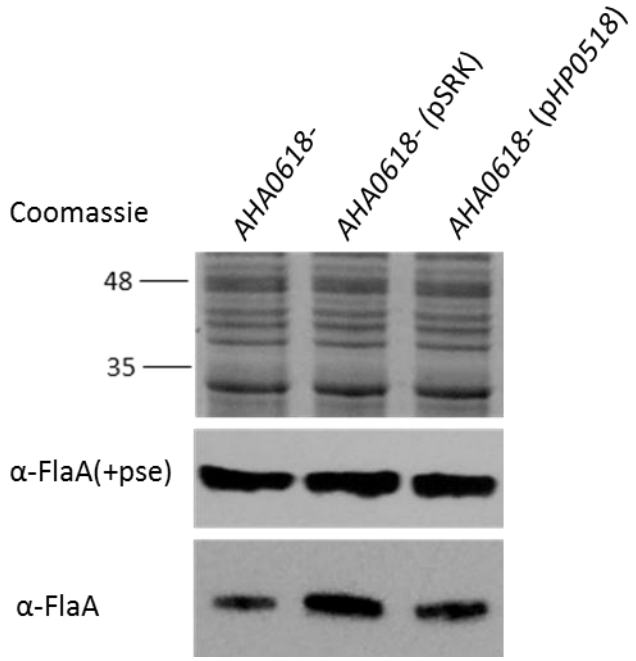


**Figure 3.12** – Whole-cell western blot analysis of the *A. caviae AHA0618* mutant (*AHA0618-*), the mutant containing pSRK(Gm) [*AHA0618-* (pSRK)] and the mutant containing pSRK_*HP0518* [*AHA0618-* (p*HP0518*)] probed with a rabbit, anti-polar flagellin antibody that recognises only glycosylated polar flagellin [α-FlaA/B(+Pse)] (1:10,000) and a rat, anti-polar flagellin antibody that recognises both glycosylated and unglycosylated polar flagellin [α-FlaA/B] (1:1,000).

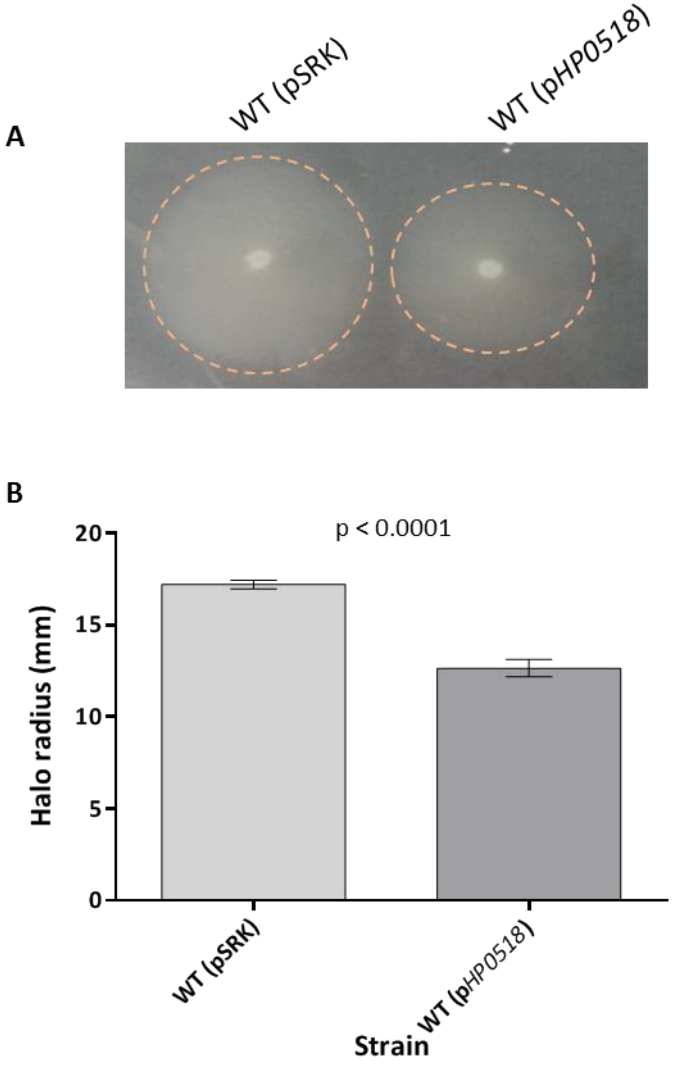


**Figure 3.13** - Analysis of pSRK_*HP0518* overexpression in *Aeromonas caviae* Sch3. (**A**) Swimming motility assays were carried out on 0.25% (w/v) agar containing 1 mM IPTG for *A. caviae* Sch3 containing pSRK(Gm) [WT (pSRK)] and pSRK_*HP0518* ) [WT (p*HP0518*)]. (**B**) The radius of each motility halo was measured and average measurements are presented here (n=10) ± the standard error of the mean. A p-value of < 0.0001 was generated when a paired T-test was carried out on the data sets.

Additionally, western blot analysis of whole cell samples revealed flagellins from each strain to be of an identical size when probed with both anti-FlaA/B(+Pse) and anti-FlaA/B, suggesting flagellin glycosylation levels to be similar in each strain (Fig. 3.14).

Figures 3.11, 3.12, 3.13 and 3.14 display the findings from one transconjugant containing pSRK_*HP0518* (*AHA0618* mutant and wild type respectively) but are representative of all three transconjugants analysed.

### 3.2.5 – Analysis of *AHA0618* mutant *A. caviae* cellular envelope

In addition to modifying its polar flagellins, FlaA/B, *A. caviae* also modifies the LPS O-antigen with pseudaminic acid (Tabei *et al.*, 2009). Once pseudaminic acid is activated with the addition of CMP, it travels down a pathway independent of flagellin glycosylation, for transfer onto the LPS O-antigen. Mutations in genes of the pseudaminic acid biosynthetic pathway (*flmA, flmB, neuA, flmD, neuB*) lead to the loss of the sugar on the LPS O-antigen and therefore the LPS profiles of these mutants differ significantly to the wild type (Tabei *et al.,* 2009).

If AHA0618 is altering LPS O-antigen glycosylation levels, this could lead to a change in bacterial cell surface charge and effect how *A. caviae* interacts with its environment (which may help to explain why we see increased motility in the *AHA0618* mutant). LPS was extracted from overnight subcultures of wild type and *AHA0618* mutant *A. caviae* using an LPS extraction kit from ChemBio (Chapter 2, section 2.7.5). Once obtained, samples were run on a 12% polyacrylamide gel containing 4 M urea to solubilise the highly hydrophobic LPS and visualised by silver staining (section 2.7.5). The LPS profiles were found to be identical indicating that AHA0618 does not affect the levels of LPS O-antigen glycosylation (Fig. 3.15). LPS extractions and gels were carried out in triplicate, with each repeat showing identical profiles for each strain.

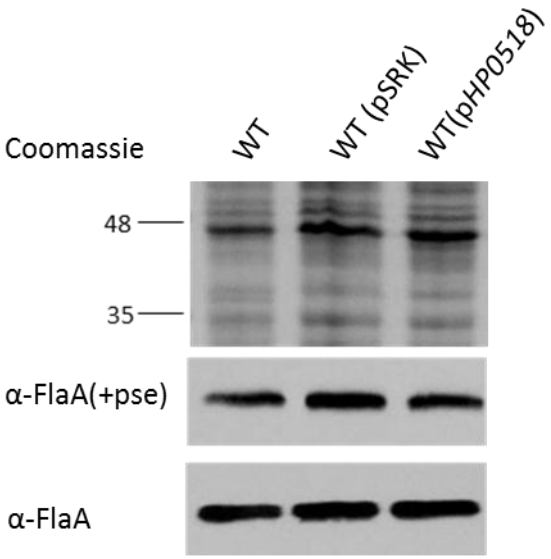


**Figure 3.14** - Whole-cell western blot analysis of *Aeromonas caviae* Sch3 (WT), Sch3 containing pSRK(Gm) [WT (pSRK)] and Sch3 containing pSRK_*HP0518* [WT (p*HP0518*)], probed with a rabbit, anti-polar flagellin antibody that recognises only glycosylated polar flagellin [α-FlaA/B(+Pse)] (1:10,000) and a rat, anti-polar flagellin antibody that recognises both glycosylated and unglycosylated polar flagellin [α-FlaA/B] (1:1,000).

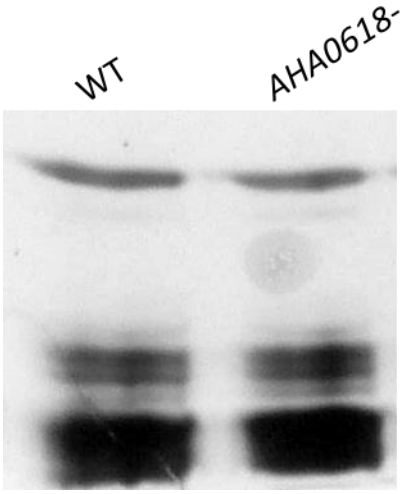


**Figure 3.15** – Lipopolysaccharide (LPS) profile analysis of *A.caviae* Sch3 (WT) and an *AHA0618* mutant (*AHA0618*-). LPS was extracted from each strain grown in BHIB at 37$^{o}$C, was analysed by SDS-PAGE (12%, containing 4 M urea) and visualised via silver staining. LPS extractions and analyses were repeated three times. One extraction is displayed here but is representative of all the repeats.

## 3.2.6 – Analysis of *A. caviae* cellular morphology

Recent cell morphology studies by Sycuro *et al.* (2013) identified a number of peptidoglycan modification enzymes important for maintaining the characteristic helical shape of *H. pylori*. HP0518 (known as Csd6 in this study) was shown to have L,D-carboxypeptidase activity and a mutant of which exhibited straight rod cellular morphology compared to the helical wild type Sycuro *et al.* (2013). The cell morphology of *AHA0618* mutant *A. caviae* was therefore investigated due to the homology between AHA0618 and HP0518 and the behavioural similarities between the corresponding mutants in each case. Initially, scanning electron microscopy (SEM) was implemented to analyse the gross cell morphology of the *AHA0618* mutant compared to the straight-rod wild type. Mutant and wild type *A. caviae* cell samples were submitted to the University of Sheffield Electron Microscopy Unit for SEM sample preparation and analysis on a Philips XL-20 SEM (Chapter 2, section 2.8). Both wild type and mutant samples were analysed in five fields of view on the SEM grids at 8000 x magnification. No drastic changes in cell shape were detected, however, a small but significant difference in cell length between strains was observed when cells were measured manually from pole to pole ($n = 100$; $p < 0.0001$) (Fig. 3.16 A/B).

The higher throughput method of fluorescence microscopy was then used to further investigate this initial difference in cell length between *A. caviae* strains (Chapter 2, section 2.8). Strains analysed included: wild type and *AHA0618* mutant alone, wild type and mutant containing empty pSRK(Gm), the mutant containing pSRK_*AHA0618* and the mutant containing pSRK_HP0518. *A. caviae* samples were grown in LB containing 1 mM IPTG and were labelled with the thiol-reactive dye, Alexa Fluor 594, to fluorescently label the cell surfaces; a DAPI mount was also used which additionally labelled the chromosomal DNA. Samples were each analysed in four fields of view on a Zeiss Axiovert fluorescence microscope at 1000 x magnification. Again, a subtle but significant difference was observed between mutant and wild type *A. caviae* cell lengths, with the mutant displaying a 14% decrease in mean cell length compared to that of the wild type ($n = 80$; $p < 0.0001$) (Fig. 3.17). Furthermore, when the cell lengths of *AHA0618* mutant strains complemented with either *AHA0618* or *HP0518* genes (in pSRK) was investigated, these strains displayed a significant increase in cell length compared to the *AHA0618* mutant containing empty pSRK(Gm) ($p = 0.0026$ and $p < 0.0001$ respectively) (Fig. 3.17).

Due to such subtle differences in cell lengths being observed between strains, the frequency distribution of cell length measurements was analysed to ensure the mean measurements acquired were not concealing important details of the spread of cell lengths across strains (Fig. 3.18). The *AHA0618* mutant (containing empty pSRK) displayed the smallest minimum cell

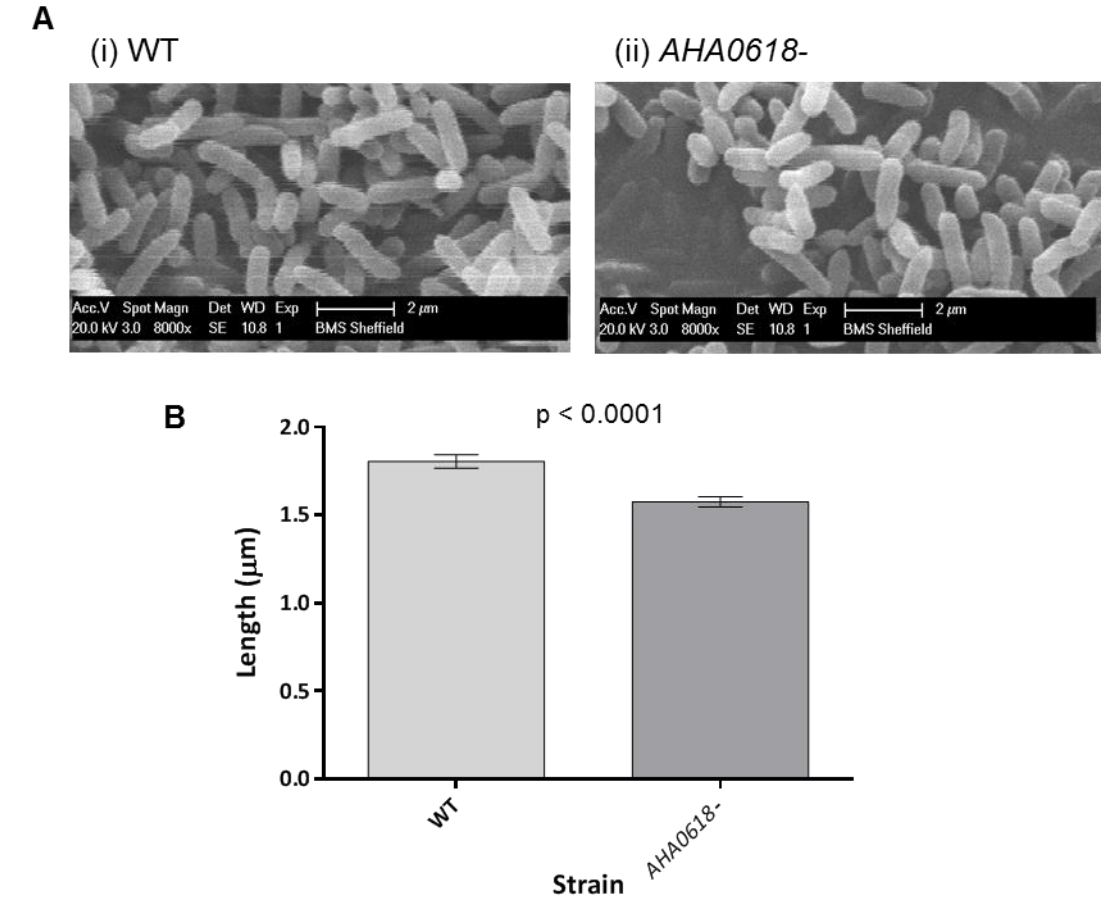


**Figure 3.16** – (**A**) Scanning electron microscopy (SEM) carried out on a Philips XL-20 SEM at 8000 x magnification of samples: (i) *Aeromonas caviae* Sch3 (WT) and (ii) *A. caviae AHA0618* mutant (*AHA0618-*). (**B**) Bacterial cell lengths from the electron micrographs were manually measured from five fields of view and average cell lengths are presented here (n=100) ± the standard error of the mean. A p-value of < 0.0001 was generated when a paired T-test was carried out on the data sets.

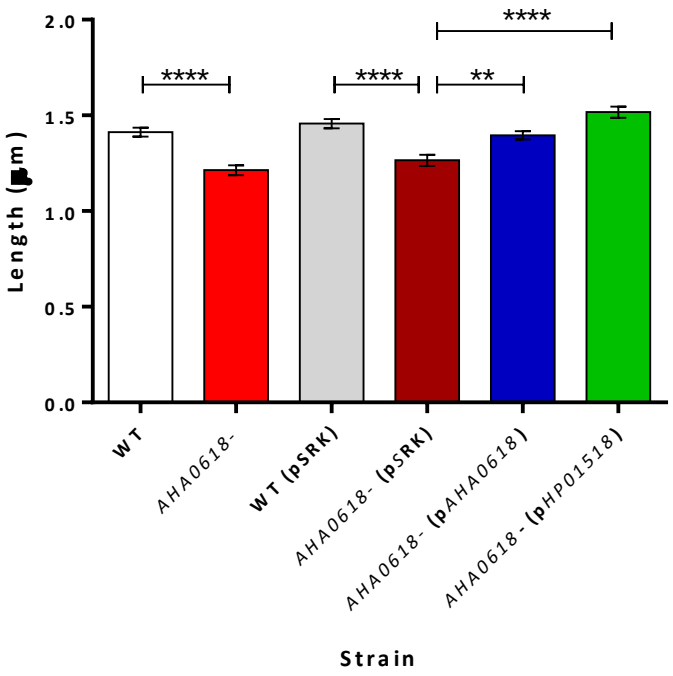


**Figure 3.17** – Investigation into differences in cell lengths of *Aeromonas caviae* strains using fluorescence microscopy. Bacterial cell lengths were manually measured from micrographs of fluorescently labelled *A. caviae* samples (Chapter 2, section 2.8): *A. caviae* Sch3 (WT), the *AHA0618* mutant (*AHA0618*-), Sch3 containing pSRK(Gm) [WT (pSRK)], the *AHA0618* mutant containing pSRK(Gm) [*AHA0618*- (pSRK)], the *AHA0618* mutant containing pSRK_*AHA0618* [*AHA0618*- (p*AHA0618*)] and the *AHA0618* mutant containing pSRK_*HP0518* [*AHA0618*- (p*HP0518*)]. Cell lengths were measured from four fields of view at 1000 x magnification and average cell lengths are presented here (n=80) ± the standard error of the mean. A one-way ANOVA, with a Tukey's multiple comparisons test, was carried out on the data sets. **p = 0.001-0.009, ****p < 0.0001.

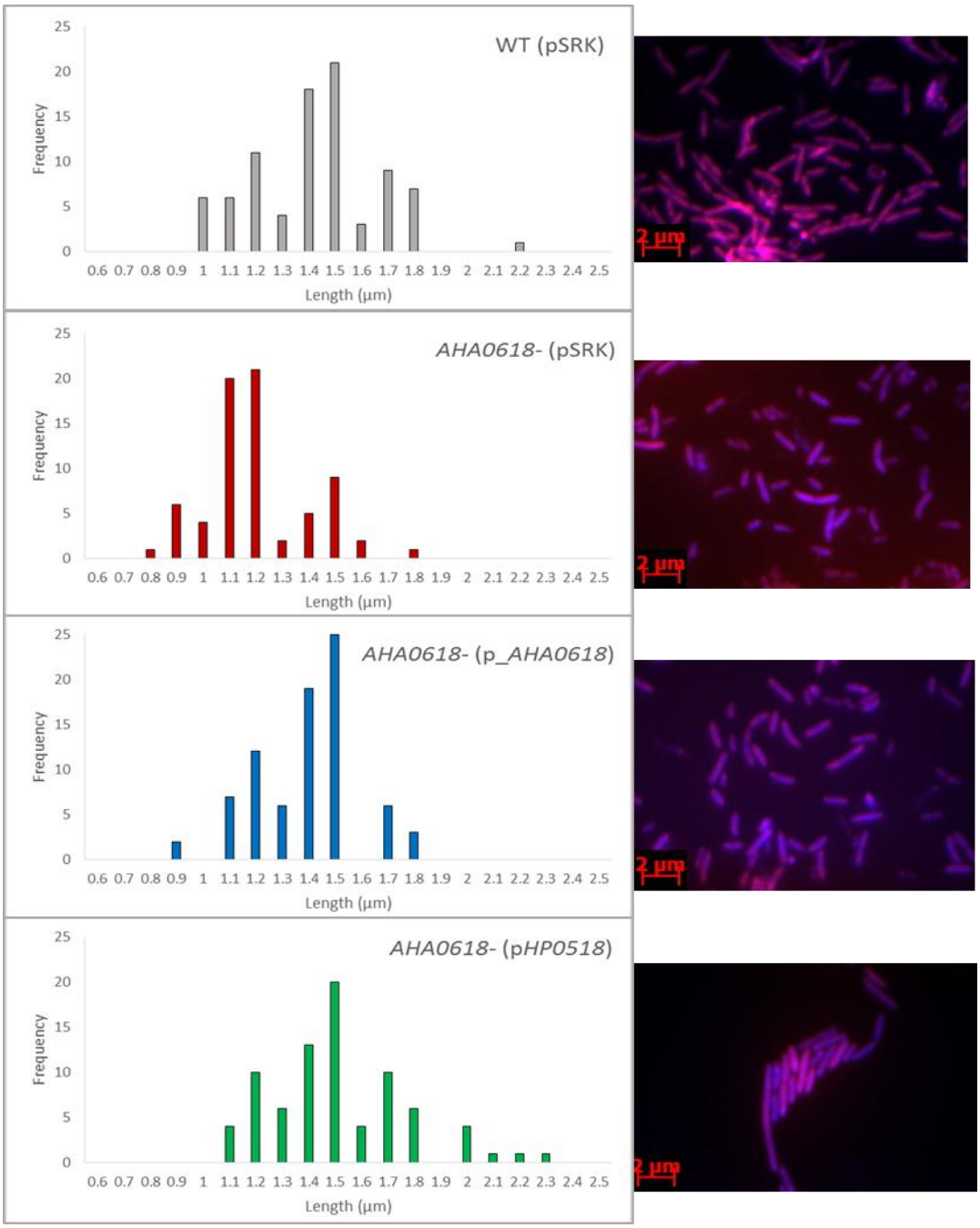


**Figure 3.18** – Frequency distribution of cell lengths of *Aeromonas caviae* strains measured fluorescence micrographs previously discussed in figure 3.17. The frequency distributions of cell length measurements from *A. caviae* Sch3 containing pSRK(Gm) [WT (pSRK)], the *AHA0618* mutant containing pSRK(Gm) [*AHA0618*- (pSRK)], the *AHA0618* mutant containing pSRK_*AHA0618* [*AHA0618*- (p*AHA0618*)] and the *AHA0618* mutant containing pSRK_*HP0518* [*AHA0618*- (p*HP0518*)], are displayed here (n=80).

length of 0.77 µm, compared to the other strains analysed, and was more frequently measured at the lower end of the frequency distribution scale, showing a shift to the left (with a mode cell length of 1.2 µm) when compared to the wild type (mode length of 1.5 µm) (Fig. 3.18). Both *AHA0618* mutant strains containing either pSRK_*AHA0618* or pSRK_*HP0518* displayed similar patterns of spread of cell length, showing a shift to the right when compared to the *AHA0618* mutant (containing empty pSRK) and both strains having a mode measurement of 1.5 µm (Fig. 3.18).

### 3.2.7 – *A. caviae* muropeptide analysis

Muropeptide analysis was carried out in conjunction with Stephane Mesnage's group in the Department of Molecular Biology and Biotechnology at the University of Sheffield.

If AHA0618 from *A. caviae* is involved in peptidoglycan processing at the cell wall, then the muropeptide profiles of the wild type and mutant strains may be different. Therefore, peptidoglycan from *A. caviae* Sch3 and the *AHA0618* mutant was extracted in triplicate and digested with mutanolysin to cleave the *N*-acetylmuramyl-β(1-4)-*N*-acetylglucosamine linkages in peptidoglycan, before being analysed via high performance liquid chromatography (HPLC) (Chapter 2, section 2.7.6). These initial studies did not show any differences between the peptidoglycan of these strains as determined by the similarity of the HPLC traces obtained (Fig. 3.19). However, very subtle differences could take much experimental optimisation and time to discover.

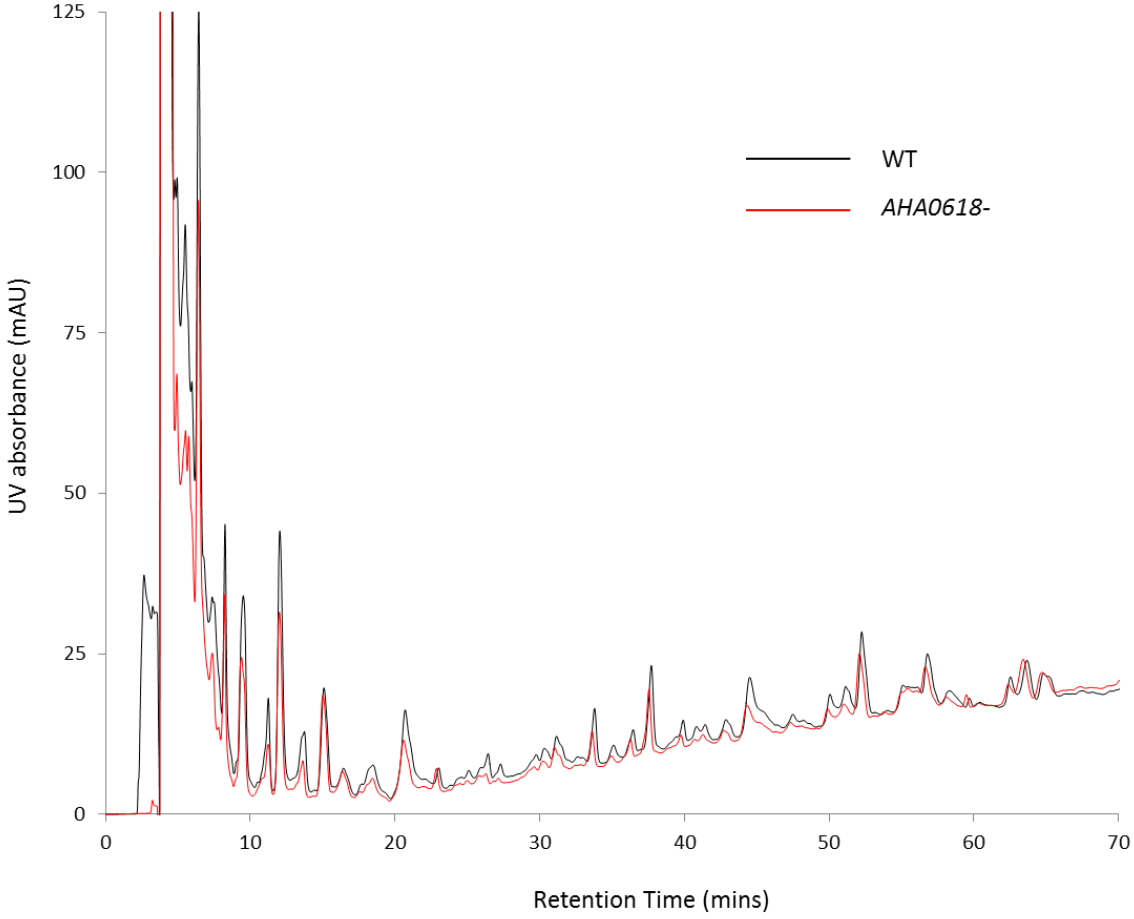


**Figure 3.19** – HPLC analysis of peptidoglycan (PG) extracted from *A. caviae* Sch3 (WT) and the *AHA0618* mutant (*AHA0618*-). A quantity of 1 mg of PG was digested with murolysin and loaded onto the HPLC for analysis. This trace was created with the help of Stephane Mesnage and displays the results from only one of the PG samples obtained from each strain, but is representative of all the samples analysed.

## 3.3 – Discussion

This chapter focused on examining the function of the protein, AHA0618, from *Aeromonas caviae*, which was identified due to its homology with a putative flagellin deglycosylation enzyme, HP0518, from *Helicobacter pylori* (Asakura *et al.*, 2010). The *AHA0618* gene is not associated with the polar flagellar locus in *A. caviae*, although a disruption mutant was shown here to display a similar hypermotile phenotype to a *H. pylori HP0518* mutant (Asakura *et al.*, 2010). These results suggested that AHA0618 may also be affecting flagellin glycosylation levels and perhaps adding a new level of complexity to this post-translational modification pathway. Although the role of flagellin glycosylation is unknown, it is tempting to speculate that this modification could be involved in mediating interactions with the bacterial environment, perhaps assisting with adherence to host cells, as the bacterial flagellum has previously been identified as a key adherence factor as well as a propeller for motility (Pratt and Kolter, 1998; Rabaan *et al.*, 2001; Giron *et al.*, 2002). If this is the case then bacteria being able to maintain or modulate their levels of flagellin glycosylation may be beneficial, perhaps in response to the environment, allowing bacterial behaviour to be altered. Modulation of flagellin glycosylation and consequently bacterial behaviour has been previously observed in *Campylobacter jejuni,* where studies by van Alphen *et al.* (2008) suggested the presence of a phase-variable glycosyltransferase (Maf4). During Maf4 expression, flagellins were modified with a new pseudaminic acid derivative and the autoagglutination ability of the bacterial population increased (van Alphen *et al.*, 2008). Furthermore, the presence of legionaminic acid on the *C. jejuni* flagellum, which is not required for flagellar assembly (as pseudaminic acid is), has been found to aid chicken colonisation (Howard *et al.*, 2009). These studies therefore demonstrate how the differential glycosylation of the *C. jejuni* flagellum with a variety of sugars can modify bacterial behaviour and aid survival in their specific niche. *A. caviae* and *H. plyori* only glycosylate their flagellins with pseudaminic acid compared to the wide variety of sugars found decorating the *Campylobacter* flagellum. Therefore, where *C. jejuni* can potentially use Maf protein expression to change flagellin glycosylation and in doing so, bacterial behaviour, an alternative pathway may be in place in other bacteria that do not possess such vast glycosylation islands, such as in *A. caviae* and *H. pylori,* enabling them to control how their flagellins are glycosylated.

Although an *AHA0618 A. caviae* mutant displays a similar hypermotile phenotype to the *HP0518 H. pylori* mutant, examination of polar flagellin glycosylation via western blot analysis suggested the glycosylation status of mutant *A. caviae* flagellins is comparable to the wild type. Furthermore, analysis of the LPS profiles from both wild type and mutant *A. caviae* strains suggested that AHA0618 is not affecting glycosylation of the LPS O-antigen, therefore the

hypermotility phenotype of the mutant is not likely due to an altered cell surface charge from elevated LPS glycosylation levels.

To further examine the role of these genes, *HP0518* was introduced into *A. caviae* and was found to reduce the motility of the *AHA0618* mutant strain similarly to when the mutant is complemented with *AHA0618.* In addition, heterologous expression of *HP0518* in the wild type strain reduced motility, in contrast to *AHA0618* overexpression which had no effect on wild type *A. caviae* motility. This suggests that AHA0618 and HP0518 are functioning similarly in *A. caviae* and there is perhaps a control mechanism in place that is not functioning with the heterologously expressed HP0518 from *H. pylori*, where possibly enzyme activity is being controlled, or AHA0618 is being targeted for degradation when present in excess amounts. Western blot analysis of the flagellins from these *A. caviae* strains containing vectors encoding *AHA0618* and *HP0518* showed there to be no discernible effect on overall levels flagellin glycosylation. *A. caviae* FlaA and FlaB are glycosylated with six-eight pseudaminic acid residues (out of a possible 19 sites on FlaA and 18 on FlaB) in the central D2/3domain of the flagellin (Tabei *et al.,* 2009), and Pse5Ac7Ac has a predicted mass of 316 Da, therefore the mass difference caused by subtle changes in glycosylation (for example, corresponding to 1 or 2 Pse5Ac7Ac residues) between wild type and mutant flagellins may be too subtle to visualise using our methodology. These data suggest that the hypermotility phenotype observed from *AHA0618* mutation is therefore unlikely to be the result of altered polar flagellin glycosylation levels in *A. caviae.*

It is also possible that AHA0618 and HP0518 are involved in pathways unrelated to flagellar assembly and glycosylation in *A. caviae.* Recently, work by Sycuro *et al.* (2013) suggested an alternative role for *HP0518* (named *csd6* in this study) as an L,D-carboxypeptidase involved in peptidoglycan modification at the cell wall, a mutant of which displayed straight-rod cell morphology compared to the helical wild type. AHA0618 may be working in a related fashion, in peptidoglycan synthesis. To strengthen this notion, this work revealed AHA0618 to have homology with proteins shown to be involved in peptidoglycan cross linking at the bacterial cell wall (YkuD superfamily) (Bielnicki *et al.*, 2006) and both AHA0618 and HP0518 were also found to possess the conserved cysteine and histidine residues found in L,D-transpeptidases of the YkuD superfamily of proteins (along with the original YkuD characterised from *B. subtilis*), reinforcing that these proteins likely play a role in peptidoglycan modification. Furthermore, SEM analysis of the *A. caviae AHA0618* mutant suggested a subtle but significant decrease in cell length compared the wild type and *AHA0618* mutant strains expressing either *HP0518* or *AHA0618* displayed overall larger cell lengths. However, when initial studies were carried out to explore the muropeptide profiles of the wild type and mutant strains, no differences were

observed. Nonetheless, these were very preliminary studies and very subtle differences in muropeptide profiles would take further work, with much experimental optimisation, to uncover.

However, *H. pylori* HP0518 is around twice the size of AHA0618 which may indicate that this protein contains a number of other domains, allowing multiple protein functions or an alternative mechanism of action to AHA0618. Penicillin binding proteins containing multiple functioning domains, such as glycosyltransferase and transpeptidase domains, have been described in a number of bacteria (Sauvage *et al.*, 2008); HP0518 is therefore potentially bifunctional, containing separate domains with carboxypeptidase and deglycosylase activities. Analysis of the HP0518 amino acid sequence through the Pfam server suggests this may be the case as it predicts there to be an uncharacterised 'SnoaL' domain of unknown function in addition to the YkuD superfamily region.

The concept that bacterial cell morphology can affect bacterial behaviour has been described by a number of studies. In addition to a *H. pylori csd6* mutant displaying a straight-rod cell shape, studies prior to this by Sycuro *et al.* (2012) on a *csd4 H. pylori* mutant (*csd4* encoding a zinc metalloprotease with carboxypeptidase activity) demonstrated that this straight-rod mutant actually has diminished directional motility through gel-like media and displayed colonisation defects in a mouse model. Therefore the helical shape of *H. pylori* appears to be beneficial for its specific niche, allowing penetration of the mucous lining of the stomach, with morphological mutants showing altered behaviour. CwpFM of *Bacillus cereus* was also identified as a putative cell wall peptidase by Tran *et al.* (2010) and deletion of the gene encoding this protein resulted in larger, 'peanut shaped' cells that appeared to be less able to divide compared to the rod-shaped wild type. Because of this, the mutant was less motile and exhibited a number of other behavioural changes, such as a reduced ability to adhere to epithelial cells and diminished biofilm formation, compared to the wild type. Additionally, virulence of this strain in an insect model was found to be compromised (Tran *et al.*, 2010). Moreover, recent work by Frirdich *et al.* (2014) demonstrated the importance of a specific L,D-carboxypeptidase (Pgp2) on helical cell morphology, motility and biofilm formation as a mutant in the gene encoding this protein resulted in a straight-rod mutant.

Another function of some peptidoglycan remodelling enzymes is to create gaps in the bacterial cell wall for structures, such as the flagellar complex, to assemble and function efficiently (Scheurwater and Burrows, 2011). Although there is no evidence for the tampering of flagellar rotation efficiency in this case and a difference in cell length has been observed between mutant and wild type strains, we cannot rule out the possibility that an *AHA0618* mutation in

*A. caviae* may actually improve efficiency of polar flagellar formation or rotation, hence the reason for enhanced motility. For example, *H. pylori* lacking the lytic transglycosylase, MltD, form flagella that cannot rotate, resulting in non-motility due to the mutants being unable to cleave the peptidoglycan backbone correctly (Roure *et al.*, 2012). The authors of this study hypothesised that the mutation may be affecting how the stator of the flagellar complex, MotB, and peptidoglycan interact, in doing so affecting torque generation (Roure *et al.*, 2012; Roujeinikova, 2008). Mutational studies on peptidoglycan remodelling enzymes that enhance bacterial motility, however, have not yet been reported and therefore the difference in bacterial cell length discussed here is likely to be the reason for the increased bacterial motility of the *AHA0618 A. caviae* mutant.

In the case of *Aeromonas caviae*, so far no flagellin deglycosylation pathway has been identified, and if polar flagellin glycosylation is modulated then this is not achieved by AHA0618. However, this Chapter, and a number of other studies, have highlighted the link between bacterial cell morphology/size and bacterial behaviour. In the case of bacterial velocity, this may be explained by the physics of bacterial motility, where differences in cell shapes result in changes in resistance when cells are moving through aqueous environments, altering speed of motility. With the condition that the efficiency of flagellar formation and rotation is not altered, then it is tempting to speculate that larger cells will produce more drag when moving through solution, resulting in slower motility, compared to smaller cells. Therefore this study supports the role of peptidoglycan remodelling/processing enzymes in bacterial cell shape development, where even the subtlest changes in cell morphology can have an effect on bacterial motility and behaviour.

# Chapter 4: Investigating the sites of *Aeromonas caviae* Sch3 Polar Flagellin Glycosylation

## 4.1 – Introduction

Many bacteria are able to *O*-glycosylate their flagellins, a number of which use nonulosonic acids. The precise role of this post-translational modification, however, remains unknown. It has been determined that *Aeromonas caviae* Sch3 glycosylates its flagellins with pseudaminic acid on six to eight serine or threonine residues within the central D2/D3 domains of the protein (Tabei *et al.*, 2009); a region which is thought to form the surface of the flagellar filament (Yonekura *et al.*, 2003). The exact sites of flagellin glycosylation have not been identified in *A. caviae*; however, how this bacterium modifies its flagellins may give an indication towards the function of this sugar at the cell surface. For example, if glycosylation is homologous, by always being present on the same serine or threonine residues, it may have a structural role, as flagellin glycosylation is essential for flagellar assembly in a variety of bacteria (Goon *et al.*, 2003; Schirm *et al.*, 2003; Twine *et al.*, 2009; Wu *et al.*, 2011; Tabei *et al.*, 2009). It is possible that the presence of sugars may also disguise surface-exposed loop-regions of the flagellins from environmental protease cleavage, as *N*-glycans at the *Campylobacter jejuni* cell surface have been shown to potentially protect proteins from gut proteases (Alemka *et al.*, 2013). It could also be required for favourable interactions with host-cell surfaces, as flagella are essential for bacterial adherence to host cells and therefore the first stages of colonisation (Haiko and Westerlund-Wikstrom, 2013). However, if flagellin glycosylation is heterologous, the movement of pseudaminic acid around the flagellum may disguise this appendage from the host's immune system during infection or it is also possible that flagellin glycosylation may vary depending on the bacterium's situation. As previously discussed in chapter 3, studies in *Campylobacter* have demonstrated that flagellar glycosylation may vary due to phase-variation of the glycosyltransferase proteins (Maf proteins) (van Alphen *et al.*, 2008), of which it has several and is capable of glycosylating its flagella with a plethora of nonulosonate sugars (Karlyshev *et al.*, 2002). Furthermore, work by Howard *et al.* (2009) demonstrated that altered glycosylation levels in *C. jejuni* affects the overall surface charge of the *Campylobacter* flagellum and in doing so, alters the behaviour of a population (Howard *et al.*, 2009). The mutational studies concluded that when *C. jejuni* (11168H) can no longer glycosylate its flagellum with legionaminic acid (and derivatives), strains are still motile (due to the presence of pseudaminic acid), but show altered behaviour, likely due to the decreased

hydrophobicity of the polar flagellum (Howard *et al.*, 2009). Mutants were less able to: autoagglutinate, form biofilms and colonise chickens (Howard *et al.*, 2009).

The previous findings that *A. caviae* Sch3 glycosylates its flagellins with six-eight pseudaminic acid residues suggests there to be some heterogeneity in the glycosylation process (Tabei *et al.*, 2009).

*O*-linked flagellin glycosylation has previously been characterised, either partially or fully, in a number of other bacteria. *Campylobacter* species possess vast and complex glycosylation islands due to being able to glycosylate their flagellins with a variety of nonulosonate sugars. Studies exploring *C. jejuni* 81-176 sites of flagellin glycosylation have revealed 19 serine and threonine residues to be modified, with all but one of these sites being present within the central region of the protein (Thibault *et al.*, 2001). Flagellin was found to be predominantly modified with pseudaminic acid, but other derivatives were also present (such as acetamidino, *O*-acetyl and dihydroxyproprionyl derivatives). Furthermore, intact mass spectrometry analysis of flagellins revealed different flagellin components to exist at one time, suggesting heterogeneity (Thibault *et al.*, 2001). However, although 81-176 glycosylates its flagella with a number of sugars and different flagellin components were identified, it was established that the identified sites are 'usually' occupied, therefore proposing only a small amount of heterogeneity with regards to the site of modification (Thibault *et al.*, 2001). Furthermore, many of the corresponding sites on other *Campylobacter* flagellins were also found to be modified (Thibault *et al.*, 2001). Glycosylation in *C. coli* VC167 has also been characterised and was found to modify 16 residues with pseudaminic acid and derivatives of legionaminic acid (acetamidino and *N*-methylacetamidoyl versions); this was the first demonstration of legionaminic acid decorating a bacterial flagellum (Logan *et al.*, 2002; McNally *et al.*, 2007). In addition, the sugars decorating the *C. jejuni* 11168 flagellum have been explored, which possesses a more complex glycosylation locus to that of other *Campylobacter* strains analysed to date (Logan *et al.*, 2009; Zampronio *et al.*, 2011). This strain was found to synthesise novel pseudaminic acid derivatives (acetamidino and di-*O*-methylglyceric derivatives), and four possible sites of flagellin modification have been so far recognised (Logan *et al.*, 2009; Zampronio *et al.*, 2011).

In contrast to the variety of sugars decorating the polar flagella of *Campylobacter* species, *Helicobacter pylori* glycosylates its polar flagellum solely with pseudaminic acid, similarly to *A. caviae (Schirm et al., 2003).* Little heterogeneity was discovered, with FlaA containing six-seven sugars and FlaB, nine-ten (Schirm *et al.*, 2003).

More recently, glycosylation in the organism, *Shewanella oneidensis*, has been investigated. Two agreeing publications discovered flagellins to be modified with a sugar related to pseudaminic acid, with five sites of modification being confirmed on the dominant flagellin, FlaB, and four sites on FlaA (Bubendorfer *et al.*, 2013; Sun *et al.*, 2013). Heterogeneity between the sites of glycosylation occupied was not reported in these studies (Bubendorfer *et al.*, 2013; Sun *et al.*, 2013). As well as glycosylation, these studies also identified methylation on both *S. oneidensis* flagellins, however, sites of methylation did not appear to be essential for either flagellin glycosylation, or the production of a functional filament (Bubendorfer *et al.*, 2013; Sun *et al.*, 2013).

Moreover, there have also been reports of Gram-positive bacteria containing genes to synthesise nonulosonic acids (Twine *et al.*, 2008; Li *et al.*, 2015), with group I *Clostridium botulinum* flagellins being modified with pseudaminic/legionaminic acid, and a currently undetermined derivative, on up to seven sites per monomer (as well as hexuronic acid derivatives) (Twine *et al.*, 2008).

Although the biological role of flagellin glycosylation is not well understood, it is clear that bacteria modify their flagella in different ways, and therefore the role of glycosylation may vary in each case.

The aims of this chapter were to develop a method of flagellin purification to obtain pure, glycosylated *A. caviae* Sch3 flagellins, and identify sites of glycosylation using mass spectrometry and in doing so, delve deeper into the role of this modification at the *A. caviae* cell surface. Two tandem mass spectrometry (MS/MS) fragmentation methods were tested to establish an appropriate method for analysing *A. caviae* Sch3 flagellin glycosylation sites. Once identified, specific sites of glycosylation were then subjected to site-directed mutagenesis studies to assess their effect on motility.

## 4.2 – Results

### 4.2.1 – Method of flagellin purification

To purify *Aeromonas caviae* Sch3 flagellins, a shearing and centrifugation method, developed from Wilhelms *et al.* (2012) was carried out (Chapter 2, section 2.7.4). In short, bacterial cells isolated from large swarming plates were vortexed to knock the fragile flagella from the cell surfaces, and three centrifugation steps implemented to pellet the flagella. The polyacrylamide gel in Figure 4.1 (A) displays the results of the flagella isolation procedure versus precipitating the supernatant of an *A. caviae* overnight culture with ice-cold ethanol to obtain flagellins. The flagella shearing method provides a clear band of flagellins that can be excised from the polyacrylamide gel for mass spectrometric analysis, with minimal background protein contamination. The presence of glycosylated flagellins was confirmed via a western blot using an antibody that only recognises glycosylated FlaA/B (Fig. 4.1 B).

To further confirm the presence of *A. caviae* Sch3 flagellins, an in-gel trypsin digestion was carried out on an *A.* caviae Sch3 flagellin sample (Chapter 2, section 2.7.7.1), which was then run on a maXis™ (Bruker) Quadrupole Time of Flight mass spectrometer (Q-TOF) for the identification of FlaA and FlaB (Chapter 2, section 2.7.7.2). Mass spectrometric data obtained was submitted to EasyProt (Gluck *et al.*, 2013) and percentage coverages of 59.5% for FlaA and 67.2% for FlaB, were obtained (Fig. 4.2A) (when *A. caviae* Sch3 flagellins were submitted as a database to EasyProt). As this was to confirm the presence of the flagellins, no modifications were considered on EasyProt except those which could result from the in-gel trypsin digestion or mass spectrometry process. Therefore only the variable oxidation of methionine residues (maximum 3) was considered. Trypsin was set as the specific protease used, allowing for two miscleavages. The central region of the proteins (the D2/D3 domains) was not detected, which is likely due to being modified with pseudaminic acid. The actual mass of the central tryptic peptides would not have matched the predicted, unglycosylated masses.

As flagella are not formed in an *A. caviae* glycosyltransferase mutant (*maf1* mutant), but flagellins are still exported (albeit less efficiently) (Parker *et al.*, 2014), these flagellins were obtained for mass spectrometry analysis via ethanol precipitation of supernatant samples. Flagellins from a *maf1* mutant can only be detected by our means when overexpressing FlaA in an inducible vector (please refer to Chapter 3, figure 3.12). A *maf1* mutant containing *flaA* on the IPTG inducible vector pSRK(Gm) was therefore utilised and flagellins cut from a 12% polyacrylamide gel after the ethanol precipitation of the supernatant of a 50 ml overnight culture. These flagellins are thought to be unglycosylated (Parker *et al.*, 2012; Parker *et al.*, 2014)

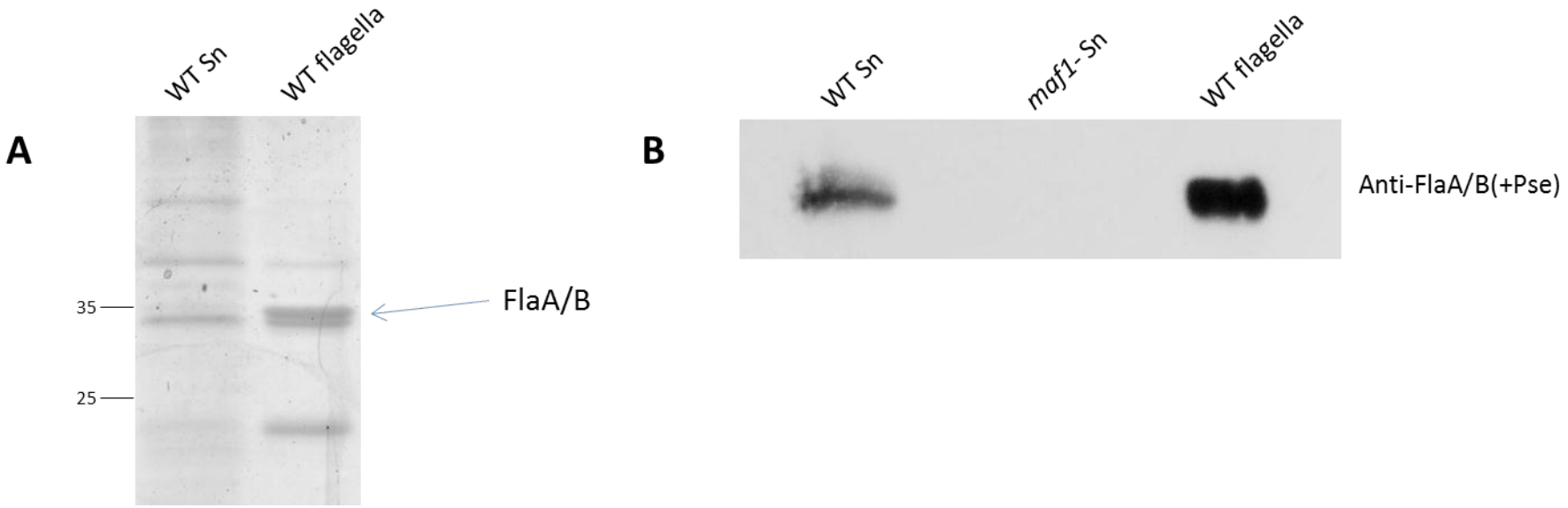


**Figure 4.1** – (**A**) A 12 % polyacrylamide gel displaying: Lane 1, an *A. caviae* Sch3 precipitated supernatant sample (WT Sn), and lane 2, *A. caviae* Sch3 flagella sample obtained from the flagella shearing method (WT flagella). (**B**) Western blot analysis of: lane 1, an *A. caviae* Sch3 precipitated supernatant sample (WT Sn); lane 2, an *A. caviae maf1* mutant precipitated supernatant sample (*maf1*- Sn), and lane 3, an *A. caviae* Sch3 flagella sample (WT flagella), probed with an anti-polar flagellin antibody that only recognises glycosylated flagellin [anti-FlaA/B(+Pse)] (1:10,000).

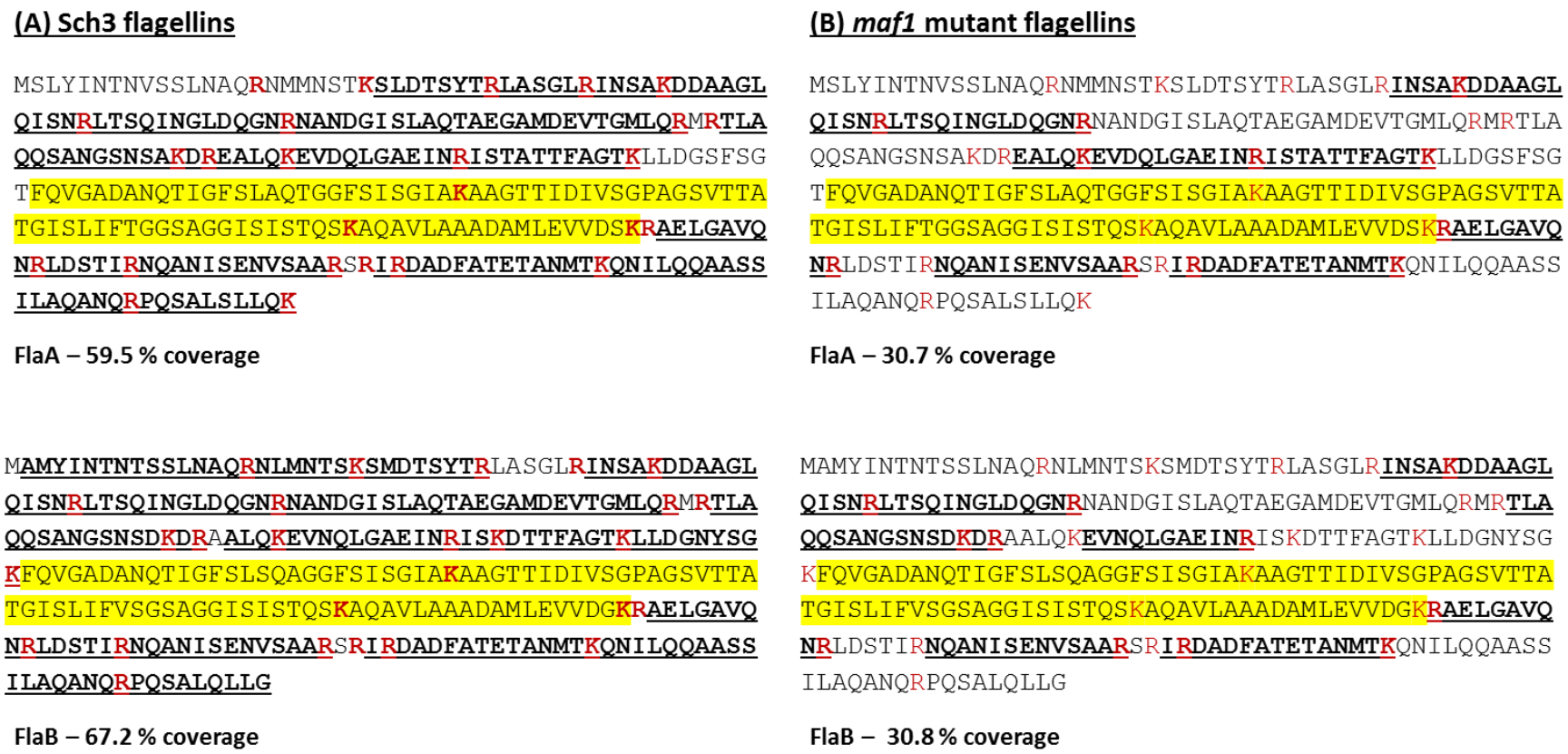


**Figure 4.2** – Percentage coverage of *A. caviae* Sch3 (**A**) and *maf1* mutant flagellins (**B**) when run analysed via CID-MS/MS. Underlined regions of the flagellins represents the peptides detected by EasyProt (Gluck *et al.,* 2009), the highlighted regions show the D2/D3 domains and the red letters demonstrate where trypsin is able to cleave the proteins.

and are extremely insoluble, so very little protein was yielded. An in-gel digest was also carried out of these flagellins samples and their presence confirmed by CID-MS/MS (via EasyProt analysis of the data); however, very few peptides were detected, likely due to the insoluble and less efficient export of these flagellins (Fig 4.2 B) (Parker *et al.*, 2014).

## 4.2.2 – Mass spectrometry analysis of *Aeromonas caviae* polar flagellins

This work was carried out in conjunction with Prof Philip Wright's group in the department of Chemical and Biological Engineering at the University of Sheffield. Samples were digested and run on the mass spectrometers with the help of a postdoctoral researcher, Dr Narciso Couto.

### 4.2.2.1 – Mass Spectrometry Methods for Glycoprotein Analysis

In gel trypsin digestions of *A. caviae* flagellin samples were carried out to yield manageable FlaA/B peptides for mass spectrometry analysis. Trypsin was found to be the best protease by cutting flagellins frequently, after arginine and lysine residues in the flagellin protein sequence (Fig. 4.2). Other enzymes were also investigated alone and in combinations, as trypsin digestion of flagellins yields extremely large peptides from the glycosylated region of interest, the central D2/D3 domain (due to the lack of lysine and arginine residues in this region) (Fig. 4.2); larger peptides are usually are too heavy to run effectively on the mass spectrometer, as they take a lot more energy to fragment (Domon and Aebersold, 2006). However, the best spectra were obtained when the tryptic peptides were subjected to the methods of mass spectrometry discussed here (section 4.2.2). Other enzymes such as LysC, GluC and Chymotrypsin, did not cut frequently enough on their own, but when used in combination, yielded peptides too small to be considered by the mass spectrometer.

Two tandem mass spectrometry (MS/MS) fragmentation methods were investigated for working with flagellin glycopeptides: collision induced dissociation (CID) MS/MS and electron transfer dissociation (ETD) MS/MS.

CID-MS/MS was carried out on a maXis$^{TM}$ Q-TOF mass spectrometer (Bruker) and mass spectra obtained were subjected to both manual and Easyprot analysis (Gluck *et al.*, 2013). CID-MS/MS cleaves the peptide backbone in the C-N peptide bond, producing a series of b and y ions (Fig. 4.3). CID-MS/MS was found to preferentially fragment the pseudaminic acid on glycopeptides present, which could be visualised in the MS/MS spectra as large, singly charged, diagnostic ion peaks at *m/z* 317.1 and 299.1, corresponding to pseudaminic acid and the sugar minus water respectively (Thibault *et al.*, 2001). The presence of these oxonium ions allowed the

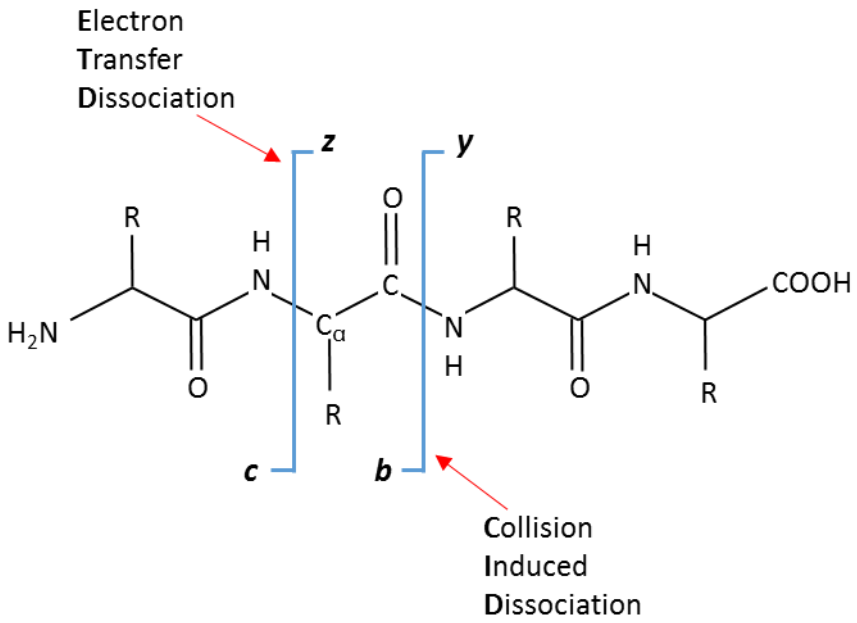


**Figure 4.3** – A schematic diagram to show how the peptide backbone is fragmented during collision induced dissociated (CID) and electron induced dissociation (ETD) tandem mass spectrometry (MS/MS). CID-MS/MS produces a series of y and b ions, whereas ETD-MS/MS produces a series of z and c ions.

manual identification of glycopeptides in the CID-MS/MS spectra. In addition, the Q-TOF used here was found to accurately detect the fragmented tryptic peptides, the results of which could then be submitted to EasyProt (Gluck *et al.*, 2013) for additional analysis of the data. ETD-MS/MS was carried out on an amaZon$^{TM}$ ion trap mass spectrometer (Bruker). This method of peptide fragmentation cleaves the peptide backbone at the N-$C_{\alpha}$ peptide bond, producing a series of c and z ions (Fig. 4.3), and has previously been utilised for glycopeptide analysis. For example, ETD-MS/MS has allowed the successful identification of: *S. onedensis*, *C. jejuni* and *C. botulinum*, sites of flagellin glycosylation (Bubendorfer *et al.*, 2013; Sun *et al.*, 2013; Twine *et al.*, 2008; Zampronio *et al.*, 2011). However, despite these findings, minimal glycopeptides could be detected using ETD for *A. caviae* flagellins. As the sugar on the glycopeptides is not fragmented so fervently during this fragmentation method, fewer to no diagnostic ions are present in the mass spectra, making manual analysis of the spectra more difficult. In theory, CID-MS/MS data could be used to identify the glycopeptides present, and then ETD-MS/MS be used for more detailed analysis of the peptide (ie. identification of sites of modification). However, no glycopeptides could be identified in this way. In addition, the ions produced from peptide fragmentation were detected at less accurate *m/z* values compared to CID-MS/MS on the Q-TOF, making EasyProt analysis of the data challenging (due to requiring extremely accurate *m/z* value information). In light of these findings, analysis of *A. caviae* flagellin glycosylation was carried out using CID-MS/MS.

#### 4.2.2.2 - Manual analysis of CID-MS/MS spectra

Protein Prospector was utilised to support the manual analysis of CID MS/MS spectra (Chapter 2, section 2.7.7.3). The Protein Prospector 'digest tool' was used to perform a theoretical trypsin digest of both FlaA and FlaB (with two miscleavages considered) to yield hypothetical *m/z* values of the tryptic peptides (up to a charge state of +6, due to high charge states of glycopeptides being visualised in the spectra). As Protein Prospector does not take into account any post-translational modifications in the digests, the predicted *m/z* values for glycosylated, tryptic peptides was manually calculated using Microsoft Excel, with up to eight pseudaminic acids being considered on appropriate peptides containing serine or threonine residues. The Protein Prospector 'MS product' tool was also used to help annotate the MS/MS spectra of peptides of interest.

Spectra obtained from trypsin digestion of *A. caviae* Sch3 flagellins was manually examined for the characteristic oxonium ions of pseudaminic acid, *m/z* $317.1^{[1+]}$ and *m/z* $299.1^{[1+]}$. These ions were present throughout the CID-MS/MS spectra of wild type flagellins, however were absent from *A. caviae maf1* mutant flagellin samples (Fig 4.4). Figure 4.4 displays the glycosylated

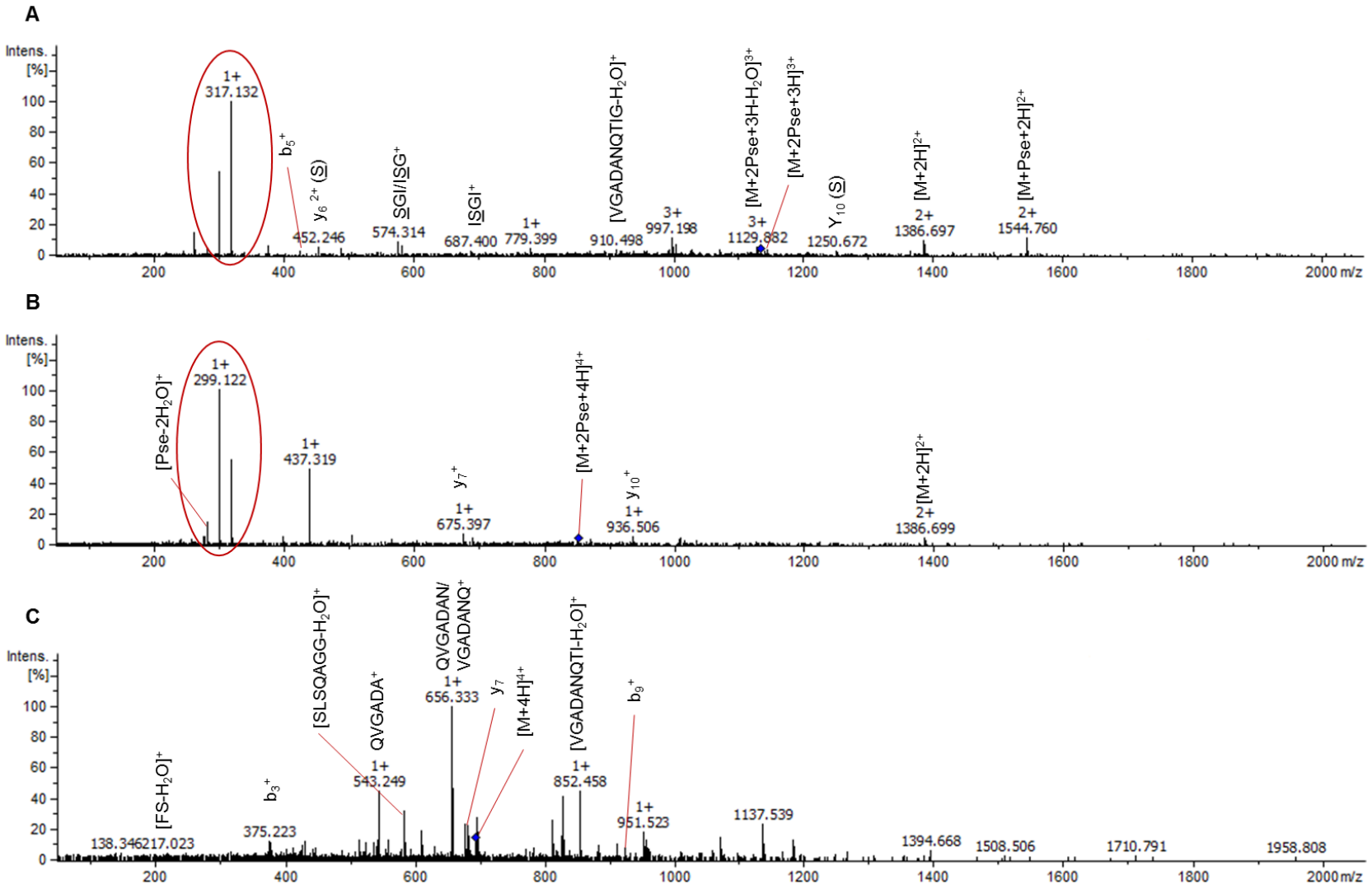


**Figure 4.4** – legend on page 109

**Figure 4.4** – CID-MS/MS spectra of the FlaB peptide, $^{146}$FQVGADANQTIGFSLSQAGGFSISGIAK$^{173}$, which contributed towards Parker *et al.* (2014). This peptide eluted multiple times between 60-100 min retention times. (**A**) MS/MS of the triply charged ion, *m/z* 1135.2, of which this particular peptide eluted at 96.22 min an *A. caviae* Sch3 sample. The ion corresponds to the peptide glycosylated with two pseudaminic acid residues. (B) MS/MS of the quadruply charged ion, *m/z* 851.7, of which this particular peptide eluted at 96.25 min an *A. caviae* Sch3 sample. The ion corresponds to the peptide glycosylated with two pseudaminic acid residues. (**C**) MS/MS spectra from an *A. caviae maf1* mutant flagellin sample. The quadruply charged ion, *m/z* 692.85, elutes here at 74.43 min and corresponds to the unglycosylated peptide. **S** refers to a potentially modified serine residue.

tryptic peptide, $^{146}$FQVGADANQTIGFSLSQAGGFSISGIAK$^{173}$, from wild type *A. caviae* FlaB (Fig 4.4 A&B). This peptide is only ever found in its glycosylated form in this strain. However, figure 4.4 C shows the corresponding, unglycosylated peptide from a *maf1* mutant strain (Fig4.4 C). Maf1 has been identified as the putative polar flagellin glycosyltransferase and these data therefore further support this notion (Parker *et al.*, 2012; Parker *et al.*, 2014).

Although many glycopeptides could be manually visualised within the spectra (recorded between 60-100 minute retention times), many difficulties were faced when trying to identify them. As previously found, FlaA/B are glycosylated with 6-8 pseudaminic acid residues in their D2/D3 domains (Tabei *et al.*, 2009) out of a possible 19 sites on each flagellin within this region. Due to the lack of lysine and arginine residues, tryptic peptides within this D2/D3 region are large; therefore there are many possible sites of glycosylation on each tryptic peptide. The FlaB peptide [146-173] was the most frequent glycopeptide observed when analysing the spectra manually; this was present at *m/z* 1135.2$^{[3+]}$ and 851.7$^{[4+]}$ corresponding to this peptide containing two pseudaminic acids, and at *m/z* 1029.8$^{[3+]}$, equivalent to the peptide containing one pseudaminic acid (Table 4.1). The exact sites of glycosylation could not be determined without the aid of EasyProt (Chapter 2, section 2.7.7.3) due to the preferential fragmentation of pseudaminic acid via CID-MS/MS; the peaks corresponding to the rest of the peptide fragmentation were therefore extremely small and largely lost in the spectra's background noise. This peptide was also found to be triply charged with two protons and one sodium ion, at *m/z* 1142.5, corresponding to the peptide containing two pseudaminic acids. This was determined to be the same peptide, as the MS/MS spectrum was similar to that of the triply and quadruply charged ions, *m/z* 1135.2 and 851.7, respectively. Furthermore, if the mass of this tryptic peptide containing two sugars is 3402.6 Da, the predicted *m/z* value of the ion, $[M+2H+Na]^{3+}$, can be estimated, which would give a value of *m/z* 1142.5 due to the following calculation: (3402.6+2+23)/3. Protein prospector MS-product confirmed that the triply charged ion of the FlaB tryptic peptide, [146-173] (with a sodium ion present), modified with two pseudaminic acid residues, is likely to have an *m/z* value of 1142.5. Table 4.1 displays the other glycopeptides that were recorded multiple times during CID-MS/MS. The table presents predicted glycopeptides which have been identified due to the observed *m/z* values matching predicted values obtained from the theoretical trypsin digest of FlaA/B carried out by Protein Prospector. However, manual analysis of MS/MS spectra could not confirm these to be the actual glycopeptides present in most cases (shown as x or ✓) (Table 4.1).

There were also peptides present that displayed the diagnostic ions of pseudaminic acid in their MS/MS spectra, but could not be assigned a protein sequence such as: 1154.2$^{[3+]}$ (which was as common as 1135.2$^{[3+]}$), 1212.6$^{[6+]}$, 1217.1$^{[2+]}$, 1250.58$^{[3+]}$, 1272.4$^{[3+]}$, 1274.3$^{[3+]}$,

| ***m/z* present** | **Potential Glycopeptide** | **Flagellin?** | **Peptide Information** | **Expected *m/z*** | **Matched peaks (y/b/internal)** |
|---|---|---|---|---|---|
| $1029.8^{[3+]}$<br>Present throughout spectra | $^{146}$FQVGADANQTIGFSLSQAGGFSISGIAK$^{173}$ | FlaB | 1 Pse5Ac7Ac – unknown position<br>$[M+3H+Pse5Ac7Ac]^{3+}$ | $1029.8^{[3+]}$ | ✓ - section 4.2.2.3, figures: 4.5, 4.6 & 4.7. |
| $1135.2^{[3+]}/851.7^{[4+]}$<br>Present throughout spectra | $^{146}$FQVGADANQTIGFSLSQAGGFSISGIAK$^{173}$ | FlaB | 2 Pse5Ac7Ac – unknown position<br>$[M+3H+Pse5Ac7Ac]^{3+}$ | $1135.2^{[3+]}/851.7^{[4+]}$ | ✓ - section 4.2.2.3. figures: 4.8 & 4.9 |
| $1142.5^{[3+]}$ | $^{146}$FQVGADANQTIGFSLSQAGGFSISGIAK$^{173}$ | FlaB | 2 Pse5Ac7Ac – unknown position<br>$[M+2H+Na+2Pse5Ac7Ac]^{3}$ | $1142.5^{[3+]}$ | ✓ |
| $1140.8^{[3+]}$<br>Present throughout spectra | Many peaks in spectra matching fragmentation pattern of $^{146}$FQVGADANQTIGFSLSQAGGFSISGIAK$^{173}$ | FlaB | Unknown | N/A | N/A |
| $1129.2^{[3+]}$ | $^{38}$INSAKDDAAGLQISNRLTSQINGLDQGNR$^{66}$<br><br>OR<br><br>$^{146}$FQVGADANQTIGFSLSQAGGFSISGIAK$^{173}$ | FlaA/B<br><br><br><br>FlaB | 1 Pse5Ac7Ac<br>$[M+3H+Pse5Ac7Ac]^{3+}$<br>2 miscleavages<br><br>2 Pse5Ac7Ac – unknown position<br>$[M+2H+Na+2Pse5Ac7Ac\text{-}H_2O]^{3+}$ | $1129.2^{[3+]}$<br><br><br><br>$1129.2^{[3+]}$ | **X - unlikely**<br><br><br><br>✓- Loss of water before fragmentation |
| $1048.99^{[2+]}$ | $^{16}$NLMNTSKSMDTSYTR$^{31}$ | FlaB | 1 Pse5Ac7Ac, 2 oxidation methionine<br>$[M+2H+Pse5Ac7Ac]^{2+}$<br>1 miscleavage | $1048.96^{[2+]}$ | **X - unlikely** |
| $1288.06^{[2+]}$ | $^{24}$SRIRDADFATETANMTK$^{42}$ | FlaB | 2 Pse5Ac7Ac. 1 oxidation methionine<br>$[M+2H+2Pse5Ac7Ac]^{2+}$<br>2 Miscleavages | $1288.09^{[2+]}$ | **X - unlikely** |
| $1292.5^{[2+]}$ | MRTLAQQSANGSNSAKDR | FlaA | 2 Pse5Ac7Ac, 1 oxidation methionine<br>$[M+2H+2Pse5Ac7Ac]^{2+}$<br>2 Miscleavages | $1292.1^{[2+]}$ | **X - unlikely** |

**Table 4.1** – The potential sequence of predicted glycopeptides identified during CID-MS/MS analysis of *Aeromonas caviae* Sch3 flagellins (FlaA/B). ✓ and X denote whether the predicted peptide is likely to be actually present depending on the presence of y and b ions in the MS/MS spectra.

1296.5$^{[2+]}$, 1317.28$^{[3+]}$, 1341.3$^{[3+]}$, 1383.99$^{[3+]}$. All of these ions were observed multiple times during manual analysis. Furthermore, there were also many glycopeptides present that only appeared once in the spectra and could not be assigned to a single peptide. This may demonstrate that *A. caviae* flagellin glycosylation is extremely variable, with many different glycopeptides, or versions of the same peptide, being present in a wild type flagellin sample.

#### 4.2.2.3 – EasyProt analysis of CID-MS/MS spectra

EasyProt (Gluck *et al.*, 2013) was utilised to complement manual analysis of CID-MS/MS data. This was carried out with the help of Andrew Landells in Chemical and Biological engineering at Sheffield University (Chapter 2, section 2.7.7.3). EasyProt parameters were updated to also consider the variable modification of serine and threonine residues with pseudaminic acid (maximum 3). Peptides with a z-score above six were considered (statistical score assigned to the peptides by EasyProt depending on the peaks present in the spectra and therefore judging the likelihood that the said peptide is actually present).

EasyProt confirmed that the FlaB peptide, $^{146}$FQVGADANQTIGFSLSQAGGFSISGIAK$^{173}$, is glycosylated either once or twice, and is never found in its unglycosylated form. In addition, it suggested the exact sites of glycosylation appear to vary on this peptide. When glycosylated once, the FlaB peptide was found to be glycosylated either on: threonine 155, serine 159 or serine 161 (Fig. 4.5, 4.6 & 4.7). When glycosylated twice (which was more common), the modification of both central serine residues (serine 159 and 161) was observed most frequently (Fig. 4.8); however, the peptide was also present with modifications on both, threonine 155 and serine 159 (Fig. 4.9).

As Sun *et al.* (2013) demonstrated that *Shewanella oneidensis* FlaB is also methylated, methylation of lysine residues was also investigated in *A. caviae.* When methylation of lysine residues (methyl/dimethyl/trimethyl) was introduced into the EasyProt search parameters as an optional, variable modification, a variety of methylated peptides were discovered. The FlaA peptide, $^{108}$DREALQKEVDQLGAEINR$^{125}$, was suggested to be present in numerous forms in a wild type *A. caviae* flagellin sample, as evidence for dimethylation and trimethylation on the central lysine 114 was discovered, along with the unmodified peptide (Fig. 4.10, 4.11 & 4.12). Furthermore, EasyProt analysis of flagellin also suggested the FlaB peptide, $^{126}$ISKDTTFAGTK$^{136}$, to be dimethylated on lysine 128 and the peptide, $^{38}$INSAKDDAAGLQISNR$^{53}$, present in both FlaA and FlaB, to be di- and trimethylated on lysine 42. Both peptides were discovered in their unmodified forms also. Please refer to figures 4.13 and 4.14 for FlaB peptide [26-136], and figures 4.15, 4.16 and 4.17 for FlaA/B peptide [38-53].

EasyProt did not identify any other modified peptides in wild type *A. caviae* flagellin samples.

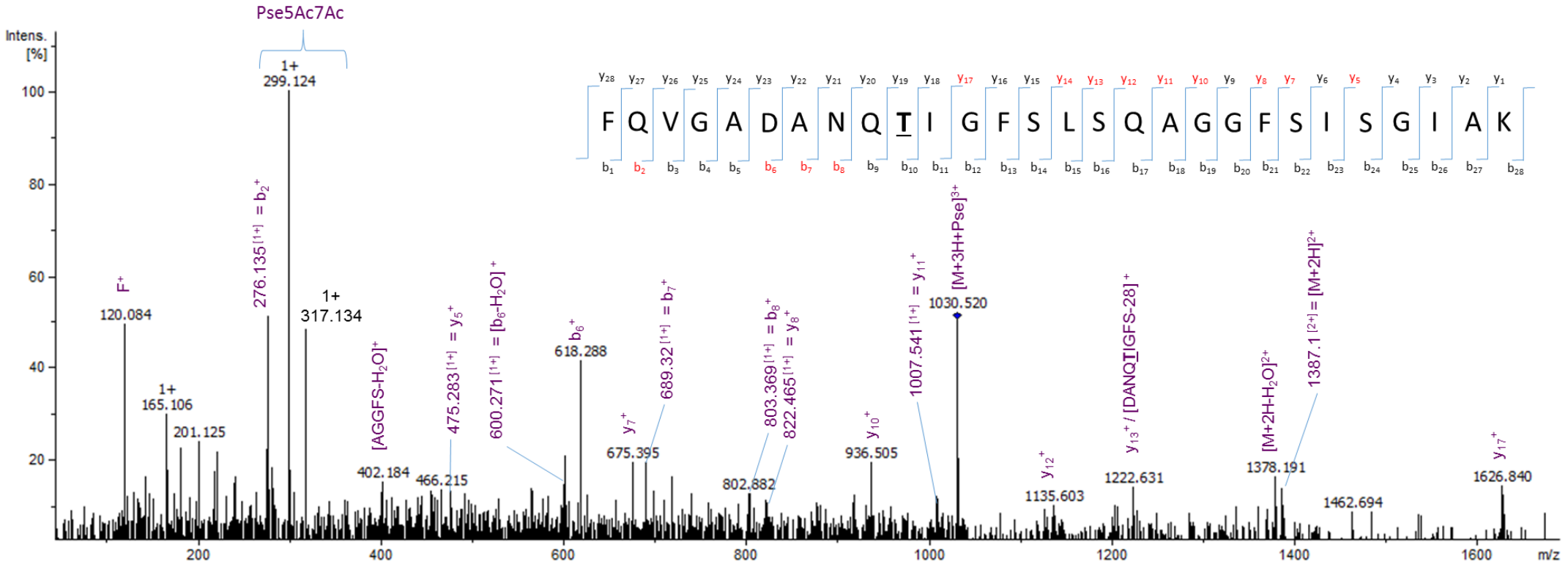


**Figure 4.5** – CID-MS/MS spectra of the triply charged ion, *m/z* 1029.8, which corresponds to the FlaB peptide, $^{146}$FQVGADANQTIGFSLSQAGGFSISGIAK$^{173}$, containing one pseudaminic acid residue at threonine 155. **T** denotes the likely position of the sugar and the red text refers to the y and b ions present in the spectra. This particular peptide eluted at 100.42 min.

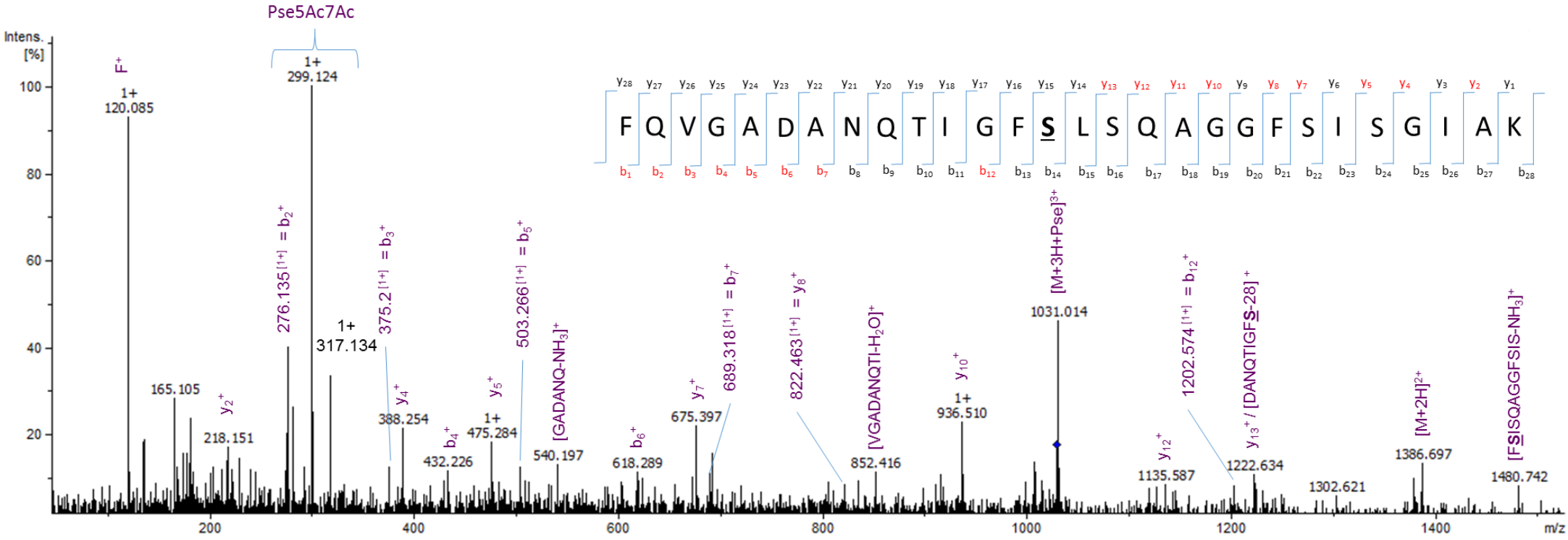


**Figure 4.6** – CID-MS/MS spectra of the triply charged ion, *m/z* 1029.8, which corresponds to the FlaB peptide, $^{146}$FQVGADANQTIGFSLSQAGGFSISGIAK$^{173}$, containing one pseudaminic acid residue at serine 159. **S** denotes the likely position of the sugar and the red text refers to the y and b ions present in the spectra. This particular peptide eluted at 79.6 min.

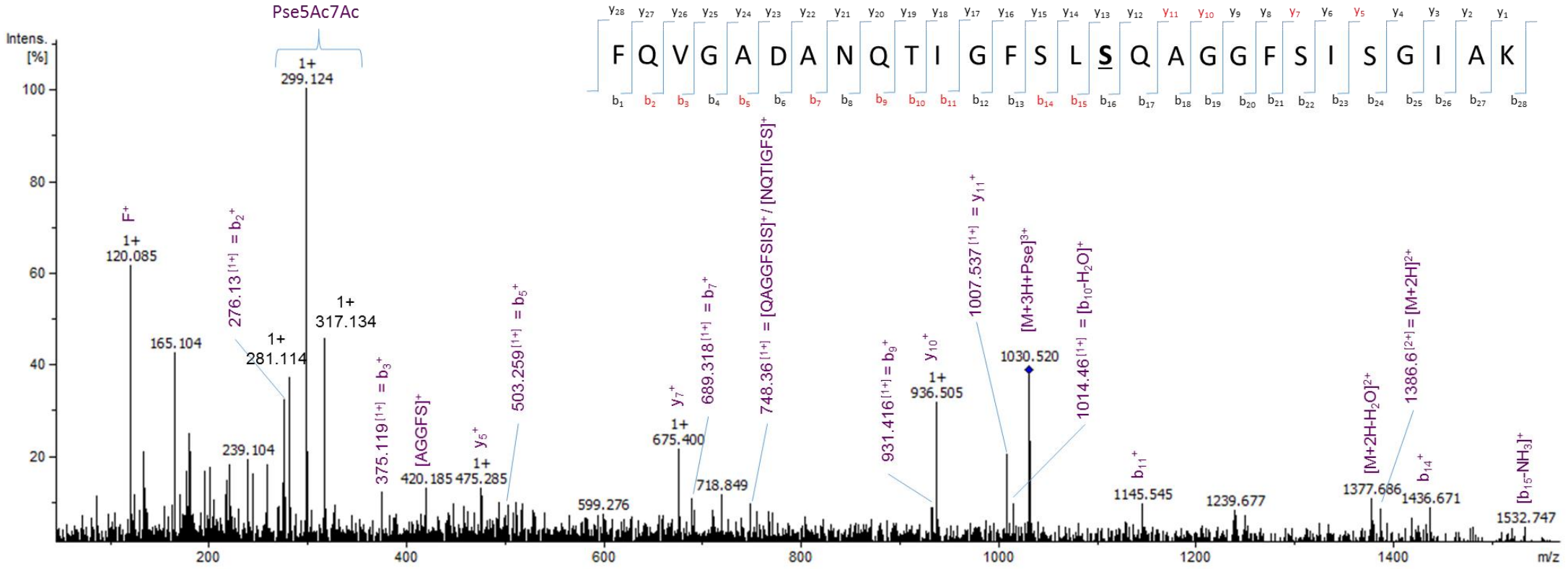


**Figure 4.7** – CID-MS/MS spectra of the triply charged ion, *m/z* 1029.8, which corresponds to the FlaB peptide, $^{146}$FQVGADANQTIGFSLSQAGGFSISGIAK$^{173}$, containing one pseudaminic acid residue at serine 161. **S** denotes the likely positions of the sugar and the red text refers to the y and b ions present in the spectra. This particular peptide eluted at 80.82 min.

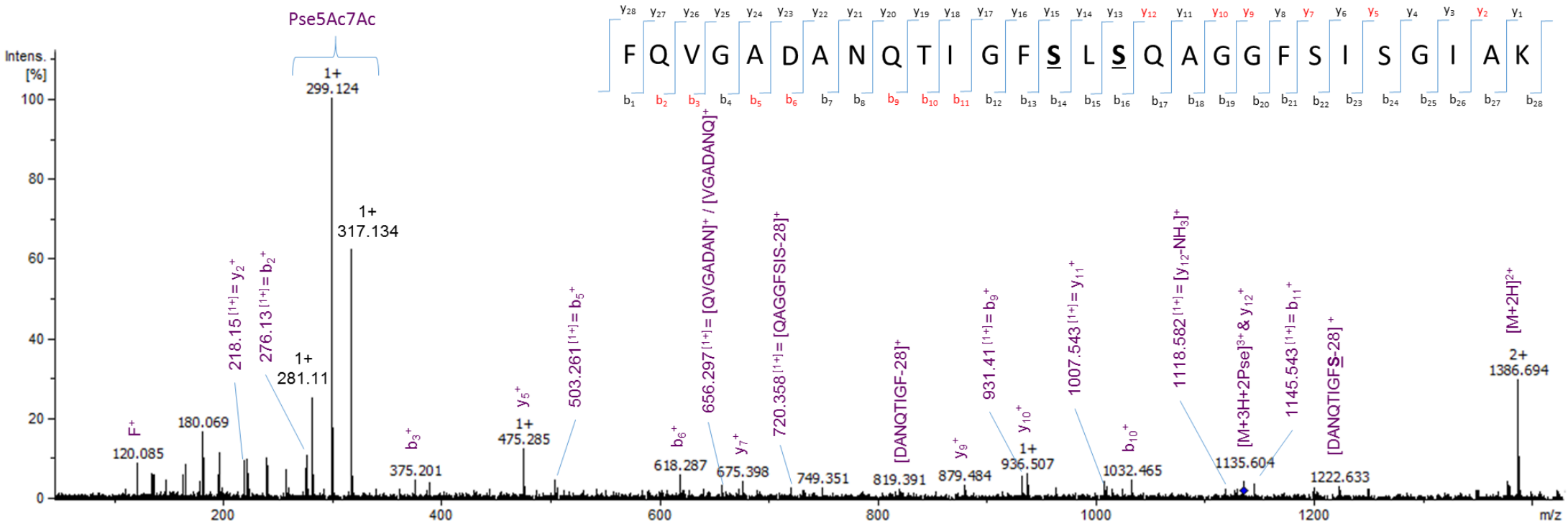


**Figure 4.8** – CID-MS/MS spectra of the triply charged ion, *m/z* 1135.2, which corresponds to the FlaB peptide, $^{146}$FQVGADANQTIGFSLSQAGGFSISGIAK$^{173}$, containing two pseudaminic acid residues at serine 159 and serine 161. **S** denotes the likely positions of the sugar and the red text refers to the y and b ions present in the spectra. This particular peptide eluted at 86.24 min.

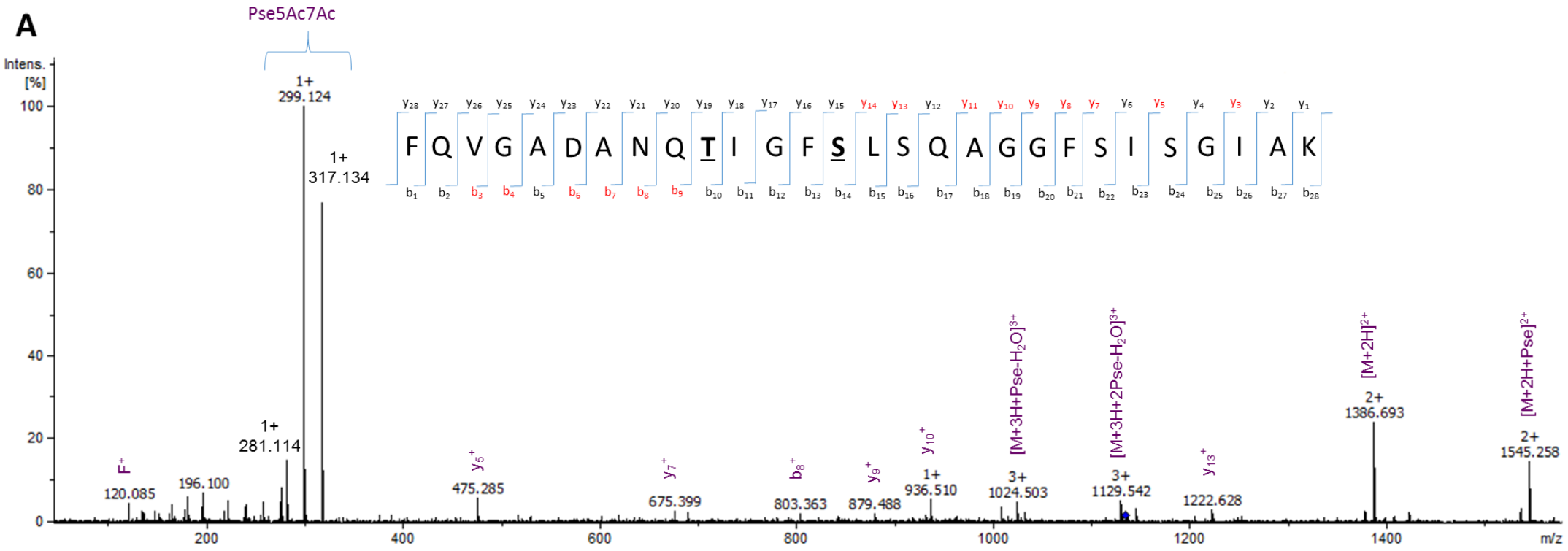


**Figure 4.9: Part A** - CID-MS/MS spectra of the triply charged ion, *m/z* 1135.2, which corresponds to the FlaB peptide, $^{146}$FQVGADANQTIGFSLSQAGGFSISGIAK$^{173}$, containing two pseudaminic acid residues at threonine 155 and serine 159. **S** and **T** denote the likely positions of the sugar and the red text shows the combination of y and b ions present in both **(A) and (B)**. Part (**B**) to this figure can be found on the following page. This particular peptide eluted at 73.53 min. Part (**B**) displays the central region of the MS/MS spectra amplified (*m/z* values between 300 and 1400).

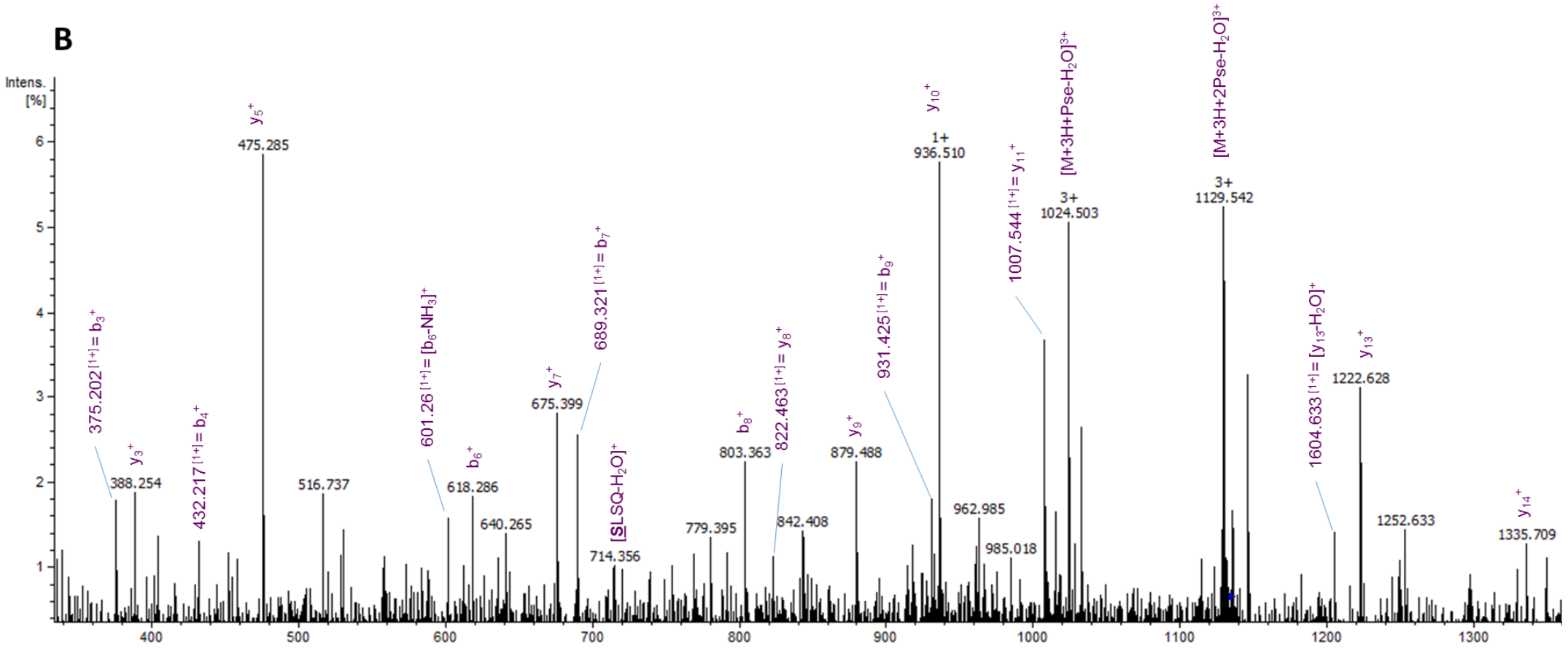


**Figure 4.9: Part B** - CID-MS/MS spectra of the triply charged ion, *m/z* 1135.2, which corresponds to the FlaB peptide, $^{146}$FQVGADANQTIGFSLSQAGGFSISGIAK$^{173}$, containing two pseudaminic acid residues at threonine 155 and serine 159. This figure shows the amplified central region (*m/z* values between 300 and 1400) from the MS/MS spectra shown in figure 4.9, part (**A**). For the combination of y and b ions present please refer to part (**A**).

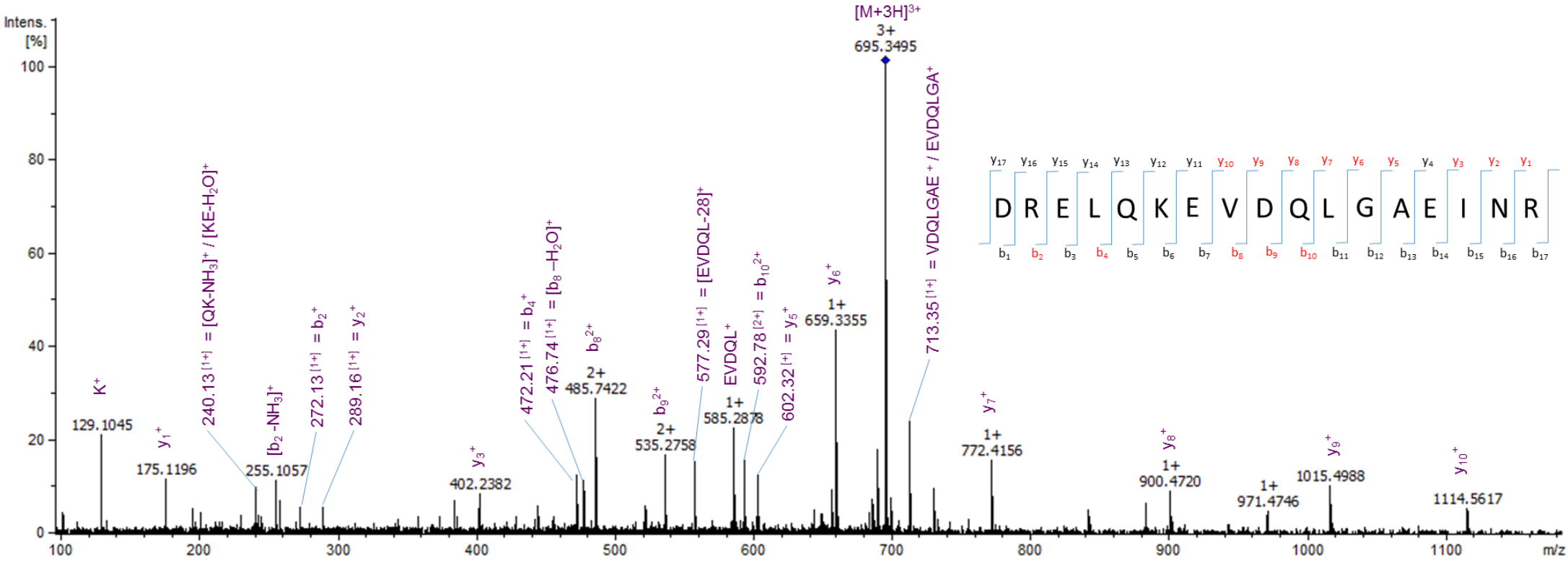


**Figure 4.10** – CID-MS/MS spectra of the triply charged ion, *m/z* 695.35, which corresponds to the unmodified FlaA peptide, $^{108}$DREALQKEVDQLGAEINR$^{125}$. The red text refers to the y and b ions present in the spectra. This particular peptide eluted at 39.19 min.

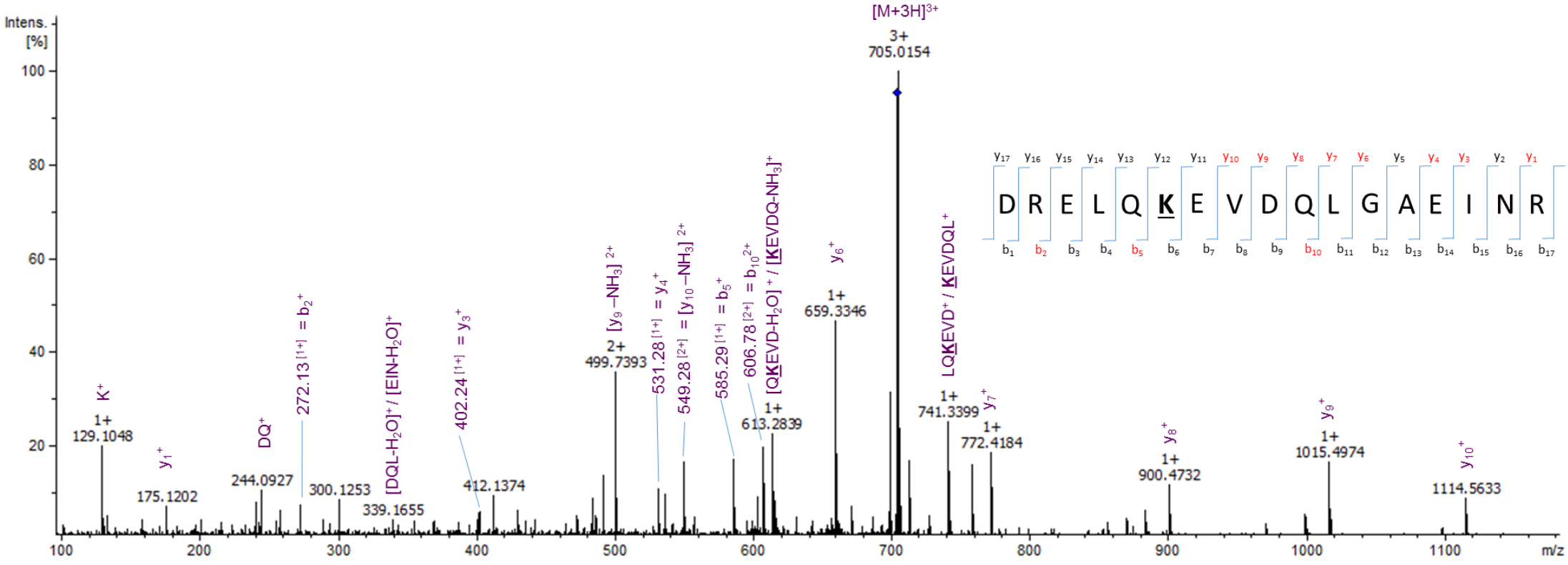


**Figure 4.11** – CID-MS/MS spectra of the triply charged ion, *m/z* 704.69, which corresponds to the dimethylated FlaA peptide, $^{108}$DREALQKEVDQLGAEINR$^{125}$. **K** denotes the likely modified residue and the red text refers to the y and b ions present in the spectra. This particular peptide eluted at 44.29 min.

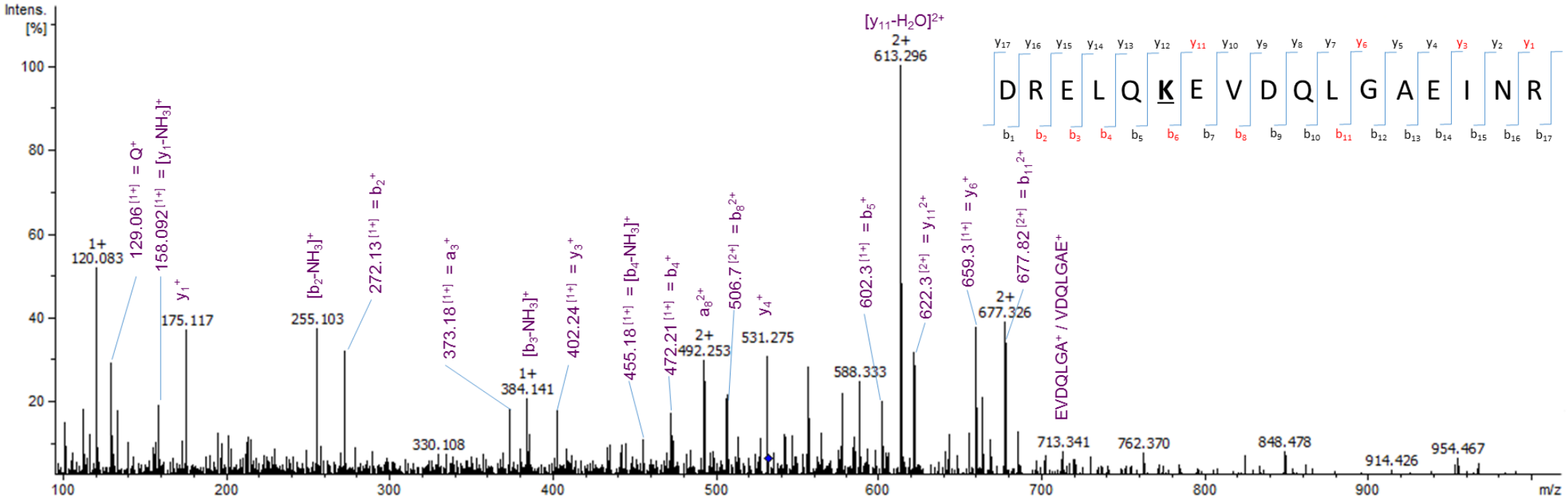


**Figure 4.12** – CID-MS/MS spectra of the quadruply charged ion, *m/z* 532.3, which corresponds to the trimethylated FlaA peptide, $^{108}$DREALQKEVDQLGAEINR$^{125}$. **K** denotes the likely modified residue and the red text refers to the y and b ions present in the spectra. This particular peptide eluted at 38.07 min.

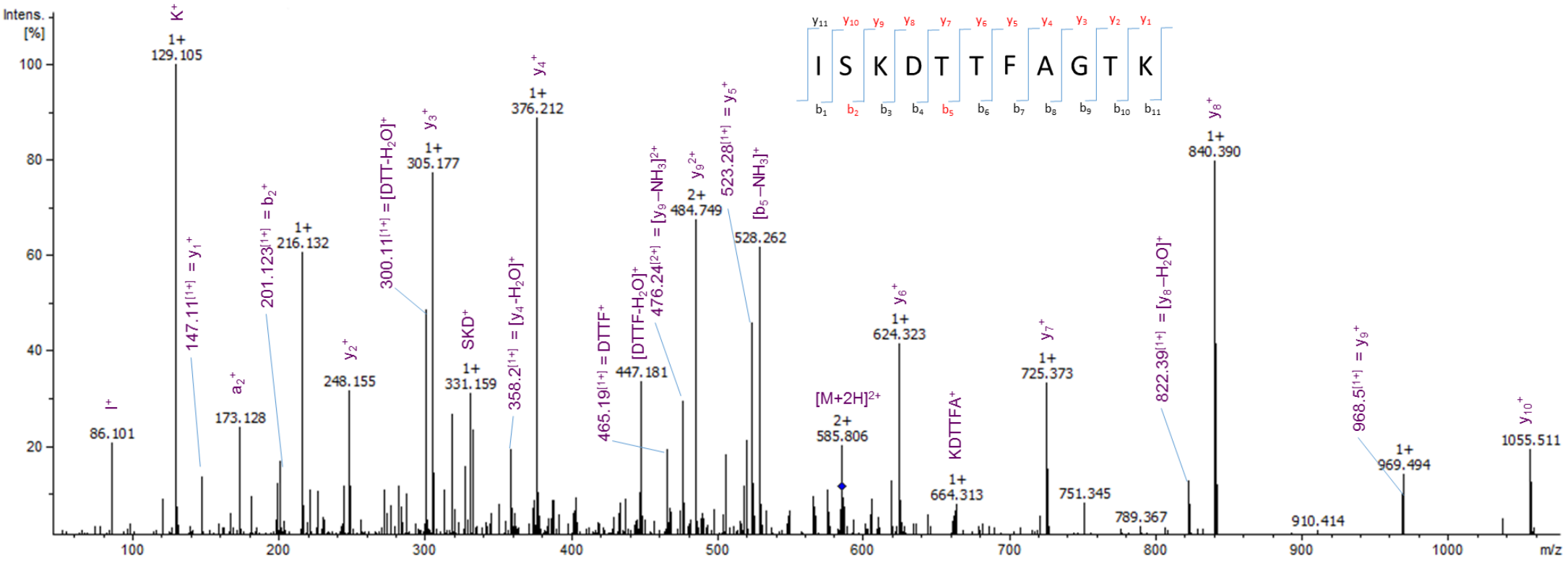


**Figure 4.13** – CID-MS/MS spectra of the doubly charged ion, *m/z* 584.8, which corresponds to the unmodified FlaB peptide, $^{126}$ISKDTTFAGTK$^{136}$. The red text refers to the y and b ions present in the spectra. This particular peptide eluted at 19.59 min.

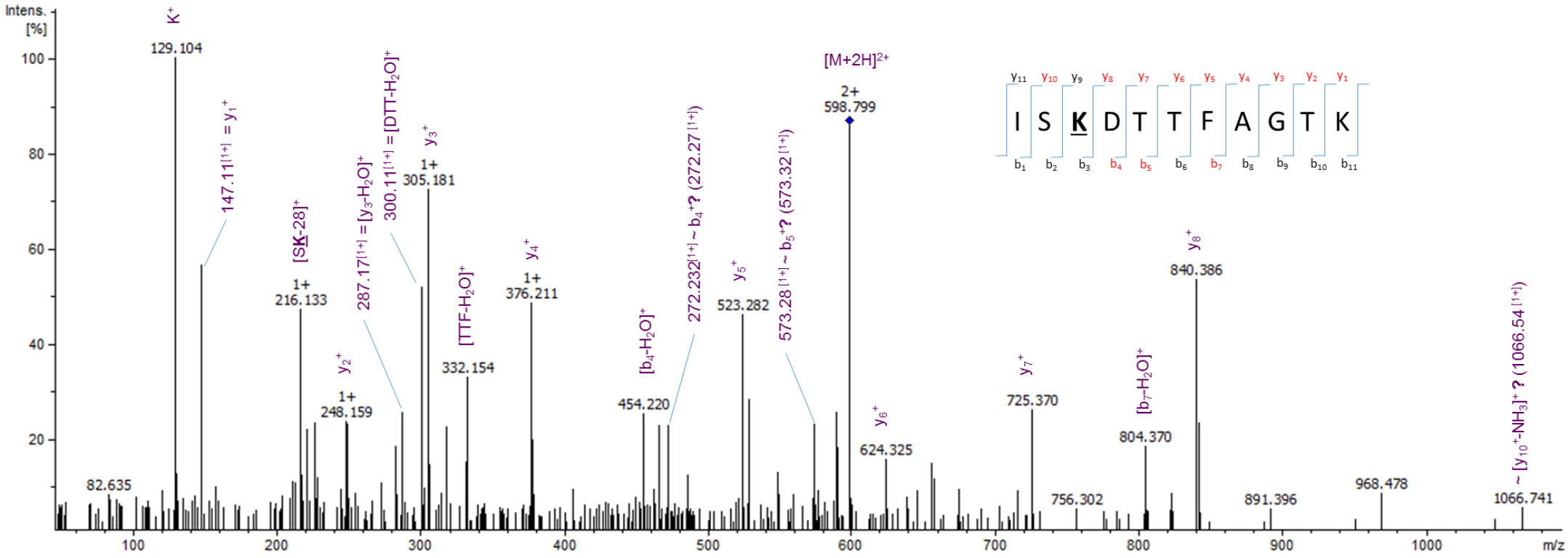


**Figure 4.14** – CID-MS/MS spectra of the doubly charged ion, *m/z* 598.8, which corresponds to the dimethylated FlaB peptide, $^{126}$ISKDTTFAGTK$^{136}$. **K** denotes the likely modified residue and the red text refers to the y and b ions present in the spectra. This particular peptide eluted at 28.87 min.

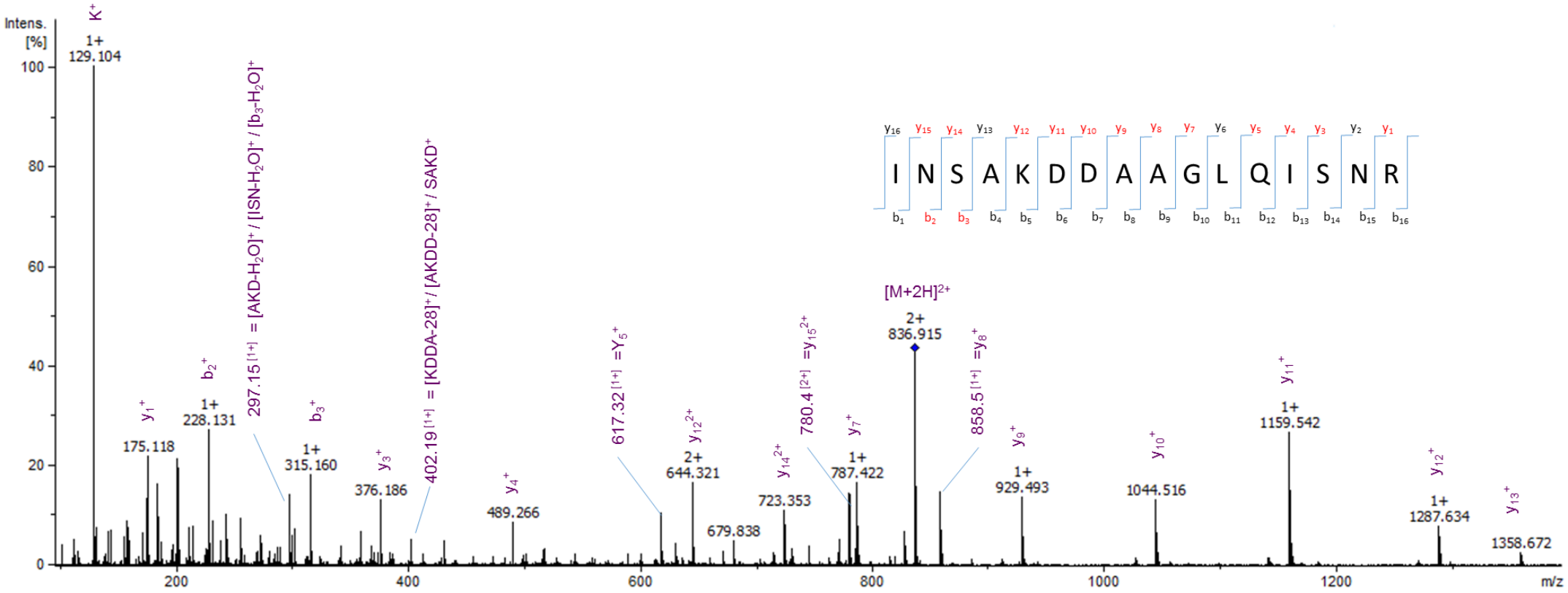


**Figure 4.15** – CID-MS/MS spectra of the doubly charged ion, *m/z* 836.9, which corresponds to the unmodified FlaA/B peptide, $^{38}$INSAKDDAAGLQISNR$^{53}$. The red text refers to the y and b ions present in the spectra. This particular peptide eluted at 23.18 min.

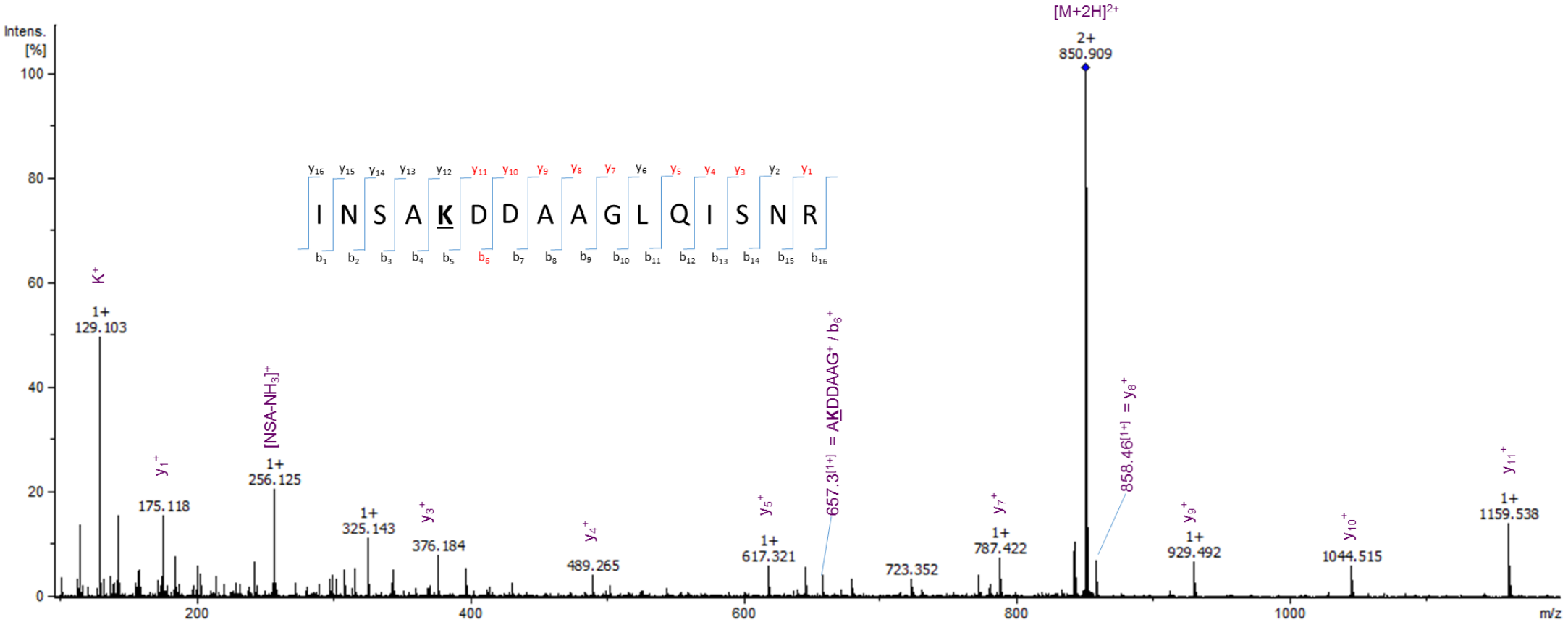


**Figure 4.16** – CID-MS/MS spectra of the doubly charged ion, *m/z* 850.9, which corresponds to the dimethylated FlaA/B peptide, [38]INSAKDDAAGLQISNR[53]. **K** denotes the likely modified residue and the red text refers to the y and b ions present in the spectra. This particular peptide eluted at 32.47 min.

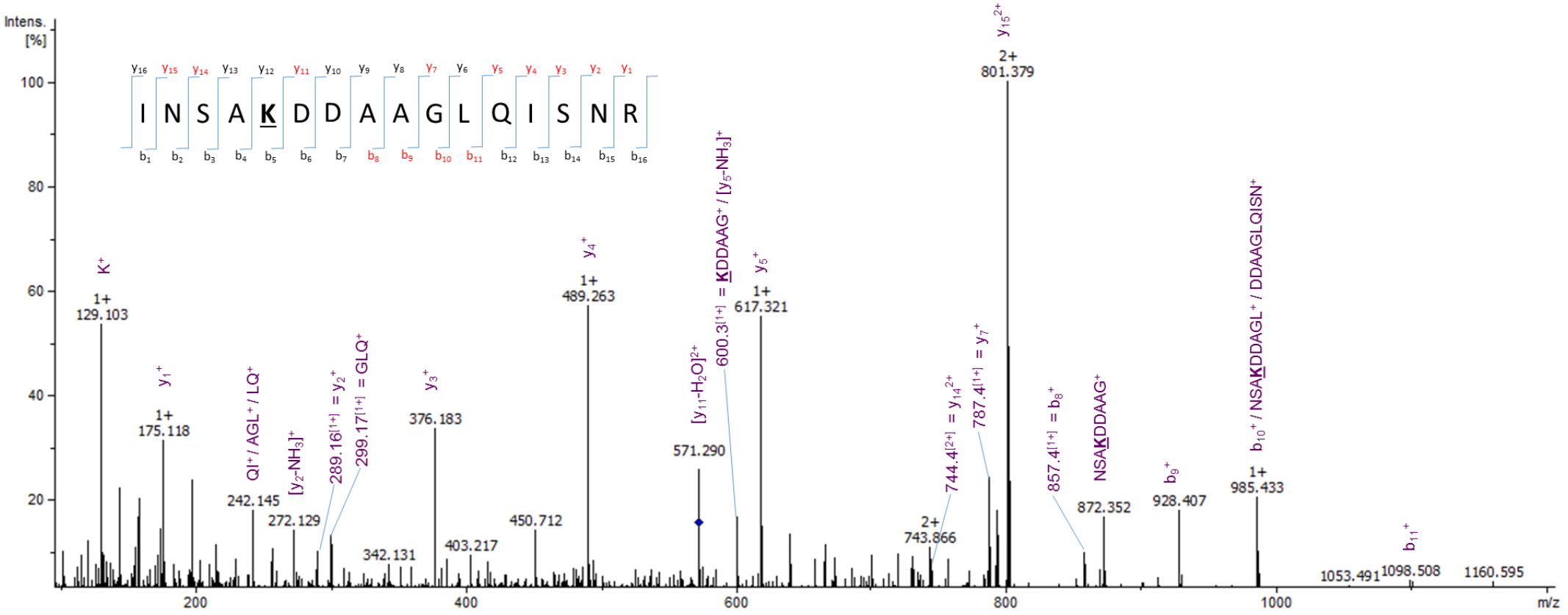


**Figure 4.17** – CID-MS/MS spectra of the triply charged ion, *m/z* 572.3, which corresponds to the trimethylated FlaA/B peptide, $^{38}$INSAKDDAAGLQISNR$^{53}$. **K** denotes the likely modified residue and the red text refers to the y and b ions present in the spectra. This particular peptide eluted at 26.99 min.

## 4.2.3 – Flagellin Mutational Studies

As the FlaB peptide, $^{146}$FQVGADANQTIGFSLSQAGGFSISGIAK$^{173}$, was identified to be glycosylated (potentially with either one or two pseudaminic acid residues), and the site of glycosylation appears to vary, FlaB was selected for site-directed mutagenesis studies to investigate whether any specific glycoforms of this peptide are particularly required for the motility of *A. caviae.* These studies were carried out in an *A. caviae flaA flaB* double mutant background (which will be referred to as *flaAB* mutant), created from the insertion of a chloramphenicol cassette into *flaA* and a kanamycin cassette into *flaB* (Rabaan *et al.*, 2001). Site-directed *flaB* mutants were cloned into the broad host range vector pBBR1MCS-5 and strains created were compared to the *flaAB* mutant containing wild type *flaB* (from Sch3 *A. caviae*) in pBBR1MCS-5, as although *flaB* can complement the non-motile phenotype of a *flaAB* mutant, motility is slightly impaired compared to the wild type (Fig. 4.18).

### 4.2.3.1 – Generation of pBBR1MCS-5_*flaB*

The *flaB* gene (918 base pairs), encoding the *A. caviae* Sch3 polar flagellin (FlaB), was cloned into pBBR1MCS-5 along with a region upstream of the transcription start site to allow expression of *flaB* from its native promoter (99 base pairs). Q5 high fidelity DNA polymerase (NEB) was used to amplify *flaB* from Sch3 *A. caviae* genomic DNA with the primers RCL_55 and RCL_56 (Fig. 4.19 A). The PCR product was directly cut with a combination of *Hin*dIII and *Bam*HI restriction enzymes before being ligated into HindIII/BamHI cut pBBR1MCS-5 (Fig. 4.19 A). The ligation was transformed into chemically competent DH5α and minipreps carried out with resulting transformants to isolate the vector DNA. The presence of *flaB* was investigated with a *Bam*HI restriction digest and agarose gel electrophoresis (compare with linearised empty pBBR1MCS-5). Likely pBBR1MCS-5_*flaB* constructs were sent for sequencing using M13 forward and reverse primers to confirm the presence of *flaB.*

### 4.2.3.2 – Site-directed Mutagenesis of FlaB Glycosylation Sites Identified via Mass Spectrometry

In order to determine whether particular glycosylation sites were important for the motility of *A. caviae,* FlaB site-directed mutants were created via overlap extension PCR (OE-PCR) (Chapter 2, section 2.6.2.3); where serine and threonine residues on the peptide, $^{146}$FQVGADANQTIGFSLSQAGGFSISGIAK$^{173}$, were mutated to alanine residues, due to the structural simplicity and non-polar properties of this amino acid. Site directed mutants created, and the primers used to generate each fragment for OE-PCR, are summarised in table 4.2 (mutants 1-4).

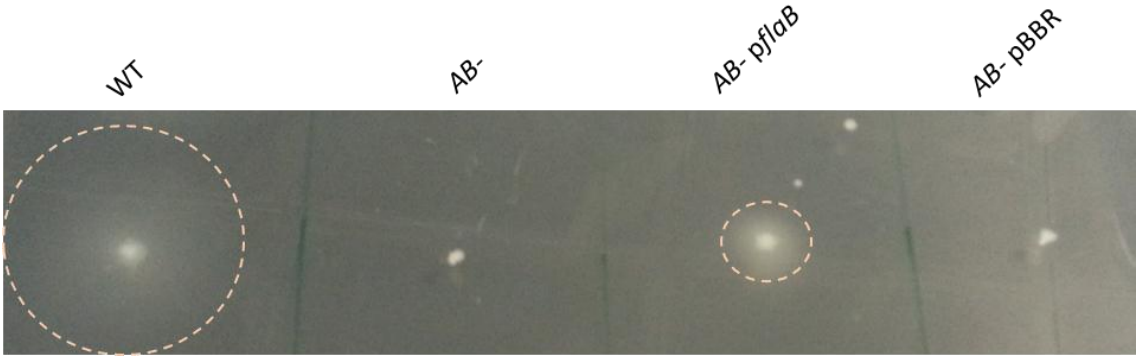


**Figure 4.18** – Swimming motility assays were carried out on 0.25% (w/v) agar of *A. caviae* Sch3 (WT), a *flaAB* mutant (*AB*-), a *flaAB* mutant containing pBBR1MCS-5_*flaB* (*AB*- p*flaB*) and a *flaAB* mutant containing empty pBBR1MCS-5 (*AB*- pBBR).

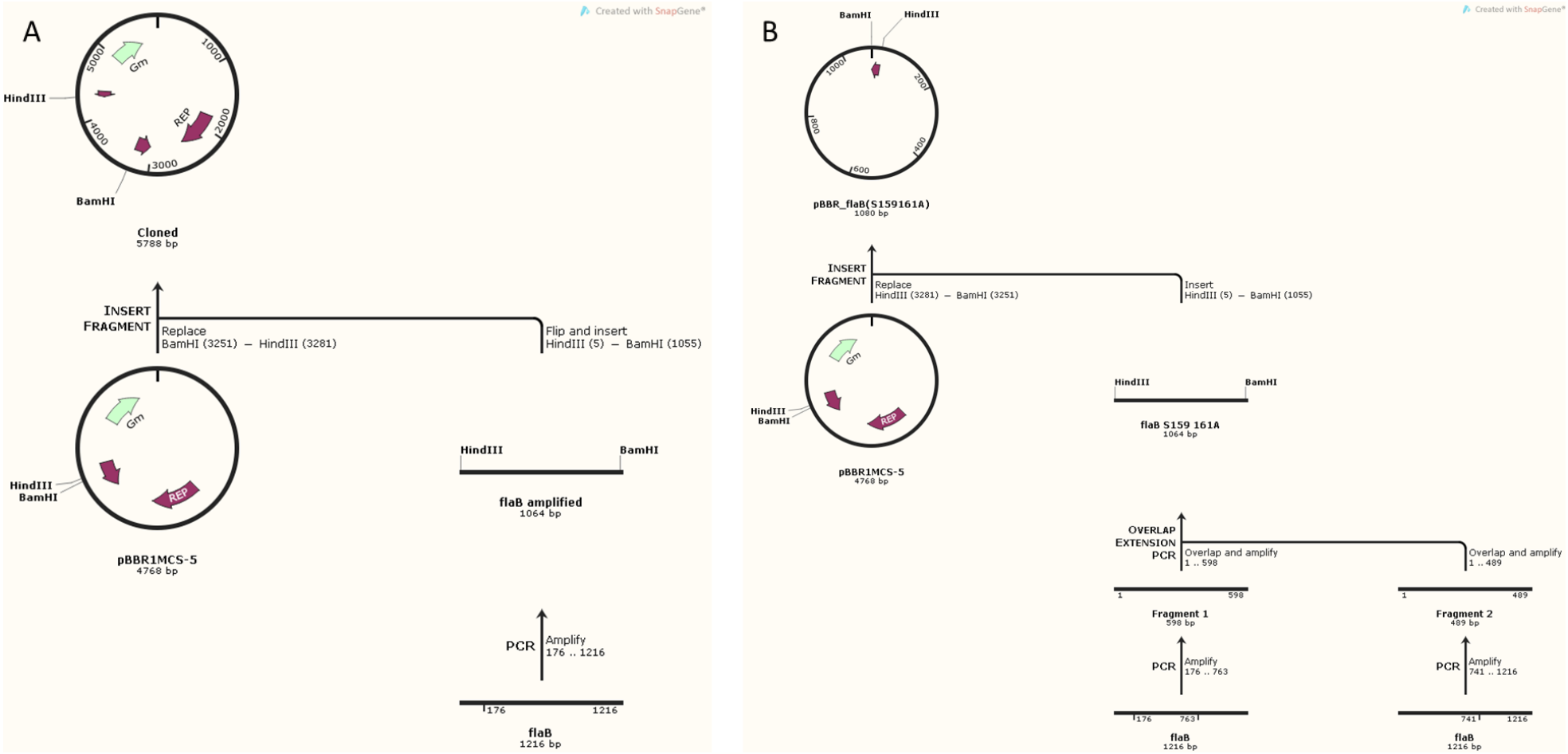


**Figure 4.19** – Diagrammatic representation of cloning methods, using SnapGene software: (**A**) the cloning method of *flaB* from *A. caviae* Sch3 into pBBR1MCS-5 (Kovach *et al.,* 1995) and (**B**) how *flaB* site-directed mutants were cloned into pBBR1MCS-5 using overlap extension PCR [using pBBR_*flaB*(S159/161A) as an example].

| | Site-directed mutant | PCR fragment 1 | PCR fragment 2 |
|---|---|---|---|
| **1** | FlaB(T155A)<br>$^{146}$FQVGADANQ**T**IGFSLSQAGGFSISGIAK$^{173}$ | RCL_55 (F) &<br>B-T155A (R) | B-T155A (F) &<br>RCL_56 (R) |
| **2** | FlaB(S159/161A)<br>$^{146}$FQVGADANQTIGF**S**L**S**QAGGFSISGIAK$^{173}$ | RCL_55 (F) &<br>B-S159/161A (R) | B-S159/161A (F) &<br>RCL_56 (R) |
| **3** | FlaB(S167/169A)<br>$^{146}$FQVGADANQTIGFSLSQAGGF**S**I**S**GIAK$^{173}$ | RCL_55 (F) &<br>B-S167/169A (R) | B-S167/169A (F) &<br>RCL_56 (R) |
| **4** | FlaB(S159/161/167/169A) or FlaB(4)<br>$^{146}$FQVGADANQTIGF**S**L**S**QAGGF**S**I**S**GIAK$^{173}$ | RCL_55 (F) &<br>B-S159/161A (R)<br>When pBBR1MCS-5_*flaB*(S167/169A) used as the template | B-S159/161A (F) &<br>RCL_56 (R)<br>When pBBR1MCS-5_*flaB*(S167/169A) used as the template |
| **5** | FlaB(L160A)<br>$^{146}$FQVGADANQTIGFS**L**SQAGGFSISGIAK$^{173}$ | RCL_55 (F) &<br>B-L160A (R) | B-L160A (F) &<br>RCL_56 (R) |
| **6** | FlaB(I168A)<br>$^{146}$FQVGADANQTIGFSLSQAGGFS**I**SGIAK$^{173}$ | RCL_55 (F) &<br>B-I168A (R) | B-I168A (F) &<br>RCL_56 (R) |
| **7** | FlaB(S208/210A)<br>…$^{195}$ISLIFVSGSAGGI**S**I**S**TQSKAQAVLA$^{220}$… | RCL_55 (F) &<br>B-S208/210A (R) | B9S208/210A (F)<br>& RCL_56 (R) |

**Table 4.2** - All serine and threonine residues highlighted in the FlaB peptide above (**S**/**T**) were mutated to alanine residues. The site-directed mutants were coded for in the *flaB* internal primers used to generate the two fragments for overlap extension PCR. For all SDMs, overlap extension PCR was carried out with fragments 1 and 2 with the primers RCL_55 and RCL_56 to create *flaB* containing the desired mutations.

Once each mutated *flaB* PCR product was generated (Fig. 4.19 B), cloning into pBBR1MCS-5 proceeded as previously described in section 4.2.3.1 for pBBR1MCS-5_*flaB.*

### 4.2.3.3 – Analysis of Site-Directed Mutant pBBR1MCS-5_*flaB* constructs in *Aeromonas caviae*

The plasmid, pBBR1MCS-5_*flaB*, and the vectors containing desired site-directed mutations (T155A; S159/161A; S167/169A; S159/161/167/169A), were transformed into the conjugal transfer strain, *E. coli* S17 1-λ *pir*, and conjugated into an *A. caviae flaAB* mutant (Rabaan *et al.*, 2001) (Chapter 2, section 2.4.13), along with the wild type *flaB* construct and the empty pBBR1MCS-5 vector, to analyse the effect of each mutation on *A. caviae* swimming motility. Three transconjugants were analysed for each strain expressing FlaB site-directed mutants.

Swimming motility assays were carried out on large swimming motility plates (Chapter 2, section 2.4.4), allowing an *A. caviae flaAB* mutant expressing a desired FlaB site-directed mutant to be analysed alongside: the *flaAB* mutant alone, the mutant containing the empty vector and the mutant containing wild type *flaB.* The large plates allowed for six biological repeats per strain to be analysed; three technical repeats were also carried out.

The *flaB*(T155A) construct was able to complement the non-motile phenotype of the *A. caviae flaAB* mutant and was found to swim significantly more (18% more) than the mutant expressing wild type FlaB (Fig. 4.20 A/B). Expression of the pBBR1MCS-5 constructs containing the double mutations, *flaB*(S159/161A) and *flaB*(S167/169A), were both found to restore motility in the *flaAB* mutant, however, the motility was significantly impaired (Fig. 4.21 A/B and Fig. 4.22 A/B). These strains displayed a reduction in motility of 26% (S159/161) and 39% (167/169) compared to the motility levels of the *flaAB* mutant containing the wild type FlaB (Fig. 4.21 A/B and Fig. 4.22 A/B).

When the motility of the quadruple mutant construct, *flaB*(S159/161/167/169A), in the *flaAB* mutant was analysed, severely impaired motility was visualised after 24 hours; this strain was therefore classed as non-motile (Fig. 4.23 A). Fig. 4.23 B shows a close up of the impaired motility of this strain compared to the *flaAB* mutant containing the empty pBBR1MCS-5 vector. The presence of an uneven colony demonstrates that there are possibly problems with flagellin export, or folding, in order to form a functional filament. Any filaments that are formed here may be weak, or not form as favourable interactions with aqueous environments due to the lack of glycosylation.

Western blot analysis was carried out on whole-cell and supernatant site-directed mutant flagellin samples, to compare the mutant flagellins to wild type FlaB. Each sample was probed with an antibody that recognises glycosylated flagellin only [anti-FlaA/B(+Pse)], and an

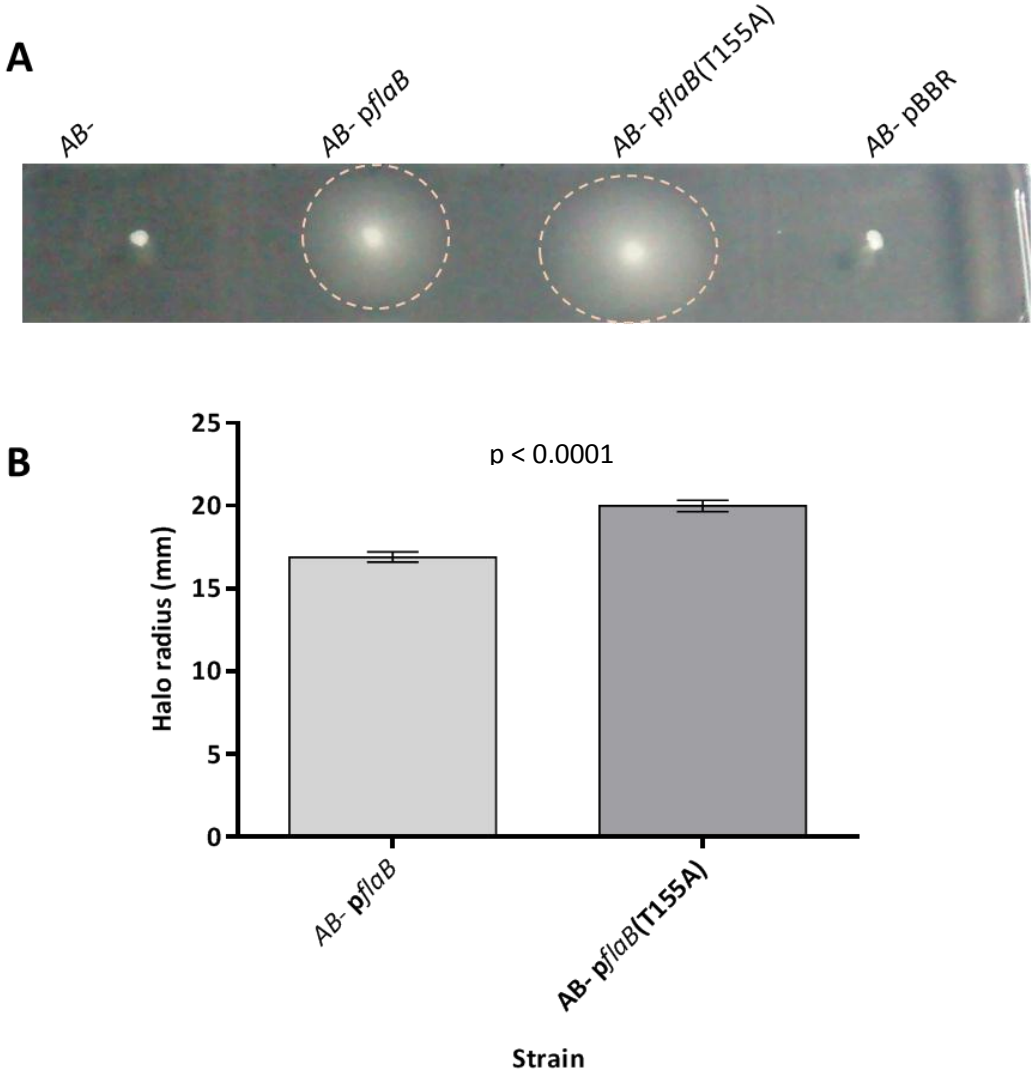


**Figure 4.20** – Analysis of a FlaB T155A site-directed mutant in an *A. caviae flaAB* mutant. (**A**) Swimming motility assays were carried out on 0.25% (w/v) agar of an *A. caviae flaAB* mutant (*AB*-), a *flaAB* mutant containing pBBR1MCS-5_*flaB* (*AB*- p*flaB*), a *flaAB* mutant containing pBBR1MCS-5_*flaB*(T155A) [*AB*- p*flaB*(T155A)] and a *flaAB* mutant containing empty pBBR1MCS-5 (*AB*- pBBR). (**B**) The radius of each motility halo was measured after 24 hours and average measurements are presented here (n=6) ± the standard error of the mean. A p value < 0.0001 was generated when a paired t-test was carried out on the data sets. Here, the *flaAB* mutant containing pBBR1MCS-5_*flaB*(T155A) swims 18% more than when the wild type flagellin is present.

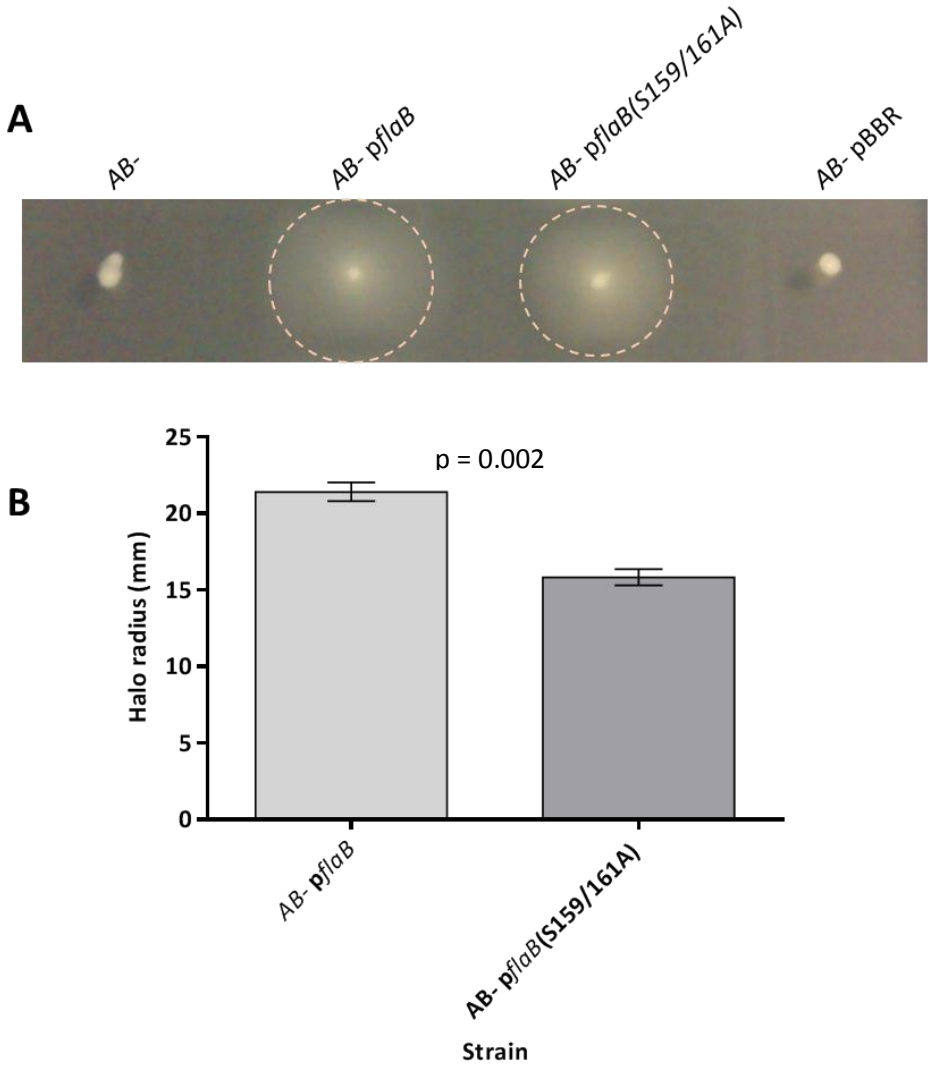


**Figure 4.21** - Analysis of a FlaB S159/161A site-directed double mutant in an *A. caviae flaAB* mutant. (**A**) Swimming motility assays were carried out on 0.25% (w/v) agar of an *A. caviae flaAB* mutant (*AB*-), a *flaAB* mutant containing pBBR1MCS-5_*flaB* (*AB*- p*flaB*), a *flaAB* mutant containing pBBR1MCS-5_*flaB*(S159/161A) [*AB*- p*flaB*(S159/161A)] and a *flaAB* mutant containing empty pBBR1MCS-5 (*AB*- pBBR). (**B**) The radius of each motility halo was measured after 24 hours and average measurements are presented here (n=6) ± the standard error of the mean. A p value of 0.002 was generated when a paired t-test was carried out on the data sets. Here, the *flaAB* mutant containing pBBR1MCS-5_*flaB*(S159/161A) displays a 26% reduction in motility levels compared to the *flaAB* mutant containing pBBR1MCS-5_*flaB.*

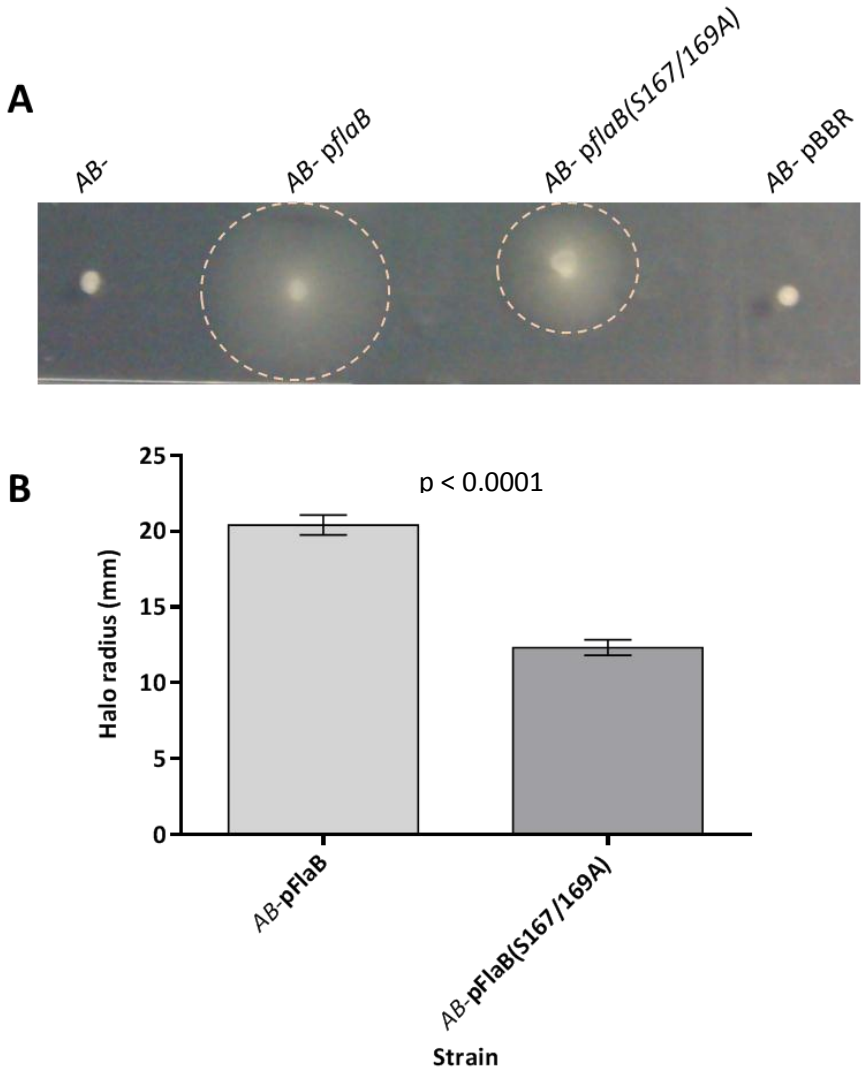


**Figure 4.22** - Analysis of a FlaB S167/169A site-directed double mutant in an *A. caviae flaAB* mutant. (**A**) Swimming motility assays were carried out on 0.25% (w/v) agar of an *A. caviae flaAB* mutant (*AB*-), a *flaAB* mutant containing pBBR1MCS-5_*flaB* (*AB*- p*flaB*), a *flaAB* mutant containing pBBR1MCS-5_*flaB*(S167/169A) [*AB*- p*flaB*(S167/169A)] and a *flaAB* mutant containing empty pBBR1MCS-5 (*AB*- pBBR). (**B**) The radius of each motility halo was measured after 24 hours and average measurements are presented here (n=6) ± the standard error of the mean. A p value of < 0.0001 was generated when a paired t-test was carried out on the data sets. Here, the *flaAB* mutant containing pBBR1MCS-5_*flaB*(S159/161A) displays a 39% reduction in motility levels compared to the *flaAB* mutant containing pBBR1MCS-5_*flaB.*

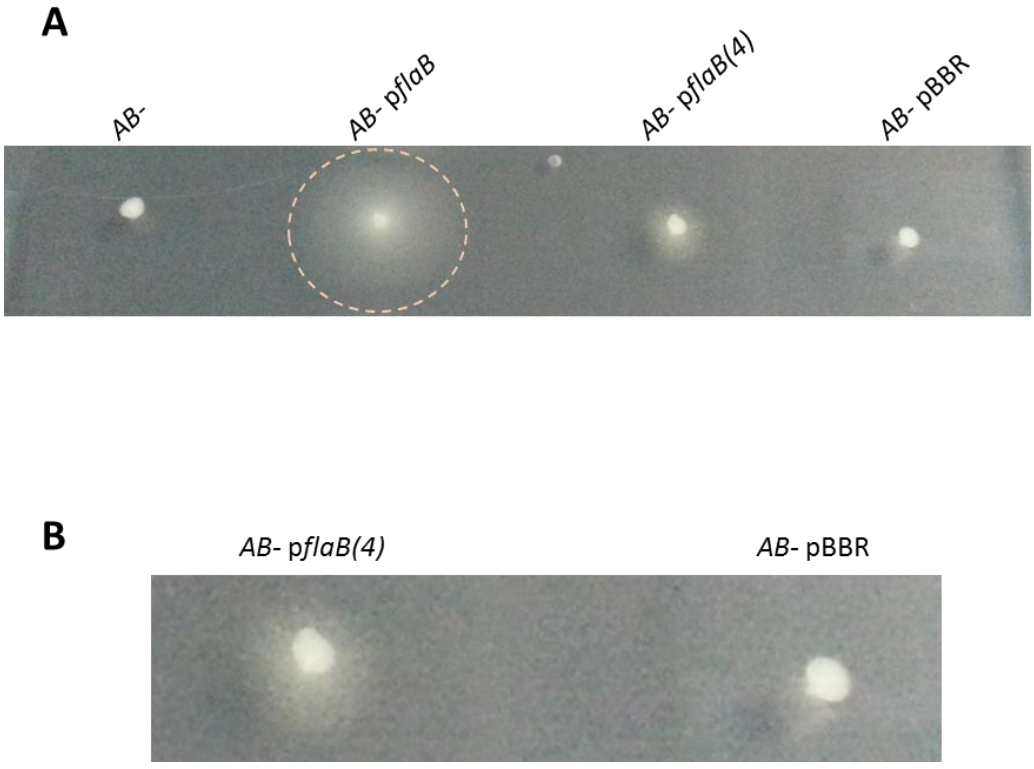


**Figure 4.23** - Analysis of a FlaB S159/161/167/169A site-directed quadruple mutant in an *A. caviae flaAB* mutant. (**A**) Swimming motility assays were carried out on 0.25% (w/v) agar of an *A. caviae flaAB* mutant (*AB*-), a *flaAB* mutant containing pBBR1MCS-5_*flaB* (*AB*- p*flaB*), a *flaAB* mutant containing pBBR1MCS-5_*flaB*(S159/161/167/169A) [*AB*- p*flaB*(4)] and a *flaAB* mutant containing empty pBBR1MCS-5 (*AB*- pBBR). Motility plates were incubated for 24 hours. (**B**) A close up of the impaired motility of the *A. caviae flaAB* mutant containing pBBR1MCS-5_*flaB*(S159/161/167/169A) [*AB*- p*flaB*(4)] compared to the non-motile *flaAB* mutant containing empty pBBR1MCS-5 (*AB*- pBBR).

antibody that recognises both glycosylated and unglycosylated flagellin forms (anti-FlaA/B) (Fig. 4.24).

When FlaB is analysed via Western blot analysis, a thick band results; most likely due to the flagellins being present in different glycoforms, with some possessing only six pseudaminic acid residues and others seven or eight sugars (Fig. 4.24) (Tabei *et al.*, 2009). When the site-directed mutant flagellins are analysed via Western blot analysis, FlaB(T155A) displays a band thickness comparable to the wild type flagellin when normalised whole cell samples and the supernatant samples are analysed with both anti-FlaA/B and anti-FlaA/B(+Pse). Therefore it is likely that FlaB(T155A) is glycosylated similarly to the wild type flagellin and the point mutation has no effect on the flagellins ability to polymerise and form a filament (which was expected due to the motility observed). However, although both FlaB(S159/161A) and FlaB(S167/169A) are able to produce a functioning flagella, they are observed as thinner bands on the Western blots compared to wild type FlaB; this is potentially due to only possessing the lower levels of flagellin glycosylation (ie. restricted to possessing only six-seven pseudaminic acid residues where as wild type flagellin is free to occupy more sites). Additionally, in the normalised whole-cell samples, the levels of both FlaB(S159/161A) and FlaB(S167/169A) visually appear to be lower than the levels of wild type FlaB or FlaB(T155A) (fig. 4.24 A); a notion which is further supported by densitometry data collected from whole-cell Western blots probed with anti-FlaA/B(+Pse) (Fig. 4.25).

Furthermore, a noticeable size shift can be observed when wild type FlaB, FlaB(T155A), FlaB(S159/161A) and FlaB(167/169A) samples are compared to the quadruple FlaB mutant flagellin sample (Fig. 4.24 A&B). This is apparent both in the whole cell and supernatant western blots (Fig. 4.24 A&B) and demonstrates that although the quadruple mutant flagellin is still glycosylated and exported, it is either not incorporated into a functional flagellar filament, or any filament formed has an impaired function. It may be that the glycosylation of this peptide is essential for the motility of *A. caviae* when FlaB is the only flagellin present. These mutations, however, may also result in the improper folding of flagellin and be the reason for the non-motile phenotype observed in the *flaAB* mutant expressing this FlaB containing quadruple serine point mutations. Densitometry analysis of whole-cell western blots also confirmed that the quadruple FlaB mutant is present at much lower levels in the cell than the other flagellins analysed (Fig. 4.25).

#### 4.2.3.4 – Mass spectrometry analysis of the site-directed mutant flagellin, FlaB(S159/161A)

The mutated FlaB(S159/161A) flagellin was selected for analysis via CID-MS/MS, due to these serine residues being the most regularly occupied sites on the wild type flagellin (observed by

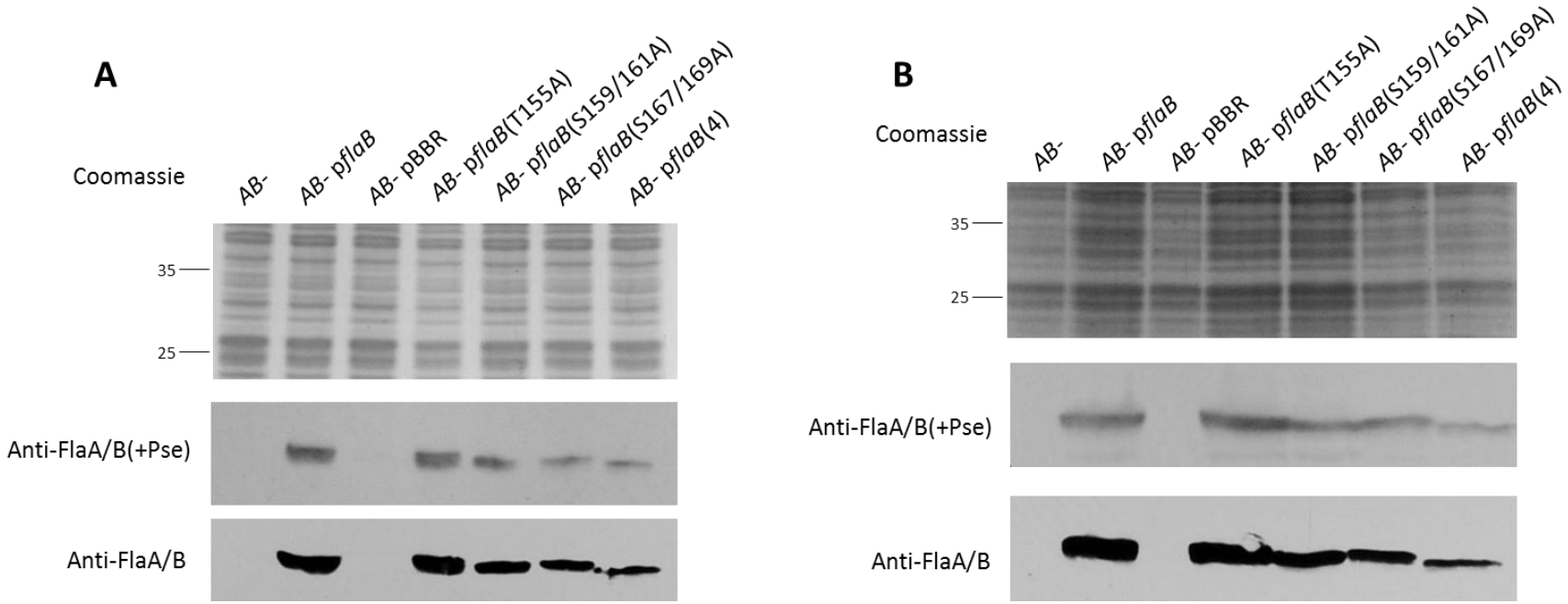


**Figure 4.24** – Western blot analysis of *Aeromonas caviae* whole cell samples (**A**), and supernatant samples (**B**). Both samples from A and B were probed with a rabbit, anti-polar flagellin antibody that recognises only glycosylated flagellin [anti-FlaA/B(+Pse)] and a mouse, anti-polar flagellin antibody that recognises both glycosylated and unglycosylated forms of flagellin (anti-FlaA/B). In each case: lane 1, the *A.caviae flaAB* mutant (*AB*-); lane 2, the *flaAB* mutant containing pBBR1MCS-5_*flaB* (*AB*- p*flaB*); lane 3, the *flaAB* mutant containing empty pBBR1MCS-5 (*AB*- pBBR); lane 4, the *flaAB* mutant containing pBBR1MCS-5_*flaB*(T155A) [*AB*- p*flaB*(T155A)]; lane 5, the *flaAB* mutant containing pBBR1MCS-5_*flaB*(S159/161A) [*AB*- p*flaB*(S159/161A)]; lane 6, the *flaAB* mutant containing pBBR1MCS-5_*flaB*(S167/169A) [*AB*- p*flaB*(S167/169A)]; lane 7, the *flaAB* mutant containing pBBR1MCS-5_*flaB*(S159/161/167/169A) [*AB*- p*flaB*(4)].

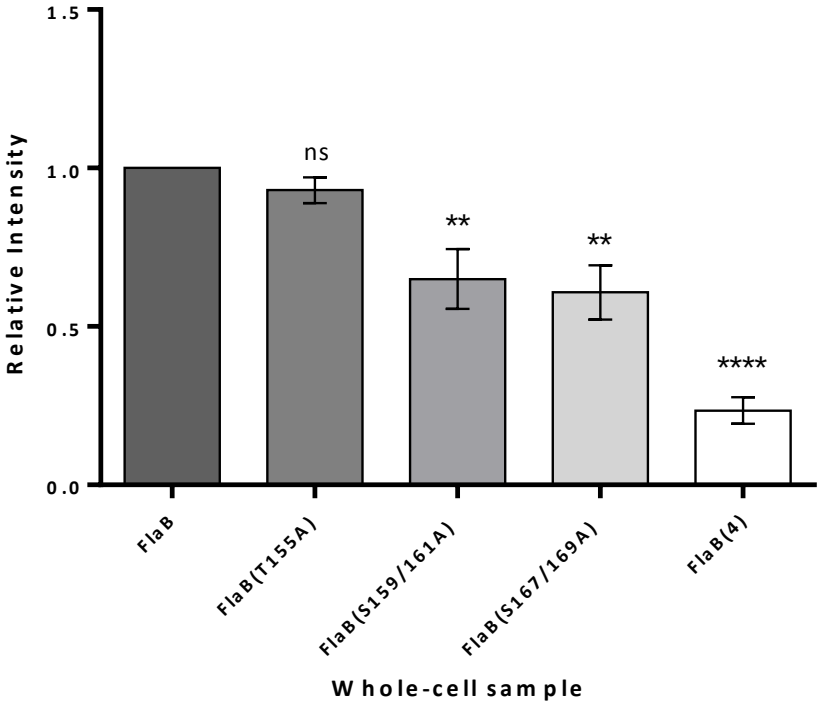


**Figure 4.25** – Densitometry analysis of whole-cell Western blots to show the level of FlaB and site-directed mutant FlaB [FlaB(T155A); FlaB(S159/161A); FlaB(S1567/169A); FlaB(S159/161/167/169A)] present in normalised *A. caviae flaAB* mutant samples when expressed from the native *flaB* promoter in pBBR1MCS-5. The relative intensity of each site-directed mutant flagellin is shown compared to wild type FlaB (n=4) ± the standard error of the mean. A one-way ANOVA, with a Tukey's multiple comparisons test, was carried out on the data sets to compare the level of site-directed mutant FlaB in whole-cell samples to levels of wild type FlaB. **p = 0.001-0.009. ****p < 0.0001, ns = not significant.

EasyProt). Flagella were purified from an *A. caviae flaAB* mutant containing pBBR1MCS-5_*flaB*(S159/161A), using the shearing method previously described and tryptically digested before being run on the maXis$^{TM}$ Q-TOF. The mutated FlaB amino acid sequence was uploaded as a database to EasyProt in order to analyse the MS/MS data. EasyProt analysis of the data suggested that when serine 159 and serine 161 are co-mutated to alanine residues, the new peptide, $^{146}$FQVGADANQTIGFALAQAGGFSISGIAK$^{173}$, is still glycosylated, but only ever with one sugar. EasyProt detected the triply charged ion, *m/z* 1019.18, corresponding to this peptide modified with one sugar. This sugar can occupy any of the remaining serine or threonine sites (T155, S167 or S169), with a pseudaminic acid at serine 167 being the predominant glycoform. Although EasyProt estimated the most probable site of glycosylation due to the ions present in the MS/MS spectra, when these glycopeptides were manually analysed, specific sites of glycosylation could not be determined due to the preferential fragmentation of the sugar and the presence of too similar fragment ions in the MS/MS spectra. Serine 167 and 169 were not found to be modified at the same time in the mutant peptide, even to replace the preferred co-modification of serine 159 and 161 observed on the wild type peptide, which may indicate that this region is required for Maf1 docking to the flagellins.

When CID-MS/MS data was manually analysed, glycopeptides were recorded between 60-100 minute retention times. The triply charged ion, *m/z* 1019.18, was recorded throughout (similarly to *m/z* 1135.3$^{[3+]}$ in the wild type flagellin spectra), with MS/MS spectra corresponding to the mutated FlaB peptide, [146-173], decorated with one pseudaminic acid residue. The doubly charged ion of this peptide containing one sugar, *m/z* 1528.27, was also observed. Furthermore, the triply charged ion, *m/z* 1026.51, was also frequently detected and found to be related to the glycosylated FlaB peptide, [146-173], due to the presence of similar peaks in the MS/MS spectra. Previously, it was observed that when wild type flagellin is analysed via CID-MS/MS, $^{146}$FQVGADANQTIGF**S**L**S**QAGGFSISGIAK$^{173}$ can also be ionised by the addition of a sodium cation (section 4.2.2.2), and this is also likely to be occurring with the mutated peptide. If the mass of the mutated tryptic peptide containing one pseudaminic acid is 3054.5 Da, then the *m/z* value of the triply charged ion, ionised with two protons and a sodium cation, $[M+2H+Na]^{3+}$, can be calculated: (3054.5+2+23)/3 = 1026.5. This *m/z* value was also predicted by Protein Prospector, showing that different ionised versions of the same glycopeptide can be present during CID-MS/MS, making analysis difficult. Moreover, another version of this peptide was also identified, with a triply charged ion of *m/z* 1025.5 being present. This was found to be related to the FlaB tryptic peptide, [146-173], due to common peaks from peptide fragmentation being present in the MS/MS spectra. As previously stated, the mass of this peptide containing one sugar is estimated at 3054.5 Da, and the mass of the

newly observed version of this peptide is 3073.5 Da [(1025.5 x 3)-3]. Therefore, a mass discrepancy of 28 Da is observed between these two related peptides, which is common with dimethylation. EasyProt identified this peptide as the dimethylated version of the FlaB [146-173] peptide (modified with one pseudaminic acid), with the dimethyl being located at the terminal lysine (K 173). This is questionable however, as trypsin would be unlikely to cleave at a modified lysine residue. Therefore the cause of this mass discrepancy cannot be confirmed currently.

The triply charged ion, *m/z* 1124.56, which would result from the ionisation of the FlaB tryptic peptide, [146-173], containing two pseudaminic acid residues, was never observed when CID-MS/MS data was analysed manually. This therefore confirms the observation from EasyProt, that the mutated tryptic FlaB peptide, [146-173], is only ever decorated with one sugar.

As with CID-MS/MS analysis of wild type flagellins, many unidentified glycopeptides were also present when mass spectrometric analysis of FlaB(S159/161A) was carried out, which possessed the diagnostic oxonium ions of pseudaminic acid (*m/z* 299.13 and 317.13) in their MS/MS spectra. This may therefore demonstrate the heterologous nature of *A. caviae* flagellin glycosylation.

As expected, ions at *m/z* values: $851.7^{[4+]}$, $1135.2^{[3+]}$, $1029.7^{[3+]}$, corresponding to the glycosylated wild type FlaB tryptic peptide, [146-173], (previously observed in section 4.2.2) did not elute from the mutant sample. However, more unexpectedly, the unidentified glycopeptide, observed throughout the wild type spectra at *m/z* $1154.2^{[3+]}$, was also not present in the mutant sample. This may show that this peptide is related to FlaB [146-173].

#### 4.2.3.5 – Further Site-Directed mutagenesis of FlaB

Although there is no consensus sequence for O-linked flagellin glycosylation to occur, unlike N-linked glycosylation (Nothaft and Szymanski, 2013), a number of studies have recognised that the specific sites of glycosylation appear to occur in highly hydrophobic regions of the protein, suggesting there to be some selectivity to the glycosylation process (Schirm *et al.*, 2003; Thibault *et al.*, 2001). Thibault *et al.* (2001) observed that the sites of *C. jejuni* flagellin glycosylation were directly preceded by hydrophobic amino acids and Schirm *et al.* (2003) suggested glycosylation of certain serine/threonine residues in *H. pylori* may occur due to the local hydrophobicity surrounding the sites. These observations, and the lack of heterogeneity in the site of flagellin modification in a number of bacteria, therefore suggest partial selectivity in the glycosylation process.

The Kyte and Doolittle hydrophobicity plot in figure 4.26 (A) shows that the hydrophobic amino acids in FlaB are clustered in the D2/D3 domain. Values above zero on the kyte-doolittle scale indicates hydrophobicity, which can be visualised on this plot as peaks above zero and predominantly arises within the D2/D3 domain of the flagellin (Fig. 4.26 A). Furthermore, these regions of hydrophobicity are most commonly separated by serine or threonine residues, unlike the rest of the protein (Fig. 4.26 B). The sites of glycosylation identified here, on the FlaB tryptic peptide [146-173], are surrounded by hydrophobicity, with the commonly, co-modified serine 159 and serine 161, being separated by a leucine residue. Furthermore, these serine residues are also flanked by hydrophobic residues (Fig. 4.26 B). Although serine 167 and 169 are not found co-modified, they are individually targeted for glycosylation (from EasyProt analysis) and are separated by an isoleucine residue, as well as being flanked by hydrophobic regions (although not quite as hydrophobic as serine 159/161). The less commonly modified threonine 155 precedes a hydrophobic amino acid sequence; however, it is itself, preceded by acidic and polar amino acids (Fig. 4.26 B). This may indicate why the mutation of this residue is not detrimental to *A. caviae* motility and why the modification of this residue is not as common as the central serine residues.

The hydrophobic amino acids, L160 and I168, separating the serine residues on the FlaB peptide [146-173], were targeted for site-directed mutational studies. The residues were individually mutated to the less hydrophobic and similarly sized amino acid, alanine. Furthermore, although the rest of the FlaB D2/D3 domain was not identified during mass spectrometric analysis (due to the size of the tryptic peptide), it was observed that there are two serine residues present here, also separated by a hydrophobic isoleucine residue and preceded by a region of hydrophobicity: serine 208 and serine 210. Due to speculation that these serine residues may be co-modified, with the glycosyltransferase recognising the local hydrophobicity and the hydrophobic iseoleucine separating these serine residues, they were co-mutated to alanine residues to analyse the effect of these mutations on *A. caviae* motility.

**A.**

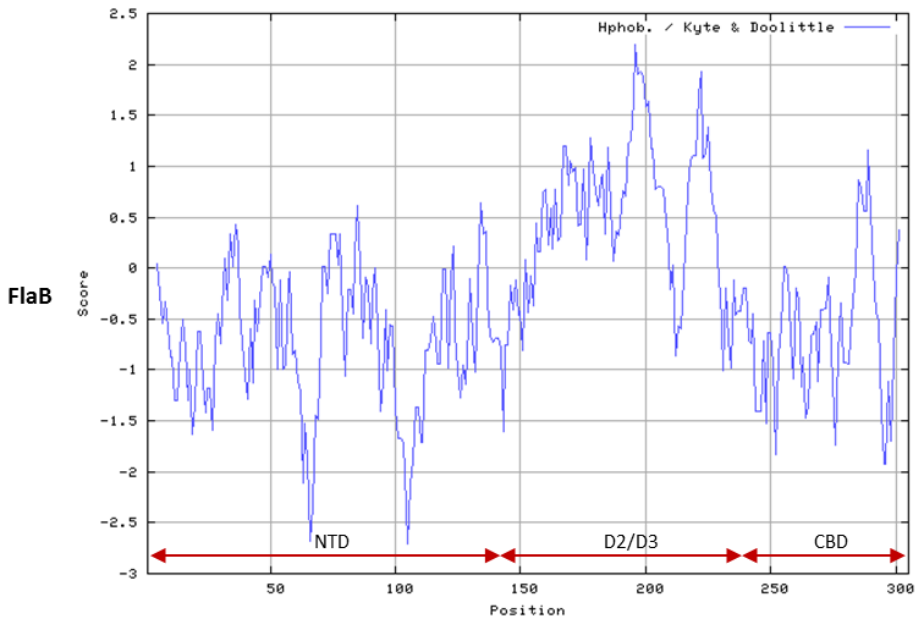


**B.**

MAMYINTNTSSLNAQRNLMNTSKSMDTSYTRLASGLRINSAKDDAAGLQISNRLTSQINGL
DQGNRNANDGISLAQTAEGAMDEVTGMLQRMRTLAQQSANGSNSDKDRAALQKEVNQLGAE
INRISKDTTFAGTKLLDGNYSGK**FQVGADANQTIGFSLSQAGGFSISGIAKAAGTTIDIVS**
**GPAGSVTTATGISLIFVSGSAGGISISTQSKAQAVLAAADAMLEVVDGK**RAELGAVQNRLD
STTRNQANISENVSAARSRIRDADFATETANMTKQNILQQAASSILAQANQRPQSALQLLG

**Figure 4.26** – The presence of hydrophobic amino acids in the *Aeromonas caviae* Sch3 polar flagellin, FlaB. **A**. A kyte and Doolittle hydrophobicity plot displaying the hydrophobicity of the FlaB N-terminal domain (NTD), D2/D3 domain and the chaperone binding domain (CBD) (scored by the kyte-doolittle scale) **B**. The amino acid sequence of FlaB highlighting the location of the hydrophobic amino acids: F, I, L, M, P and V and the slightly hydrophobic amino acids, A and G.

FlaB site-directed mutants were created by overlap-extension PCR and cloned into pBBR1MCS-5 as previously described in section 4.2.3.2 (Table 4.2, mutants 5-7). Once created, the vectors were analysed in an *A. caviae flaAB* mutant, as described in section 4.2.3.3. Both the leucine 160 and isoleucine 168 point mutations individually had a detrimental effect on *A. caviae* motility. The mutant FlaB containing the leucine mutation (L160A), could not restore the motility of a *flaAB* mutant after 24 hours (Fig. 4.27 A), however, after 40 hours, impaired, speckled motility was observed, but could not be quantified due to the irregular halo formation (Fig. 4.27 B). This was observed with all three *A. caviae* transconjugants analysed. When the isoleucine FlaB mutant (I168A) was introduced into the *A. caviae flaAB* mutant, all three transconjugants analysed displayed inconsistent motility. Fig. 4.28 displays the motility of the same transconjugant during different technical repeats, after 24 hours. Motility was extremely inconsistent, and when it was observed, only minimal amounts of motility were present, showing the I168A mutation to have a serious, detrimental effect on the motility of *A. caviae* (Fig. 4.28).

Furthermore, as observed with the previous double serine mutations (S159/161A & S167/169A), the co-mutation of serine 208 and 210 to alanine residues still complements the motility of a *flaAB* mutant; however, motility is drastically reduced when compared to the mutant containing the wild type flagellin (FlaB) (Fig. 4.29). A 50% reduction in motility was observed (Fig. 4.29). It is possible that glycosylation is targeted to serine/threonine residues that are surrounded by hydrophobicity, and in doing so counteracts this hydrophobicity allowing the formation of a fully functional flagellum. The reduced motility of the double mutant here, however, may be due to increasing the local hydrophobicity of this area of the D2/D3 domain (due to mutating two serine residues to alanine residues), and may not be due to reduced glycosylation of the area, as we currently do not have proof of which amino acids in this region are glycosylated.

The FlaB site-directed mutant flagellins were also subjected to Western blot analysis. Normalised whole-cell Western blots were carried out (Chapter 2, section 2.7.3) of the *flaAB* mutant strains containing the site-directed mutant FlaB, were probed with both anti-FlaA/B(+Pse) (recognises only glycosylated flagellin) and anti-FlaA/B (recognises both flagellin forms) (Fig. 4.30 A). All mutated flagellins were shown to be present in their glycosylated form [when probed with anti-FlaA/B(+Pse)], but only very low levels of FlaB(L160A) and FlaB(I168A) were detected, and these levels could not be detected in the whole-cell samples using anti-FlaA/B that recognises both forms of the flagellins (Fig. 4.30 A). FlaB(S208/210A) was present

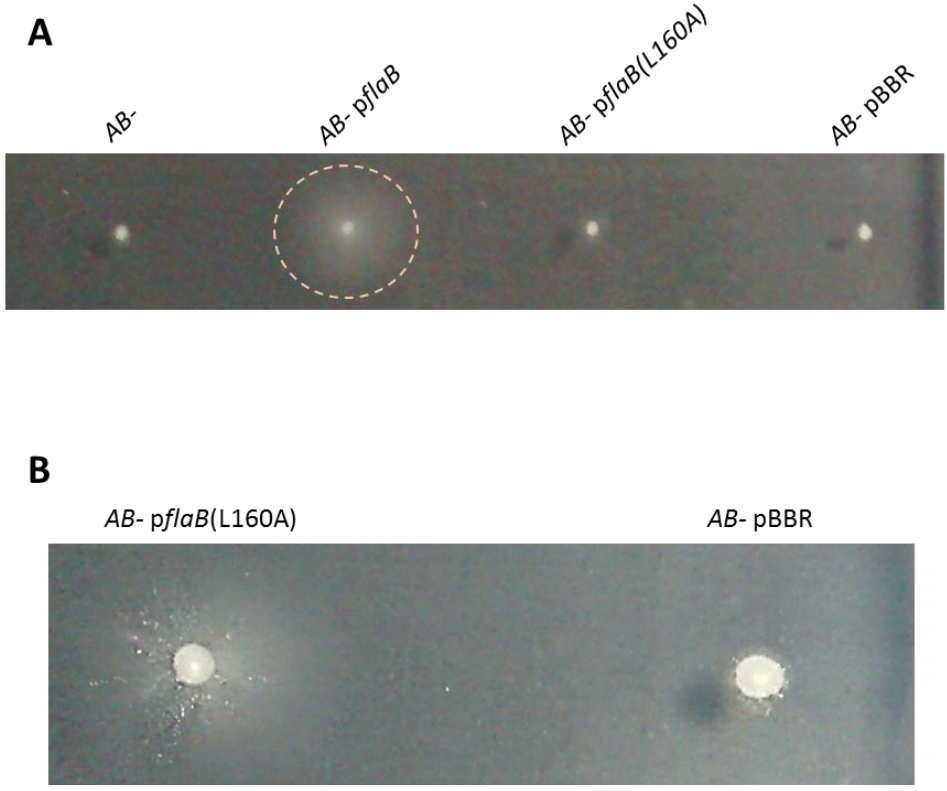


**Figure 4.27** - Analysis of a FlaB L160A site-directed mutant in an *A. caviae flaAB* mutant. (**A**) Swimming motility assays were carried out on 0.25% (w/v) agar of an *A. caviae flaAB* mutant (*AB*-), a *flaAB* mutant containing pBBR1MCS-5_*flaB* (*AB*- p*flaB*), a *flaAB* mutant containing pBBR1MCS-5_*flaB*(L160A) [*AB*- p*flaB*(L160A)] and a *flaAB* mutant containing empty pBBR1MCS-5 (*AB*- pBBR). Motility plates were incubated for 24 hours. (**B**) A close up of the impaired, speckled motility of the *A. caviae flaAB* mutant containing pBBR1MCS-5_*flaB*(L160A) [*AB*- p*flaB*(L160A)] compared to the non-motile *flaAB* mutant containing empty pBBR1MCS-5 (*AB*- pBBR) after 40 hours incubation.

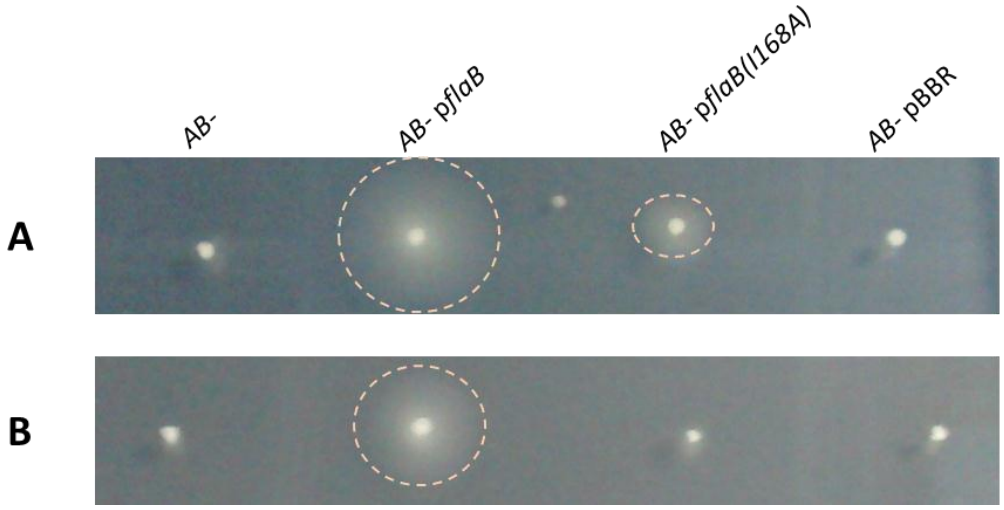


**Figure 4.28** - Analysis of a FlaB I168A site-directed mutant in an *A. caviae flaAB* mutant. Swimming motility assays were carried out on 0.25% (w/v) agar of an *A. caviae flaAB* mutant (*AB*-), a *flaAB* mutant containing pBBR1MCS-5_*flaB* (*AB*- p*flaB*), a *flaAB* mutant containing pBBR1MCS-5_*flaB*(I168A) [*AB*- p*flaB*(I168A)] and a *flaAB* mutant containing empty pBBR1MCS-5 (*AB*- pBBR). Motility plates were incubated for 24 hours. Both (**A**) and (**B**) display the variable motility of the sample *AB*- p*flaB*(I168A) transconjugant during different biological replicates.

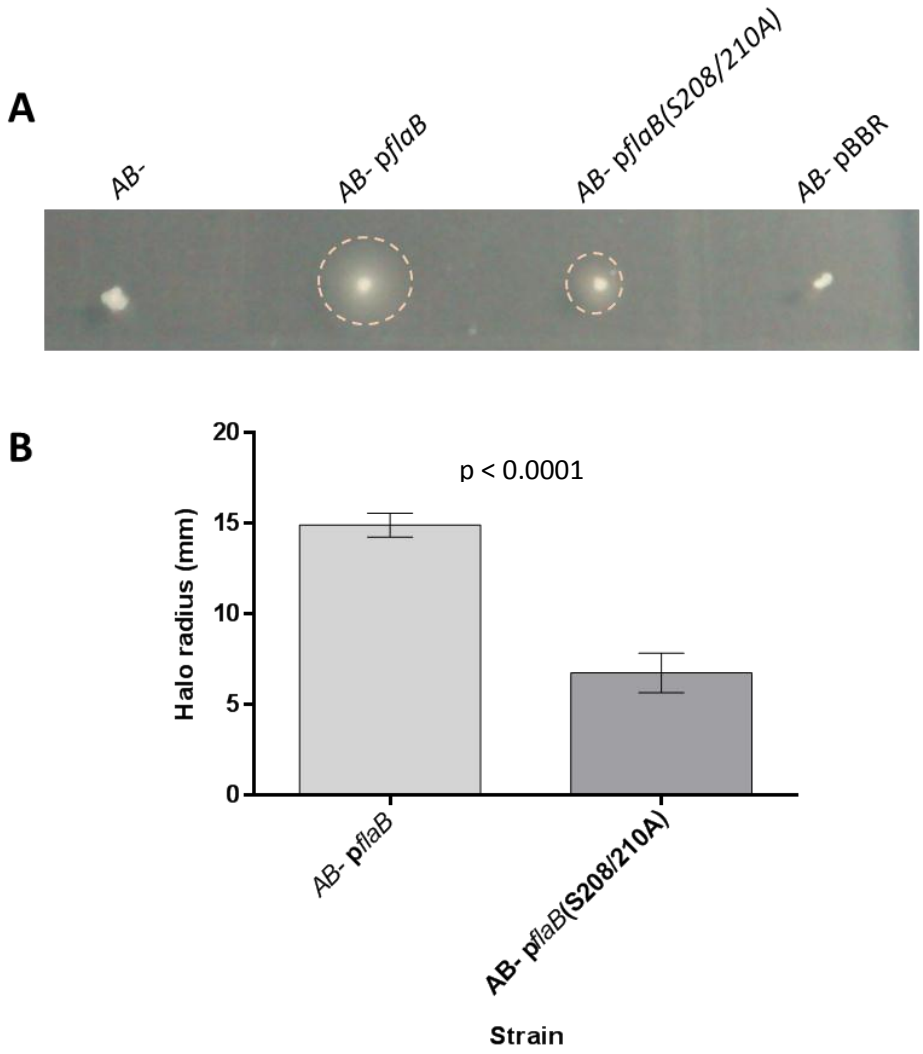


**Figure 4.29** - Analysis of a FlaB S208/210A site-directed double mutant in an *A. caviae flaAB* mutant. (**A**) Swimming motility assays were carried out on 0.25% (w/v) agar of an *A. caviae flaAB* mutant (*AB*-), a *flaAB* mutant containing pBBR1MCS-5_*flaB* (*AB*- p*flaB*), a *flaAB* mutant containing pBBR1MCS-5_*flaB*(S208/210A) [*AB*- p*flaB*(S208/210A)] and a *flaAB* mutant containing empty pBBR1MCS-5 (*AB*- pBBR). (**B**) The radius of each motility halo was measured after 24 hours and average measurements are presented here (n=6) ± the standard error of the mean. A p value of < 0.0001 was generated when a paired t-test was carried out on the data sets. Here, the *flaAB* mutant containing pBBR1MCS-5_*flaB*(S208/210A) displays a 50% reduction in motility compared to the *flaAB* mutant containing pBBR1MCS-5_*flaB.*

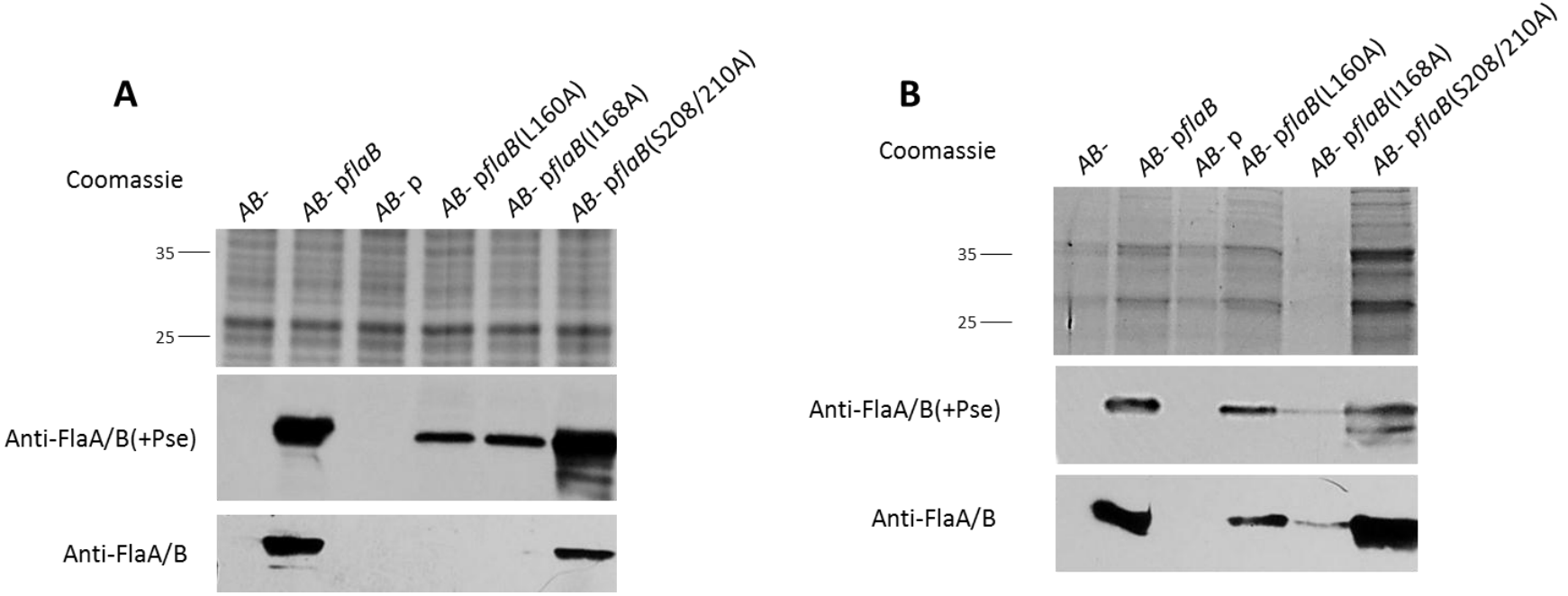


**Figure 4.30** – Western blot analysis of *Aeromonas caviae* whole cell samples (**A**), and supernatant samples (**B**). Both samples from **A** and **B** were probed with a rabbit, anti-polar flagellin antibody that recognises only glycosylated flagellin [anti-FlaA/B(+Pse)] and a mouse, anti-polar flagellin antibody that recognises both glycosylated and unglycosylated forms of flagellin (anti-FlaA/B). In each case: lane 1, the *A.caviae flaAB* mutant (*AB*-); lane 2, the *flaAB* mutant containing pBBR1MCS-5_*flaB* (*AB*- p*flaB*); lane 3, the *flaAB* mutant containing empty pBBR1MCS-5 (*AB*- pBBR); lane 4, the *flaAB* mutant containing pBBR1MCS-5_*flaB*(L160A) [*AB*- p*flaB*(L160A)]; lane 5, the *flaAB* mutant containing pBBR1MCS-5_*flaB*(I168A) [*AB*- p*flaB*(I168A)]; lane 6, the *flaAB* mutant containing pBBR1MCS-5_*flaB*(S208/210A) [*AB*- p*flaB*(S208/210A)].

in whole-cell samples in comparable amounts to the wild type (Fig. 4.30 A). In addition, Western blots of supernatant samples were carried out to analyse the export of these mutated flagellins (Fig. 4.30 B). As expected, FlaB(S208/210A) was found to be present in supernatant smaples (Fig. 4.30 B). Furthermore, even though FlaB(L160A) and FlaB(I168A) caused impaired, inconsistent motility in *A. caviae,* glycosylated flagellins were still found to be exported but only in small amounts (Fig. 4.30 B). Although these samples could not be normalised due to the inconsistent precipitation of proteins, it is likely that these proteins are present in smaller amounts due to the levels observed in whole-cell samples (Fig. 4.30). Additionally, the detection of these mutated flagellins in supernatant samples with the anti-FlaA/B antibody, shows that these mutations do not affect antibody recognition of these proteins and that extremely low protein levels are why this antibody could not detect these mutated proteins in whole-cell samples (Fig. 4.30).

The flagella shearing method was carried out in an attempt to purify glycosylated FlaB(L160A) and FlaB(I168A) for mass spectrometry analysis. Only very small amounts of flagella could be pelleted in each case by this method. Samples were tryptically digested and run on the maXis$^{TM}$ Q-TOF for CID-MS/MS analysis of the samples, however, no glycopeptides could be detected via manual analysis and EasyProt detected limited peptides for each mutant. Therefore, analysis of the glycosylation of these flagellins could not be carried out due to being unable to obtain sufficient amount of protein. This, however, could indicate that although these mutated flagellins are still glycosylated and exported, these mutations may have a severe effect of flagellar assembly, or export, and may be the reason for the lack of flagella pelleted during the shearing method of flagellin purification.

## 4.3 – Discussion

Here, CID-MS/MS was chosen to analyse *A. caviae* Sch3 flagellin glycosylation, as the manual analysis of the data acquired could be complemented with EasyProt analysis (Gluck *et al.*, 2013). However, many difficulties were faced when working with the flagellins, as trypsin digestion of the D2/D3 domain (the glycosylated region of interest) resulted in large, heavy, tryptic peptides, making analysis of this region problematic. This is likely to be why only the smallest tryptic peptide, FlaB [146-173], could be identified from this region. Furthermore, there are also many limitations of using CID as the fragmentation method when working with glycopeptides. Although the diagnostic ions of the sugar can be seen in the MS/MS spectra allowing identification of glycopeptides, the sugar is preferentially fragmented, resulting in large peaks in the MS/MS spectra corresponding to pseudaminic acid and very small peaks corresponding to the rest of the peptide (such as y and b ions). This therefore makes analysis of the specific site of glycosylation challenging. Despite these difficulties, manual analysis of CID-MS/MS spectra concluded that flagellins from an *A. caviae maf1* mutant are not glycosylated, due to the lack of pseudaminic acid oxonium ions in the MS/MS spectra (Parker *et al.*, 2014), providing further support to the findings in Parker *et al.* (2012), that Maf1 is the flagellin-specific glycosyltransferase.

Further manual analysis of wild type *A. caviae* flagellins by CID-MS/MS demonstrated that many glycopeptides are present in a sample, although the majority could not be designated a peptide sequence due to the limitations of CID-MS/MS. Some eluted multiple times, whereas others were only detected once; which may show the heterogeneity of *A. caviae* flagellin glycosylation. One glycopeptide was confidently identified from FlaB: $^{146}$FQVGADANQTIGFSLSQAGGFSISGIAK$^{173}$; however, analysis of this single glycopeptide was extremely complex due to several glycoforms being present and the ionisation of the peptide with sodium cations also being a possibility. It was observed that this peptide can be glycosylated with either one or two pseudaminic acid residues; with EasyProt data analysis suggesting that the site of modification can vary on the peptide. This was confirmed with manual annotation of the MS/MS spectra, however glycosylation of the two central serine residues (Serine 159 and 161) was detected most frequently. This peptide was never found in its unmodified form in wild type flagellin samples, suggesting that the glycosylation of this D2/D3 domain peptide in particular, is essential for the formation of a functional flagellar filament. This was also hinted at with site-directed mutagenesis studies, where serine and threonine residues on this FlaB peptide were mutated to alanine residues.

A FlaB T155A mutation had no detrimental effect on *A. caviae* motility and was found to be present in comparable amounts to wild type FlaB in the whole-cell. However, the double mutations at: S159/161A and S167/169A, caused a significant decrease in *A. caviae* motility, and a lower level of flagellin was found to be present in the whole-cell. This may show that these mutant flagellins are more readily degraded, maybe due to their less efficient polymerisation, or they are perhaps less stable compared to the wild type flagellins. Alternatively, this region of FlaB, at the beginning of the D2/D3 domain, may be important for Maf1 docking to the flagellin, and when mutated may lead to the less efficient glycosylation of flagellins by Maf1, which may be having an effect on flagellation, and therefore, motility.

Mass spectrometric analysis of the mutated flagellin, FlaB(S159/161A) uncovered that the mutated FlaB [146-173, S159/161A] peptide is still glycosylated, but only ever with a single sugar. Here, pseudaminic acid had the ability to occupy any of the remaining serine and threonine sites, with serine 167 being identified as the most frequently glycosylated site on this peptide by EasyProt. It is therefore possible that the decreased *A. caviae* motility observed when only this mutated flagellin is present, may be due to the flagella formed having a decreased hydrophilicity, and therefore impaired ability to move through an aqueous environment. In addition, it has previously been noted that unglycosylated flagellin is recognised less by the chaperone, FlaJ (Parker *et al.*, 2014). Therefore, reduced flagellin glycosylation may lead to reduced recognition of the flagellins by FlaJ, leading to decreased flagellin export and therefore filament polymerisation. However, there is also less protein present within the bacterial whole-cells which may be affecting flagellar assembly and filament length. On the other hand, a slight decrease in glycosylation levels may cause the formation of more delicate flagella that are readily broken, causing impaired motility compared to when wild type FlaB is present. Site-directed mutagenesis studies of the 19 sites of glycosylation in *C. jejuni* have also shown specific glycosylation sites to have an impact on motility, where the individual mutation of three serine residues in particular (in *C. jejuni* 81-176) caused the formation of truncated flagellar filaments and therefore reducing bacterial motility (Ewing *et al.*, 2009). Furthermore, the modification of other sites were also shown to be crucial for the autoagglutination behaviour of *C. jejuni* which demonstrates that different glycosylation sites may play a different role in bacterial behaviour *(Ewing et al., 2009).*

Impaired motility is also observed when the mutated flagellin, FlaB(S167/169A), is the only flagellin present. The two mutated residues here were never found to be co-modified in wild type flagellin samples, and therefore it is likely that the serine residues, 159 and 161, are still the predominantly modified residues on the FlaB peptide [146-173, S167/169A]. As impaired motility is also seen with the co-mutation of these residues, it is possible that this

phenomenon is not related to flagellin glycosylation, but occurs due to the increased hydrophobicity of the peptide (from mutating serine to alanine) resulting in an overall increase in the hydrophobicity of the polar flagellum. This may lead to less favourable interactions with the aqueous environment. Alanine is only slightly hydrophobic and can exist in all environments, so is unlikely to have drastic effects on flagellar function, which may be why these mutant flagellins still produce functional flagella, and only display slightly impaired motility. However, again, the point mutations here may also have an effect on the stability or the overall form of the flagella, compared to flagella polymerised from wild type flagellin.

When all four serine residues on this peptide (159, 161, 167, 169) were mutated to alanine residues, although glycosylated flagellin was still detected both in whole-cell and supernatant samples, motility of an *A. caviae flaAB* mutant could not be restored. This quadruple mutant flagellin was found to be smaller than the wild type and other site-directed mutant flagellins, due to a clear size-shift being detected via Western blot analysis. This suggests that the glycosylation status of this flagellin differs to that of the wild type and that these sites are unequivocally the target of Maf1 glycosylation. Furthermore, the size of this flagellin also demonstrates that when this region of the protein cannot be glycosylated and that the glycosylation status is not made up for with the modification of other serine/threonine residues. This further indicates, for unknown reasons, that the glycosylation of this peptide is essential for motility. The D2/D3 domain is situated in the centre of the primary amino acid sequence of the flagellin, but folds in order to form the flagellar surface once polymerised into a filament (Fig. 4.31). Figure 4.31 displays the predicted folding of FlaB and the location of the serine and threonine residues on FlaB peptide [146-173]. It is possible that the mutation of these residues may result in the improper folding of the flagellin, or these flagellins may polymerise differently to the wild type flagellins, and be the reason for the impaired and non-motile phenotypes visualised here (although a FlaB T155A mutation appear to increase *A. caviae* motility, not have a detrimental effect on motility).

As serine residues, 159 and 161, were found to be the most frequently modified sites on FlaB peptide [146-173], and the site-directed mutagenesis of these residues (S159/161A) did not result in the co-modification of the neighbouring serine 167 and 169 residues, it is likely S159 and S161 are the preferred sites of modification. A consensus sequence for *O*-linked flagellin glycosylation has never been identified, but it is intriguing as to why these two sites are predominantly glycosylated over the other three sites of glycosylation available on this peptide, suggesting there to be some selectivity to the glycosylation process.


**Figure 4.31** – Predicted *Aeromonas caviae* Sch3 FlaB folding, generated using the Phyre2 server and analysed using Jmol software. The structure is based on the phase 1 flagellin from *Salmonella enterica* (Accession: 1UCU_A) (Mimori *et al.,* 1995). The predicted locations of the serine and threonine residues on the FlaB peptide [146-173] (T155, S159, S161, S167, S169), are also shown.

Previous studies into bacterial *O*-linked flagellin glycosylation have suggested that local regions of hydrophobicity may play a role in glycosyltransferase selection of these residues (Schirm *et al.*, 2003; Thibault *et al.*, 2001). In particular, Thibault *et al.* (2001) identified hydrophobic amino acid sequences preceding their identified sites of flagellin modification in *C. jejuni.* Hydrophobic amino acids are also focused in the D2/D3 domain of *A. caviae* flagellins, preceding the serine residues 159 and 161, and the serine 167 and 169 residues. However, hydrophobic amino acids are not preceding threonine 155, which may show that this residue is not the desired target for the glycosyltransferase and be why mutation of this residue does not impair motility. Furthermore, the double serine residues on this peptide are both separated by hydrophobic amino acids, which led to the selection of leucine 160 and isoleucine 168 for further site-directed mutagenesis studies (L160A and I168A). Both mutations resulted in severely reduced *A. caviae* motility compared to when wild type FlaB was present, and only very low levels of these proteins were detected in whole-cell and supernatant samples. It is therefore possible that these mutated proteins are readily degraded, or less stable than their wild type counterparts. The substitutions, L160A and I168A, may also result in decreased hydrophobicity on the FlaB [146-173] peptide of the D2/D3 domain, which may result in an impaired ability for Maf1 to bind this region of the flagellin, resulting in the reduced motility seen. However, these flagellins were still found to be glycosylated, the glycosylation status of which did not appear to differ drastically from that of the wild type flagellin when analysed via Western blot analysis, showing that Maf1 is still able to identify and modify these flagellins. It is also possible that the mutations present may affect the ability of these flagellins to be secreted, or affect the folding of FlaB, having an effect on flagellar assembly. When purification of these mutant flagellins was attempted for mass spectrometry analysis, only small amounts of flagella could be isolated by the methods used here, further indicating that these mutations affect flagellar assembly.

As the serine residues identified on the FlaB peptide [146-173] (S159/161 and S167/169) are separated by a hydrophobic isoleucine or leucine residue, it was speculated that similar sites may be targeted by Maf1 for modification within the rest of the FlaB D2/D3 domain. Therefore, S208 and S210, separated by an isoleucine residue, were co-mutated to alanine residues which resulted in significantly reduced motility in an *A. caviae flaAB* mutant. However, the level of flagellins present, and their glycosylation status, appeared to be comparable to the wild type when investigated by Western blot analysis. If these residues are modified in wild type FlaB, it is possible that their co-mutation cause the site of modification to move to another residue, as serine 201 and 203 are located close upstream. This could not be explored, however, as the tryptic peptide on which these residues are located, was not

observed during CID-MS/MS. With regards to the local hydrophobicity of this region of the D2/D3 domain, it is possible that not only serine 208 and 210 are modified, but also the double serine residues upstream (S201/203). There residues are surrounded by more local hydrophobicity and may suggest that these are the preferred glycosylation sites of Maf1.

Although there is no consensus sequence for *O*-linked glycosylation, it is tempting to speculate that these local regions of hydrophobicity within the D2/D3 domains of the flagellins, may guide the glycosyltransferase, Maf1, to the preferred residues for modification, allowing more frequent glycosylation of these residues and the production of a polar flagellum functioning at its optimum. As this is not a fixed consensus sequence, it indicates the modification process to be flexible, permitting other residues to also be modified, although less commonly.

To continue on from these studies, future work could concentrate on exploring the flagella structures formed by these mutant flagellins (if any are formed at all), as motility can be affected by a number of factors such as the amino acid sequence, pH and temperature, which can alter the flagellar wave formation (Turner *et al.*, 2000). In addition the regions of flagellins important for Maf1 docking could be explored, by carrying out Maf1 binding affinity studies to different flagellin regions, as the mutations carried out here may be altering how Maf1 recognises and modifies the flagellins (please see the short-term perspectives in Chapter 6, the general discussion).

Another post-traslational modification, methylation, was also detected on lysine residues on both *A. caviae* flagellins (FlaA/B). Methylation is important in biological systems for a number of processes, such as regulation of gene expression or protein activity. This modification did not appear to be essential for flagellar formation and motility, however, as the methylated peptides were also identified in their unmodified forms. This is not the first time that methylation has been identified on bacterial flagellins, as *S. oneidensis* flagellins have also been found to be methylated on at least five lysine residues on the dominant flagellin, FlaB (Bubendorfer *et al.*, 2013; Sun *et al.*, 2013). The role of flagellin methylation in *S. onedensis* is unclear, however, mutation of the putative methyltransferase had no effect on bacterial motility (Sun *et al.*, 2013). Although not associated with the genetic loci for polar flagellum biogenesis, a putative methyltransferase has been identified in the lateral flagellar operon in *A. caviae* Sch3; however mutation of this gene had no effect on swimming motility (Shaw, unpublished). It is possible that if this putative methyltransferase is associated with modifying the lateral flagellar system, there may be some cross-talk between the polar and lateral systems, resulting in the methylation of the polar flagellins also. Although methylation may not have a role in *A. caviae* motility, its presence does highlight the future difficulties that could be

faced when further characterising *A. caviae* flagellin glycosylation by mass spectrometric methods. Not only may different peptide glycoforms be present (as observed with the FlaB peptide [146-173]), but also other modifications such as methyl groups. This may be why such a large number of glycopeptides identified during CID-MS/MS could not be assigned a peptide sequence here.

The biological role of flagellin glycosylation is still to be determined, however, the function may be unique to the individual bacterium itself. For example, the ability of *Camplylobacter* species to modify their flagellins with a variety of nonulosonate sugars, may aid the bacterium in different circumstances. The presence of pseudaminic acid is essential for *Campylobacter* flagellation; however, the presence of other sugars, such as legionaminic acid in *C. jejuni* on the hypermotile strain 11168H (Howard *et al.*, 2009), is not required for motility, but is required for certain behaviours of this bacterium. *C. jejuni* (11168H) unable to produce legionaminic acid to decorate their flagella showed reduced ability to form biofilms and colonise chickens, demonstrating this sugar is important for the colonisation and persistence of this species (Howard *et al.*, 2009).

Furthermore, *H. pylori* has a sheathed polar flagellum (Geis *et al.*, 1993) and so the modification of the filament surface is unlikely to aid interactions with the environment. Furthermore, *H. pylori* flagellins have been shown to evade TLR-5 recognition by the host's innate immune system, due to changes in the conserved sequences of the D0 region of the flagellin (Gewirtz *et al.*, 2004), and so glycosylation is not required for host immune evasion. Therefore, glycosylation may have a different role here, although explanations for why this modification is involved in flagellation, and consequently virulence, have not yet been explored.

It is now becoming clear that flagellin glycosylation is more widespread than originally believed, with reports of Gram- positive bacteria also modifying their flagella. Some are able to glycosylate their flagellins with nonulosonic acids, such as *C. botulinum,* where it is clear that the presence of these sugars play a role in pathogenicity, as strains isolated from infant botulism patients were more frequently found to modify their flagella with nonulosonic acids compared to strains that did not cause disease (Twine *et al.*, 2008). Furthermore, although *C. difficile* flagellins are not modified with nonulosonic acids, their modification with *N*-acetylglucosamine has been found to be essential for flagellation (Twine *et al.*, 2009). Recent work by Faulds-Pain *et al.* (2014), whereby the glycan at the *C. difficile* flagellar surface was altered, has demonstrated that motility is not essential for colonisation, but the specific structure of the sugar is. *C. difficile* glycan-structural mutants displayed a reduced ability to

colonise a mouse model of infection compared to the wild type strain (Faulds-Pain *et al.*, 2014). Furthermore, some mutants exhibited altered behaviours, such as motility defects and increased cellular aggregation (Faulds-Pain *et al.*, 2014).

Likewise, the non-pathogenic microorganism, *S. onedensis,* also requires glycosylation for flagellar assembly (Bubendorfer *et al.*, 2013; Sun *et al.*, 2013), and site-directed mutagenesis studies on the dominant flagellin FlaB have demonstrated that each glycosylation site contributes towards flagellar function, with the modification of one site in particular being critical for the motility of *S. oneidensis* (Sun *et al.*, 2013). Therefore this modification is not only utilised by pathogenic bacteria, but contributes to the bacterial colonisation of a variety of environments.

There are also a number of bacteria that are able to glycosylate their flagellins but do not require this modification for flagellar formation and motility; although, it is clear that this modification aids bacterial colonisation and virulence. For example, *P. syringae*, a tobacco plant pathogen, is able to *O*-glycosylate its flagellins with modified rhamnose residues (Takeuchi *et al.*, 2003), and although this is not essential for swimming and swarming motility, glycosylation mutants have a decreased ability to adhere to surfaces and cause disease in the plant (Taguchi *et al.*, 2006). Site-directed mutagenesis studies have revealed that sites of modification located on the surface of the flagellum are more essential for bacterial virulence, than sites located away from this area (Taguchi *et al.*, 2006). However, the individual site-directed mutagenesis of the known sites of modification were all found to impair motility, compared to when optimum levels of flagellin glycosylation are present (Taguchi *et al.*, 2010). The role of glycosylation has been explored here and glycosylated flagellins have been found to polymerise into a more stable flagellum, being more heat resistant that the unglycosylated equivalent (Taguchi *et al.*, 2009). Furthermore, it is thought this stability may aid evasion of host defences, as the host immune system (TLR-5) recognises an N-terminal region of the flagellins (Andersen-Nissen *et al.*, 2005), so once polymerised, this N-terminal region is hidden. The unglycosylated monomer and polymerised flagellins, and glycosylated monomer flagellins, displayed increased interactions with the host immune system, leading to increase apoptosis, compared to the glycosylated, polymerised flagellins (Taguchi *et al.*, 2009). This indicates that the increased stability of the glycosylated flagellum may aid immune evasion by preventing flagellum breakdown and exposure of flagellin N-terminal regions (Taguchi *et al.*, 2009).

Similarly to *P. syringae, P. aeruginosa* strains do not require glycosylation for flagellation, but are still capable of O-linked flagellin glycosylation, with type ‘a’ strains glycosylating with rhamnose-linked oligosaccharides (extremely heterologous sugars) and type ‘b’ strains

modifying with less heterologous hexose residues linked to an undermined 209 Da mass (Schirm *et al.*, 2004; Verma *et al.*, 2006). It has been demonstrated that glycosylation in this case may also be involved in virulence, as strains were found to be more virulent in a burned mouse model of infection compared to strains that did not glycosylate (Arora *et al.*, 2005). Furthermore, instead of to evade the host defences, flagellin glycosylation here may actually enhance bacterial interactions with the host immune system, as unglycosylated *P. aeruginosa* flagellins were found to have a reduced ability to stimulate the release of IL-8 (in the human lung cancer cell line, A549) (Verma *et al.*, 2005). This may be why hyper-inflammation is usually present in *P. aeruginosa* respiratory infections, especially in cystic fibrosis patients.

These studies therefore show the importance of flagellin modification to a wide variety of bacteria and the potential different roles of glycosylation in each case.

A number of the bacteria discussed here require flagellin modification for the assembly of polar flagella, and are capable of colonising the gastrointestinal tract, causing human disease (*Aeromonas, Campylobacter* and *Helicobacter*). It is intriguing as to why these polar flagellated microorganisms require this modification, whereas other gut pathogens such as, *E. coli* and *Salmonella* (that possess peritrichous flagella) do not. It is already well established that flagella contribute towards adhesion to host cell and colonisation (Haiko and Westerlund-Wikstrom, 2013), so it may be that glycosylated flagella allow bacteria that possess only polar flagella in this gastrointestinal environment to compete with other pathogenic microorganisms. The mass spectrometry and site-directed mutagenesis work carried out in this chapter suggests that the *A. caviae* Sch3 flagellum can be created from a variety of flagellin glycoforms, with some sites of glycosylation being preferred and occupied more frequently, suggesting partial selectivity (likely due to regions of local hydrophobicity) in Maf1 selection of modification sites. Site-directed mutagenesis studies have suggested that optimal flagellar function may not be possible with the elimination of certain glycosylation sites, and therefore the removal of certain flagellin glycoforms. This may show that flagella are made up of a variety of flagellin glycoforms that allow efficient motility through aqueous environments and the production of favourable interactions with host cell surfaces.

# Chapter 5: Investigations into Maf1 dependent polar flagellin glycosylation

## 5.1 – Introduction

Limited studies have been carried out on *O*-linked glycosylation, compared to N-linked protein glycosylation in bacteria. In Gram-negative bacteria, *N*-linked glycosylation requires the oligosaccharide to be synthesised on the cytoplasmic side of the inner membrane before it is flipped across the cytoplasmic membrane into the periplasm, via the action of a flippase enzyme. The glycan is then passed onto a periplasmic oligosaccharyltransferase and subsequently transferred onto the target protein; much of this knowledge comes from studies on the *N*-linked glycosylation process in *Campylobacter jejuni* (Baker *et al.*, 2013; Nothaft and Szymanski, 2010; Nothaft and Szymanski, 2013). Similar events also take place with some *O*-linked protein glycosylation pathways, such as pilin glycosylation in *Pseudomonas* and *Neisseria* species (see Chapter 1); however, the *O*-linked glycosylation described in this thesis, with the transfer of nonulosonic acids onto flagellin monomers, requires a flagellin specific glycosyltransferase to transfer the sugar directly onto the target protein. The Maf proteins are putative flagellin glycosyltransferases that have been identified in a number of bacteria (Canals *et al.*, 2007; Karlyshev *et al.*, 2002; Parker *et al.*, 2012; Schirm *et al.*, 2003), however, very little is known about their mechanism of action. Furthermore, prior to the studies carried out here (and by other members of the Shaw group), it was unknown as to where in the flagellar assembly pathway that glycosylation actually occurred. Some of the studies carried out in this chapter were in conjunction with Dr Jennifer Parker and contributed towards Parker *et al.* (2014), where the location of flagellin glycosylation was assessed.

Exploring out how specific these glycosyltransferase enzymes are (ie. the Maf proteins) and identifying where in the flagellar assembly pathway they actually carry out their function, would allow us to begin understanding these novel proteins, which could potentially be an antimicrobial target in the future as they play such an essential role in the virulence of a number of pathogens. Furthermore, these studies would also give a good indication as to whether these proteins would be of use for industrial or pharmaceutical applications in the future. For example, currently the *N*-linked bacterial protein glycosylation system (*C. jejuni* system reconstituted in *E. coli*) is being manipulated for eukaryotic protein glycosylation (for the production of therapeutic glycoproteins); however, these proteins first have to be targeted to the periplasm of the bacterium before they can be glycosylated, and then they have to be

isolated (Baker *et al.*, 2013). Therefore, simpler methods for therapeutic protein glycosylation would be useful.

The aim of the work carried out in this chapter was to contribute towards investigating where in the flagellar assembly pathway glycosylation occurs, by carrying out interaction studies with proteins of the flagellar assembly pathway, and analysing whether the polar flagellar cap protein, FlaH, is required for flagellin glycosylation. FlaH, which is known as FliD in *Escherichia coli* and *Salmonella*, is required for the formation of the flagellar filament, and for incorporating the flagellins into the growing filament (Yonekura *et al.*, 2000). When deleted, flagellin monomers are exported into the supernatant, but are not incorporated into a functional filament, rendering bacteria non-motile (Yonekura *et al.*, 2000). However, in *A. caviae* the glycosylation status of these exported flagellins is unknown [results have now been published in Parker *et al.* (2014)].

In addition, flagellin D2/D3 domain swapping studies, from other *Aeromonas* strains, were also undertaken to begin assessing the specificity of the glycosyltransferase, Maf1, from *A. caviae* (Chapter 1, figure 1.3). Furthermore, investigations were also carried out to examine whether *A. caviae* is a good model of flagellin glycosylation for the heterologous study of *H. pylori* glycosylation proteins. *H. pylori* possesses two Maf proteins (referred to as Maf1 and Maf2 here), however it only glycosylates its polar flagella with pseudaminic acid, similarly to *A. caviae* Sch3 (Josenhans *et al.*, 2002; Schirm *et al.*, 2003). Why two Maf proteins are present in *H. pylori* is unknown, however as *A. caviae* is genetically amenable and possesses the simplest system currently known for *O*-linked flagellin glycosylation (Tabei *et al.*, 2009), it may be a useful tool for the study of the *H. pylori* flagellin glycosylation pathway.

## 5.2 – Results

### 5.2.1 – Interaction studies of the proteins of the *Aeromonas caviae* polar flagellum

The bacterial adenylate cyclase two-hybrid (BACTH) system (EUROMEDEX) was utilised to explore the protein interactions between the polar flagellar proteins of *A. caviae* Sch3 in a non-glycosylating system (*E. coli* BTH101) (Fig. 5.1). *E. coli* BTH101 is an adenylate cyclase mutant (*cyaA*-) and is unable to ferment lactose. Each gene of interest was cloned into the four vectors of the BACTH system to tag each protein with one of the two domains of adenylate cyclase (CyaA), T18 or T25 (Fig. 5.2). Cloning into all four BACTH vectors allowed the proteins to be tagged at either their N or C termini with both domains (Fig. 5.2). Protein interactions could then be assessed *in vivo*, whereby any protein interactions taking place would bring together the two domains of adenylate cyclase, triggering a rise in the second messenger, cyclic adenosine monophosphate (cAMP) (Fig. 5.1 A). The second messenger is then able to bind to the transcriptional activator, CAP (catabolite gene activator protein) and switch on target operons, such as the maltose or lactose operons (Fig. 5.1 A). Here, interaction studies were carried out on MacConkey agar supplemented with 1% maltose, to allow *E. coli* BTH101 to utilise maltose in the instance of a protein interaction. Bacterial colonies able to utilise maltose appeared purple on the agar due to a change in pH being detected on the agar from maltose fermentation (Fig. 5.1 B).

#### 5.2.1.1 – Generation of the Bacterial two-hybrid system vectors

The *A. caviae* Sch3 genes of interest: *flaA, flaA-CBD* (*flaA* minus the chaperone binding domain), *flaA-D2/D3* (*flaA* minus the D2/D3 domain) (Chapter 1, figure 1.3), *flaB, flaJ* and *maf1,* were individually cloned into all four BACTH vectors (Fig. 5.2). The genes were amplified using the Expand high fidelity PCR system (Roche) (Chapter 2, section 2.6.2.1) using *A. caviae* Sch3 genomic DNA as the template. Two PCR reactions were set up for each gene to produce one fragment compatible for insertion into pUT18 and pKNT25, and the other fragment for insertion into pUT18C and pKT25. The primers used and the expected size of the PCR product in each case are specific in table 5.1. Once the correct sized PCR products were obtained, the gene fragments were ligated into pGEM-T EASY (as in Chapter 3, section 3.2.3), which were subsequently transformed into chemically competent *E. coli* DH5α and plasmids purified from the resulting transformants. The presence of correct sized inserts was checked with EcoRI restriction digests of pGEM-T EASY (as in Chapter 3, section 3.2.3), and the presence of the desired genes was confirmed by sequencing using T7 forward and SP6 reverse primers. Fragments were engineered with BamHI and EcoRI restriction sites at their 5’ and 3’ ends

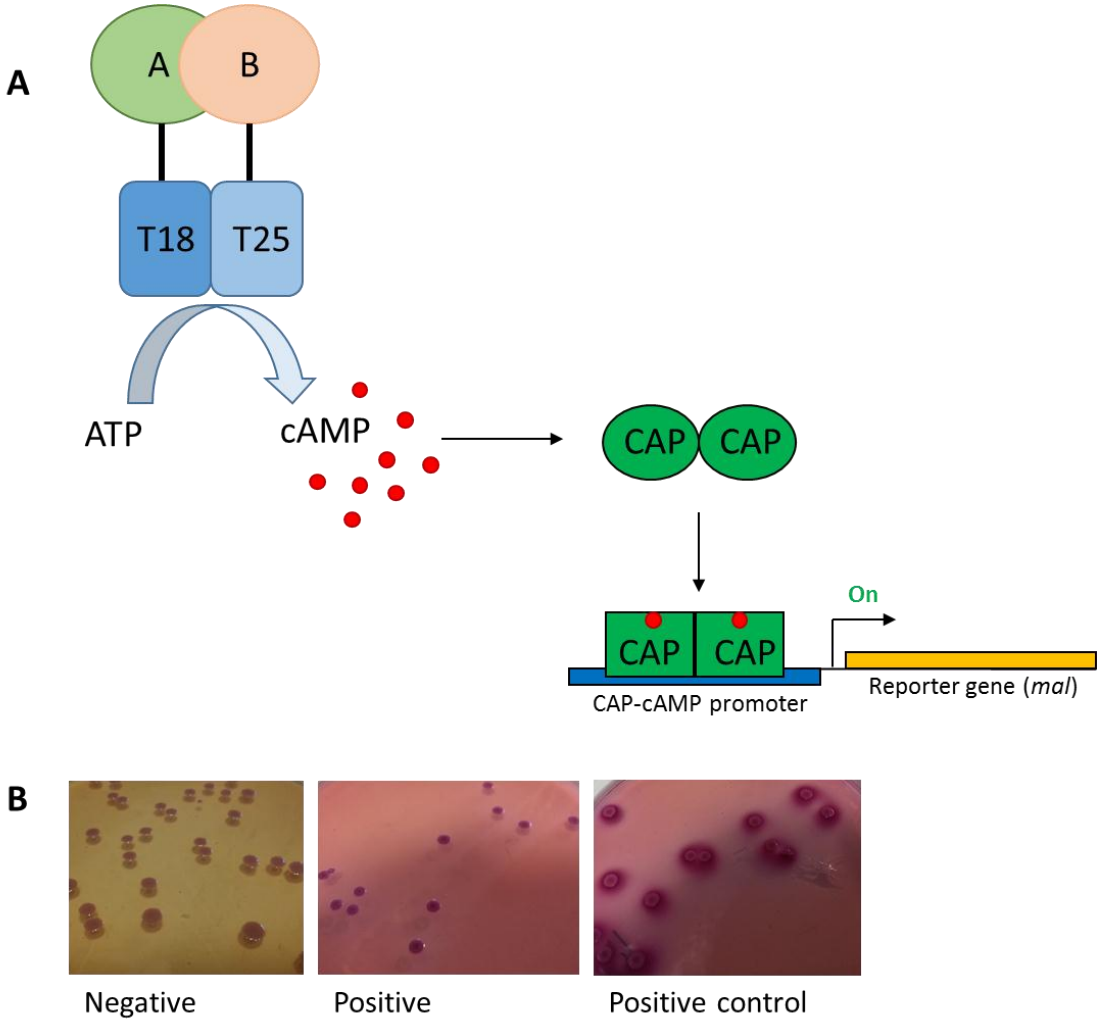


**Figure 5.1** – (**A**) The principle of the bacterial two-hybrid system, where proteins of interest, tagged with the domains of adenylate cyclase (CyaA) (T18 and T25), are expressed in a non-lactose fermenting strain of *E. coli* (BTH101). The different domains of CyaA are brought together if an interaction occurs, causing the levels of cAMP in the cell rise and bind to the catabolite gene activator protein (CAP). CAP then binds to target promoters and switches on gene expression. (**B**) The appearance of *E. coli* BTH101 colonies on MacConkey agar once cotransformed with the bacterial two-hybrid vectors. Yellow colonies occur when no interactions take place between the proteins of interest; however, if an interaction occurs, purple colonies result due to the pH that occurs when *E. coli* is able to ferment maltose.

| Gene | Primers for insertion into pUT18 and pKNT25 | Primers for insertion into pUT18C and pKT25 |
|---|---|---|
| ***flaA*** | JLP_39 (F) & JLP_53 (R)<br>(930 bp) | JLP_39 (F) & JLP_40 (R)<br>(933 bp) |
| ***flaA-CBD*** | JLP_39 (F) & RCL_01 (R)<br>(703 bp) | JLP_39 (F) & RCL_02 (R)<br>(701 bp) |
| ***flaA-D2/D3*** | OE-PCR was used first to create *flaA-D2/D3* domain:<br>Fragment 1 – JLP_39 (F) & RCL_17 (R)<br>Fragment 2 – RCL_18 (F) & JLP_53 (R)<br><br>JLP_39 (F) & JLP_53 (R) were then used to amplify the whole PCR product.<br>(673 bp) | OE-PCR was used first to create *flaA-D2/D3* domain:<br>Fragment 1 – JLP_39 (F) & RCL_17 (R)<br>Fragment 2 – RCL_18 (F) & JLP_40 (R)<br><br>JLP_39 (F) & JLP_40 (R) were then used to amplify the whole PCR product.<br>(672 bp) |
| ***flaB*** | JLP_47 (F) & JLP_47 (R)<br>(927 bp) | JLP_47 (F) & JLP_48 (R)<br>(930 bp) |
| ***flaJ*** | JLP_41 (F) & RCL_20 (R)<br>(432 bp) | JLP_41 (F) & RCL_21 (R)<br>(435 bp) |
| ***maf1*** | JLP_79 (F) & JLP_50 (R)<br>(2097 bp) | JLP_79 & JLP_44 (R)<br>(2100 bp) |

**Table 5.1 –** Summary of the primers used to amplify the genes of interest for insertion into the bacterial two-hybrid vectors. Spliced overlap-extension PCR (OE-PCR) was used to generate *flaA*-D2/D3. Please refer to Chapter 2 table 2.6 for the details of the primers.

respectively. Therefore once confirmed, the genes of interest were excised from pGEM-T EASY using these restriction enzymes, and then ligated into the corresponding BamHI and EcoRI digested BACTH vector (table 5.1). Ligations were then transformed into *E. coli* DH5α and selected for on agar plates containing appropriate antibiotics (pUT18/pUT18C on ampicillin; pKT25/pKNT25 on kanamycin). BACTH vectors were then purified from the resulting transformants, digested with BamHI to linearise, and the presence of the correct gene confirmed on an agarose gel (when compared to empty, linearised BACTH vectors) (as in Chapter 3, section 3.2.3).

#### 5.2.1.2 – Interaction studies

Interaction studies were carried out with the recombinant plasmids generated (Chapter 2, table 2.2). Briefly, pUT18 or pUT18C (containing gene) was cotransformed into *E. coli* BTH101 with pKT25 or pKNT25 (containing gene), and plated onto MacConkey agar supplemented with maltose. Table 5.2 displays all of the interaction studies carried out, which also included testing for the self-interaction of each protein. All of the necessary negative controls were carried out with empty BACTH vectors, and the positive controls were supplied with the Euromedex BACTH system kit. If the proteins of interest interacted, co-transformed *E. coli* BTH101 formed bright purple colonies on the MacConkey agar; whereas if no interaction occurred, yellow colonies formed (Fig. 5.1 B). At least three biological repeats were carried out for each interaction tested, and up to five were carried out in the case of inconsistent interactions (where the majority of time an interaction was observed, although sometimes negative results also detected or if the colonies were only marginally purple).

No self-interactions, interactions between the flagellins (FlaA and FlaB), or interactions between the flagellins and the flagellin-specific chaperone (FlaJ), were detected using the BACTH system. However, Maf1 was found to interact, either consistently (+) or inconsistantly (+/-) with FlaA when tagged at the C-terminus with the T25 fragment of CyaA, or at both the N or C-termi with the T25 fragment (with FlaA tagged at both termini with the opposite CyaA fragment) (Table 5.3). Furthermore, interactions were also detected between Maf1 (+ or +/-) and FlaB, when Maf1 was tagged at the C-terminus with T25 (FlaB with T18 at either terminal region, similarly to FlaA) (Table 5.3). However, no interactions between Maf1 and FlaB were detected here when Maf1 was tagged at the N-terminus with either CyaA domain. The inconsistent results seen here between Maf1 and flagellin interactions may be due to unglycosylated flagellin from *A. caviae* Sch3 being highly insoluble [as observed in Parker *et al.* (2014)]. Interactions were also assessed when the chaperone binding domain and the D2/D3 region of FlaA were deleted (Chapter 1, figure 1.3). Maf1 was found to strongly interact (+)

| | Plasmid 1 | Plasmid 2 | Expected Phenotype? |
|---|---|---|---|
| A | pUT18_geneA | pKT25_geneA | Unknown – to be tested |
| | pUT18_geneA | pKNT25_geneA | |
| | pUT18C_geneA | pKT25_geneA | |
| | pUT18C_geneA | pKNT25_geneA | |
| | pKT25_geneA | pUT18_geneA | |
| | pKT25_geneA | pUT18C_geneA | |
| | pKNT25_geneA | pUT18_geneA | |
| | pKNT25_geneA | pUT18C_geneA | |
| B | pUT18_geneB | pKT25_geneB | Unknown – to be tested |
| | pUT18_geneB | pKNT25_geneB | |
| | pUT18C_geneB | pKT25_geneB | |
| | pUT18C_geneB | pKNT25_geneB | |
| | pKT25_geneB | pUT18_geneB | |
| | pKT25_geneB | pUT18C_geneB | |
| | pKNT25_geneB | pUT18_geneB | |
| | pKNT25_geneB | pUT18C_geneB | |
| C | pUT18_geneA | pKT25_geneB | Unknown – to be tested |
| | pUT18_geneA | pKNT25_geneB | |
| | pUT18C_geneA | pKT25_geneB | |
| | pUT18C_geneA | pKNT25_geneB | |
| | pKT25_geneA | pUT18_geneB | |
| | pKT25_geneA | pUT18C_geneB | |
| | pKNT25_geneA | pUT18_geneB | |
| | pKNT25_geneA | pUT18C_geneB | |
| D | pUT18_gene? | pKT25 | Negative |
| | pUT18_gene? | pKNT25 | Negative |
| | pUT18C_gene? | pKT25 | Negative |
| | pUT18C_gene? | pKNT25 | Negative |
| | pKT25_gene? | pUT18 | Negative |
| | pKT25_gene? | pUT18C | Negative |
| | pKNT25_gene? | pUT18 | Negative |
| | pKNT25_gene? | pUT118C | Negative |
| | pUT18_zip | pKT25_zip | Positive |

**Table 5.2** – A summary of all bacterial two-hybrid vector combinations carried out to analyse a pair of protein interactions. Vectors were cotransformed into *Escherichia coli* BTH101. **A** & **B**: The combinations here were used to test for protein self-interactions. **C**: The combinations here were used to test for interactions between two different proteins. **D**: The control plasmid combinations are shown here.

with FlaA-CBD when tagged at the C-terminus (with T25) and the mutant flagellin was tagged at either terminus (with T25) (Table 5.3). Furthermore, a strong interaction was also detected when Maf1 was tagged at the N-terminus (with T18) and FlaA-CBD tagged at the N-terminus (with T25), a consistent result of which was not observed between Maf1 and wild type FlaA/B (Table 5.3). This may show that the deletion of the CBD may make the D2/D3 domain more accessible for Maf1 binding. Interactions were also detected between Maf1 and FlaA-D2/D3, in the same combinations as were detected for Maf1 and FlaA (Table 5.3). Although results were again inconsistent, this shows that Maf1 is not only recognising the D2/D3 region of the flagellin.

Although interactions were not detected between the flagellins and the chaperone here, FlaJ was found to interact, although inconsistently so, with Maf1 (Table 5.3). This interaction was only detected when Maf1 was tagged at the N-terminus (with T18) and FlaJ at the C-terminus (with T25) (Table 5.3). The inconsistent results here suggest that a transient interaction between Maf1 and FlaJ may occur, perhaps in order to allow FlaJ binding of glycosylated flagellin (which has not been investigated here).

| | T18::Maf1 | Maf1::T18 | T18::FlaA | FlaA::T18 | T18::FlaB | FlaB::T18 | T18::FlaA$^{-CBD}$ | FlaA$^{-CBD}$::T18 | T18::FlaA$^{-D2/D3}$ | FlaA$^{-D2/D3}$::T18 | T18::FlaJ | FlaJ::T18 |
|---|---|---|---|---|---|---|---|---|---|---|---|---|
| T25::Maf1 | - | - | - | - | - | - | - | - | - | - | - | - |
| Maf1::T25 | - | - | +/- | + | +/- | + | + | + | + | + | - | - |
| T25::FlaA | +/- | +/- | - | - | - | - | - | - | - | - | - | - |
| FlaA::T25 | +/- | +/- | - | - | - | - | - | - | - | - | - | - |
| T25::FlaB | - | - | - | - | - | - | - | - | - | - | - | - |
| FlaB::T25 | - | - | - | - | - | - | - | - | - | - | - | - |
| T25::FlaA$^{-CBD}$ | + | - | - | - | - | - | - | - | - | - | - | - |
| FlaA$^{-CBD}$::T25 | - | - | - | - | - | - | - | - | - | - | - | - |
| T25::FlaA$^{-D2/D3}$ | +/- | +/- | - | - | - | - | - | - | - | - | - | - |
| FlaA$^{-D2/D3}$::T25 | +/- | +/- | - | - | - | - | - | - | - | - | - | - |
| T25::FlaJ | - | - | - | - | - | - | - | - | - | - | - | - |
| FlaJ::T25 | +/- | - | - | - | - | - | - | - | - | - | - | - |

**Table 5.3** – A summary of the results obtained from the bacterial two-hybrid interaction studies, showing the position of the CyaA tag (T18/T25), at either the N- or C-terminus of the protein of interest.

## 5.2.2 – The polar flagellar cap protein, FlaH, is not required for flagellin glycosylation

In *A. caviae,* FlaH is the polar flagellar cap protein, and is required for polymerising the flagellins into a functional flagellar filament. Studies were undertaken to analyse whether the polar flagellar cap protein (FlaH) is required for flagellin glycosylation, in order to give an indication as to: where flagellin glycosylation may be occurring in the flagellar assembly pathway, if FlaH is required for glycosylation, or, if a mechanism is in place to prevent the glycosylation of flagellin when *A. caviae* is unable to form a flagellar filament. Investigations carried out here contributed towards Parker *et al.* (2014). To investigate whether FlaH is involved in flagellin glycosylation, flagellins from an *A. caviae flaH* mutant, previously created in the Shaw group, were analysed (Rabaan *et al.*, 2001).

The presence of glycosylated flagellin was analysed in normalised whole-cell sample and ethanol precipitated supernatant samples of *A. caviae* Sch3 and the *flaH* mutant. Western blot analysis was carried out on the samples, whereby they were probed with an anti-polar flagellin antibody that only recognises the glycosylated form of flagellin [anti-FlaA/B(+Pse)] (Fig. 5.8). No glycosylated flagellin could be detected in the whole-cell *flaH* mutant sample; however it could be detected in the supernatant sample. This demonstrates that FlaH is not required for flagellin glycosylation and that even though a filament cannot be produced, glycosylated flagellin is still readily exported in the absence of FlaH (in monomeric form) (Fig. 5.2).

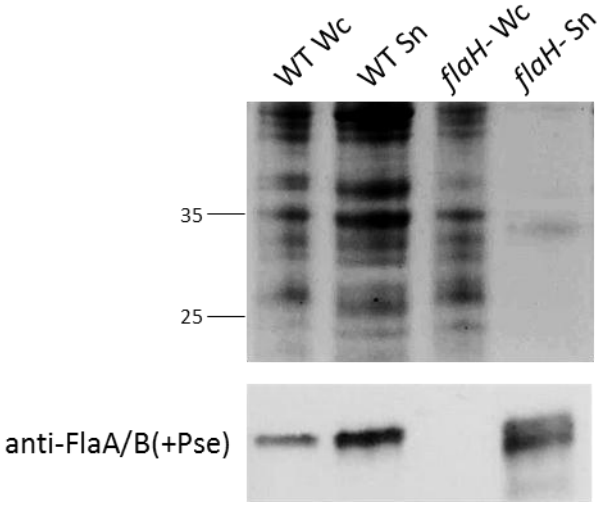


**Figure 5.2** – Western blot analysis of *Aeromonas* whole-cell and supernatant samples probed with a rabbit, anti-polar flagellin antibody that recognises only glycosylated flagellin [anti-FlaA/B(+Pse)] (Parker *et al.,* 2014). The samples were as follows: *A. caviae* Sch3 whole-cell (WT Wc), *A. caviae* Sch3 supernatant (WT Sn), *flaH* mutant whole-cell (*flaH*- Wc) and *flaH* mutant supernatant (*flaH*- Sn).

## 5.2.3 – Flagellin swapping studies

O-linked flagellin glycosylation is known to be widespread amongst *Aeromonas* spp., with many aeromonads possessing *maf* homologues in their genomes thought to encode the flagellin specific glycosyltransferase, such as the clinically relevant species: *A. caviae* (Parker *et al.*, 2012), *A. piscicola* (originally classed as *A. hydrophila*) (Canals *et al.*, 2007) and *A. hydrophila* (Seshadri *et al.*, 2006). Very little is known about the Maf proteins mechanism of action or how specific they are, as there is no consensus sequence for O-linked flagellin glycosylation. Polar flagellins from these clinically relevant *Aeromonas* species are extremely similar, showing highly conserved D0 and D1 regions, with only their central D2/D3 domain regions being variable. Therefore, D2/D3 domain swapping investigations were carried out in *A. caviae* Sch3, whereby flagellins from different *Aeromonas* strains were expressed in an *A. caviae* double flagellin mutant (*flaAB* mutant) in order to determine if the *A. caviae* Sch3 glycosyltransferase, Maf1, is able to glycosylate these foreign D2/D3 domains. Polar flagellin A (FlaA) from the following strains: *A. caviae* Ae398 (Beatson *et al.*, 2011), *A. piscicola* AH-3 (Merino *et al.*, 1991) and *A. hydrophila* ATCC 7966 (Seshadri *et al.*, 2006), were analysed. Alignment studies were carried out to determine how identical the flagellins from these strains are to FlaA from *A. caviae* Sch3 (Fig. 5.3). *A. caviae* Sch3 FlaA shares the highest identity with *A. caviae* Ae398 FlaA, at 86%, then with *A. hydrophila* ATCC 7966 FlaA, at 73%, and finally with *A. piscicola* AH-3 FlaA at 71%, with primarily the central regions of these proteins varying the most (Fig. 5.3).

### 5.2.3.1 – Generation of pBBR1MCS-5 constructs containing *Aeromonas* flagellins

The *flaA* genes from a variety of *Aeromonas* species: *A. caviae* Ae398 (891 bp), *A. piscicola* AH-3 (915 bp), *A. hydrophila* ATCC 7966 (906 bp) and *A. caviae* Sch3 (921 bp) as a positive control, were cloned into pBBR1MCS-5 along with a region upstream of the transcription start site to allow expression of flagellins from their native promoters (Table 5.4). Q5 high fidelity DNA polymerase (NEB) was used to amplify *flaA* genes from the corresponding genomic DNA. The sets of primers used in each case are shown in table 5.4. Restriction sites encoded for in the primers used allowed the PCR products to be directly cut with a combination of HindIII and BamHI (apart from the *A. hydrophila* ATCC 7966 *flaA* PCR product which was cut with HindIII and XbaI) restriction enzymes before being ligated into HindIII/BamHI (or HindIII/XbaI) cut pBBR1MCS-5 (As in Chapter 4, section 4.2.3, figure 4.19 A). The ligations were transformed into chemically competent *E.* coli DH5α and vector DNA isolated from the resulting transformants. Likely pBBR1MCS-5_*flaA* constructs were sent for sequencing using M13 forward and reverse primers to confirm the presence of the correct *flaA* gene.

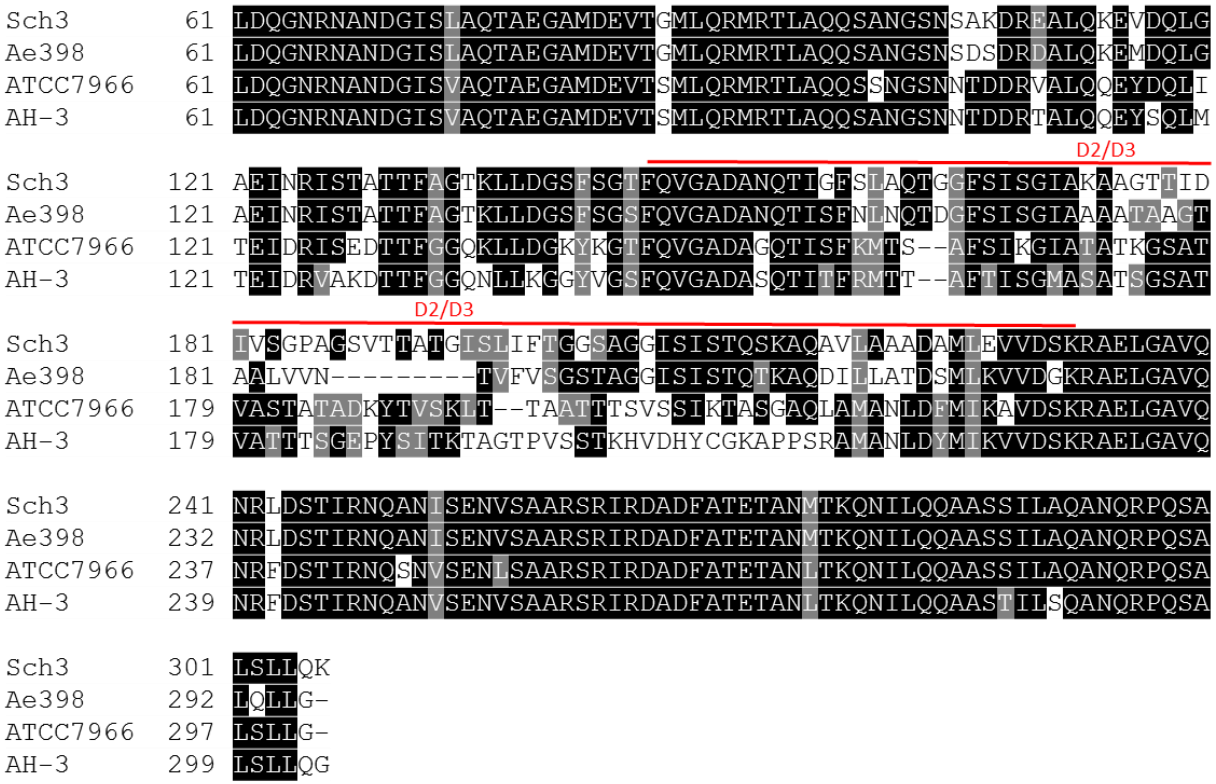


**Figure 5.3** – Alignment of FlaA from: *Aeromonas caviae* Sch3 (accession: AAF19179), *A. caviae* Ae398 (Beatson *et al*., 2011), *A. hydrophila* ATCC 7966 (Seshadri *et al.,* 2006) and *A. piscicola* AH-3 (accession ABA01569). *A. caviae* Sch3 FlaA shows 86% identity with FlaA from *A. caviae* Ae398, 73% identity with FlaA from *A. hydrophila* ATCC 7966, and 71% identifity with FlaA from *A. piscicola* AH-3, The alignment was executed using CLUSTALW (Thompson *et al.*, 1994) and displayed with box-shade. The location of the D2/D3 region is highlighted (amino acids 146-231 in *A. caviae* Sch3 FlaA).

| Gene | Information | Primers for pBBR1MCS-5 | Primers for pSRK(Gm) |
|---|---|---|---|
| *flaA* (Sch3) | Gene – 921 bp<br>Upstream region – 99 bp | RCL_71 (F) & RCL_72 (R) | RCL_53 (F) & RCL_54 (R) |
| *flaA* (Ae398) | Gene – 891 bp<br>Upstream region – 84 bp | RCL_28 (F) & RCL_29 (R) | |
| *flaA* (AH-3) | Gene – 915 bp<br>Upstream region – 72 bp | RCL_30 (F) & RCL_31 (R) | RCL_49 (F) & RCL_50 (R) |
| *flaA* (ATCC 7966) | Gene – 906 bp<br>Upstream region – 84 bp | RCL_32 (F) & RCL_34 (R) | RCL_51 (F) & RCL_52 (R) |

**Table 5.4** – Flagellin swapping gene and primer information: The *flaA* genes described here were amplified for insertion into pBBR1MCS-5 and pSRK(Gm). For insertion into pBBR1MCS-5, a region upstream of the gene was also amplified (sizes of these regions are given here), however these were not included when cloned into pSRK(Gm). The primers used in each case are presented here. Please refer to Chapter 2 table 2.6 for the details of the primers

#### 5.2.3.2 – Analysis of pBBR1MCS-5_*flaA* constructs in *Aeromonas caviae*

The resulting pBBR1MCS-5 vectors containing the desired flagellin genes were conjugated into an *A. caviae flaAB* mutant (as previously described in Chapter 4, section 4.2.3), along with the empty vector and three transconjugants selected for analysis.

Swimming motility assays were carried out with the *flaAB* mutant strains containing the various *flaA* genes from other *Aeromonas* strains. The motility assays were carried out on large agar plates, as described previously, to analyse the motility of the *flaAB* mutant, the mutant containing the Sch3 flagellin, the mutant containing one of the other aeromonad flagellins (Ae398/AH-3/ATCC 7966) and the mutant containing the empty vector, on a single plate, also allowing for six technical repeats per strain (Fig. 5.4). Figure 5.4 displays the results of a single transconjugant in each case, but represents the motility of all transconjugants analysed.

FlaA from *A. caviae* Ae398 was able to complement the non-motile phenotype of an *A. caviae* (Sch3) *flaAB* mutant; the other flagellins expressed in pBBR1MCS-5, however, could not.

Western blot analysis was carried out on normalised whole-cell and supernatant *A. caviae* samples to test whether the heterologous flagellins could be glycosylated by Maf1 from *A. caviae* Sch3 (Fig. 5.5 and 5.6), as it is possible that Maf1 is still able to glycosylate the AH-3 and ATCC 7966 flagellins, but they are just unable to form a flagellar filament. A rabbit anti-polar flagellin antibody, that recognises the pseudaminic acid on glycosylated flagellin (described previously), was used to probe the whole-cell and supernatant samples, as work in the Shaw group has demonstrated that this antibody is able to recognise pseudaminic acid decorating a variety of flagellins (such as *Aeromonas, H. pylori, C. jejuni, C. coli*) (Shaw, unpublished), and so would recognise any glycosylation on these *Aeromonas* flagellins (Fig. 5.5 and 5.6). Glycosylated FlaA (Ae398) was, as expected (due to the motility phenotype observed), found to be present in whole cell and supernatant samples (Fig. 5.5 A and 5.6 A). FlaA from AH-3 and ATCC 7966 strains, however, were not found to be glycosylated (Fig. 5.5 B/C and 5.6 B/C).

#### 5.2.3.3 – Generation of pSRK(Gm) constructs containing *Aeromonas* flagellins

The *Aeromonas* flagellins that did not complement the *A. caviae* (Sch3N) *flaAB* mutant (and could not be detected by western blot analysis) were cloned into the IPTG inducible vector pSRK(Gm), to ensure that the results obtained were not down to *A. caviae* (Sch3) being unable to express these other *Aeormonas spp* flagellins, as expression in pBBR1MCS-5 relies on the genes native promoter.

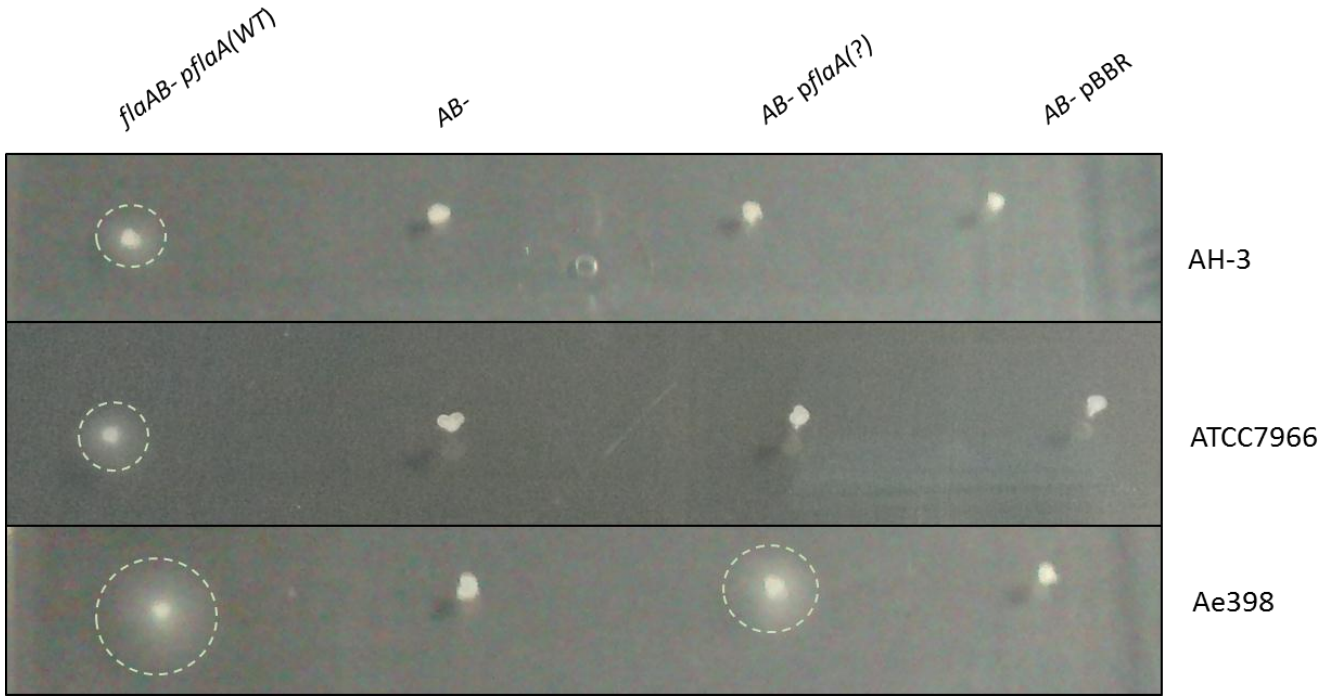


**Figure 5.4** – Motility analysis of an *Aeromonas caviae flaAB* mutant expressing heterologous *Aeromonas* flagellins (AH-3, ATCC 7966 and Ae398). Assays were carried out on 0.25% agar. The motility of the *A. caviae flaAB* mutant containing pBBR1MCS-5_*flaA* from Sch3 [*flaAB- pflaA*(WT)], the *flaAB* mutant alone (*flaAB-*), the mutant containing a heterologous *flaA* gene [*flaAB-* p*flaA*(?)] and the mutant containing empty pBBR1MCS-5 (*flaAB-* pBBR), are shown.

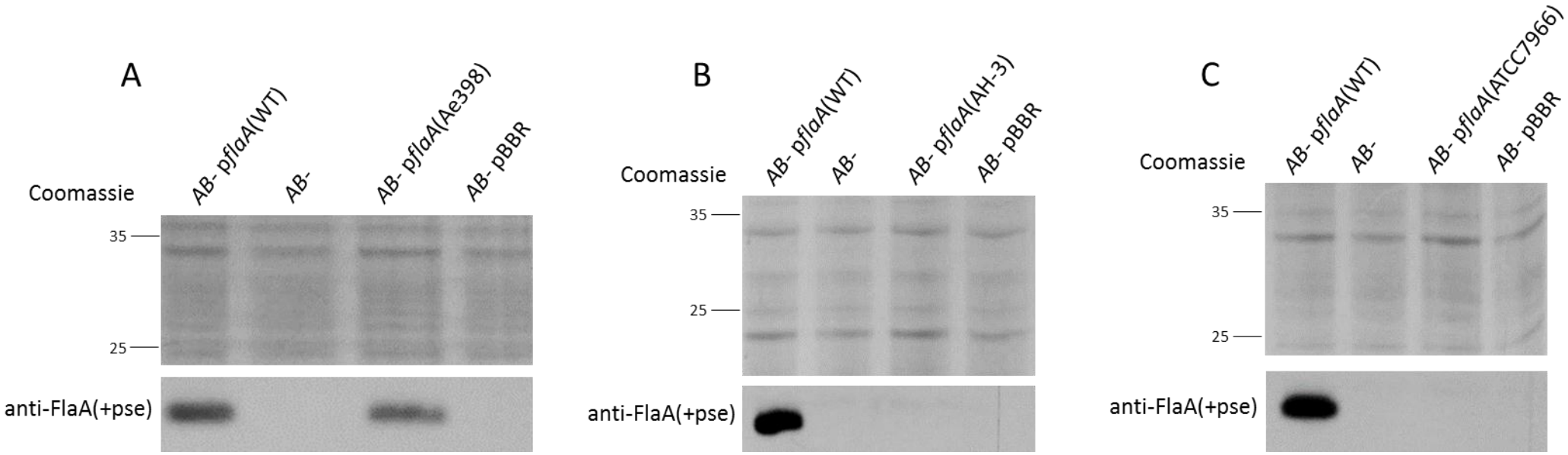


**Figure 5.5** – Western blot analysis of *Aeromonas caviae* whole-cell samples probed with a rabbit, anti-polar flagellin antibody that recognises only glycosylated flagellin [anti-FlaA/B(+Pse)]. (**A**) Lane 1, *A. caviae flaAB* mutant containing pBBR1MCS-5_*flaA* from Sch3 [*flaAB- pflaA*(WT)]; lane 2, the *flaAB* mutant alone (*flaAB-*); lane 3, the mutant containing pBBR1MCS-5_*flaA* from Ae398 [*flaAB-* p*flaA*(Ae398)]; and lane 4, the mutant containing the empty vector (*flaAB-* pBBR). (**B**) As before, but lane 3, displays the mutant containing pBBR1MCS-5_*flaA* from AH-3 [*flaAB-* p*flaA*(AH-3)]. (**C**) As before, but lane 3, displays the mutant containing pBBR1MCS-5_*flaA* from ATCC 7966 [*flaAB-* p*flaA*(ATCC 7966)].

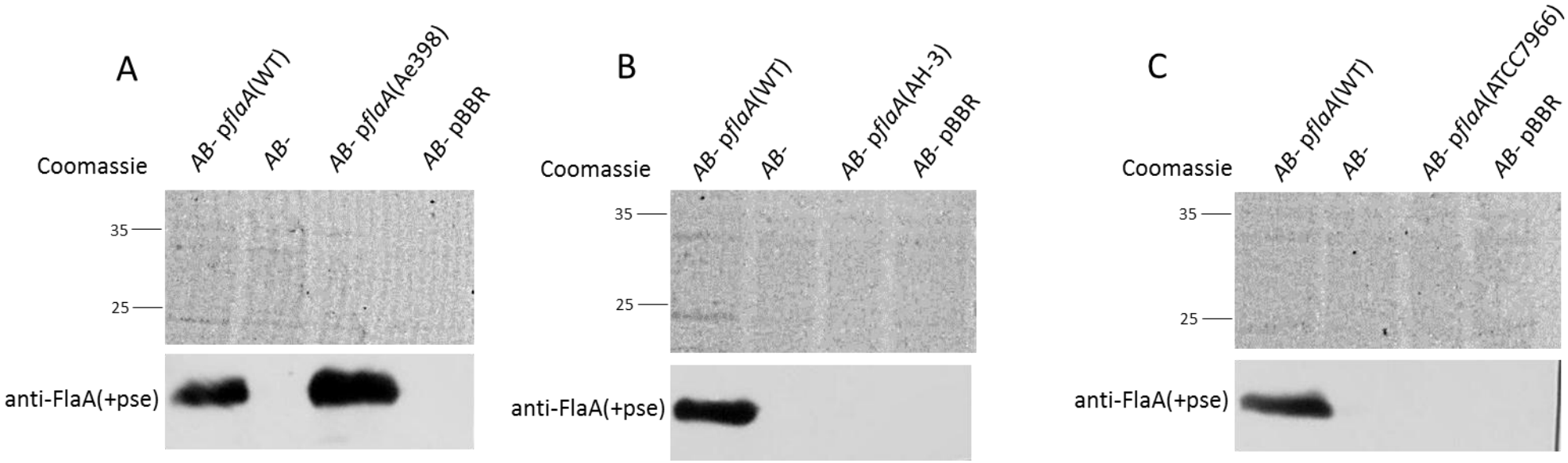


**Figure 5.6** – Western blot analysis of *Aeromonas caviae* supernatant samples probed with a rabbit, anti-polar flagellin antibody that recognises only glycosylated flagellin [anti-FlaA/B(+Pse)]. (**A**) Lane 1, *A. caviae flaAB* mutant containing pBBR1MCS-5_*flaA* from Sch3 [*flaAB*- *pflaA*(WT)]; lane 2, the *flaAB* mutant alone (*flaAB*-); lane 3, the mutant containing pBBR1MCS-5_*flaA* from Ae398 [*flaAB*- p*flaA*(Ae398)]; and lane 4, the mutant containing the empty vector (*flaAB*- pBBR). (**B**) As before, but lane 3, displays the mutant containing pBBR1MCS-5_*flaA* from AH-3 [*flaAB*- p*flaA*(AH-3)]. (**C**) As before, but lane 3, displays the mutant containing pBBR1MCS-5_*flaA* from ATCC 7966 [*flaAB*- p*flaA*(ATCC 7966)].

For insertion into pSRK(Gm), the *A. piscicola* AH-3, *A. hydrophila* ATCC 7966 and *A. caviae* Sch3 (positive control) *flaA* genes were amplified using the Expand high fidelity PCR system (Roche), using the corresponding *Aeromonas* genomic DNA and the sets of primers summarised in table 5.4. These genes were cloned into pGEM-T EASY, as in section 5.2.1.1. Once the correct *flaA* genes were present and then excised from pGEM-T EASY (using a combination of NdeI and HindIII restriction enzymes), they were ligated into *Nde*I/*Hin*dIII cut pSRK(Gm) (section 3.2.3, figure 3.7). The ligations were transformed into *E. coli* DH5α and vector DNA isolated from the resulting transformants. A HindIII restriction digest and agarose gel electrophoresis confirmed the presence of the correct genes in pSRK(Gm).

#### 5.2.3.4 – Analysis of pSRK_*flaA* constructs in *Aeromonas caviae*

The resulting pSRK(Gm) vectors containing the desired flagellin genes were conjugated into an *A. caviae flaAB* mutant, along with the empty vector. Three transconjugants were selected for analysis. As in section 5.2.3.2, motility assays were carried out with the resulting transconjugants, and the glycosylation status, of the flagellins present in whole-cell and supernatant *A. caviae* samples, was analysed by immunoblotting.

Again, both FlaA proteins from AH-3 and ATCC 7966 *Aeromonas* strains were unable to restore the motility of an *A. caviae* (Sch3) *flaAB* mutant (Fig. 5.7) and glycosylated flagellin could not be detected in either whole-cell or supernatant samples when they were probed with the anti-polar flagellin antibody that only recognises glycosylated flagellin (Fig 5.8). This may indicate that Maf1 is an extremely specific enzyme. Although no consensus sequence for O-linked glycosylation has been identified, these data suggest, in addition to the results obtained in Chapter 4, that there is selectivity to the Maf1-dependent flagellin glycosylation process.

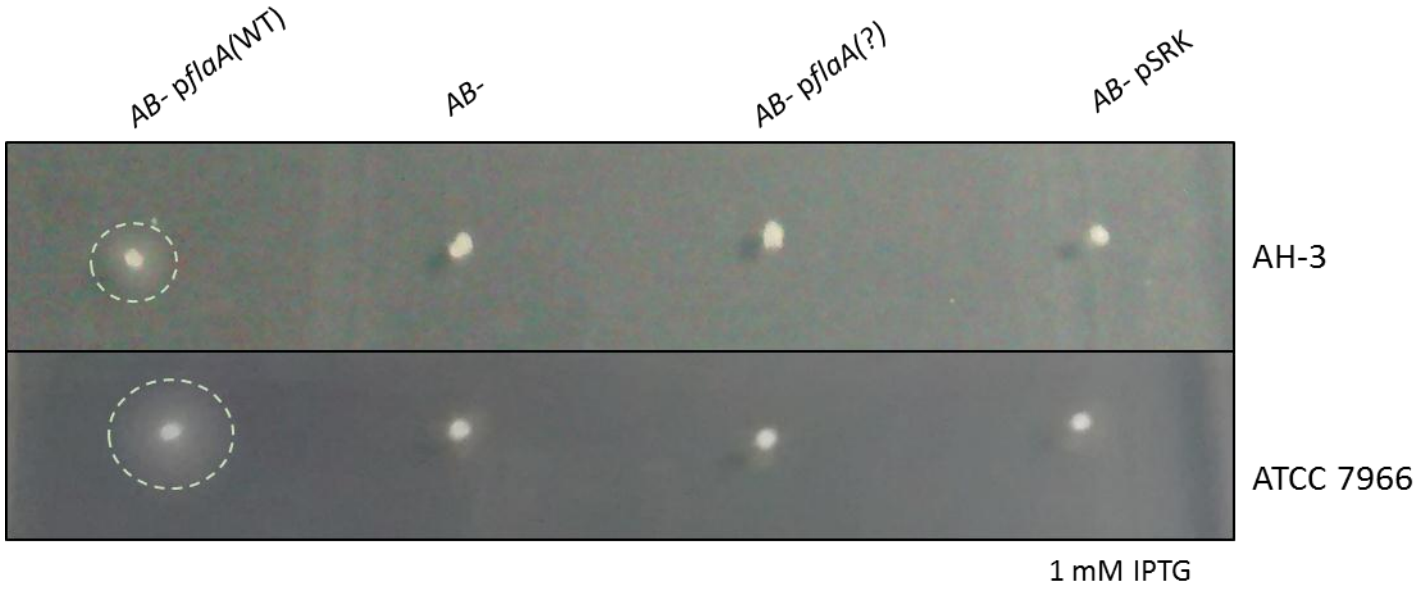


**Figure 5.7** – Motility analysis of an *Aeromonas caviae flaAB* mutant expressing heterologous *Aeromonas* flagellins (AH-3 and ATCC 7966). Assays were carried out on 0.25% agar containing 1 mM IPTG. The motility of the *A. caviae flaAB* mutant containing pSRK_*flaA* from Sch3 [*flaAB*- *pflaA*(WT)], the *flaAB* mutant alone (*flaAB*-), the mutant containing a heterologous *flaA* gene [*flaAB*- p*flaA*(?)] and the mutant containing empty pSRK(Gm) (*flaAB*- pSRK), are shown.

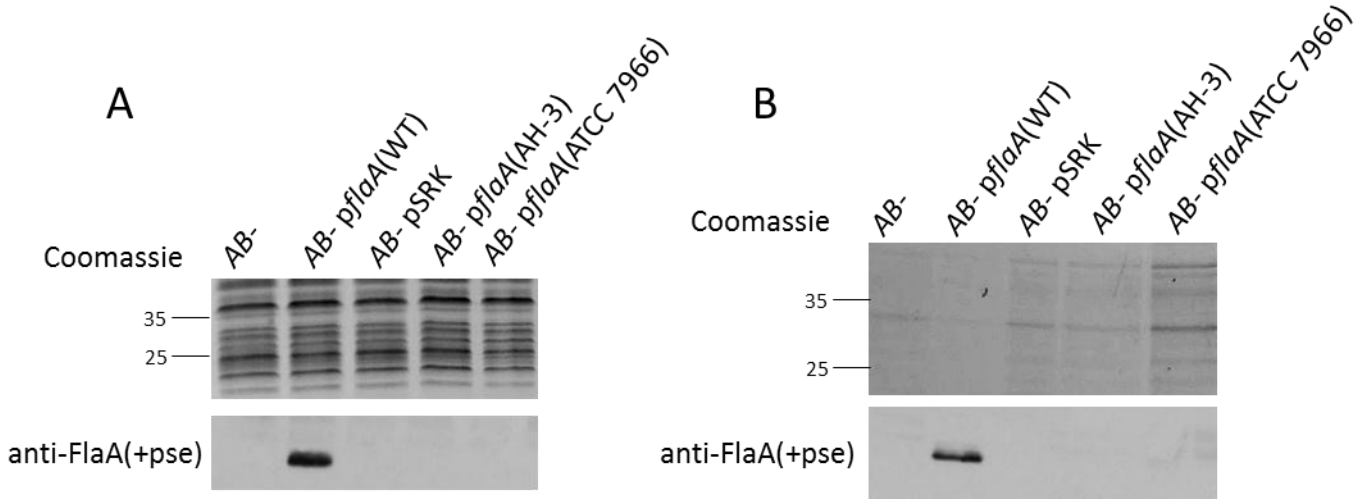


**Figure 5.8** – Western blot analysis of *Aeromonas caviae* whole-cell (**A**) and supernatant samples (**B**) probed with a rabbit, anti-polar flagellin antibody that recognises only glycosylated flagellin [anti-FlaA/B(+Pse)]. In each case: lane 1, the *A. caviae flaAB* mutant (*flaAB*-); lane 2, the *flaAB* mutant containing pSRK_*flaA* from Sch3 [*flaAB*- *pflaA*(WT)]; lane 3, the *flaAB* mutant containing the empty vector (*flaAB*- pSRK); lane 4, the mutant containing pSRK_*flaA* from AH-3 [*flaAB*- p*flaA*(AH-3)] and pSRK_*flaA* from ATCC 7966 [*flaAB*- p*flaA*(ATCC 7966)].

## 5.2.4 – *Helicobacter pylori* Maf studies

These studies were carried in conjunction with Corrie Porter, a second year undergraduate student from the department of Molecular Biology and Biotechnology, who carried out a summer research project in the Shaw group (SURE scheme, 2014).

*H. pylori* glycosylates its polar flagella solely with pseudaminic acid (Josenhans *et al.*, 2002; Schirm *et al.*, 2003), similarly to *A. caviae* (Tabei *et al.*, 2009); however, for unclear reasons, *H. pylori* possesses two *maf* homologues in its genome (Fig. 5.9) (Tomb *et al.*, 1997) (described as *maf1 and maf2* here). In *H. pylori* 26695, *maf1* is located directly next to the gene for flagellin B (*flaB*), whereas *maf2* is located entirely in a separate region of the genome (Fig. 5.9) (Tomb *et al.*, 1997). The initial studies carried out here were to determine whether *A. caviae* Sch3 is a good model of O-linked glycosylation for the heterologous expression of *H. pylori* glycosylation proteins, to see if the function of these proteins can be explored. Additionally these studies also allow the further exploration of whether the Maf proteins have broader specificity for other flagellins, or whether they are specific for their own cognate flagellins.

### 5.2.4.1 – Generation of pSRK_*maf (H. pylori)* constructs

The *H. pylori* 26695 *maf* genes, *maf1* and *maf2*, thought to each encode a 72 kDa protein (628 and 631 amino acids respectively), were cloned into the IPTG inducible vector pSRK(Gm). The *maf* genes were cloned into pSRK(Gm) using the same cloning method as previously described in section 5.2.3.3, using the primers, RCL_61 (F) and RCL_62 (R) for the amplification of *maf1,* and RCL_63 (F) and RCL_64 (R) for *maf2,* from *H. pylori* 26695 genomic DNA (Chapter 2, Table 2.6).

### 5.2.4.2 - Analysis of pSRK_*maf (H. pylori)* constructs in *Aeromonas caviae*

The pSRK_*maf* constructs were individually conjugated into the *A. caviae maf1* mutant previously created in the Shaw group (Parker *et al.*, 2012), along with empty pSRK(Gm), and three transconjugants were selected for analysis in each case.

Swimming motility assays were carried out on the strains created, again on the large motility plates discussed previously, allowing for the analysis of multiple strains, and six technical repeats per strain, per plate. *A. caviae* was used as a positive motility control during these motility assays.

When the motility of the *maf1* mutant containing *maf1* from *H. pylori* was analysed, inconsistent motility phenotypes were observed (Fig. 5.10). Out of the three transconjugants

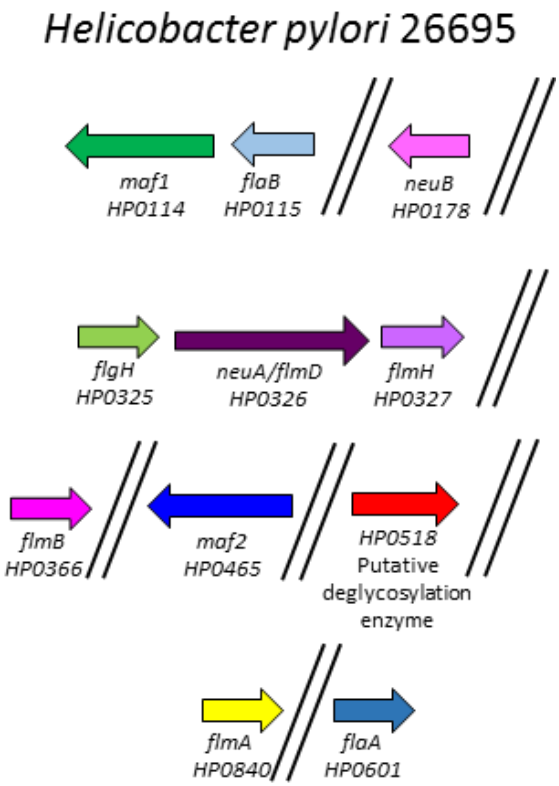


**Figure 5.9** – The genetic organisation of the polar flagellar and pseudaminic acid biosynthetic genes in *Helicobacter pylori* 26695 (Tomb *et al.,* 1997).

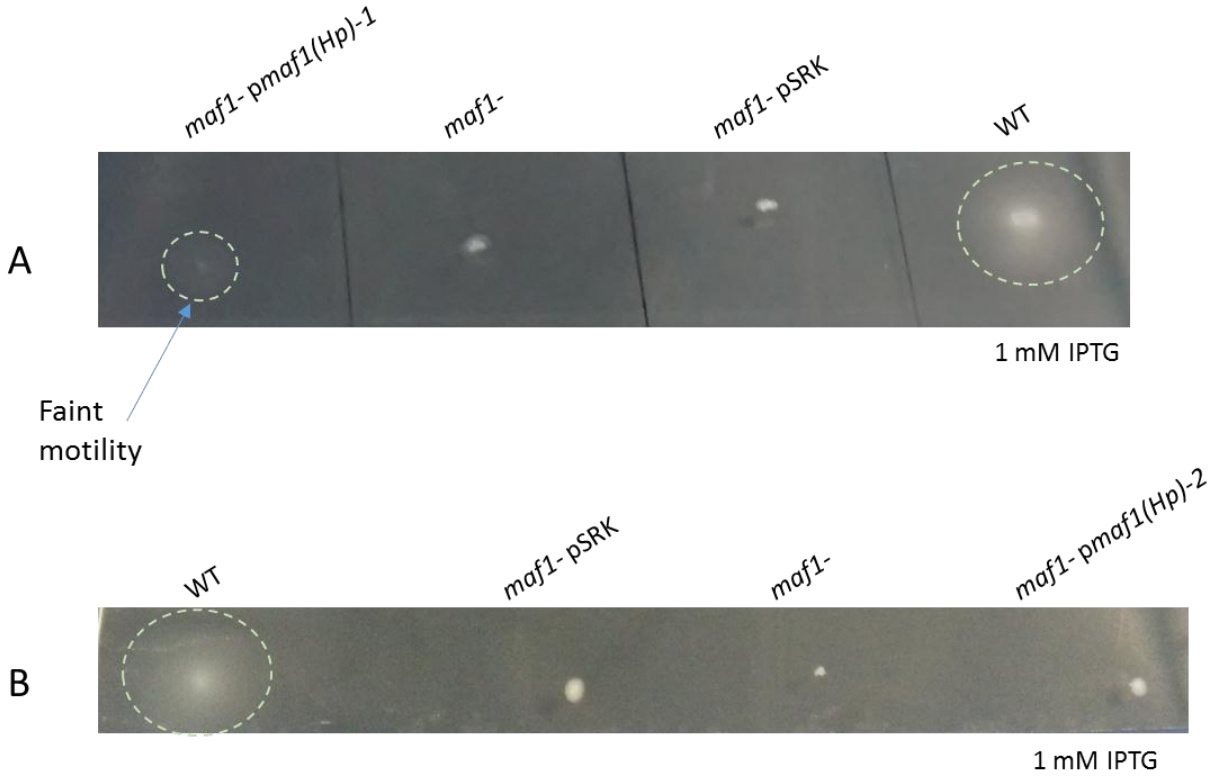


**Figure 5.10** - Motility analysis of an *Aeromonas caviae maf1* mutant containing *maf1* from *Helicobacter pylori* 26695 [*maf1- pmaf1*(Hp)]. (A) and (B) show the motility of two different transconjugants [*maf1- pmaf1*(Hp)-1 and *maf1- pmaf1*(Hp)-2]. Assays were carried out alongside: *A. caviae* Sch3 (WT), the *maf1* mutant (*maf1-*) and the mutant containing empty pSRK(Gm) (*maf1-* pSRK), on 0.25% agar containing 1 mM IPTG.

analysed, two displayed a non-motile phenotype, whereas one showed faint, highly impaired, motility (not the characteristic motility halos produced by wild type *A. caviae*) (Fig. 5.10). Figure 5.10 displays the motile transconjugant (A), and one of the non-motile transconjugants (B). Three biological repeats of these motility assays were also carried out, but the plates shown here are representative of them all. Furthermore, when normalised whole-cell and precipitated supernatant samples from these transconjugants were probed with the anti-polar flagellin antibody that only recognises glycosylated flagellin, the motile transconjugant was shown to be producing glycosylated flagellin, whereas the non-motile strains were not (Fig. 5.11). The conjugations of these pSRK_*maf1* vectors into the *A. caviae maf1* mutant were repeated twice more, with one repeat showing three fully motile transconjugants, and the other resulting in non-motile transconjugants (data not shown). Extremely variable results were observed here.

However, when the motility of the *maf1* mutant containing *maf2* from *H. pylori* was analysed, all transconjugants displayed non-motile phenotypes (Fig. 5.12) and no glycosylated flagellins could be detected by Western blot analysis (Fig. 5.13).

Therefore, some promiscuity was detected with Maf1 from *H. pylori*, which suggests that this protein in *H. pylori* is a flagellin-specific glycosyltransferase. Although as inconsistent results were observed here, it is possible that both Maf proteins are required for efficient *H. pylori* flagellin glycosylation to take place. However, it is possible that Maf2 from *H. plyori* has an alternative target in the cell.

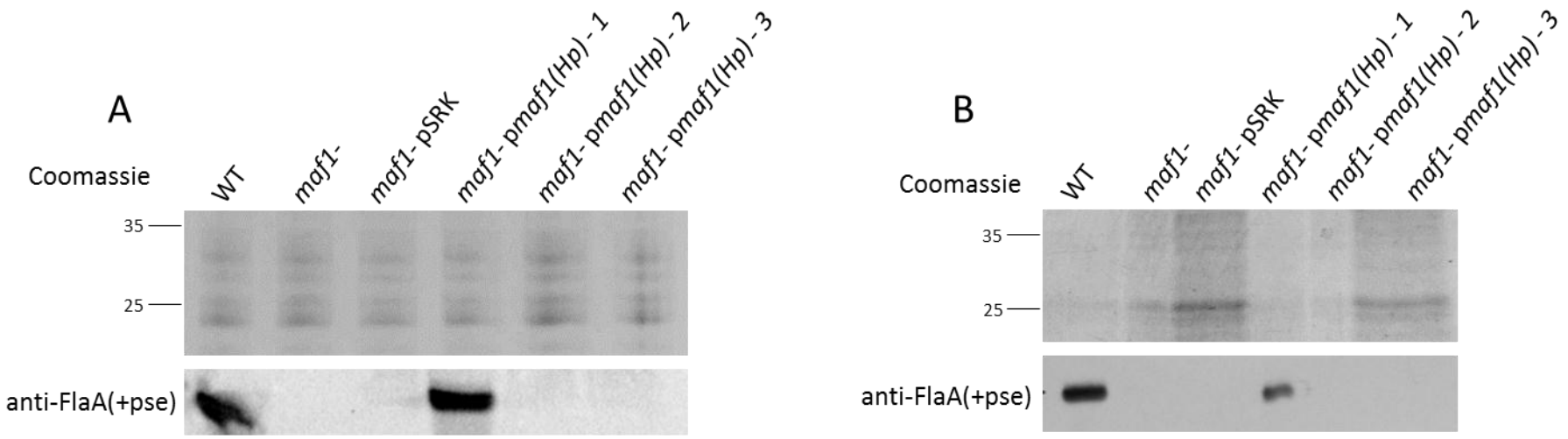


**Figure 5.11** - Western blot analysis of the glycosylation status of flagellin present in *Aeromonas caviae* whole-cell (**A**) and supernatant (**B**) samples, when Maf1 from *Helicobacter pylori* 26695 is heterologously expressed in an *A. caviae maf1* mutant. In each case: lane 1, *A. caviae* Sch3 (WT); lane 2, the *maf1* mutant (*maf1*- ); lane 3, the *maf1* mutant empty pSRK(Gm) (*maf1*- pSRK); and lanes 4-6, show the three transconjugants which are the *A. caviae maf1* mutant containing pSRK_*maf1* from *H. pylori* [*maf1*- p*maf1*(Hp)-1/2/3].

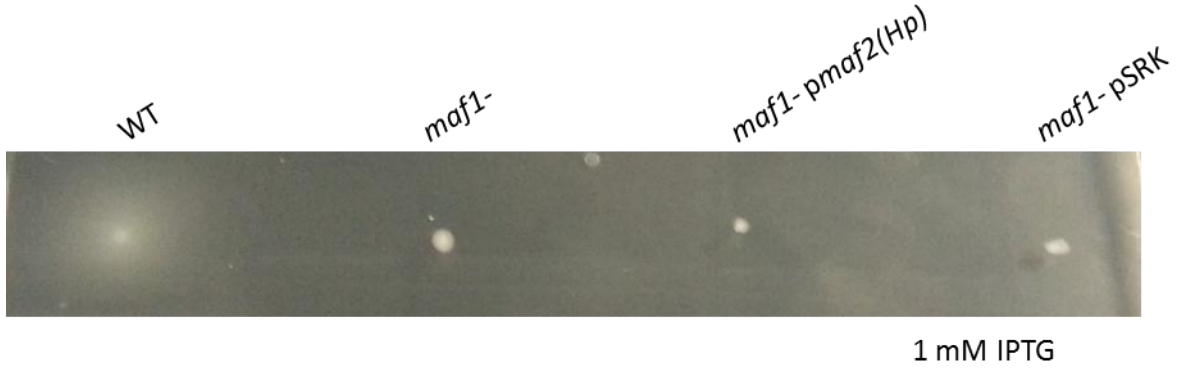


**Figure 5.12** - Motility analysis of an *Aeromonas caviae maf1* mutant containing *maf2* from *Helicobacter pylori* 26695 [*maf1- pmaf2*(Hp)]. The motility of one transconjugant is shown but is representative of all analysed. Assays were carried out alongside: *A. caviae* Sch3 (WT), the *maf1* mutant (*maf1*-) and the mutant containing empty pSRK(Gm) (*maf1*- pSRK), on 0.25% agar containing 1 mM IPTG.

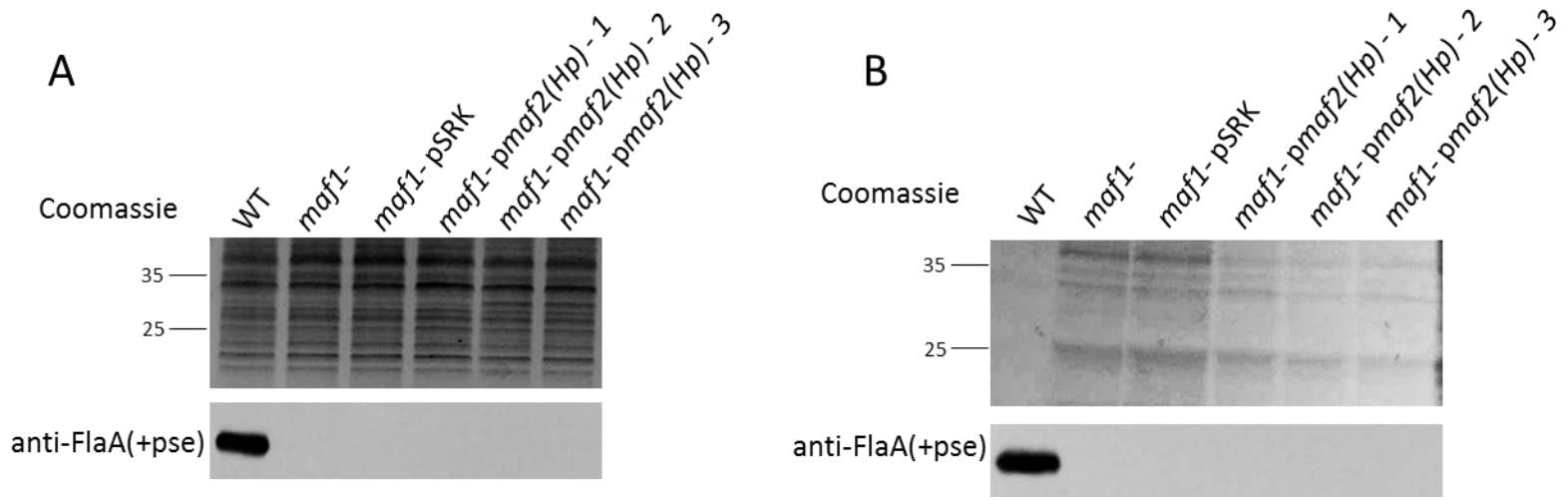


**Figure 5.13** - Western blot analysis of the glycosylation status of flagellin present in *Aeromonas caviae* whole-cell (**A**) and supernatant (**B**) samples, when Maf2 from *Helicobacter pylori* 26695 is heterologously expressed in an *A. caviae maf1* mutant. In each case: lane 1, *A. caviae* Sch3 (WT); lane 2, the *maf1* mutant (*maf1*- ); lane 3, the *maf1* mutant empty pSRK(Gm) (*maf1*- pSRK); and lanes 4-6, show the three transconjugants which are the *A. caviae maf1* mutant containing pSRK_*maf2* from *H. pylori* [*maf1*- p*maf2*(Hp)-1/2/3].

## 5.3 – Discussion

Continuing on from section 5.2.1, the bacterial adenylate cyclase two-hybrid system was utilised to explore the interactions between proteins associated with *A. caviae* Sch3 flagellin glycosylation and polar flagellar assembly. This system allowed *in vivo* interactions between these proteins, in a non-glycosylating system (*E.coli* BTH101), to be explored. No self-interactions, interactions between the unglycosylated flagellins (FlaA and FlaB), or interactions between the flagellins and the flagellin-specific chaperone (FlaJ) were observed. This further demonstrates that glycosylation is likely to be required for the correct folding of flagellin and for polymerisation, as it has previously been determined that glycosylation is essential for the formation of *A. caviae* polar flagellum ((Tabei *et al.*, 2009). However, when flagellins fold, the N and C termini come together to form conserved D0 and D1 domains, which are required for polymerisation (Auvray *et al.*, 2001). Therefore the presence of the adenylate cyclase tags at the N or C termini of these proteins may have had an effect on their ability to interact with other proteins (such as each other) here. These results also suggest that chaperone binding of the flagellins may occur after glycosylation, as no interactions were detected between the unglycosylated flagellins and FlaJ (Table 5.3). This agrees with the work from Parker *et al.* (2014), where interactions between glycosylated and unglycosylated *A. caviae* flagellins were explored by Far Western blot analysis. Only very minor interactions could be detected between FlaJ and the unglycosylated form of flagellin, compared to the strong interactions observed when the glycosylated flagellin was present (Parker *et al.*, 2014). Therefore, the likelihood of detecting interactions between these proteins in an *in vivo*, non-glycosylating system is extremely slim.

It was concluded, however, that Maf1 is able to interact with the unglycosylated flagellins, FlaA and FlaB, and in the absence of pseudaminic acid; although a number of the results obtained were inconsistent. Maf1 interacted with both flagellins when tagged at either the N or C termini with either domains of CyaA, but particularly strong interactions were observed between Maf1 tagged at the C-terminus (with T25) and both the flagellins tagged at their C-termini (with T18). This suggests that the N-terminal region of Maf1 may be important for flagellin recognition, and when the N-terminal region of the flagellin is free, this may allow Maf1 access to the D2/D3 domain for glycosylation to occur. It has been previously determined that the chaperone binding domain of glycosylated flagellin is essential for FlaJ binding and export of the flagellin (Parker *et al.*, 2014), therefore another region of the flagellin, such as the N-terminal domain, may be important for Maf1 docking. It is also known that the flagellin N-terminus is important for secretion, and in addition, the D0 regions of the

flagellins are essential for the newly proposed chain mechanism of flagellar assembly (Evans *et al.*, 2013). Therefore if Maf1 docks to thisregion, it may the block signals for flagellin export, resulting in the decreased export of unglycosylated flagellin that cannot be incorporated into a filament. Other interactions observed were very inconsistent, likely due to the insoluble nature of unglycosylated *A. caviae* flagellins (Parker *et al.*, 2014). Additionally, the large tags of CyaA may also affect correct protein folding, leading to inconsistent results.

Strong positive interactions were, however, detected between Maf1 tagged at the C-terminus (with T25) and FlaA-CBD (FlaA minus the chaperone binding domain) when tagged at either the N or C-termini (with T18). Furthermore interactions were also detected when Maf1 was tagged at the N-terminus (with T18) and FlaA-CBD tagged at the N-terminal region (with T25). A strong positive interaction had previously not been detected between Maf1 and either flagellin tagged at their N-termini (inconsistent results); however, the removal of the chaperone binding domain may make the glycosylated region of flagellin, the D2/D3 domain (Tabei *et al.*, 2009), more accessible for Maf1 to bind and allow access even when the flagellin is tagged at the N-terminus. In addition, the combination of the removal of the CBD and being tagged by a domain of adenylate cyclase may also make the flagellin more soluble, allowing for more interactions to be observed *in vivo* between the mutant flagellin and Maf1 here.

More unexpectedly, however, was that when interactions between Maf1 and FlaA-D2/D3 (FlaA minus the D2/D3 domain) were assessed, interactions were observed (either strong or inconsistent) in all the combinations previously witnessed between FlaA and Maf1. This was surprising as although the central region that Maf1 glycosylates has been removed, Maf1 is still able to recognise and bind to the mutant flagellin (though interactions were again extremely inconsistent). However, as it was previously discussed in chapter 4, hydrophobic residues appear to be clustered in the central (D2/D3) region of flagellins and glycosylation may mask these hydrophobic regions. So when removed, a mutant flagellin made up of only D0 and D1 domains may allow the production of a soluble flagellin (compared to the usual, highly insoluble, wild type version). This mutant flagellin may therefore exist more freely in *E. coli* and be available to interact with Maf1. These results also suggest that Maf1 can interact with other regions of the flagellins and is not solely recognising the D2/D3 region. It is therefore possible that the N-terminal region of flagellin is required for Maf1 docking, before glycosylation occurs, as interactions are observed between Maf1 and both the mutant flagellins investigated here (FlaA-CBD and FlaA-D2/D3). In addition, these observations also indicate that glycosylation occurs before chaperone binding of flagellin, and therefore, likely to

occur in the cytoplasm of the bacterium (Fig. 5.14). The 'handover' experiment carried out in Parker *et al.* (2014) further supports these observations, as it was concluded that Maf1 and glycosylated flagellin co-purify from *A. caviae*, and the *in vitro* experiments demonstrated that FlaJ is able to take this glycosylated flagellin directly from the glycosyltransferase. This is thought to mimic the events that are occurring inside the cell. Moreover, as FlaJ also appears to have a higher affinity for glycosylated flagellin, it is likely to only interact with these proteins inside the cell once glycosylated, to allow the efficient export of only the modified version of the flagellins for incorporation into the flagellar filament (Fig. 5.14) (Parker *et al.*, 2014). This also agrees with studies in *C. jejuni* whereby mutant strains incapable of producing basal body and hook proteins, and therefore deficient in a flagellar export system, were still able to produce glycosylated flagellins, suggesting glycosylation occurs in the cytoplasm (Ewing *et al.*, 2009).

An inconsistent interaction was also detected between Maf1 and FlaJ, which would be expected if this 'handover' event takes place within the cell (Parker *et al.*, 2014). However, again, the bulky CyaA tags may be affecting protein folding, leading to the inconsistent interactions observed. Interactions were only detected here when Maf1 had a free C-terminal region, which suggests that this region may be more important for the recognition of FlaJ, and the N-terminus for the recognition of flagellins.

Continuing on from section 5.2.2, FlaH is the polar flagellar cap protein in *A. caviae* and carries out the same job as FliD from *E. coli* and *Salmonella* (Yonekura *et al.*, 2000). Although it is known that the filament cap is required for incorporation of the flagellins into a functional filament, and that flagellar cap mutants are non-motile (Yonekura *et al.*, 2000); it was not known if FlaH in *A. caviae* had a role in the flagellin glycosylation process. Here, the flagellins of an *A. caviae flaH* mutant were analysed and it was confirmed by Western blot analysis that the flagellins present in this strain are still glycosylated and are readily exported into the culture supernatant. These data therefore demonstrate that FlaH is not involved in the glycosylation process and together with the results from the interaction studies, suggest that flagellin modification occurs in the cytoplasm before protein targeting to the type III export apparatus and incorporation into the flagellar filament (Parker *et al.*, 2014). Furthermore, these data also show that there is no mechanism to prevent flagellin glycosylation in the occurrence that the bacterium is unable to form a functional filament (Parker *et al.*, 2014).

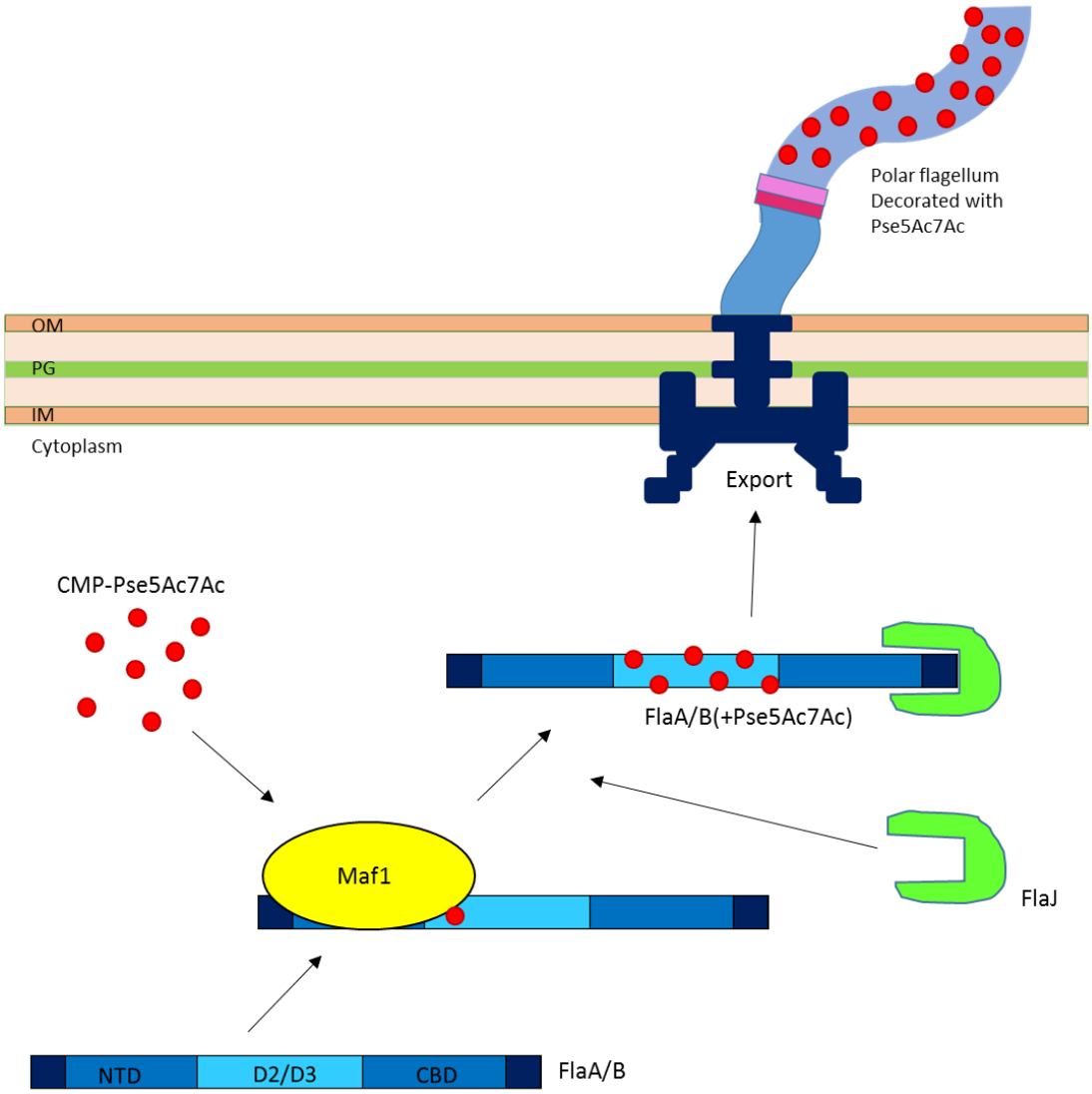


**Figure 5.14** – A theoretical model of the pathway of flagellin glycosylation. Pseudaminic acid (Pse5Ac7Ac) is activated via the addition of cytidine monophosphate (CMP) before it is transferred onto the D2/D3 domain of the flagellin by Maf1 in the cytoplasm. FlaJ binding is likely to occur after glycosylation, which depends on the presence of the chaperone binding domain (CBD) of the flagellin (Parker *et al.*, 2014), resulting in the export of glycosylated flagellins [FlaA/B(+Pse)] that can be incorporated into a flagellar filament. This model of flagellin glycosylation agrees with that from Parker *et al.* (2014).

In section 5.2.3, flagellin swapping studies were carried out to assess whether Maf1 from *A. caviae* is a promiscuous enzyme capable of glycosylating alternative *Aeromonas* flagellin D2/D3 domains. The ability of Maf1 from *A. caviae* to glycosylate flagellins from: *A. piscicola* AH-3 (Merino *et al.*, 1991), *A. hydrophila* ATCC 7966 (Seshadri *et al.*, 2006) and *A. caviae* Ae398 (Beatson *et al.*, 2011), was explored. Of the flagellins analysed, FlaA from *A. caviae* Sch3 displays the highest sequence identity (of 86%) with FlaA from *A. caviae* Ae398; however, their D2/D3 regions only display 58% identity. It was found that *A. caviae* Ae398 flagellins could restore the motility of an *A. caviae flaAB* mutant, with Western blot analysis confirming that the flagellins were glycosylated. In contrast, *A. piscicola* AH-3 and *A. hydrophila* ATCC 7966 flagellins (FlaA) could not complement the motility of a *flaAB* mutant, and glycosylated flagellin could not be detected in the whole-cell or supernatant samples analysed here. The flagellins show 71% (*A. piscicola* AH-3) and 73% (*A. hydrophila* ATCC 7966) identity to *A. caviae* Sch3 FlaA, with the most variation being located in the D2/D3 regions of the proteins. *A. caviae* displays less identity with the D2/D3 domains of these proteins compared to with *A. caviae* Ae398 FlaA, at 40% identity with the D2/D3 region of *A. piscicola* AH-3 flagellin, and 51% with *A. hydrophila* ATCC 7966 flagellin. This therefore suggests that although some promiscuity is detected with Maf1, this enzyme does show some specificity. Interaction studies carried out here and by Parker *et al.* (2014) also suggest that Maf1 does not only recognise the D2/D3 region of the flagellins, but may recognise the N-terminus also. Therefore, Maf1 may not actually be binding to and glycosylating flagellins due to their D2/D3 domain sequences, but due to another site perhaps located in the N-terminal region of the protein. *A. caviae* Sch3 and Ae398 FlaA show the highest level of identity in their N-terminal regions, at 98%. However, the FlaA N-terminal regions from *A. piscicola* AH-3 and *A. hydrophila* ATCC 7966 only show 80% and 82% identity respectively with *A. caviae* Sch3 FlaA. This therefore suggests that the N-terminal regions of the flagellins could be responsible for Maf1 docking and glycosylation.

However, flagellin glycosylation from *A. piscicola* AH-3 and *A. hydrophila* ATCC 7966 is thought to be more complex than *A. caviae* Sch3. *A. piscicola* AH-3 possess more complex glycosylation loci than *A. caviae*, due to the presence of two *maf* genes (Chapter 1, figure 1.7) (Canals *et al.,* 2007), and recent work from Wilhelms *et al.* (2012) also suggests that flagellins are modified with a heterogenous heptasaccharide (376 Da) which includes pseudaminic acid. Furthermore, the flagellin glycosylation loci in *A. hydrophila* ATCC7966 (Seshadri *et al.*, 2006) is also far more complex than that of *A. caviae* Sch3, as it possesses two *maf* homologues, similarly to *A. piscicola* AH-3 (Chapter 1, figure 1.7). These studies may demonstrate that the Maf proteins are extremely specific enzymes, or perhaps glycosylation in bacteria that contain multiple Maf

proteins, and are known likely to modify their flagellins with a variety of sugars, require specific interactions between their Maf proteins, which Maf1 from *A. caviae* Sch3 is incapable of due to pseudaminic acid being the only sugar present in this system (Tabei *et al.*, 2009).

Continuing on from section 5.2.4, although Maf1 from *A. caviae* Sch3 could not glycosylate *A. piscicola* AH-3 and *A. hydrophila* ATCC 7966 flagellins (FlaA), the effect of heterologously expressing *H. pylori* Maf proteins (Maf1 and Maf2) was investigated here due to *H. pylori* solely glycosylating its flagellins with pseudaminic acid, similarly to *A. caviae* Sch3 (Josenhans *et al.*, 2002; Schirm *et al.*, 2003). These studies were also carried out to give an indication as to whether *A. caviae* Sch3 is a good model for the study of O-linked glycosylation, as it grows well aerobically, and contains the smallest set of genes required for pseudaminic acid biosynthesis. Little is known about the Maf proteins from *H. pylori,* or why two proteins are present when the bacterium only modifies its flagella with pseudaminic acid; however *H. pylori* requires nutrient rich media and a microaerobic environment for growth, so other means of analysing the flagellin glycosylation process of this pathogen would be desirable. It is possible that both Maf proteins have a role in flagellin glycosylation in *H. pylori*; however, they may also have different roles within the cell.

Maf2 from *H. pylori* was unable to restore the motility of an *A. caviae maf1* mutant, and no evidence of flagellin glycosylation was observed. However, Maf1 from *H. pylori* was found to possibly, although inconsistently, recognise and modify *A. caviae* flagellins. This may show that Maf proteins from similar glycosylating systems, (ie. can only glycosylate with pseudaminic acid here) are able to compensate for one another. The preliminary results obtained, however, were extremely inconsistent and would require further investigation. The results are intriguing, as the flagellins from *H. pylori* are much larger than those from *A. caviae*, with their sequences showing only 37% identity (Fig. 5.15). These proteins do, however, share some identical runs of amino acids, such as 'FQVGA', located at the start of the *A. caviae* FlaA D2/D3 region (Fig. 5.15). It was found in Chapter 4 of this work, that FlaB is glycosylated on residues that occur shortly after this sequence. It may be that this region is involved in Maf recognition of, and docking to, the flagellins; although this sequence is present in all the *Aeromonas* flagellins involved in the flagellin swapping studies here where glycosylation by *A. caviae* Sch3 Maf1 was not detected. The position of *maf1* in the *H. pylori* 26995 genome suggests it to be a flagellin specific glycosyltransferase as it is located next to the gene encoding flagellin B (FlaB) (Fig. 5.9). Whereas, *maf2* is not associated with any genes for pseudaminic acid biosynthesis or

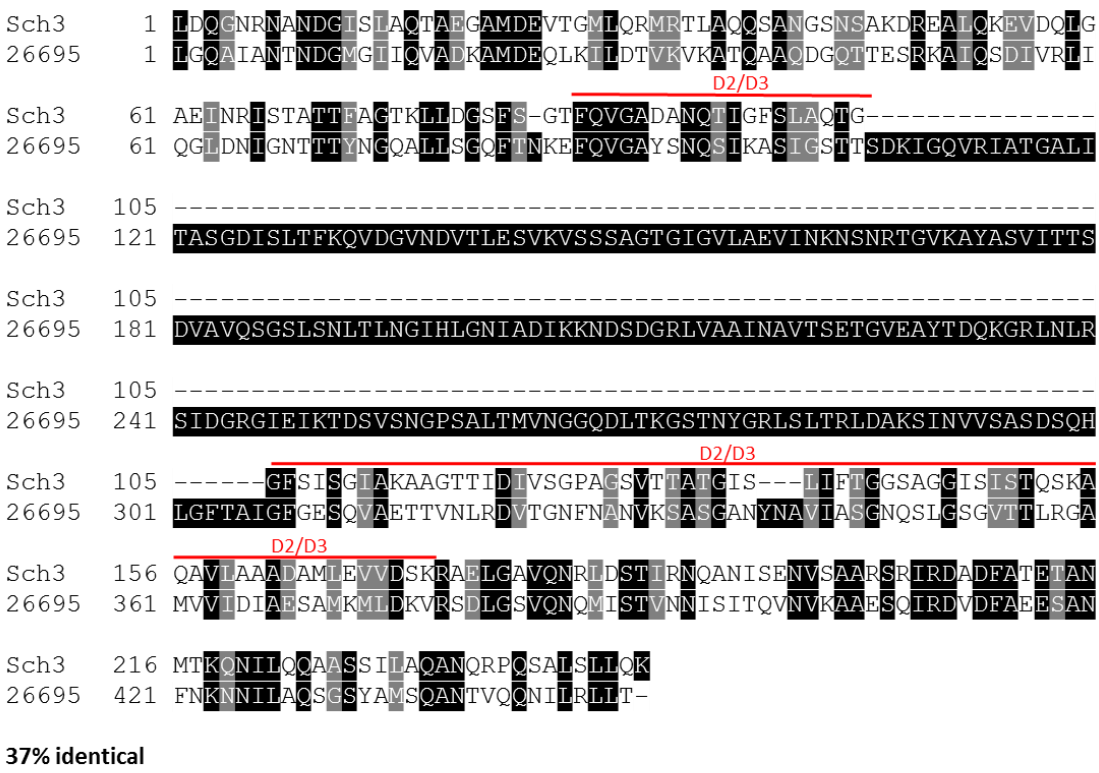


**37% identical**

**Figure 5.15** – Alignment of *Aeromonas caviae* Sch3 FlaA (Sch3) (accession: AAF19179) with FlaA from *Helicobacter pylori* 26695 (Tomb *et al.,* 1997). The alignment was executed using CLUSTALW (Thompson *et al.*, 1994) and displayed with box-shade. The D2/D3 domain of *A. caviae* Sch3 FlaA is highlighted.

polar flagellum assembly (Fig. 5.9), which may indicate that this protein is not required for flagellin modification at all and may target other proteins in *H. pylori.* Recent studies by Hopf *et al.* (2011) have demonstrated that although pseudaminic acid solely decorates *H. pylori* polar flagella, there is evidence that this bacterium is also capable of synthesising other pseudaminic acid derivatives, and possibly legionaminic acid. This work presented nine candidate glycoproteins that all reside either within the bacterial cytoplasm or embedded in the inner membrane (Hopf *et al.*, 2011); however, the importance of glycosylation for these proteins has not yet been determined. Furthermore, Champasa *et al.* (2013) identified 125 putative glycoproteins in *H. pylori* using metabolic glycan labelling studies. The proteins identified carry out a diverse range of functions within the cell and reside in a variety of cellular locations (such as, the cytoplasm, the periplasm, and the inner and outer membranes) (Champasa *et al.*, 2013). It is therefore possible that Maf2 from *H. pylori* does not target the flagellins, and is targeting another protein for glycosylation. It is clear from these investigations that there is still much to discover about protein glycosylation in this microorganism. However, there have not yet been reports in any other bacteria of the Maf proteins having alternative target proteins to the flagellins.

To follow on from these studies, both *maf* homologues could be expressed in *A. caviae*, to see whether both of these proteins are required for efficient flagellin glycosylation. Also, as *A. caviae* is genetically amenable and easy to culture, it could be a good tool in the future to study how *H. plylori* glycosylates its own flagellins, by expressing *H. pylori* Maf proteins and flagellins in *A. caviae*. Although these are very preliminary studies, they show promise that *A. caviae* Sch3 may be used and manipulated as a model organism for the study of glycosylation in the future.

This work has therefore provided evidence, together with the studies from Parker *et al.* (2014), that Maf1 functions in the cytoplasm to glycosylate target flagellins before chaperone binding and export (Fig. 5.14). As Maf1 is a cytoplasmic enzyme, it may be of use in the future for the glycosylation of therapeutic proteins, or may itself be a useful antimicrobial target; however, further work is required to fully understand how these enzymes identify and glycosylate their target proteins, and their precise mechanism of action. This work (and the work from Chapter 4) has raised many questions as to the site on the flagellins for Maf1 recognition and docking. The interaction studies carried out here, together with the D2/D3 domain swapping studies, suggest this site to reside upstream of the D2/D3 domain. Maf1 binding investigations to N-terminal flagellin regions, along with site-directed mutational studies of the flagellins, would

allow the region of Maf1 docking to be further explored. In addition, structural studies with the Maf proteins would reveal the protein domains present, perhaps pockets for pseudaminic

acid binding, and would provide information that could be used to create a model of Maf1 mechanism of action. Moreover, putative thiamine pyrophosphokinase (TPK) domains have been previously found to be highly conserved amongst the Maf proteins, which suggests that this domain has an important role (Parker *et al.*, 2012). TPK domains catalyse the transfer of phosphate groups from a nucleoside triphosphate (ie. ATP) to the thiamine hydroxyl group, producing thiamine pyrophosphate, and it would be interesting to explore the specific role of this domain in Maf1 also.

# Chapter 6: General Discussion

## 6.1 – General discussion of results

In this thesis, the pathway and role of flagellin glycosylation was explored in *Aeromonas caviae* Sch3, a clinically relevant aeromonad that requires pseudaminic acid for flagellation and virulence, and possesses the simplest set of genes currently known for glycosylation and polar flagellum assembly.

In Chapter 3, the existence of a potential flagellin deglycosylation pathway was investigated due to a homologue of a putative flagellin deglycosylase (HP0518) from *H. pylori* (Asakura *et al.,* 2010), being identified in the *A. caviae* Sch3 genome (AHA0618) (Lowry *et al.*, 2014b). Although an *A. caviae AHA0618* mutant was found to be hypermotile compared to the wild type strain [similarly to the findings in Asakura *et al.* (2010)], the mutation had no effect on flagellin glycosylation. Therefore the altered behaviour exhibited here was not due to flagellin glycosylation levels, which have been shown to have an effect on bacterial behaviour previously (with studies in *Campylobacter*) (Howard *et al.*, 2009; van Alphen *et al.*, 2008). An alternative function for HP0518 was suggested by Sycuro *et al.* (2013), as an L,D-carboxypeptidase involved in peptidoglycan processing at the cell wall. The mutant also displayed a straight-rod morphology compared to the helical wild type (Sycuro *et al.*, 2013). Bioinformatic analysis of AHA0618 revealed this protein to be in the YkuD superfamily of proteins, a family of L,D-transpeptidases involved in peptidoglycan processing, that contain a characteristic catalytic tetrad of amino acids in their active sites (Bielnicki *et al.*, 2006), of which were present in both AHA0618 and HP0518. When the cell shape of an *A. caviae AHA0618* mutant was analysed here, it was concluded that the mutant is significantly shorter than the wild type strain; a phenomenon that could be complemented by either *AHA0618* or *HP0518* expressed in the mutant, demonstrating that HP0518 is having a similar effect to AHA0618 in *A. caviae*. Although preliminary studies did not identify any differences between the muropeptide profiles of the wild type and *AHA0618* mutant strains, these data still suggest that AHA0618 is not involved in a flagellin deglycosylation pathway, but instead it is the cell shape which is responsible for the differences in bacterial behaviour observed between the strains analysed. The results obtained demonstrate that even the subtlest changes in cellular morphology can affect bacterial behaviour, an observation which has been documented from the study of a number of other bacterial cell-wall enzyme mutants also. For example, in the Gram-positive bacterium *Bacillus cereus*, mutants of the cell wall peptidase, CwpFM, were

found to be larger than the wild type, and as a result were less motile (Tran *et al.*, 2010). Likewise, when the carboxypeptidase, Pgp2, was mutated in *C. jejuni*, the straight rod cellular morphology that resulted affected bacterial motility and biofilm formation (Frirdich *et al.*, 2014).

Although no flagellin deglycosylation pathway has been identified in *A. caviae* to alter flagellin glycosylation levels, it has been suggested that *Campylobacter* strains may regulate the expression of their Maf proteins in order to do this. The presence of different sugars have been shown to provide *C. jejuni* with diverse abilities, such as the presence of legionaminic acid on the polar flagellum enables this pathogen to efficiently colonise chickens compared to when this sugar is absent (Howard *et al.*, 2009). Therefore, it is intriguing as to whether alternative mechanisms of tailoring bacterial flagellin glycosylation are present in bacteria that solely modify their flagellins with one sugar, and do not possesses a vast array of Maf proteins, such as in *H. pylori* and *A. caviae* (Parker *et al.*, 2012; Schirm *et al.*, 2003) (Tabei *et al.,* 2009).

Chapter 4 of this work has unequivocally identified for the first time, using mass spectrometric methods, sites of glycosylation at the very start of the D2/D3 domain of the flagellin, FlaB, from *A. caviae* Sch3. It was determined that one or two sugars are able to decorate the FlaB peptide [146-173], and in addition, these sites of glycosylation can vary from peptide to peptide. However, two sites in particular (serine 159 and 161) were found to be predominantly co-modified in the wild type strain. These results show that although no consensus sequence for *O*-linked protein glycosylation has been identified, there is partial selectivity to the Maf1-dependent flagellin glycosylation process. This has also been observed in *Campylobacter* and *Helicobacter* where the sites of glycosylation identified were found to be 'usually' glycosylated (Schirm *et al.*, 2003; Thibault *et al.*, 2001). Furthermore, this work also agrees with the studies in these bacteria*,* that glycosylation may occur in regions of local hydrophobicity within the D2/D3 domain of the flagellin (Schirm *et al.*, 2003; Thibault *et al.*, 2001). It was particularly observed in *C. jejuni* that the sites of glycosylation are more commonly preceded by runs of hydrophobic amino acids. All of the serine residues present on the *A. caviae* FlaB [146-173] peptide are surrounded by hydrophobic amino acids, the mutation of which had a detrimental effect on *A. caviae* motility, demonstrating that these residues may indeed be the preferred targets on Maf1. Additionally, when all of the serine residues on this peptide were mutated at the same time, the mutant flagellin was unable to restore the motility of an *A. caviae flaAB* mutant. This flagellin was also smaller than the wild type flagellin, demonstrating that the glycosylation of this peptide is essential and cannot be made up for by the glycosylation of

alternative residues within the protein. The reason for the impaired motility phenotypes observed here are not yet clear. It is possible that impaired motility may result from the less efficient recognition of the flagellins by Maf1, which may have arisen from these mutations, or through the flagella having a different overall form when polymerised from the mutant monomers. In contrast, the mutation of threonine 155 on this same peptide, which is not preceded by hydrophobic amino acids, did not have a detrimental effect on *A. caviae* motility. Furthermore, the glycosylation status and level of this flagellin found in the *A. caviae* whole-cell was comparable to that of wild type FlaB.

As hydrophobicity appears to play a role in Maf1 flagellin glycosylation, the hydrophobic amino acids leucine 160 and isoleucine 168 were targeted for further mutagenesis studies. The individual mutation of these residues had a severely detrimental effect on *A. caviae* motility. Again it is possible that these mutated regions impede Maf1's ability to dock to the flagellin, perhaps through decreasing the hydrophobicity of this region; although flagellins were still identified to be glycosylated. The effect of these mutations on flagellin glycosylation could not be explored here as all attempts to pellet any flagella formed from these mutant flagellins failed, suggesting that a flagellar filament cannot form, or any filaments that do form are fragile and break off before full length flagella are polymerised.

Although it has been suggested that flagellin glycosylation may be coupled to export (Logan, 2006), the interaction studies carried out in chapter 5, along with the recent work by Parker *et al.* (2014), have contributed towards determining that *A. caviae* Sch3 flagellin glycosylation by Maf1 is likely to occur in the cytoplasm, before chaperone binding and export (Chapter 5, figure 5.14). The lack of interactions observed between the flagellins and the flagellin-specific chaperone, Maf1, is likely to be due to the conclusions from Parker *et al.* (2014), that FlaJ has less affinity for the unglycosylated flagellin, which would therefore promote the export of the modified flagellin rather than the unmodified version. In addition, the 'handover' experiment carried out by Parker *et al.* (2014), suggests that Maf1 and FlaJ could come into contact within the cell to pass the glycosylated flagellin onto its chaperone, to prevent the premature folding and polymerisation of the flagellins within the cytoplasm. This may be why inconsistent interactions were observed here between Maf1 and FlaJ, further demonstrating that FlaJ is likely to take the flagellin from the glycosyltransferase after glycosylation has occurred (Parker *et al.*, 2014). Furthermore, as FlaJ is able to take the flagellin from Maf1, it is likely that these proteins are binding to different parts of the flagellin. The chaperone binding domain is essential for FlaJ binding and flagellin export, but not for glycosylation to occur (Parker *et al.*,

2014), which therefore suggests another part of the protein is required for Maf1 docking (possibly the N-terminal region). These studies agree with work carried out in *C. jejuni* 81-176, demonstrating that mutant strains which are unable to produce basal body and hook proteins, and are therefore deficient in a flagellar export system, are still able to produce glycosylated flagellins, suggesting that glycosylation occurs before export (Ewing *et al.*, 2009). Cytoplasmic Maf-dependent flagellin glycosylation is therefore likely to be occurring in other O-linked glycosylation pathways; although, how multiple Maf proteins fit into this pathway, for example in the case of *Campylobacter* species where up to seven Maf proteins can be present (Karlyshev *et al.*, 2002; van Alphen *et al.*, 2008), has not yet been investigated.

Furthermore, the D2/D3 domain swapping investigations carried out here have called into question the specificity of the Maf proteins and the location on the flagellin to which these enzymes dock. Maf1 from *A. caviae* Sch3 was only found to recognise and glycosylate flagellin from *A. caviae* Ae398, of the *Aeromonas* flagellins investigated here, which may show that these enzymes are very specific for their target proteins; however, the D2/D3 domain of the *A. caviae* Ae398 FlaA, of which is the glycosylated region, only shares 58% identity with the *A. caviae* Sch3 FlaA. This therefore further suggests that the initial recognition of the flagellins may not involve the D2/D3 domain of the flagellin. Through the interaction studies carried out in Chapter 5, it was shown that Maf1 is likely to interact with the N-terminal region of the flagellin, and so it may be this region that is important for Maf1 flagellin recognition and docking. The N-terminus of *A. caviae* Sch3 FlaA was found to display the highest identity to the N-terminal region of FlaA from *A. caviae* Ae398, at 98%, of the flagellins examined, further demonstrating that this N-terminal region may be required for Maf1 docking.

On the other hand, Maf1 from *H. pylori* 26695*,* appeared to show some promiscuity and was able to modify the much smaller flagellins of *A. caviae* Sch3 (although inconsistently). Although *H. pylori* possesses two *maf* homologues in its genome, it only modifies its polar flagella with pseudaminic acid (Josenhans *et al.*, 2002; Schirm *et al.*, 2003), similarly to *A. caviae*, which may be why we are seeing some cross over between these systems, even though flagellins from these bacteria only display 37% identity. Therefore, there is much still to be understood about the mechanism of action of these novel glycosyltransferases, that have a clear role in bacterial virulence.

## 6.2 – Future perspectives

### 6.2.1 – Short-term perspectives

In the short-term, there are a number of investigations that can be carried out to help answer some of the questions that have arisen from this work.

With regards to Chapter 3, further muropeptide analysis could be carried out with the peptidoglycan from *A. caviae* Sch3 and the *AHA0618* mutant, in order to investigate any subtle differences in the muropeptide profiles of these strains which may arise from the lack of AHA0618 in the mutant. Furthermore, the peptidoglycan from the complementation strains (the mutant containing either *AHA0618* or *HP0518* on an inducible vector) could also be analysed, as overexpression of these proteins in the mutant may have a more pronounced effect on the peptidoglycan, allowing any differences to be more clearly observed.

To continue investigating the effect of the sites of glycosylation (identified in Chapter 4) on *A. caviae* Sch3 motility and flagellar assembly, transmission electron microscopy studies could be carried out with the *A. caviae* strains expressing the site-directed flagellin mutants created. Flagella shape can be altered due to a variety of factors, such as: the flagellin amino acid sequence, temperature and pH, which can change the wave form of the filament and alter how bacteria swim (Turner *et al.,* 2000). The diminished motility visualised may therefore result from the mutant flagellins polymerising to form different shaped flagella than the wild type flagellins. Additionally, studies in *P. syringae* have demonstrated that the unglycosylated form of their flagella are less stable than the glycosylated versions (Taguchi *et al.*, 2009), and studies on the sites of flagellin glycosylation in *C. jejuni* have shown that the mutation of specific sites lead to the production of truncated filaments, suggesting flagellar fragility (Ewing *et al.*, 2009). Therefore mutation of the glycosylation sites in *A. caviae* may also be producing more fragile flagella, resulting in decreased motility, which could also be explored by microscopy studies. To add to this, lower levels of mutated flagellins (FlaB with the following mutations: S159/161A; S167/169A; S159/161/167/169A; L160A; I168A) were observed in the *A. caviae* whole-cell, therefore half-life experiments could also be carried out to determine whether these flagellins are more unstable than the wild type, or whether they are being readily targeted for degradation by the bacterium, perhaps to prevent a build-up of glycosylated flagellins that are able to self-polymerise, in the cytoplasm of the cell, which could occur if the mutant flagellins are not exported and incorporated into a filament as efficiently.

In addition to exploring the role of these glycosylation sites on flagellar function, other sites of modification can also be investigated now this work has uncovered a reliable method of mass spectrometry for the analysis of *A. caviae* flagellin glycosylation. However, trypsin digestion of the flagellins resulted in the formation of large tryptic peptides from the D2/D3 domain, making it difficult for the sites of glycosylation to be analysed in this work. Therefore site-directed mutagenesis of the flagellins, whereby lysine residues are engineered into the flagellins, may allow these proteins to be digested into more manageable pieces by trypsin for mass spectrometry analysis, allowing the sites of glycosylation on FlaA to also be examined.

Both Chapters 4 and 5 have raised questions about the site of Maf1 docking to the flagellin and how partial selectivity observed in the process of Maf-dependent flagellin glycosylation is achieved without the existence of a specific consensus sequence within the protein, in contrast to N-linked protein glycosylation. From Chapter 4 it would now be interesting to look at whether the flagellin regions that underwent site-directed mutagenesis are important for Maf1 docking, as reduced ability of Maf1 to dock may also result in impaired motility through the slower modification of the flagellins, and therefore targeting to the cell surface for incorporation into the flagellar filament. This could be achieved through affinity binding studies of these mutant flagellins to Maf1, via a technique such as isothermal titration calorimetry (ITC), where interactions between proteins, or even peptides, can be quantified. Or as the mutations may alter the peptide hydrophobicity, and it is the local regions of hydrophobicity that Maf1 is targeting, then it is possible that this may be affecting the ability of Maf1 to scan and select residues in the D2/D3 domain to modify. Furthermore, the interaction studies from Chapter 5, along with the D2/D3 domain swapping studies, and the work from Parker *et al.* (2014), suggest that a region for Maf1 recognition of the flagellin may reside within the N-terminal region. Further protein interaction studies, along with binding affinity studies, could be carried out with Maf1 and different N-terminal regions of the *A. caviae* flagellins, to assess whether there is a location upstream of the D2/D3 domain essential for Maf1 docking.

Additionally, the Maf proteins contain a putative thiamine pyrophosphokinase (TPK) domain, likely to have an important role in Maf function due to their conservation amongst these proteins (Parker *et al.*, 2012). This domain generally functions in nucleotide biosynthesis, and catalyses the transfer of phosphate from ATP to thiamine (producing thiamine pyrophosphate). As pseudaminic acid is nucleotide activated (with the addition of CMP) before it can be transferred onto the flagellins, this domain may function in binding to the nucleotide

activated sugar. Investigations into the ability of Maf1, and a variety of Maf1 site-directed mutants (mutated within this TPK domain), to interact with CMP-activated pseudaminic acid would give an indication as to whether this domain is operating as pseudaminic acid binding pocket. This could also be assessed by ITC as it allows the interactions between small molecules and proteins to be quantified.

### 6.2.2 – Long-term perspectives

The importance of bacterial flagellin glycosylation has been determined in a number of bacteria, with many showing specific sites to be essential for motility, virulence and particular bacterial behaviours (discussed throughout this work). However, the precise role of flagellar modification still remains unclear and further work is required to fully uncover why this modification has evolved. It is possible that this modification has alternative roles in different bacteria. Investigations, so far, have largely identified Gram-negative bacteria with polar flagella, such as *Aeromonas, Campylobacter* and *Helicobacter* species, to require this modification for flagellation and virulence. This therefore may show that this modification aids the ability of these microorganisms to colonise their specific gastrointestinal niche. The hydrophilic properties of the nonulosonic acids may allow these bacteria to produce favourable interactions with their environments and compete with other enteric pathogens, such as *E. coli* and *Salmonella* that possess peritrichous flagella. It is tempting to speculate that this modification may have evolved to be essential for flagellation as without it, these microorganisms would not be able to compete for a place in this niche. However, why *H. pylori* requires flagellin glycosylation, when they possess sheathed flagella, remains a mystery, as the sugars are unlikely to aid interactions with the external environment. However, it may have more of a structural role, by providing further stability to this appendage in the harsh environment of the stomach, perhaps by also interacting with the sheath for extra reinforcement. As previously mentioned glycosylation has also been reported to stabilise the *P. syringae* flagellum, where flagellin glycosylation is not essential for flagellation, but the enhanced stability provided by this modification enables flagellins to evade the host immune response (Taguchi *et al.*, 2009). This modification also appears to augment the ability of this microorganism to colonise its plant host (Taguchi *et al.*, 2006). In contrast, reports on *P. aeruginosa* flagellin glycosylation have indicated that this modification enhances interactions of the flagellins with the immune system, which may allow respiratory infections to progress (Verma *et al.*, 2005). In addition, the modification of *P. aeruginosa* flagellins have also been shown to aid bacterial colonisation (Arora *et al.*, 2005).

Recently it was established that the receptor binding protein (Gp047) on the *Campylobacter* lytic phage (NCTC 12673) is able to specifically bind to acetamidino-modified pseudaminic acid linked to *C. jejuni* flagellins, and that binding is towards the C-terminus of the flagellins (Javed *et al.*, 2015). It is therefore possible with regards to *A. caviae* that varying the sites of flagellin glycosylation may provide resistance to predation by bacteriophage. This theory, however, has not yet been investigated in *A. caviae* but would be an exciting prospect for future studies.

In recent years there have also been increasing reports of flagellin glycosylation in Gram-positive bacteria, and also in some non-pathogenic species, such as *Shewanella* (Bubendorfer *et al.*, 2013; Sun *et al*., 2013). It is therefore clear that the modification of this appendage with sugars is extremely widespread, and therefore very important for the ability of bacteria to thrive in a variety of environments. Therefore, glycosylation may have a specific role to individual bacteria, allowing them to thrive in their specific niche. With regards to *A. caviae*, once all of the sites of flagellin glycosylation have been deduced, further mutational studies with the flagellins, such as analysis of: the flagella formed (if any flagella are formed at all as a result from the mutations), the levels of *A. caviae* motility, and their ability to adhere to mammalian cell lines, will allow the role of flagellin glycosylation in *A. caviae* to be fully explored.

As glycosylation of flagellins, in particular with nonulosonic acids, is essential for the formation of flagella in a number of bacteria, this pathway has the potential to be a therapeutic target. Therefore, the structural and biochemical characterisation of the Maf proteins would allow the mechanism of action of these novel proteins to be investigated. This would allow the study of how Maf1 binds to pseudaminic acid, and the region of the protein responsible for this essential step in flagellin glycosylation. Pseudaminic acid structural analogues could be designed to compete with pseudaminic acid for the specific site of sugar binding on the Maf proteins, preventing flagellin modification from taking place, and therefore preventing bacterial flagellation. This may not only be a useful antimicrobial target for Gram-negative pathogens, but also for the clinically relevant Gram-positive species, such as *C. botulinum,* where the modification of their flagellins, in particular with nonulosonic acids, is likely to be involved in their ability to colonise humans (Twine *et al.*, 2008).

Glycosylation is also useful for increasing the stability of pharmaceutical proteins, such as antibodies (Sola and Griebenow, 2009). Therefore, in addition, characterisation of the Maf proteins could allow these novel enzymes to be used for the glycosylation of therapeutic proteins in the future. Currently, the bacterial N-linked glycosylation process is being

manipulated for increasing the stability of therapeutic proteins; however, this requires targeting the protein of interest to the periplasm before glycosylation can take place. Therefore, these cytoplasmic enzymes may be useful when more is known about how they recognise their target proteins and what in the flagellin peptide sequences allows the Maf proteins to select their glycosylation sites.

The work carried out in this thesis has therefore provided a further understanding of the O-linked flagellin glycosylation pathway, essential for the virulence of a number of pathogenic bacteria. Evidence has been provided here, and by Parker *et al.* (2014), that the Maf proteins are cytoplasmic enzymes and glycosylate the flagellins before chaperone binding, and subsequent export. In addition, this work has demonstrated that Maf1 shows partial selectivity for both its target proteins and the sites it modifies on these proteins, despite the lack of consensus sequence present. These studies have paved the way for the continued research of O-linked glycosylation pathways, in particular by raising questions about the mechanism of action of the glycosyltransferases involved, such as the Maf proteins, which show the exciting prospect of being novel therapeutic targets, or being manipulated for industrial and pharmaceutical purposes, in the future.

# Chapter 7 - References


AAS, F. E., VIK, A., VEDDE, J., KOOMEY, M. & EGGE-JACOBSEN, W. 2007. Neisseria gonorrhoeae O-linked pilin glycosylation: functional analyses define both the biosynthetic pathway and glycan structure. *Molecular Microbiology,* 65**,** 607-624.

ABRAHAMIAN, F. M. & GOLDSTEIN, E. J. C. 2011. Microbiology of Animal Bite Wound Infections. *Clinical Microbiology Reviews,* 24**,** 231-246.

ABRUSCI, P., VERGARA-IRIGARAY, M., JOHNSON, S., BEEBY, M. D., HENDRIXSON, D. R., ROVERSI, P., FRIEDE, M. E., DEANE, J. E., JENSEN, G. J., TANG, C. M. & LEA, S. M. 2013. Architecture of the major component of the type III secretion system export apparatus. *Nature Structural & Molecular Biology,* 20**,** 99-U126.

ALAIMO, C., CATREIN, I., MORF, L., MAROLDA, C. L., CALLEWAERT, N., VALVANO, M. A., FELDMAN, M. F. & AEBI, M. 2006. Two distinct but interchangeable mechanisms for flipping of lipid-linked oligosaccharides. *Embo Journal,* 25**,** 967-976.

ALEMKA, A., NOTHAFT, H., ZHENG, J. & SZYMANSKI, C. M. 2013. N-Glycosylation of Campylobacter jejuni Surface Proteins Promotes Bacterial Fitness. *Infection and Immunity,* 81**,** 1674-1682.

ALMAGRO-MORENO, S. & BOYD, E. F. 2010. Bacterial catabolism of nonulosonic (sialic) acid and fitness in the gut. *Gut microbes,* 1**,** 45-50.

ALTARRIBA, M., MERINO, S., GAVíN, R., CANALS, R. O., RABAAN, A., SHAW, J. G. & TOMÁS, J. M. 2003. A polar flagella operon (flg) of Aeromonas hydrophila contains genes required for lateral flagella expression. *Microbial Pathogenesis,* 34**,** 249-259.

ANDERSEN-NISSEN, E., SMITH, K. D., STROBE, K. L., BARRETT, S. L. R., COOKSON, B. T., LOGAN, S. M. & ADEREM, A. 2005. Evasion of Toll-like receptor 5 by flagellated bacteria. *Proceedings of the National Academy of Sciences of the United States of America,* 102**,** 9247-9252.

ARORA, S. K., NEELY, A. N., BLAIR, B., LORY, S. & RAMPHAL, R. 2005. Role of Motility and Flagellin Glycosylation in the Pathogenesis of Pseudomonas aeruginosa Burn Wound Infections. *Infection and Immunity,* 73**,** 4395-4398.

ASAKURA, H., CHURIN, Y., BAUER, B., BOETTCHER, J. P., BARTFELD, S., HASHII, N., KAWASAKI, N., MOLLENKOPF, H. J., JUNGBLUT, P. R., BRINKMANN, V. & MEYER, T. F. 2010. *Helicobacter pylori* HP0518 affects flagellin glycosylation to alter bacterial motility. *Molecular Microbiology,* 78**,** 1130-1144.

AUVRAY, F., THOMAS, J., FRASER, G. M. & HUGHES, C. 2001. Flagellin polymerisation control by a cytosolic export chaperone. *Journal of Molecular Biology,* 308**,** 221-229.

BAKER, J. L., CELIK, E. & DELISA, M. P. 2013. Expanding the glycoengineering toolbox: the rise of bacterial N-linked protein glycosylation. *Trends in Biotechnology,* 31**,** 49-59.

BAKER, M. D., WOLANIN, P. M. & STOCK, J. B. 2006. Signal transduction in bacterial chemotaxis. *Bioessays,* 28**,** 9-22.

BARILLO, D. J., MCMANUS, A. T., CIOFFI, W. G., MCMANUS, W. F., KIM, S. H. & PRUITT, B. A. 1996. Aeromonas bacteraemia in burn patients. *Burns,* 22**,** 48-52.

BEATSON, S. A., DE LUNA, M. D. G., BACHMANN, N. L., ALIKHAN, N.-F., HANKS, K. R., SULLIVAN, M. J., WEE, B. A., FREITAS-ALMEIDA, A. C., DOS SANTOS, P. A., DE MELO, J. T. B., SQUIRE, D. J. P., CUNNINGHAM, A. F., FITZGERALD, J. R. & HENDERSON, I. R. 2011. Genome Sequence of the Emerging Pathogen Aeromonas caviae. *Journal of Bacteriology,* 193**,** 1286-1287.

BEAZ-HIDALGO, R., ALPERI, A., BUJAN, N., ROMALDE, J. L. & JOSE FIGUERAS, M. 2010. Comparison of phenotypical and genetic identification of Aeromonas strains isolated from diseased fish. *Systematic and Applied Microbiology,* 33**,** 149-153.

BEAZ-HIDALGO, R. & FIGUERAS, M. J. 2013. Aeromonas spp. whole genomes and virulence factors implicated in fish disease. *Journal of Fish Diseases,* 36**,** 371-388.

BIELNICKI, J., DEVEDJIEV, Y., DEREWENDA, U., DAUTER, Z., JOACHIMIAK, A. & DEREWENDA, Z. S. 2006. *B. subtilis* ykuD protein at 2.0 Å resolution: Insights into the structure and function of a novel, ubiquitous family of bacterial enzymes. *Proteins: Structure, Function, and Bioinformatics,* 62**,** 144-151.

BLAKE, D. J., WEIR, A., NEWEY, S. E. & DAVIES, K. E. 2002. Function and genetics of dystrophin and dystrophin-related proteins in muscle. *Physiological Reviews,* 82**,** 291-329.

BOMAR, L., MALTZ, M., COLSTON, S. & GRAF, J. 2011. Directed Culturing of Microorganisms Using Metatranscriptomics. *mBio,* 2.

BOYD, J. M., DACANAY, A., KNICKLE, L. C., TOUHAMI, A., BROWN, L. L., JERICHO, M. H., JOHNSON, S. C. & REITH, M. 2008. Contribution of type IV pili to the virulence of Aeromonas salmonicida subsp salmonicida in Atlantic salmon (Salmo salar l.). *Infection and Immunity,* 76**,** 1445-1455.

BUBENDORFER, S., ISHIHARA, M., DOHLICH, K., HEISS, C., VOGEL, J., SASTRE, F., PANICO, M., HITCHEN, P., DELL, A., AZADI, P. & THORMANN, K. M. 2013. Analyzing the Modification of the <italic>Shewanella oneidensis</italic> MR-1 Flagellar Filament. *Plos One,* 8**,** e73444.

CANALS, R., ALTARRIBA, M., VILCHES, S., HORSBURGH, G., SHAW, J. G., TOMAS, J. M. & MERINO, S. 2006a. Analysis of the lateral flagellar gene system of Aeromonas hydrophila AH-3. *Journal of Bacteriology,* 188**,** 852-862.

CANALS, R., JIMENEZ, N., VILCHES, S., REGUE, M., MERINO, S. & TOMAS, J. M. 2006b. The UDP N-acetylgalactosamine 4-epimerase gene is essential for mesophilic Aeromonas hydrophila serotype O34 virulence. *Infection and Immunity,* 74**,** 537-548.

CANALS, R., RAMIREZ, S., VILCHES, S., HORSBURGH, G., SHAW, J. G., TOMAS, J. A. & MERINO, S. 2006c. Polar flagellum biogenesis in Aeromonas hydrophila. *Journal of Bacteriology,* 188**,** 542-555.

CANALS, R., VILCHES, S., WILHELMS, M., SHAW, J. G., MERINO, S. & TOMAS, J. M. 2007. Non-structural flagella genes affecting both polar and lateral flagella-mediated motility in *Aeromonas hydrophila*. *Microbiology-Sgm,* 153**,** 1165-1175.

CERQUEIRA, G. M., MCBRIDE, A. J. A., PICARDEAU, M., RIBEIRO, S. G., MOREIRA, A. N., MOREL, V., REIS, M. G., KO, A. I. & DELLAGOSTIN, O. A. 2009. Distribution of the leptospiral immunoglobulin-like (lig) genes in pathogenic Leptospira species and application of ligB to typing leptospiral isolates. *Journal of Medical Microbiology,* 58**,** 1173-1181.

CHAMPASA, K., LONGWELL, S. A., ELDRIDGE, A. M., STEMMLER, E. A. & DUBE, D. H. 2013. Targeted Identification of Glycosylated Proteins in the Gastric Pathogen Helicobacter pylori (Hp). *Molecular & Cellular Proteomics,* 12**,** 2568-2586.

CHEN, S., BEEBY, M., MURPHY, G. E., LEADBETTER, J. R., HENDRIXSON, D. R., BRIEGEL, A., LI, Z., SHI, J., TOCHEVA, E. I., MUELLER, A., DOBRO, M. J. & JENSEN, G. J. 2011. Structural diversity of bacterial flagellar motors. *Embo Journal,* 30**,** 2972-2981.

CHEVANCE, F. F. V., TAKAHASHI, N., KARLINSEY, J. E., GNERER, J., HIRANO, T., SAMUDRALA, R., AIZAWA, S.-I. & HUGHES, K. T. 2007. The mechanism of outer membrane penetration by the eubacterial flagellum and implications for spirochete evolution. *Genes & Development,* 21**,** 2326-2335.

CHOI, K.-J., GRASS, S., PAEK, S., ST. GEME, J. W., III & YEO, H.-J. 2010. The Actinobacillus pleuropneumoniae HMW1C-Like Glycosyltransferase Mediates N-Linked Glycosylation of the Haemophilus influenzae HMW1 Adhesin. *Plos One,* 5.

CHOY, H. A., KELLEY, M. M., CHEN, T. L., MOLLER, A. K., MATSUNAGA, J. & HAAKE, D. A. 2007. Physiological osmotic induction of Leptospira interrogans adhesion: LigA and LigB bind extracellular matrix proteins and fibrinogen. *Infection and Immunity,* 75**,** 2441-2450.

DACANAY, A., KNICKLE, L., SOLANKY, K. S., BOYD, J. M., WALTER, J. A., BROWN, L. L., JOHNSON, S. C. & REITH, M. 2006. Contribution of the type III secretion system (TTSS) to virulence of Aeromonas salmonicida subsp salmonicida. *Microbiology-Sgm,* 152**,** 1847-1856.

DOMON, B. & AEBERSOLD, R. 2006. Review - Mass spectrometry and protein analysis. *Science,* 312**,** 212-217.

EASOW, J. M. & TULADHAR, R. 2007. Aeromonas hydrophila wound infection following a tiger bite in Nepal. *Southeast Asian Journal of Tropical Medicine and Public Health,* 38**,** 867-870.

ERHARDT, M., HIRANO, T., SU, Y., PAUL, K., WEE, D. H., MIZUNO, S., AIZAWA, S.-I. & HUGHES, K. T. 2010. The role of the FliK molecular ruler in hook-length control in Salmonella enterica. *Molecular Microbiology,* 75**,** 1272-1284.

EVANS, L. D. B., HUGHES, C. & FRASER, G. M. 2014. Building a flagellum outside the bacterial cell. *Trends in Microbiology*.

EVANS, L. D. B., POULTER, S., TERENTJEV, E. M., HUGHES, C. & FRASER, G. M. 2013. A chain mechanism for flagellum growth. *Nature,* 504**,** 287-+.

EWING, C. P., ANDREISHCHEVA, E. & GUERRY, P. 2009. Functional Characterization of Flagellin Glycosylation in Campylobacter jejuni 81-176. *Journal of Bacteriology,* 191**,** 7086-7093.

FAULDS-PAIN, A., TWINE, S. M., VINOGRADOV, E., STRONG, P. C. R., DELL, A., BUCKLEY, A. M., DOUCE, G. R., VALIENTE, E., LOGAN, S. M. & WREN, B. W. 2014. The post-translational modification of the Clostridium difficile flagellin affects motility, cell surface properties and virulence. *Molecular Microbiology,* 94**,** 272-289.

FERRIS, H. U., FURUKAWA, Y., MINAMINO, T., KROETZ, M. B., KIHARA, M., NAMBA, K. & MACNAB, R. M. 2005. FlhB regulates ordered export of flagellar components via autocleavage mechanism. *Journal of Biological Chemistry,* 280**,** 41236-41242.

FERRIS, H. U. & MINAMINO, T. 2006. Flipping the switch: bringing order to flagellar assembly. *Trends in Microbiology,* 14**,** 519-526.

FRASER, G. M., GONZALEZ-PEDRAJO, B., TAME, J. R. H. & MACNAB, R. M. 2003a. Interactions of FliJ with the Salmonella type III flagellar export apparatus. *Journal of Bacteriology,* 185**,** 5546-5554.

FRASER, G. M., HIRANO, T., FERRIS, H. U., DEVGAN, L. L., KIHARA, M. & MACNAB, R. M. 2003b. Substrate specificity of type III flagellar protein export in Salmonella is controlled by subdomain interactions in FlhB. *Molecular Microbiology,* 48**,** 1043-1057.

FRIRDICH, E., VERMEULEN, J., BIBOY, J., SOARES, F., TAVEIRNE, M. E., JOHNSON, J. G., DIRITA, V. J., GIRARDIN, S. E., VOLLMER, W. & GAYNOR, E. C. 2014. Peptidoglycan LD-carboxypeptidase Pgp2 influences *Campylobacter jejuni* helical cell shape and pathogenic properties and provides the substrate for the DL-carboxypeptidase Pgp1. *The Journal of biological chemistry,* 289**,** 8007-18.

FUCHS, T. M., BRANDT, K., STARKE, M. & RATTEI, T. 2011. Shotgun sequencing of *Yersinia enterocolitica* strain W22703 (biotype 2, serotype O:9): genomic evidence for oscillation between invertebrates and mammals. *Bmc Genomics,* 12.

GAVIN, R., RABAAN, A. A., MERINO, S., TOMAS, J. M., GRYLLOS, I. & SHAW, J. G. 2002. Lateral flagella of Aeromonas species are essential for epithelial cell adherence and biofilm formation. *Molecular Microbiology,* 43**,** 383-397.

GEIS, G., SUERBAUM, S., FORSTHOFF, B., LEYING, H. & OPFERKUCH, W. 1993. ULTRASTRUCTURE AND BIOCHEMICAL-STUDIES OF THE FLAGELLAR SHEATH OF HELICOBACTER-PYLORI. *Journal of Medical Microbiology,* 38**,** 371-377.

GEWIRTZ, A. T., YU, Y., KRISHNA, U. S., ISRAEL, D. A., LYONS, S. L. & PEEK, R. M. 2004. Helicobacter pylori Flagellin Evades Toll-Like Receptor 5-Mediated Innate Immunity. *Journal of Infectious Diseases,* 189**,** 1914-1920.

GIRON, J. A., TORRES, A. G., FREER, E. & KAPER, J. B. 2002. The flagella of enteropathogenic *Escherichia coli* mediate adherence to epithelial cells. *Molecular Microbiology,* 44**,** 361-379.

GLUCK, F., HOOGLAND, C., ANTINORI, P., ROBIN, X., NIKITIN, F., ZUFFEREY, A., PASQUARELLO, C., FÉTAUD, V., DAYON, L., MÜLLER, M., LISACEK, F., GEISER, L., HOCHSTRASSER, D., SANCHEZ, J.-C. & SCHERL, A. 2013. EasyProt — An easy-to-use graphical platform for proteomics data analysis. *Journal of Proteomics,* 79**,** 146-160.

GOON, S., KELLY, J. F., LOGAN, S. M., EWING, C. P. & GUERRY, P. 2003. Pseudaminic acid, the major modification on *Campylobacter flagellin*, is synthesized via the Cj1293 gene. *Molecular Microbiology,* 50**,** 659-671.

GRASS, S., LICHTI, C. F., TOWNSEND, R. R., GROSS, J. & ST GEME, J. W., III 2010. The Haemophilus influenzae HMW1C Protein Is a Glycosyltransferase That Transfers Hexose Residues to Asparagine Sites in the HMW1 Adhesin. *Plos Pathogens,* 6.

GRYLLOS, I., SHAW, I. G., GAVIN, R., MERINO, S. & TOMAS, J. M. 2001. Role of flm locus in mesophilic Aeromonas species adherence. *Infection and Immunity,* 69**,** 65-74.

GUARDPETTER, J., LAKSHMI, B., CARLSON, R. & INGRAM, K. 1995. CHARACTERIZATION OF LIPOPOLYSACCHARIDE HETEROGENEITY IN SALMONELLA-ENTERITIDIS BY AN IMPROVED GEL-ELECTROPHORESIS METHOD. *Applied and Environmental Microbiology,* 61**,** 2845-2851.

GUERRA, I. M. F., FADANELLI, R., FIGUEIRO, M., SCHREINER, F., DELAMARE, A. P. L., WOLLHEIM, C., COSTA, S. O. P. & ECHEVERRIGARAY, S. 2007. Aeromonas associated diarrhoeal disease in south Brazil: Prevalence, virulence factors and antimicrobial resistance. *Brazilian Journal of Microbiology,* 38**,** 638-643.

GUERRY, P. 2007. *The role of flagella in Campylobacter virulence*.

HADI, N., YANG, Q., BARNETT, T. C., TABEI, S. M. B., KIROV, S. M. & SHAW, J. G. 2012. Bundle-Forming Pilus Locus of Aeromonas veronii bv. Sobria. *Infection and Immunity,* 80**,** 1351-1360.

HAIKO, J. & WESTERLUND-WIKSTROM, B. 2013. The role of the bacterial flagellum in adhesion and virulence. *Biology,* 2**,** 1242-67.

HAN, H. J., KIM, D. Y., KIM, W. S., KIM, C. S., JUNG, S. J., OH, M. J. & KIM, D. H. 2011. Atypical Aeromonas salmonicida infection in the black rockfish, Sebastes schlegeli Hilgendorf, in Korea. *Journal of Fish Diseases,* 34**,** 47-55.

HAYASHI, F., SMITH, K. D., OZINSKY, A., HAWN, T. R., YI, E. C., GOODLETT, D. R., ENG, J. K., AKIRA, S., UNDERHILL, D. M. & ADEREM, A. 2001. The innate immune response to bacterial flagellin is mediated by Toll-like receptor 5. *Nature,* 410**,** 1099-1103.

HERRERO, M., DELORENZO, V. & TIMMIS, K. N. 1990. TRANSPOSON VECTORS CONTAINING NON-ANTIBIOTIC RESISTANCE SELECTION MARKERS FOR CLONING AND STABLE CHROMOSOMAL INSERTION OF FOREIGN GENES IN GRAM-NEGATIVE BACTERIA. *Journal of Bacteriology,* 172**,** 6557-6567.

HIRANSUTHIKUL, N., TANTISIRIWAT, W., LERTUTSAHAKUL, K., VIBHAGOOL, A. & BOONMA, P. 2005. Skin and soft-tissue infections among tsunami survivors in southern Thailand. *Clinical Infectious Diseases,* 41**,** E93-E96.

HOPF, P. S., FORD, R. S., ZEBIAN, N., MERKX-JACQUES, A., VIJAYAKUMAR, S., RATNAYAKE, D., HAYWORTH, J. & CREUZENET, C. 2011. Protein Glycosylation in <italic>Helicobacter pylori</italic>: Beyond the Flagellins? *Plos One,* 6**,** e25722.

HOWARD, S. L., JAGANNATHAN, A., SOO, E. C., HUI, J. P. M., AUBRY, A. J., AHMED, I., KARLYSHEV, A., KELLY, J. F., JONES, M. A., STEVENS, M. P., LOGAN, S. M. & WREN, B. W. 2009. *Campylobacter jejuni* Glycosylation Island Important in Cell Charge, Legionaminic Acid Biosynthesis, and Colonization of Chickens. *Infection and Immunity,* 77**,** 2544-2556.

IBUKI, T., IMADA, K., MINAMINO, T., KATO, T., MIYATA, T. & NAMBA, K. 2011. Common architecture of the flagellar type III protein export apparatus and F- and V-type ATPases. *Nature Structural & Molecular Biology,* 18**,** 277-U56.

JANDA, J. M. & ABBOTT, S. L. 2010. The Genus Aeromonas: Taxonomy, Pathogenicity, and Infection. *Clinical Microbiology Reviews,* 23**,** 35-73.

JAVED, M. A., VAN ALPHEN, L. B., SACHER, J., DING, W., KELLY, J., NARGANG, C., SMITH, D. F., CUMMINGS, R. D. & SZYMANSKI, C. M. 2015. A receptor-binding protein of Campylobacter jejuni bacteriophage NCTC 12673 recognizes flagellin glycosylated with acetamidino-modified pseudaminic acid. *Molecular Microbiology,* 95**,** 101-115.

JOSENHANS, C., VOSSEBEIN, L., FRIEDRICH, S. & SUERBAUM, S. 2002. The *neuA/flmD* gene cluster of *Helicobacter pylori* is involved in flagellar biosynthesis and flagellin glycosylation. *Fems Microbiology Letters,* 210**,** 165-172.

KARIMOVA, G., PIDOUX, J., ULLMANN, A. & LADANT, D. 1998. A bacterial two-hybrid system based on a reconstituted signal transduction pathway. *Proceedings of the National Academy of Sciences of the United States of America,* 95**,** 5752-5756.

KARLYSHEV, A. V., EVEREST, P., LINTON, D., CAWTHRAW, S., NEWELL, D. G. & WREN, B. W. 2004. The Campylobacter jejuni general glycosylation system is important for attachment to human epithelial cells and in the colonization of chicks. *Microbiology-Sgm,* 150**,** 1957-1964.

KARLYSHEV, A. V., LINTON, D., GREGSON, N. A. & WREN, B. W. 2002. A novel paralogous gene family involved in phase-variable flagella-mediated motility in *Campylobacter jejuni*. *Microbiology-Sgm,* 148**,** 473-480.

KAWAGISHI, I., IMAGAWA, M., IMAE, Y., MCCARTER, L. & HOMMA, M. 1996. The sodium-driven polar flagellar motor of marine Vibrio as the mechanosensor that regulates lateral flagellar expression. *Molecular Microbiology,* 20**,** 693-699.

KEARNS, D. B. 2010. A field guide to bacterial swarming motility. *Nat Rev Micro,* 8**,** 634-644.

KHAN, S. R., GAINES, J., ROOP, R. M., II & FARRAND, S. K. 2008. Broad-host-range expression vectors with tightly regulated promoters and their use to examine the influence of TraR and TraM expression on Ti plasmid quorum sensing. *Applied and Environmental Microbiology,* 74**,** 5053-5062.

KIENZLE, N., MULLER, M. & PEGG, S. 2000. Aeromonas wound infection in burns. *Burns,* 26**,** 478-482.

KINOSHITA, M., HARA, N., IMADA, K., NAMBA, K. & MINAMINO, T. 2013. Interactions of bacterial flagellar chaperone-substrate complexes with FlhA contribute to co-ordinating assembly of the flagellar filament. *Molecular Microbiology,* 90**,** 1249-1261.

KIROV, S. M., TASSELL, B. C., SEMMLER, A. B. T., O'DONOVAN, L. A., RABAAN, A. A. & SHAW, J. G. 2002. Lateral flagella and swarming motility in Aeromonas species. *Journal of Bacteriology,* 184**,** 547-555.

KOSTRZYNSKA, M., BETTS, J. D., AUSTIN, J. W. & TRUST, T. J. 1991. Identification, characterization, and spatial localization of two flagellin species in Helicobacter pylori flagella. *Journal of Bacteriology,* 173**,** 937-946.

KOVACH, M. E., ELZER, P. H., HILL, D. S., ROBERTSON, G. T., FARRIS, M. A., ROOP, R. M. & PETERSON, K. M. 1995. 4 NEW DERIVATIVES OF THE BROAD-HOST-RANGE CLONING VECTOR PBBR1MCS, CARRYING DIFFERENT ANTIBIOTIC-RESISTANCE CASSETTES. *Gene,* 166**,** 175-176.

KOWARIK, M., YOUNG, N. M., NUMAO, S., SCHULZ, B. L., HUG, I., CALLEWAERT, N., MILLS, D. C., WATSON, D. C., HERNANDEZ, M., KELLY, J. F., WACKER, M. & AEBI, M. 2006. Definition of the bacterial N-glycosylation site consensus sequence. *Embo Journal,* 25**,** 1957-1966.

KU, S. C., SCHULZ, B. L., POWER, P. M. & JENNINGS, M. P. 2009. The pilin O-glycosylation pathway of pathogenic Neisseria is a general system that glycosylates AniA, an outer

membrane nitrite reductase. *Biochemical and Biophysical Research Communications,* 378**,** 84-89.
LAMY, B., KODJO, A., LAURENT, F. & COL, B. V. H. S. G. 2009. Prospective Nationwide Study of Aeromonas Infections in France. *Journal of Clinical Microbiology,* 47**,** 1234-1237.
LI, G., MILLER, A., BULL, H. & HOWARD, S. P. 2011. Assembly of the Type II Secretion System: Identification of ExeA Residues Critical for Peptidoglycan Binding and Secretin Multimerization. *Journal of Bacteriology,* 193**,** 197-204.
LI, Z., HWANG, S., ERICSON, J., BOWLER, K. & BAR-PELED, M. 2015. Pen and Pal Are Nucleotide-Sugar Dehydratases That Convert UDP-GlcNAc to UDP-6-Deoxy-d-GlcNAc-5,6-ene and Then to UDP-4-Keto-6-deoxy-l-AltNAc for CMP-Pseudaminic Acid Synthesis in Bacillus thuringiensis. *Journal of Biological Chemistry,* 290**,** 691-704.
LINTON, D., DORRELL, N., HITCHEN, P. G., AMBER, S., KARLYSHEV, A. V., MORRIS, H. R., DELL, A., VALVANO, M. A., AEBI, M. & WREN, B. W. 2005. Functional analysis of the Campylobacter jejuni N-linked protein glycosylation pathway. *Molecular Microbiology,* 55**,** 1695-1703.
LOGAN, S. M. 2006. Flagellar glycosylation – a new component of the motility repertoire? *Microbiology,* 152**,** 1249-1262.
LOGAN, S. M., HUI, J. P. M., VINOGRADOV, E., AUBRY, A. J., MELANSON, J. E., KELLY, J. F., NOTHAFT, H. & SOO, E. C. 2009. Identification of novel carbohydrate modifications on Campylobacter jejuni 11168 flagellin using metabolomics-based approaches. *Febs Journal,* 276**,** 1014-1023.
LOGAN, S. M., KELLY, J. F., THIBAULT, P., EWING, C. P. & GUERRY, P. 2002. Structural heterogeneity of carbohydrate modifications affects serospecificity of Campylobacter flagellins. *Molecular Microbiology,* 46**,** 587-597.
LOMMEL, M. & STRAHL, S. 2009. Protein O-mannosylation: Conserved from bacteria to humans. *Glycobiology,* 19**,** 816-828.
LOWRY, R., BALBOA, S., PARKER, J. L. & SHAW, J. G. 2014a. Chapter Five - Aeromonas Flagella and Colonisation Mechanisms. *In:* ROBERT, K. P. (ed.) *Advances in Microbial Physiology.* Academic Press.
LOWRY, R. C., PARKER, J. L., KUMBHAR, R., MESNAGE, S., SHAW, J. G. & STAFFORD, G. P. 2014b. The Aeromonas caviae AHA0618 gene modulates cell length and influences swimming and swarming motility. *MicrobiologyOpen***,** n/a-n/a.
LYE, D. J., RODGERS, M. R., STELMA, G., VESPER, S. J. & HAYES, S. L. 2007. Characterization of Aeromonas virulence using an immunocompromised mouse model. *Current Microbiology,* 54**,** 195-198.
MAGNET, S., BELLAIS, S., DUBOST, L., FOURGEAUD, M., MAINARDI, J.-L., PETIT-FRERE, S., MARIE, A., MENGIN-LECREULX, D., ARTHUR, M. & GUTMANN, L. 2007. Identification of the L,D-transpeptidases responsible for attachment of the Braun lipoprotein to *Escherichia coli* peptidoglycan. *Journal of Bacteriology,* 189**,** 3927-3931.
MAGNET, S., DUBOST, L., MARIE, A., ARTHUR, M. & GUTMANN, L. 2008. Identification of the L,D-transpeptidases for peptidoglycan cross-linking in Escherichia coli. *Journal of Bacteriology,* 190**,** 4782-4785.
MATTICK, J. S. 2002. Type IV pili and twitching motility. *Annual Review of Microbiology,* 56**,** 289-314.
MCCARTER, L., HILMEN, M. & SILVERMAN, M. 1988. Flagellar dynamometer controls swarmer cell differentiation of V. parahaemolyticus. *Cell,* 54**,** 345-351.
MCNALLY, D. J., AUBRY, A. J., HUI, J. P. M., KHIEU, N. H., WHITFIELD, D., EWING, C. P., GUERRY, P., BRISSON, J.-R., LOGAN, S. M. & SOO, E. C. 2007. Targeted Metabolomics Analysis of Campylobacter coli VC167 Reveals Legionaminic Acid Derivatives as Novel Flagellar Glycans. *Journal of Biological Chemistry,* 282**,** 14463-14475.

MCNALLY, D. J., HUI, J. P. M., AUBRY, A. J., MUI, K. K. K., GUERRY, P., BRISSON, J.-R., LOGAN, S. M. & SOO, E. C. 2006. Functional Characterization of the Flagellar Glycosylation Locus in Campylobacter jejuni 81–176 Using a Focused Metabolomics Approach. *Journal of Biological Chemistry,* 281**,** 18489-18498.

MERINO, S., CAMPRUBI, S. & TOMAS, J. M. 1991. THE ROLE OF LIPOPOLYSACCHARIDE IN COMPLEMENT-KILLING OF AEROMONAS-HYDROPHILA STRAINS OF SEROTYPE O-34. *Journal of General Microbiology,* 137**,** 1583-1590.

MERINO, S., FULTON, K. M., TWINE, S. M., WILHELMS, M., MOLERO, R. & TOMAS, J. M. 2014. Aeromonas hydrophila Flagella Glycosylation: Involvement of a Lipid Carrier. *Plos One,* 9.

MERINO, S., SHAW, J. G. & TOMÁS, J. M. 2006. Bacterial lateral flagella: an inducible flagella system. *Fems Microbiology Letters,* 263**,** 127-135.

MERINO, S. & TOMAS, J. M. 2014. Gram-Negative Flagella Glycosylation. *International Journal of Molecular Sciences,* 15**,** 2840-2857.

MESCHER, M. F. & STROMINGER, J. L. 1976. PURIFICATION AND CHARACTERIZATION OF A PROKARYOTIC GLYCOPROTEIN FROM CELL-ENVELOPE OF HALOBACTERIUM-SALINARIUM. *Journal of Biological Chemistry,* 251**,** 2005-2014.

MINAMINO, T. & NAMBA, K. 2008. Distinct roles of the FliI ATPase and proton motive force in bacterial flagellar protein export. *Nature,* 451**,** 485-U12.

MOLERO, R., WILHELMS, M., INFANZON, B., TOMAS, J. M. & MERINO, S. 2011. Aeromonas hydrophila motY is essential for polar flagellum function, and requires coordinate expression of motX and Pom proteins. *Microbiology-Sgm,* 157**,** 2772-2784.

NAMDARI, H. & BOTTONE, E. J. 1990. MICROBIOLOGIC AND CLINICAL-EVIDENCE SUPPORTING THE ROLE OF AEROMONAS-CAVIAE AS A PEDIATRIC ENTERIC PATHOGEN. *Journal of Clinical Microbiology,* 28**,** 837-840.

NELSON, M. C. & GRAF, J. 2012. Bacterial symbioses of the medicinal leech Hirudo verbana. *Gut microbes,* 3**,** 322-31.

NEUBERGER, A. 1938. Carbohydrates in proteins I. The carbohydrate component of crystalline egg albumin. *Biochemical Journal,* 32**,** 1435-1451.

NOTHAFT, H. & SZYMANSKI, C. M. 2010. Protein glycosylation in bacteria: sweeter than ever. *Nature Reviews Microbiology,* 8**,** 765-778.

NOTHAFT, H. & SZYMANSKI, C. M. 2013. Bacterial Protein N-Glycosylation: New Perspectives and Applications. *Journal of Biological Chemistry,* 288**,** 6912-6920.

OSEI-POKU, J., MBOGO, C. M., PALMER, W. J. & JIGGINS, F. M. 2012. Deep sequencing reveals extensive variation in the gut microbiota of wild mosquitoes from Kenya. *Molecular Ecology,* 21**,** 5138-5150.

PARKER, J. L., DAY-WILLIAMS, M. J., TOMAS, J. M., STAFFORD, G. P. & SHAW, J. G. 2012. Identification of a putative glycosyltransferase responsible for the transfer of pseudaminic acid onto the polar flagellin of *Aeromonas caviae* Sch3N. *MicrobiologyOpen,* 1**,** 149-160.

PARKER, J. L., LOWRY, R. C., COUTO, N. A. S., WRIGHT, P. C., STAFFORD, G. P. & SHAW, J. G. 2014. Maf dependent bacterial flagellin glycosylation occurs before chaperone binding and flagellar T3SS export. *Molecular Microbiology*.

PARKER, J. L. & SHAW, J. G. 2011. *Aeromonas spp*. clinical microbiology and disease. *Journal of Infection,* 62**,** 109-118.

PORTER, S. L., WADHAMS, G. H. & ARMITAGE, J. P. 2008. Rhodobacter sphaeroides: complexity in chemotactic signalling. *Trends in Microbiology,* 16**,** 251-260.

POWER, P. M., RODDAM, L. F., DIECKELMANN, M., SRIKHANTA, Y. N., TAN, Y. C., BERRINGTON, A. W. & JENNINGS, M. P. 2000. Genetic characterization of pilin glycosylation in Neisseria meningitidis. *Microbiology-Uk,* 146**,** 967-979.

PRATT, L. A. & KOLTER, R. 1998. Genetic analysis of *Escherichia coli* biofilm formation: roles of flagella, motility, chemotaxis and type I pili. *Molecular Microbiology,* 30**,** 285-293.

RABAAN, A. A., GRYLLOS, I., TOMAS, J. M. & SHAW, J. G. 2001. Motility and the polar flagellum are required for *Aeromonas caviae* adherence to HEp-2 cells. *Infection and Immunity,* 69**,** 4257-4267.

RANGREZ, A. Y., DAYANANDA, K. M., ATANUR, S., JOSHI, R., PATOLE, M. S. & SHOUCHE, Y. S. 2006. Detection of Conjugation Related Type Four Secretion Machinery in Aeromonas culicicola. *Plos One,* 1.

REITH, M. E., SINGH, R. K., CURTIS, B., BOYD, J. M., BOUEVITCH, A., KIMBALL, J., MUNHOLLAND, J., MURPHY, C., SARTY, D., WILLIAMS, J., NASH, J. H. E., JOHNSON, S. C. & BROWN, L. L. 2008. The genome of Aeromonas salmonicida subsp salmonicida A449: insights into the evolution of a fish pathogen. *Bmc Genomics,* 9.

RIBEIRO, N. F. F., HEATH, C. H., KIERATH, J., REA, S., DUNCAN-SMITH, M. & WOOD, F. M. 2010. Burn wounds infected by contaminated water: Case reports, review of the literature and recommendations for treatment. *Burns,* 36**,** 9-22.

ROBERTS, M. A. J., PAPACHRISTODOULOU, A. & ARMITAGE, J. P. 2010. Adaptation and control circuits in bacterial chemotaxis. *Biochemical Society Transactions,* 38**,** 1265-1269.

ROCHA-DE-SOUZA, C. M., COLOMBO, A. V., HIRATA, R., MATTOS-GUARALDI, A. L., MONTEIRO-LEAL, L. H., PREVIATO, J. O., FREITAS, A. C. & ANDRADE, A. F. B. 2001. Identification of a 43-kDa outer-membrane protein as an adhesin in Aeromonas caviae. *Journal of Medical Microbiology,* 50**,** 313-319.

ROUJEINIKOVA, A. 2008. Crystal structure of the cell wall anchor domain of MotB,, a stator component of the bacterial flagellar motor: Implications for peptidoglycan recognition. *Proceedings of the National Academy of Sciences of the United States of America,* 105**,** 10348-10353.

ROURE, S., BONIS, M., CHAPUT, C., ECOBICHON, C., MATTOX, A., BARRIERE, C., GELDMACHER, N., GUADAGNINI, S., SCHMITT, C., PREVOST, M.-C., LABIGNE, A., BACKERT, S., FERRERO, R. L. & BONECA, I. G. 2012. Peptidoglycan maturation enzymes affect flagellar functionality in bacteria. *Molecular Microbiology,* 86**,** 845-856.

SAMATEY, F. A., IMADA, K., NAGASHIMA, S., VONDERVISZT, F., KUMASAKA, T., YAMAMOTO, M. & NAMBA, K. 2001. Structure of the bacterial flagellar protofilament and implications for a switch for supercoiling. *Nature,* 410**,** 331-337.

SAMATEY, F. A., MATSUNAMI, H., IMADA, K., NAGASHIMA, S., SHAIKH, T. R., THOMAS, D. R., CHEN, J. Z., DEROSIER, D. J., KITAO, A. & NAMBA, K. 2004. Structure of the bacterial flagellar hook and implication for the molecular universal joint mechanism. *Nature,* 431**,** 1062-1068.

SANDERS, A. N. & PAVELKA, M. S. 2013. Phenotypic analysis of *Eschericia coli* mutants lacking L,D-transpeptidases. *Microbiology-Sgm,* 159**,** 1842-1852.

SAUVAGE, E., KERFF, F., TERRAK, M., AYALA, J. A. & CHARLIER, P. 2008. The penicillin-binding proteins: structure and role in peptidoglycan biosynthesis. *Fems Microbiology Reviews,* 32**,** 234-258.

SCHEURWATER, E. M. & BURROWS, L. L. 2011. Maintaining network security: how macromolecular structures cross the peptidoglycan layer. *Fems Microbiology Letters,* 318**,** 1-9.

SCHIRM, M., ARORA, S. K., VERMA, A., VINOGRADOV, E., THIBAULT, P., RAMPHAL, R. & LOGAN, S. M. 2004. Structural and genetic characterization of glycosylation of type a flagellin in Pseudomonas aemginosa. *Journal of Bacteriology,* 186**,** 2523-2531.

SCHIRM, M., SOO, E. C., AUBRY, A. J., AUSTIN, J., THIBAULT, P. & LOGAN, S. M. 2003. Structural, genetic and functional characterization of the flagellin glycosylation process in *Helicobacter pylori*. *Molecular Microbiology,* 48**,** 1579-1592.

SCHOENHOFEN, I. C., MCNALLY, D. J., BRISSON, J.-R. & LOGAN, S. M. 2006. Elucidation of the CMP-pseudaminic acid pathway in Helicobacter pylori: synthesis from UDP-N-acetylglucosamine by a single enzymatic reaction. *Glycobiology,* 16**,** 8C-14C.

SCHWARZ, F. & AEBI, M. 2011. Mechanisms and principles of N-linked protein glycosylation. *Current Opinion in Structural Biology,* 21**,** 576-582.

SESHADRI, R., JOSEPH, S. W., CHOPRA, A. K., SHA, J., SHAW, J., GRAF, J., HAFT, D., WU, M., REN, Q., ROSOVITZ, M. J., MADUPU, R., TALLON, L., KIM, M., JIN, S., VUONG, H., STINE, O. C., ALI, A., HORNEMAN, A. J. & HEIDELBERG, J. F. 2006. Genome sequence of Aeromonas hydrophila ATCC 7966(T): Jack of all trades. *Journal of Bacteriology,* 188**,** 8272-8282.

SHA, J., WANG, S. F., SUAREZ, G., SIERRA, J. C., FADL, A. A., EROVA, T. E., FOLTZ, S. M., KHAJANCHI, E. K., SILVER, A., GRAF, J., SCHEIN, C. H. & CHOPRA, A. K. 2007. Further characterization of a type III secretion system (T3SS) and of a new effector protein from a clinical isolate of Aeromonas hydrophila - Part I. *Microbial Pathogenesis,* 43**,** 127-146.

SHIMADA, T., SAKAZAKI, R. & SUZUKI, K. 1985. PERITRICHOUS FLAGELLA IN MESOPHILIC STRAINS OF AEROMONAS. *Japanese Journal of Medical Science & Biology,* 38**,** 141-145.

SIERRA, J. C., SUAREZ, G., SHA, J., FOLTZ, S. M., POPOV, V. L., GALINDO, C. L., GARNER, H. R. & CHOPRA, A. K. 2007. Biological characterization of a new type III secretion system effector from a clinical isolate of Aeromonas hydrophila - Part II. *Microbial Pathogenesis,* 43**,** 147-160.

SILVER, A. C., RABINOWITZ, N. M., KUEFFER, S. & GRAF, J. 2007. Identification of Aeromonas veronii genes required for colonization of the medicinal leech, Hirudo verbana. *Journal of Bacteriology,* 189**,** 6763-6772.

SLEYTR, U. B. & THORNE, K. J. I. 1976. CHEMICAL CHARACTERIZATION OF REGULARLY ARRANGED SURFACE-LAYERS OF CLOSTRIDIUM-THERMOSACCHAROLYTICUM AND CLOSTRIDIUM-THERMOHYDROSULFURICUM. *Journal of Bacteriology,* 126**,** 377-383.

SMEDLEY, J. G., JEWELL, E., ROGUSKIE, J., HORZEMPA, J., SYBOLDT, A., STOLZ, D. B. & CASTRIC, P. 2005. Influence of pilin glycosylation on Pseudomonas aeruginosa 1244 pilus function. *Infection and Immunity,* 73**,** 7922-7931.

SOLA, R. J. & GRIEBENOW, K. 2009. Effects of Glycosylation on the Stability of Protein Pharmaceuticals. *Journal of Pharmaceutical Sciences,* 98**,** 1223-1245.

SOWA, Y. & BERRY, R. M. 2009. The Bacterial Flagellar Motor. *Single Molecule Biology***,** 105-142.

SPIRO, R. G. 2002. Protein glycosylation: nature, distribution, enzymatic formation, and disease implications of glycopeptide bonds. *Glycobiology,* 12**,** 43R-56R.

STAFFORD, G. P., EVANS, L. D. B., KRUMSCHEID, R., DHILLON, P., FRASER, G. M. & HUGHES, C. 2007. Sorting of early and late flagellar subunits after docking at the membrane ATPase of the type III export pathway. *Journal of Molecular Biology,* 374**,** 877-882.

STEWART, B. J. & MCCARTER, L. L. 2003. Lateral flagellar gene system of Vibrio parahaemolyticus. *Journal of Bacteriology,* 185**,** 4508-4518.

SUAREZ, G., SIERRA, J. C., EROVA, T. E., SHA, J., HORNEMAN, A. J. & CHOPRA, A. K. 2010. A Type VI Secretion System Effector Protein, VgrG1, from Aeromonas hydrophila That Induces Host Cell Toxicity by ADP Ribosylation of Actin. *Journal of Bacteriology,* 192**,** 155-168.

SUAREZ, G., SIERRA, J. C., SHA, J., WANG, S., EROVA, T. E., FADL, A. A., FOLTZ, S. M., HORNEMAN, A. J. & CHOPRA, A. K. 2008. Molecular characterization of a functional type VI secretion system from a clinical isolate of Aeromonas hydrophila. *Microbial Pathogenesis,* 44**,** 344-361.

SUN, L., JIN, M., DING, W., YUAN, J., KELLY, J. & GAO, H. 2013. Posttranslational Modification of Flagellin FlaB in Shewanella oneidensis. *Journal of Bacteriology,* 195**,** 2550-61.

SYCURO, L. K., RULE, C. S., PETERSEN, T. W., WYCKOFF, T. J., SESSLER, T., NAGARKAR, D. B., KHALID, F., PINCUS, Z., BIBOY, J., VOLLMER, W. & SALAMA, N. R. 2013. Flow cytometry-based enrichment for cell shape mutants identifies multiple genes that influence *Helicobacter pylori* morphology. *Molecular Microbiology,* 90**,** 869-83.

SYCURO, L. K., WYCKOFF, T. J., BIBOY, J., BORN, P., PINCUS, Z., VOLLMER, W. & SALAMA, N. R. 2012. Multiple Peptidoglycan Modification Networks Modulate *Helicobacter pylori's* Cell Shape, Motility, and Colonization Potential. *Plos Pathogens,* 8.

SZYMANSKI, C. M., YAO, R. J., EWING, C. P., TRUST, T. J. & GUERRY, P. 1999. Evidence for a system of general protein glycosylation in Campylobacter jejuni. *Molecular Microbiology,* 32**,** 1022-1030.

TABEI, S. M. B., HITCHEN, P. G., DAY-WILLIAMS, M. J., MERINO, S., VART, R., PANG, P.-C., HORSBURGH, G. J., VICHES, S., WILHELMS, M., TOMAS, J. M., DELL, A. & SHAW, J. G. 2009. An Aeromonas caviae Genomic Island Is Required for both O-Antigen Lipopolysaccharide Biosynthesis and Flagellin Glycosylation. *Journal of Bacteriology,* 191**,** 2851-2863.

TAGUCHI, F., SUZUKI, T., TAKEUCHI, K., INAGAKI, Y., TOYODA, K., SHIRAISHI, T. & ICHINOSE, Y. 2009. Glycosylation of flagellin from Pseudomonas syringae pv. tabaci 6605 contributes to evasion of host tobacco plant surveillance system. *Physiological and Molecular Plant Pathology,* 74**,** 11-17.

TAGUCHI, F., TAKEUCHI, K., KATOH, E., MURATA, K., SUZUKI, T., MARUTANI, M., KAWASAKI, T., EGUCHI, M., KATOH, S., KAKU, H., YASUDA, C., INAGAKI, Y., TOYODA, K., SHIRAISHI, T. & ICHINOSE, Y. 2006. Identification of glycosylation genes and glycosylated amino acids of flagellin in Pseudomonas syringae pv. tabaci. *Cellular Microbiology,* 8**,** 923-938.

TAGUCHI, F., YAMAMOTO, M., OHNISHI-KAMEYAMA, M., IWAKI, M., YOSHIDA, M., ISHII, T., KONISHI, T. & ICHINOSE, Y. 2010. Defects in flagellin glycosylation affect the virulence of Pseudomonas syringae pv. tabaci 6605. *Microbiology-Sgm,* 156**,** 72-80.

TAKEUCHI, K., TAGUCHI, F., INAGAKI, Y., TOYODA, K., SHIRAISHI, T. & ICHINOSE, Y. 2003. Flagellin Glycosylation Island in Pseudomonas syringae pv. glycinea and Its Role in Host Specificity. *Journal of Bacteriology,* 185**,** 6658-6665.

TERASHIMA, H., FUKUOKA, H., YAKUSHI, T., KOJIMA, S. & HOMMA, M. 2006. The Vibrio motor proteins, MotX and MotY, are associated with the basal body of Na+-driven flagella and required for stator formation. *Molecular Microbiology,* 62**,** 1170-1180.

TERASHIMA, H., KOJIMA, S. & HOMMA, M. 2008. FLAGELLAR MOTILITY IN BACTERIA: STRUCTURE AND FUNCTION OF FLAGELLAR MOTOR. *International Review of Cell and Molecular Biology, Vol 270,* 270**,** 39-85.

THIBAULT, P., LOGAN, S. M., KELLY, J. F., BRISSON, J. R., EWING, C. P., TRUST, T. J. & GUERRY, P. 2001. Identification of the carbohydrate moieties and glycosylation motifs in *Campylobacter jejuni* flagellin. *Journal of Biological Chemistry,* 276**,** 34862-34870.

THOMPSON, J. D., HIGGINS, D. G. & GIBSON, T. J. 1994. ClustalW - Improving the sensitivity of progressive multiple sequence alignment through sequence weighting, position-specific gap penalties and weight matric choice. *Nucleic Acids Research,* 22**,** 4673-4680.

TOMAS, J. M. 2012. The main Aeromonas pathogenic factors. *ISRN microbiology,* 2012**,** 256261-256261.

TOMB, J. F., WHITE, O., KERLAVAGE, A. R., CLAYTON, R. A., SUTTON, G. G., FLEISCHMANN, R. D., KETCHUM, K. A., KLENK, H. P., GILL, S., DOUGHERTY, B. A., NELSON, K., QUACKENBUSH, J., ZHOU, L. X., KIRKNESS, E. F., PETERSON, S., LOFTUS, B., RICHARDSON, D., DODSON, R., KHALAK, H. G., GLODEK, A., MCKENNEY, K., FITZEGERALD, L. M., LEE, N., ADAMS, M. D., HICKEY, E. K., BERG, D. E., GOCAYNE, J. D., UTTERBACK, T. R., PETERSON, J. D., KELLEY, J. M., COTTON, M. D., WELDMAN, J. M.,

FUJII, C., BOWMAN, C., WATTHEY, L., WALLIN, E., HAYES, W. S., WEIDMAN, J. M., BORODOVSKY, M., KARP, P. D., SMITH, H. O., FRASER, C. M. & VENTER, J. C. 1997. The complete genome sequence of the gastric pathogen Helicobacter pylori. *Nature,* 388**,** 539-547.

TRAN, S.-L., GUILLEMET, E., GOHAR, M., LERECLUS, D. & RAMARAO, N. 2010. CwpFM (EntFM) Is a *Bacillus cereus* Potential Cell Wall Peptidase Implicated in Adhesion, Biofilm Formation, and Virulence. *Journal of Bacteriology,* 192**,** 2638-2642.

TURNER, L., RYU, W. S. & BERG, H. C. 2000. Real-Time Imaging of Fluorescent Flagellar Filaments. *Journal of Bacteriology,* 182**,** 2793-2801.

TURNER, L., STERN, A. S. & BERG, H. C. 2012. Growth of Flagellar Filaments of Escherichia coli Is Independent of Filament Length. *Journal of Bacteriology,* 194**,** 2437-2442.

TWINE, S. M., PAUL, C. J., VINOGRADOV, E., MCNALLY, D. J., BRISSON, J.-R., MULLEN, J. A., MCMULLIN, D. R., JARRELL, H. C., AUSTIN, J. W., KELLY, J. F. & LOGAN, S. M. 2008. Flagellar glycosylation in Clostridium botulinum. *Febs Journal,* 275**,** 4428-4444.

TWINE, S. M., REID, C. W., AUBRY, A., MCMULLIN, D. R., FULTON, K. M., AUSTIN, J. & LOGAN, S. M. 2009. Motility and Flagellar Glycosylation in Clostridium difficile. *Journal of Bacteriology,* 191**,** 7050-7062.

VAN ALPHEN, L. B., WUHRER, M., BLEUMINK-PLUYM, N. M. C., HENSBERGEN, P. J., DEELDER, A. M. & VAN PUTTEN, J. P. M. 2008. A functional *Campylobacter jejuni maf4* gene results in novel glycoforms on flagellin and altered autoagglutination behaviour. *Microbiology-Sgm,* 154**,** 3385-3397.

VAN SORGE, N. M., BLEUMINK, N. M. C., VAN VLIET, S. J., SAELAND, E., VAN DER POL, W. L., VAN KOOYK, Y. & VAN PUTTEN, J. P. M. 2009. N-glycosylated proteins and distinct lipooligosaccharide glycoforms of Campylobacter jejuni target the human C-type lectin receptor MGL. *Cellular Microbiology,* 11**,** 1768-1781.

VERMA, A., ARORA, S. K., KURAVI, S. K. & RAMPHAL, R. 2005. Roles of specific amino acids in the N terminus of Pseudomonas aeruginosa flagellin and of flagellin glycosylation in the innate immune response. *Infection and Immunity,* 73**,** 8237-8246.

VERMA, A., SCHIRM, M., ARORA, S. K., THIBAULT, P., LOGAN, S. M. & RAMPHAL, R. 2006. Glycosylation of b-type flagellin of Pseudomonas aeruginosa: Structural and genetic basis. *Journal of Bacteriology,* 188**,** 4395-4403.

VIK, A., AAS, F. E., ANONSEN, J. H., BILSBOROUGH, S., SCHNEIDER, A., EGGE-JACOBSEN, W. & KOOMEY, M. 2009. Broad spectrum O-linked protein glycosylation in the human pathogen Neisseria gonorrhoeae. *Proceedings of the National Academy of Sciences of the United States of America,* 106**,** 4447-4452.

VILA, J., RUIZ, J., GALLARDO, F., VARGAS, M., SOLER, L., FIGUERAS, M. J. & GASCON, J. 2003. Aeromonas spp. and traveler's diarrhea: Clinical features and antimicrobial resistance. *Emerging Infectious Diseases,* 9**,** 552-555.

WILCOX, M. H., COOK, A. M., ELEY, A. & SPENCER, R. C. 1992. AEROMONAS SPP AS A POTENTIAL CAUSE OF DIARRHEA IN CHILDREN. *Journal of Clinical Pathology,* 45**,** 959-963.

WILHELMS, M., FULTON, K. M., TWINE, S. M., TOMAS, J. M. & MERINO, S. 2012. Differential Glycosylation of Polar and Lateral Flagellins in *Aeromonas hydrophila* AH-3. *Journal of Biological Chemistry,* 287**,** 27851-27862.

WILHELMS, M., GONZALEZ, V., TOMAS, J. M. & MERINO, S. 2013. Aeromonas hydrophila Lateral Flagellar Gene Transcriptional Hierarchy. *Journal of Bacteriology,* 195**,** 1436-1445.

WILHELMS, M., MOLERO, R., SHAW, J. G., TOMAS, J. M. & MERINO, S. 2011. Transcriptional Hierarchy of Aeromonas hydrophila Polar-Flagellum Genes. *Journal of Bacteriology,* 193**,** 5179-5190.

WILHELMS, M., VILCHES, S., MOLERO, R., SHAW, J. G., TOMAS, J. M. & MERINO, S. 2009. Two Redundant Sodium-Driven Stator Motor Proteins Are Involved in Aeromonas hydrophila Polar Flagellum Rotation. *Journal of Bacteriology,* 191**,** 2206-2217.

WU, L., WANG, J., TANG, P., CHEN, H. & GAO, H. 2011. Genetic and Molecular Characterization of Flagellar Assembly in Shewanella oneidensis. *Plos One,* 6.

XING, J. H., BAI, F., BERRY, R. & OSTER, G. 2006. Torque-speed relationship of the bacterial flagellar motor. *Proceedings of the National Academy of Sciences of the United States of America,* 103**,** 1260-1265.

YONEKURA, K., MAKI-YONEKURA, S. & NAMBA, K. 2003. Complete atomic model of the bacterial flagellar filament by electron cryomicroscopy. *Nature,* 424**,** 643-650.

YONEKURA, K., MAKI, S., MORGAN, D. G., DEROSIER, D. J., VONDERVISZT, F., IMADA, K. & NAMBA, K. 2000. The bacterial flagellar cap as the rotary promoter of flagellin self-assembly. *Science,* 290**,** 2148-2152.

YOUNG, N. M., BRISSON, J. R., KELLY, J., WATSON, D. C., TESSIER, L., LANTHIER, P. H., JARRELL, H. C., CADOTTE, N., MICHAEL, F. S., ABERG, E. & SZYMANSKI, C. M. 2002. Structure of the N-linked glycan present on multiple glycoproteins in the gram-negative bacterium, Campylobacter jejuni. *Journal of Biological Chemistry,* 277**,** 42530-42539.

ZAMPRONIO, C. G., BLACKWELL, G., PENN, C. W. & COOPER, H. J. 2011. Novel Glycosylation Sites Localized in Campylobacter jejuni Flagellin FlaA by Liquid Chromatography Electron Capture Dissociation Tandem Mass Spectrometry. *Journal of Proteome Research,* 10**,** 1238-1245.

ZARSCHLER, K., JANESCH, B., PABST, M., ALTMANN, F., MESSNER, P. & SCHAEFFER, C. 2010. Protein tyrosine O-glycosylation-A rather unexplored prokaryotic glycosylation system. *Glycobiology,* 20**,** 787-798.

ZUNK, M. & KIEFEL, M. J. 2014. The occurrence and biological significance of the [small alpha]-keto-sugars pseudaminic acid and legionaminic acid within pathogenic bacteria. *RSC Advances,* 4**,** 3413-3421.

## pSRK(Gm)

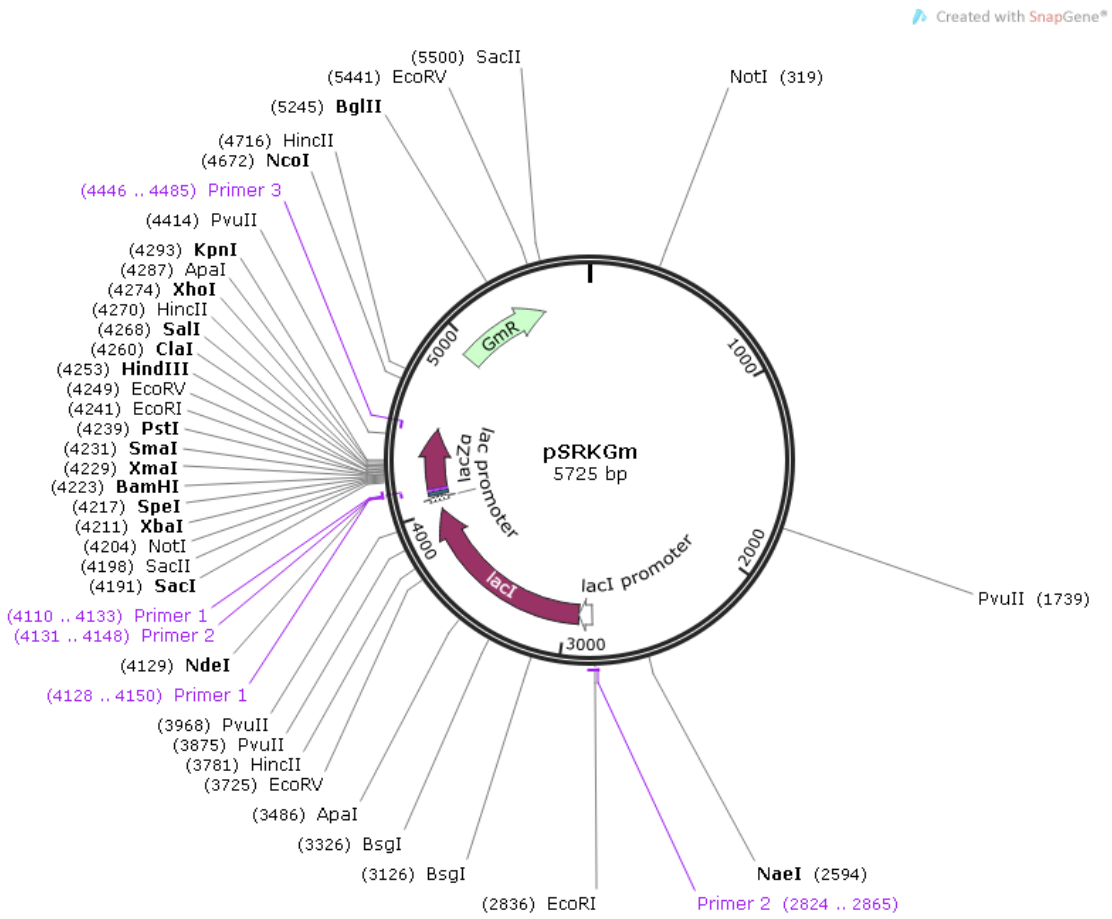
Created with SnapGene®
pSRKGm
5725 bp
GmR
lacZα
lac promoter
lacI
lacI promoter
1000
2000
3000
4000
5000
(5500) SacII
(5441) EcoRV
(5245) BglII
(4716) HincII
(4672) NcoI
(4446 .. 4485) Primer 3
(4414) PvuII
(4293) KpnI
(4287) ApaI
(4274) XhoI
(4270) HincII
(4268) SalI
(4260) ClaI
(4253) HindIII
(4249) EcoRV
(4241) EcoRI
(4239) PstI
(4231) SmaI
(4229) XmaI
(4223) BamHI
(4217) SpeI
(4211) XbaI
(4204) NotI
(4198) SacII
(4191) SacI
(4110 .. 4133) Primer 1
(4131 .. 4148) Primer 2
(4129) NdeI
(4128 .. 4150) Primer 1
(3968) PvuII
(3875) PvuII
(3781) HincII
(3725) EcoRV
(3486) ApaI
(3326) BsgI
(3126) BsgI
(2836) EcoRI
NaeI (2594)
Primer 2 (2824 .. 2865)
PvuII (1739)
NotI (319)

## pBBR1MCS-5

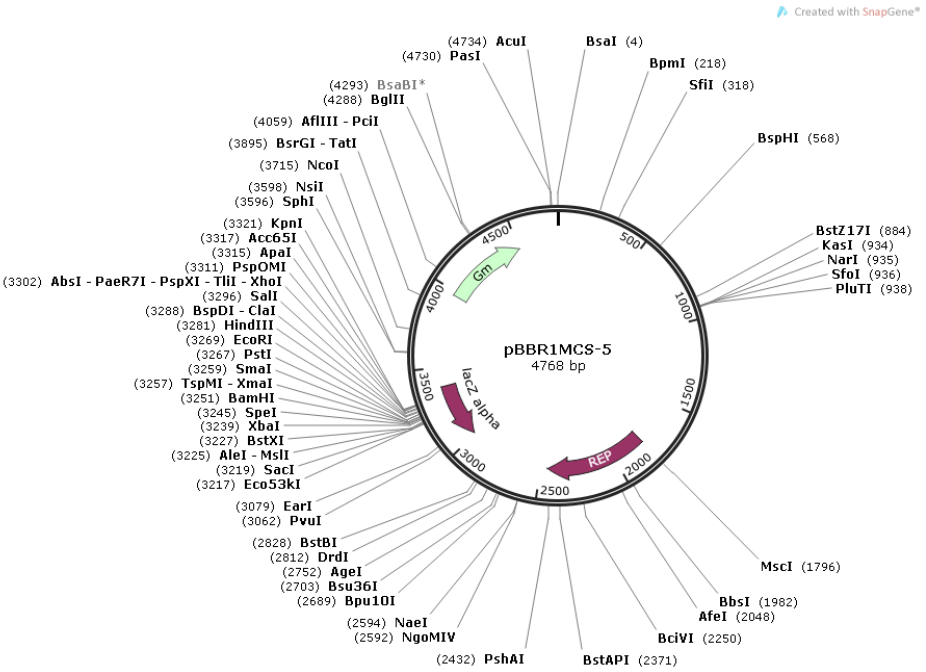


## pGEM-T EASY

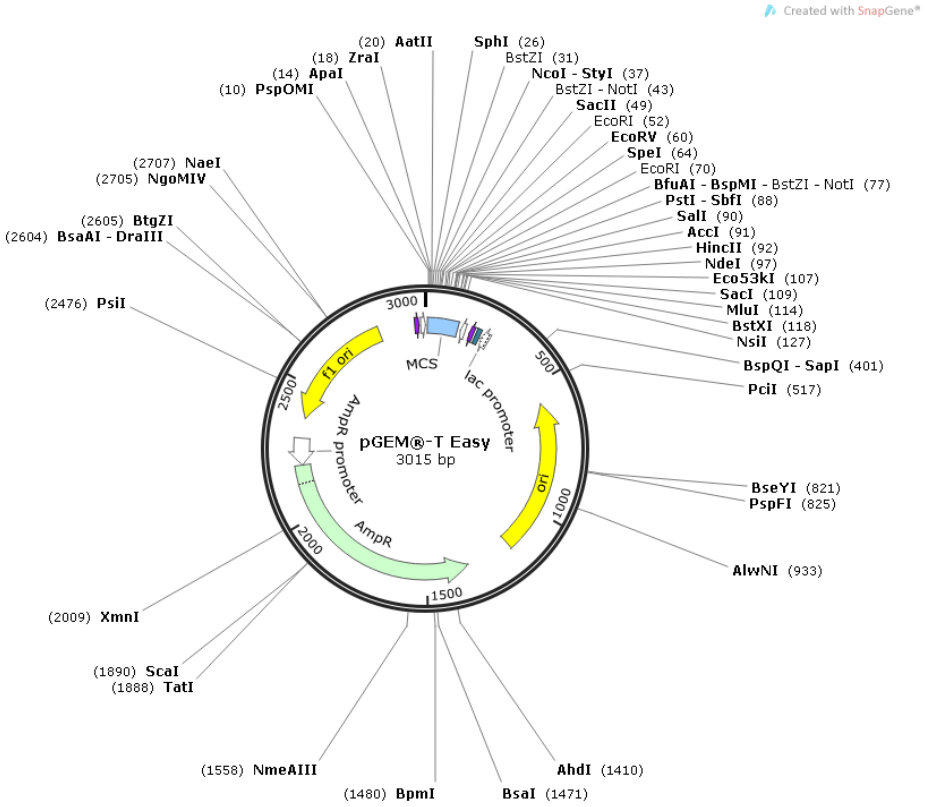

# BACTH vectors

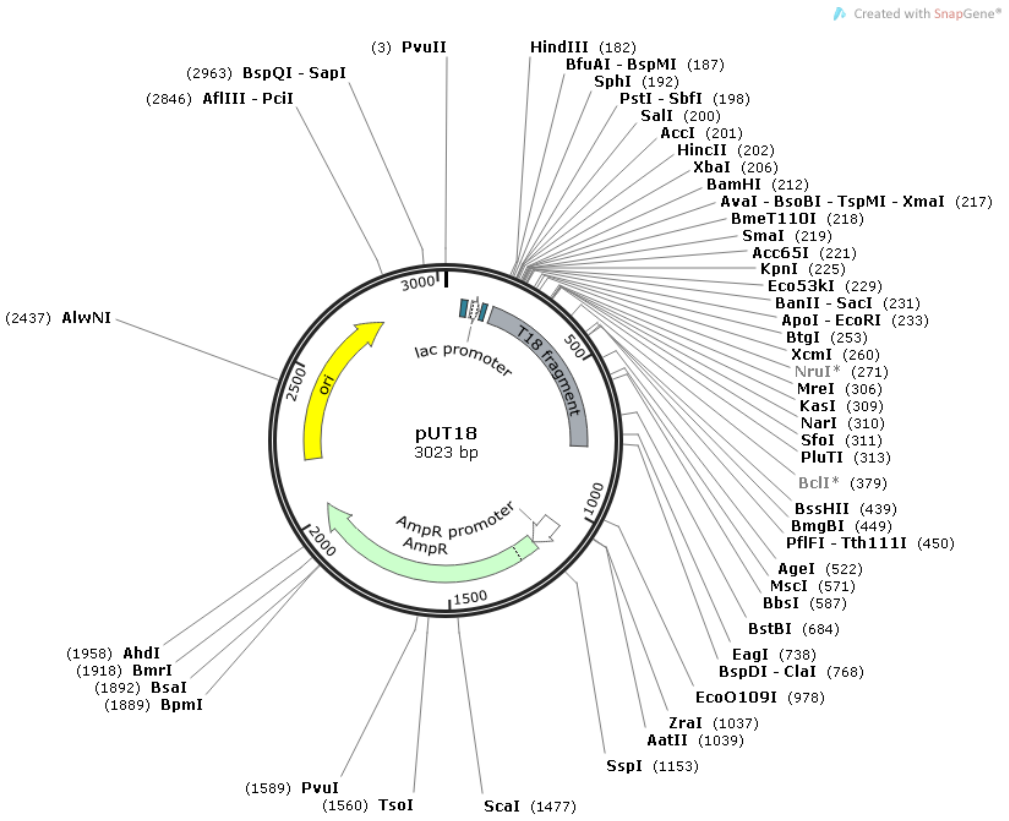


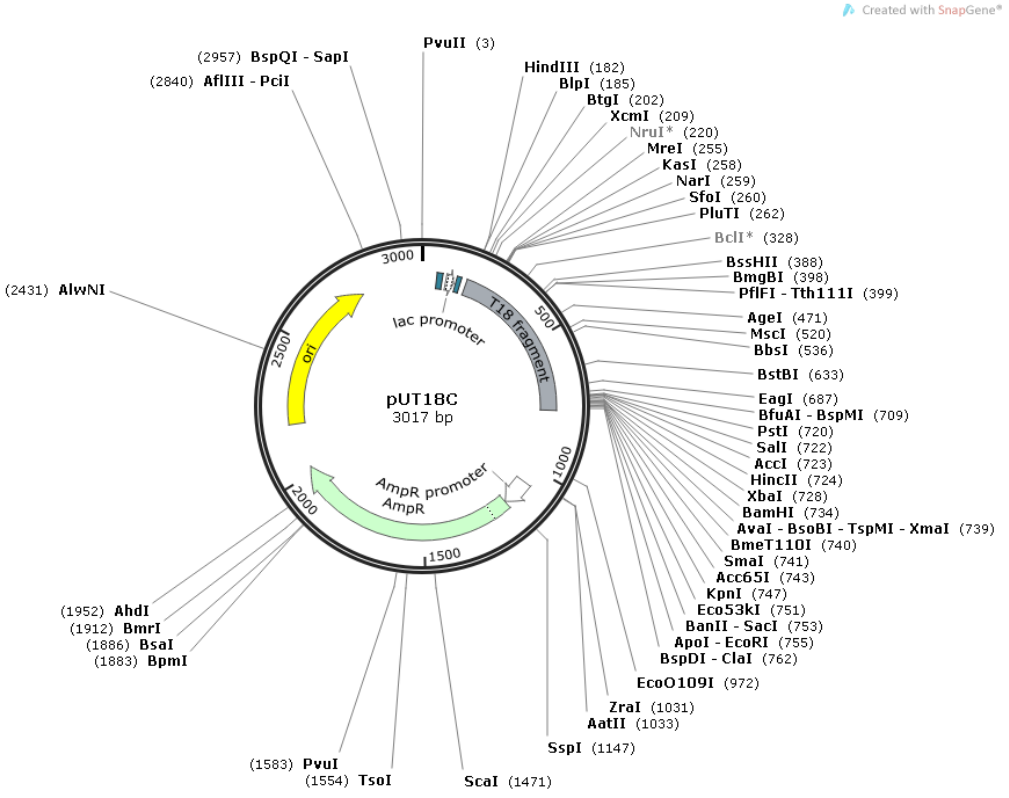

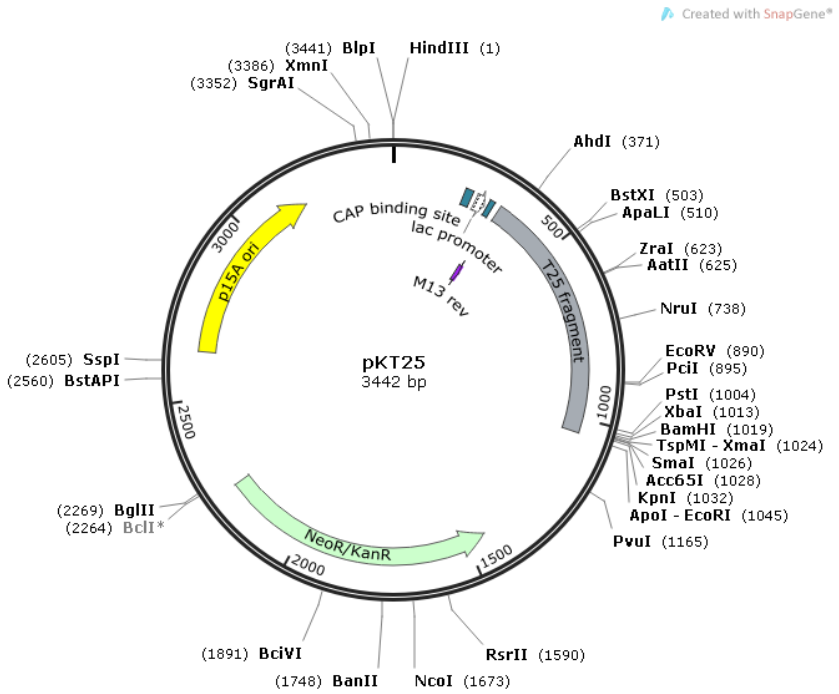
Created with SnapGene®
(3441) BlpI
HindIII (1)
(3386) XmnI
(3352) SgrAI
AhdI (371)
BstXI (503)
ApaLI (510)
ZraI (623)
AatII (625)
NruI (738)
EcoRV (890)
PciI (895)
PstI (1004)
XbaI (1013)
BamHI (1019)
TspMI - XmaI (1024)
SmaI (1026)
Acc65I (1028)
KpnI (1032)
ApoI - EcoRI (1045)
PvuI (1165)
RsrII (1590)
NcoI (1673)
BanII (1748)
BciVI (1891)
BglII
BclI*
(2269)
(2264)
(2560) BstAPI
(2605) SspI
CAP binding site
lac promoter
M13 rev
T25 fragment
p15A ori
NeoR/KanR
pKT25
3442 bp
500
1000
1500
2000
2500
3000

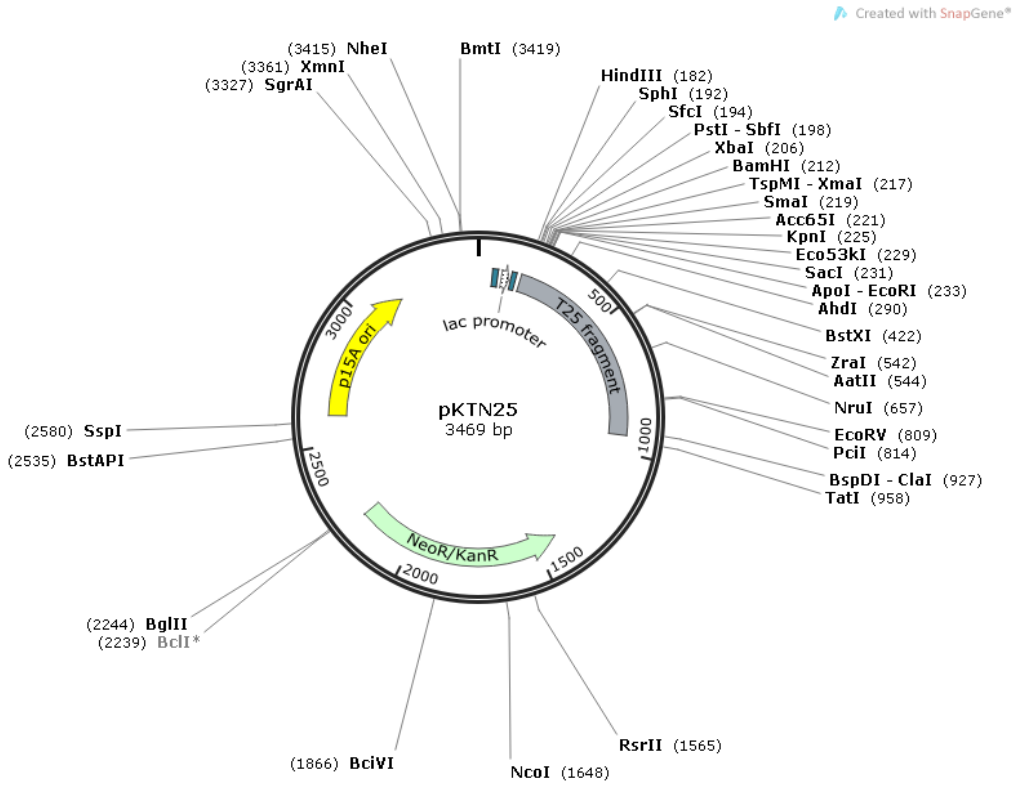
Created with SnapGene®
(3415) NheI
BmtI (3419)
(3361) XmnI
(3327) SgrAI
HindIII (182)
SphI (192)
SfcI (194)
PstI - SbfI (198)
XbaI (206)
BamHI (212)
TspMI - XmaI (217)
SmaI (219)
Acc65I (221)
KpnI (225)
Eco53kI (229)
SacI (231)
ApoI - EcoRI (233)
AhdI (290)
BstXI (422)
ZraI (542)
AatII (544)
NruI (657)
EcoRV (809)
PciI (814)
BspDI - ClaI (927)
TatI (958)
RsrII (1565)
NcoI (1648)
BciVI (1866)
BglII
BclI*
(2244)
(2239)
(2535) BstAPI
(2580) SspI
lac promoter
T25 fragment
p15A ori
NeoR/KanR
pKTN25
3469 bp
500
1000
1500
2000
2500
3000

## BACTH vector multiple cloning sites